Title

Evaluating the Private and External Costs and Benefits of Select Large-Scale Li-ion Battery Energy Storage Applications

Author

Porzio, Jason

Publication Date

2024

Peer reviewed|Thesis/dissertation

Evaluating the Private and External Costs and Benefits of Select Large-Scale Li-ion Battery Energy Storage Applications

By

Jason Edward Porzio

A dissertation submitted in partial satisfaction of the

requirements for the degree of

Doctor of Philosophy

in

Engineering - Civil & Environmental Engineering

in the

Graduate Division

of the

University of California, Berkeley

Committee in Charge:

Professor Scott Moura
Dr. Corinne Scown
Professor Maximillian Auffhammer
Professor Arpad Horvath

Spring 2024

Abstract

Evaluating the Private and External Costs and Benefits of Select Large-Scale Li-ion Battery Energy Storage Applications

By

Jason Edward Porzio

Doctor in Philosophy in Engineering – Civil and Environmental Engineering

University of California, Berkeley

Professor Scott Moura, Chair

Lithium-ion (Li-ion) batteries have experienced a massive rise in popularity since their initial commercial introduction in 1991. Their implementation into several economic sectors has been instrumental in achieving large-scale electrification, with the eventual goal of sector-wide decarbonization. However, there has been little consensus on how to report the impacts associated with Li-ion batteries, and the standard of modeling the use-phase of Li-ion technologies often relies on broad assumptions, particularly with the future prices of Li-ion batteries. Additionally, there is little consensus on whether the integration of Li-ion technologies provides net positive impacts in several sectors. My research aims to provide recommendations for life-cycle assessments (LCA) on Li-ion technologies with the intent of helping future studies be more interpretable, representative, and impactful, as well as critically examine the assumptions used to forecast Li-ion prices. I then employ LCA and technoeconomic analysis (TEA) to model the climate, human health, and economic impacts of Li-ion technologies serving in peaker replacement and heavy-duty long-haul freight roles. The results from these studies show that the relative net impact of using Li-ion batteries in these roles can be positive or negative depending on several factors. Greater details of these studies are provided below.

Life-cycle Assessment Consideration for Batteries and Battery Materials

Rechargeable batteries are necessary for the decarbonization of the energy systems, but life-cycle environmental impact assessments have not achieved consensus on the environmental impacts of producing these batteries. Nonetheless, life cycle assessment (LCA) is a powerful tool to inform the development of better-performing batteries with reduced environmental burden. This review explores common practices in lithium-ion battery LCAs and makes recommendations for how future studies can be more interpretable, representative, and impactful. First, LCAs should focus analyses of resource depletion on long-term trends toward more energy and resource-intensive material extraction and processing rather than treating known reserves as a fixed quantity being depleted. Second, future studies should account for extraction and processing operations that deviate from industry best-practices and may be responsible for an outsized share of sector-wide

impacts, such as artisanal cobalt mining. Third, LCAs should explore at least 2–3 battery manufacturing facility scales to capture size- and throughput-dependent impacts such as dry room conditioning and solvent recovery. Finally, future LCAs must transition away from kg of battery mass as a functional unit and instead make use of kWh of storage capacity and kWh of lifetime energy throughput.

Temporal Variations in Learning Rates of Li-ion Technologies: Insights for Price Forecasting and Policy through Segmented Regression Analysis

Since their initial development in 1991, Li-ion cell prices have decreased by over 97%. However, decades of lithium-ion battery cost reductions are often represented by a single learning rate in an experience curve. Learning rates are not inherently constant, however, and changes in learning rates can have dramatic impacts on cost forecasts and subsequent policy and investment decisions. This analysis is the first study to employ segmented regression to describe how learning rates have historically changed for lithium-ion technologies in different periods of time. Additionally, the distinctions between *cost* and *price* data are highlighted to emphasize the value of allowing learning rates to vary over time when performing experience curves for lithium-ion batteries. This analysis identifies past changes in the learning rate of lithium-ion cells, modules, and installations: for lithium-ion cells, the learning rate was 4% through 1997, 34% through 2003, and 24.4% onward. This dynamic learning behavior is explained as periods of market development, shakeout, and stabilization respectively. By allowing greater flexibility in the experience curve, a secondary shakeout period emerges from 2013 onward, with a learning rate of 40.9%. While this secondary shakeout has less statistical significance, we find that it aligns well with the growth of Li-ion markets and may emerge as significant as more data becomes available. Modules and installed costs follow a similar trend, with low learning (6-8% for 4-6 years) followed by an acceleration to 31-37%. The importance of capturing these historical variances is highlighted by demonstrating the impact of varying learning rates on forecasted lithium-ion cell prices through scenario analysis. We observe that price forecasts are much more sensitive to the uncertainty in learning rate compared to the uncertainty in technology deployment. Utilizing multiple learning rates from a segmented experience curve can enhance future Li-ion technology price projections, improving both price forecasting and policy development.

Private and External Costs and Benefits of Replacing High-Emitting Peaker Plants with Batteries

Falling costs of Li-ion batteries have made them attractive for grid-scale energy storage applications. Energy storage will become increasingly important as intermittent renewable generation and more frequent extreme weather events put stress on the electricity grid. Environmental groups across the United States are advocating for the replacement of the highest-emitting power plants, which run only at times of peak demand, with Li-ion battery systems. We analyze the life-cycle cost, climate, and human health impacts of replacing the 19 highest-emitting peaker plants in California with Li-ion battery energy storage systems (BESS). Our results show that designing Li-ion BESS to replace peaker plants puts them at an economic disadvantage, even if facilities are only sized to meet 95% of the original plants' load events and are free to engage in arbitrage. However, five of 19 potential replacements do achieve a positive net present value after including monetized climate and human health impacts. These BESS cycle far less than typical front-of-the-meter batteries and rely on the frequency regulation

market for most of their revenue. All projects offer net air pollution benefits but increase net greenhouse gas emissions due to electricity demand during charging and upstream emissions from battery manufacturing.

Private and External Costs and Benefits of Electrifying Heavy-Duty Long-Haul Trucking with Li-ion Batteries

The electrification of long-haul heavy-duty vehicles (HDVs) is necessary for the decarbonization of the transportation sector in the United States, but there is no clear technological pathway to replace the diesel internal combustion engine enabling this transport mode. Li-ion batteries have emerged as a popular candidate when exploring options to electrify HDVs, largely due to the rapidly growing popularity of Li-ion battery passenger electric vehicles and decreasing Li-ion battery prices. While many studies point to the climate and human health benefits that will arise from replacing diesel HDVs with Li-ion HDVs, other studies claim that technological limitations will make Li-ion HDVs economically inviable for long-haul freight. We use life-cycle assessment and technoeconomic analysis to model the total ownership cost, climate, and human health impacts associated with replacing a diesel Class 8 truck performing long-haul freight with a Li-ion Class 8 truck in the United States. Our results show that when including monetized contributions to global warming potential and human health burden, Li-ion Class 8 trucks in long-haul freight have greater lifetime costs per mile than diesel Class 8 trucks due to the high price and specific energy of Li-ion batteries, as well as high costs associated with the use of charging infrastructure. Additionally, the current use of Li-ion Class 8 trucks results in marginal improvements to social impacts relative to diesel Class 8 trucks under a high renewable energy cost scenario, but worse social impacts under a low renewable cost scenario. However, by 2035, the social impacts of Li-ion Class 8 trucks are substantially less than diesel Class 8 trucks under both renewable energy cost scenarios as more renewable energy is integrated into the electricity grid.

Table of Contents

List of Figures

List of Tables

Acknowledgements

This dissertation is the result of all the learning, research, and work throughout my graduate career, none of which would be possible without my advisor at Berkeley Lab, Dr. Corinne Scown, my advisor at UC Berkeley, Professor Scott Moura, and the greater research community at Berkeley Lab and UC Berkeley. I thank Dr. Corinne Scown for providing the invaluable mentorship and guidance I needed throughout the entirety of my Ph.D. Since hiring me as a Master's student, Dr. Scown provided ample funding, time, and support to pursue the development of my own knowledge. Thank you for the amazing opportunity to fulfill this lifetime achievement and for serving as an outstanding role model over the years. I thank Dr. Scott Moura for allowing me to pursue this career at UC Berkeley. After agreeing to serve as an advisor for my Ph.D., Professor Moura always made time to provide mentorship on navigating academia and perspective on complex research questions. Thank you for your continued guidance and for contributing to the friendly working environment I found at UC Berkeley.

Beyond my primary advisors, I am truly grateful to have received mentorship from numerous esteemed individuals at UC Berkeley and Berkeley Labs. I thank Professor Maximillian Auffhammer and Professor Arpad Horvath for serving on my exam committee and their general support. Both have been the source of much inspiration and joy over the course of my Ph.D. I also thank Dr. Sarah Smith for serving as a fantastic PI while working at Berkeley Lab. I am extremely fortunate to have worked with wonderful collaborators including Wilson McNeil, Dr. Derek Wolfson, Dr. Jingjing Zhang, and Dr. Fan Tong as well as the numerous other peers who have provided their expert perspectives towards my work. I give a special thanks to Professor Robert Harley and the entire Airheads family for welcoming me into their collaborative and friendly research group. I am especially grateful for the member of my cohort, Dr. Sarah Nordahl and Dr. Pietro Vanucci, who have made this journey full of joy.

I recognize all the individuals at the Energy and Bioscience Institute, Shell, and the Department of Energy who enabled the funding for this work. I give a special thanks to Dr. Huan Yang for being a wonderful funder over the years.

Finally, I extend endless gratitude to the friends and family who have shared my labor, my pain, and my happiness over the years. I give the warmest thanks to my partner, Allison Yip. None of this would have been possible without your endless love, support, and joy. Thank you for everything.

Chapter 1

Introduction

The price of Lithium-ion (Li-ion) batteries has decreased by over 97% since their commercial introduction in 1991, currently allowing for the storage of electricity at unprecedented prices.[1–3] This rapid price drop, along with the relatively high specific energy of Li-ion batteries, has created unique opportunities to electrify sectors that were previously dependent on the combustion of fossil fuels.[4–6] While the reduction of fossil fuel combustion is essential for the decarbonization of sectors,[7–9] it is still unclear whether the integration of Li-ion technologies provides net positive impacts in these sectors. This is largely due to the lack of consensus on how to report the impacts associated with Li-ion batteries as well as high levels of uncertainty on the future prices of Li-ion batteries.[10,11] Additionally, when examining the impacts associated with Li-ion battery application, studies have historically only modeled their private monetary impacts or their external social impacts, never both. However, decision makers need to simultaneously examine private monetary and external social costs in order to determine where Li-ion batteries can feasible provide a net positive impact.

This dissertation aims to aid decision makers in this role by providing recommendations for life-cycle assessments (LCA) on Li-ion technologies with the intent of helping future studies be more interpretable, representative, and impactful. Additionally, this dissertation critically examines the assumptions used to forecast Li-ion prices to provide recommendations on how to develop Li-ion price scenarios when examining future Li-ion costs. LCA sand technoeconomic analyses (TEAs) are then performed to model the climate, human health, and economic impacts of Li-ion technologies serving in peaker replacement and heavy-duty long-haul freight roles. The results from these studies show that the relative net impact of using Li-ion batteries in these roles can be positive or negative depending on several factors.

1.1 Background on Li-ion Battery Technologies

A schematic breakdown of the different tiers of Li-ion battery systems is visualized in Figure 1, highlighting the primary components of each tier that will be frequently referenced throughout this dissertation.

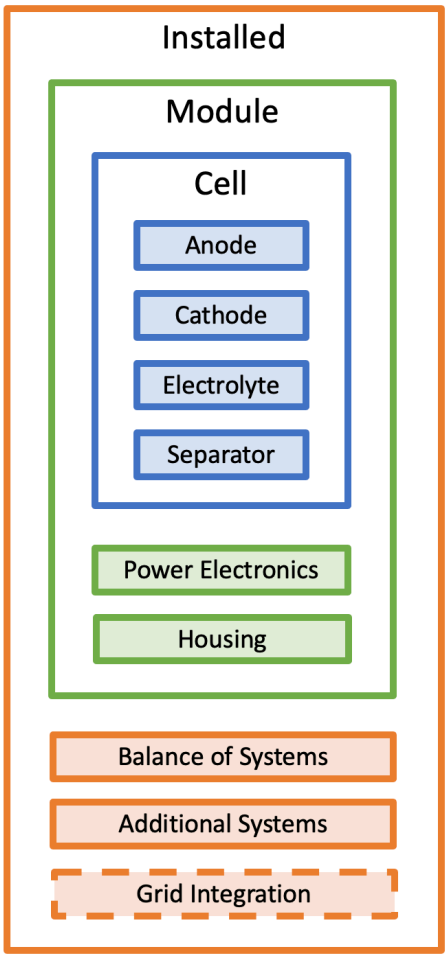

Figure 1.1. Sub-system schematics of stationary Li-ion system tiers.

1.1.1 Cell

The cathode acts as the source of ions that move from cathode to anode and vice versa to create a voltage drop. There are numerous cathode chemistries available on the market, but some of the most widely used include lithium nickel manganese cobalt (NMC), lithium nickel cobalt aluminum (NCA), lithium iron phosphate (LFP) and lithium manganese oxide (LMO). Within each cathode chemistry, the exact material ratio can vary, thus creating different cathodes. Different cathodes have different properties such as energy density, voltage, duration, and more. The electrolyte is the medium that enables the movement of ions. For Li-ion cells, it is most commonly lithium salt in an organic solution, often with additives to improve cell stability and performance overtime. The separator acts as a barrier for electrons between the cathode and the anode, forcing electrons to flow through the "wire" or the grid infrastructure which the cell is a part of as the ions pass through the separator. Separators are commonly synthetic resins like polyethylene (PE) and polypropylene (PP). A single cell "unit" consists of a cathode and an anode physically separated by a separator, all within an electrolyte.

Additionally, Li-ion cells have different designs dictating the configuration of cell sub-systems and potentially influencing cell characteristics. Three major categories of cells exist: *cylindrical*,

prismatic, and *pouch*. Cylindrical cells are the most widely used and have the recognizable cylindrical casing. They consist of alternating sheets of electrodes (anode and cathode), with a separator in between each sheet. These can then be rolled up and packed into cylindrical casings with an electrolyte solution. They have a high durability due to the tight electrode-separator packing and can be quickly and cheaply produced due to their robust pre-existing supply chain. Multiple types of cells (18650, 21700, and more) exist under this categorization.

Prismatic cells consist of many stacked flat units of cells, or flattened cylindrical cells. These are packaged into small rectangular casings. Despite being less durable, prismatic cells have seen a growth in popularity due to their application in consumer electronics, like cell phones, thanks to convenient sizing and greater energy density. Pouch cells further improve upon these benefits by replacing a rigid rectangular casing with a flexible "pouch casing". This allows for an even greater packaging density, but at the cost of a reduced durability. Similar to cylindrical cells, multiple types of cells exist within the prismatic and pouch categories. The preferred type of cell depends on the energy storage application. General schematics for Li-ion cells can be found in Smith et al. 2022.[11]

1.1.2 Module

The module is the next tier of Li-ion system, which consists of many Li-ion *cells*, supporting *power electronics*, and the *housing* containing all these sub-systems. The physical attributes and subsystems of modules can vary greatly, depending on the application, manufacturer, and cell type of the batteries.

Within a module, multiple cells are connected to achieve a greater rated power and energy capacity. The power electronics in a module ensure that the battery cells are operated within appropriate and safe conditions. This can include regulating the charging and discharging current, ensuring capacity is kept within the set depth of discharge, maintaining cell temperature within an appropriate range, and more. However, different applications of energy storage operate within different ranges, and different cell types have different properties. Therefore, an optimally designed module would have power electronics that reflect how the battery is used. Some common power electronics include heat sinks, gas collectors, open circuit voltmeters, and air/liquid cooling components.

Similarly, module housing varies greatly by the application, manufacturer, and cell type of the batteries. The primary purpose of the housing is to contain and protect the module as a single unit. The housing may be removable or opened in order to access and replace individual components. Additionally, battery housing may play a large role in thermal regulation.
Li-ion battery modules are frequently categorized into two primary groups based on their application: electric vehicles (EV) and stationary storage. While there are many potential applications for Li-ion battery modules, these two applications are of particular interest to the study. The characteristics of modules for these two applications may vary greatly.

1.1.3 Installed System

The installed system is the highest tiered Li-ion system and may vary greatly between EVs and stationary storage. In electric vehicles, the installed system has a relatively small energy capacity, ranging between 10 to 100 kWh. The installed system is often referred to as a "pack", which consists of many connected modules and additional power electronics for thermal, safety and performance regulation. The installed systems for stationary storage consist of battery *modules*, the *balance of systems* (BOS), and *additional systems*.

Within an installed system, multiple battery modules are connected to achieve a greater rated power and energy capacity. Individual modules are often easily accessible and can be replaced if degradation occurs, while the rest of the system remains. This can extend the lifespan of the total installed system. The BOS consists of the equipment required to operate and monitor the battery modules and those connecting batteries to the electrical infrastructure. This typically includes bidirectional inverters, transformers, circuit breakers, heating, ventilation, and air conditioning (HVAC), and fire suppression. The quantity/type of modules and the equipment in the BOS can vary greatly by the application of the installed system. Additional systems refers to the equipment required to perform the function of the installed system that is not inherently related to the Li-ion battery system. For example, the body of an EV would be considered an additional system, as it is essential for an EV but not needed for the operation of the Li-ion battery system.

Finally, an installed system may have an impact on the operation of the electrical infrastructure it is a part of, especially if it has a large rated power or energy capacity. Its participation on the electric power grid may cause congestion of distribution and transmission infrastructure and imbalances of reactive/active power. As a result, the party managing the electrical infrastructure will have to perform upgrades, the cost of which may be assigned to the owner of the installed system.

1.2 Research Objectives

Four primary research objectives are present in this dissertation. Each objective is the primary focus of one of the following chapters. The objectives are as follows:

1) Review the present body of literature on the life-cycle assessment of batteries and develop recommendations to improve the quality of future studies

2) Examine the temporal variations in Li-ion technology prices to develop insights for price forecasting

3) Identify the private and external costs and benefits of replacing high-emitting peaker plants with Li-ion batteries

4) Identify the private and external costs and benefits of electrifying heavy-duty long-haul trucking with Li-ion batteries

1.3 Approach and Methodology

The goal of the first and second research objectives is to understand the intricacies of the external life-cycle impacts and private costs associated with Li-ion batteries. Methods in these sections will be focused on the review of current and historic literature to understand shortcomings with the current methodologies used to assess private and external costs.

This knowledge is then applied to the third and fourth objectives to produce results that report the combined private and external impacts associated with a Li-ion battery application. In these chapters, a combined TEA and LCA will be performed to model the behavior and the consequent impact of Li-ion batteries operating in peaker replacement and heavy-duty, long-haul trucking. Both the private monetary considerations and the external societal impacts will be presented as results. Capturing both these impact categories and their combined value is vital in determining if a Li-ion technology will be easily adopted in sectors without incentive, and whether this adoption will be associated with benefits to society. Using this approach, this dissertation aims to provide novel perspectives on the use of Li-ion batteries in these sectors while emphasizing the importance that both economic and societal costs have on the impacts associated with technology adoption.

1.4 New Contributions

The following four chapters of this dissertation address one of the main objectives outlined in section 1.2. Each chapter contains novel contributions to the existing research landscape relevant to each objective. The contributions in each chapter are summarized below.

Life-cycle Assessment Considerations for Batteries and Battery Materials

- *Recommendations and best practices for battery LCAs*. The publication associated with this chapter is the first to recommend best practices for battery LCAs. While no novel methods or results are produced, the review and subsequent recommendations aim to make battery LCAs more interpretable, representative, and impactful. (Section 2.3)

Temporal Variations in Learning Rates of Li-ion Technologies: Insights for Price Forecasting and Policy through Segmented Regression Analysis

- *Segmented regression of Li-ion technology prices*: The study associated with this chapter is the first to apply segmented regression to the price of Li-ion technologies, thus deriving periods of statistically distinct learning rates. (Section 3.3.1)
- *Definition of statistically distinct Li-ion market periods*: The periods of statistically distinct learning are compared to market behavior of Li-ion technologies in order to define distinct market periods. (Section 3.4.1)
- *Li-ion technology price uncertainty forecasting by market scenarios*: The current standard practice for the forecasting the uncertainty of Li-ion technology prices is to vary learning rates by several percentages in each direction and observe the range of projected prices. This chapter performs a novel uncertainty forecast by modeling independent

market scenarios associated with historic Li-ion technology learning rates from the previously defined market periods. (Section 3.4.2)

Private and External Costs and Benefits of Replacing High-Emitting Peaker Plants with Batteries

- *Simultaneous modeling of life-cycle costs, climate, and human health impacts of replacing peaker plants with batteries*: The publication associated with this chapter is the first to concurrently model monetary life-cycle costs, climate impacts, and contributions to human health burden from replacing peaker plants with Li-ion batteries. (Section 4.3.1)
- *Sizing of Li-ion battery energy storage systems to replace peaker plants*: Novel conclusions on the sizing of Li-ion battery energy storage systems are reached by comparing the battery size against the throughput of the system. (Section 4.2.2)
- *Considering battery degradation impacts when modeling costs of large-scale Li-ion battery energy storage systems*: This chapter includes a simple model of battery degradation in order to include the impacts of battery degradation when determining potential costs of large-scale Li-ion BESS. (Section 4.2.2)

Private and External Costs and Benefits of Electrifying Heavy-Duty Long-Haul Trucking with Li-ion Batteries

- *Simultaneous modeling of life-cycle costs, climate, and human health impacts of electrifying heavy-duty long-haul trucking with Li-ion batteries*: The study associated with this chapter is the first to concurrently model monetary life-cycle costs, climate impacts, and contributions to human health burden from *electrifying heavy-duty long-haul trucking with Li-ion batteries*. (Section 5.3.1)
- *Sensitivity of total lifetime costs of heavy-duty trucking*: A preliminary sensitivity analysis is performed to explore how the monetary and social costs of Class 8 trucks operating in long-haul frieght may vary by scenario and impact valuation. (Section 5.3.3)

References

1. Ziegler, M. & Trancik, J. *Re-examining Rates of Lithium-ion Battery Technology Improvement and Cost Declines*. (2020).

2. BloombergNEF. *2022 Lithium-Ion Battery Price Survey*. (2022).

3. Whittingham, M. S. History, evolution, and future status of energy storage. *Proc. IEEE* **100**, 1518–1534 (2012).

4. Ferreira, H. L., Garde, R., Fulli, G., Kling, W. & Lopes, J. P. Characterisation of electrical energy storage technologies. *Energy* **53**, 288–298 (2013).

5. Beuse, M., Steffen, B. & Schmidt, T. S. Projecting the Competition between Energy-Storage Technologies in the Electricity Sector. *Joule* (2020) doi:10.1016/j.joule.2020.07.017.

6. Yuan, M., Thellufsen, J. Z., Lund, H. & Liang, Y. The electrification of transportation in energy transition. *Energy* **236**, 121564 (2021).

7. Papadis, E. & Tsatsaronis, G. Challenges in the decarbonization of the energy sector. *Energy* **205**, 118025 (2020).

8. Åhman, M., Nilsson, L. J. & Johansson, B. Global climate policy and deep decarbonization of energy-intensive industries. *Climate Policy* **17**, 634–649 (2017).

9. Tian, X., An, C. & Chen, Z. The role of clean energy in achieving decarbonization of electricity generation, transportation, and heating sectors by 2050: A meta-analysis review. *Renew. Sustain. Energy Rev* **182**, 113404 (2023).

10. Porzio, J. & Scown, C. D. Life-cycle assessment considerations for batteries and battery materials. *Adv. Energy Mater.* 2100771 (2021) doi:10.1002/aenm.202100771.

11. Smith, S. J., Porzio, J. & Zhang, J. *Unveiling historical Li-ion cost trends and opportunities for domestic manufacturing: Development of a technology learning framework and analysis of implications for the future*. (2022).

12. Cadex Electronics. Types of Battery Cells. *Battery University* https://batteryuniversity.com/learn/article/types_of_battery_cells (2019).

Chapter 2

Life-cycle Assessment Consideration for Batteries and Battery Materials

The text and research in this chapter was published in *Advanced Energy Materials*. The citation for the published article is as follows:

> Porzio, J., & Scown, C. D. (2021). Life-cycle assessment considerations for batteries and battery materials. *Advanced Energy Materials*, 2100771.

2.1 Introduction

Energy storage is essential to the rapid decarbonization of the electric grid and transportation sector.[1,2] Batteries are likely to play an important role in satisfying the need for short-term electricity storage on the grid and enabling electric vehicles (EVs) to store and use energy on-demand.[3] However, critical material use and upstream environmental impacts from manufacturing are often cited as a drawback to widespread use of rechargeable batteries.[4,5] Life-cycle assessment (LCA) is a widely used approach for examining the potential impacts of large-scale battery production, use, and disposal and/or recycling. At its core, LCA is a methodology for quantifying the direct and indirect environmental burdens associated with a product or service.[6] It is also a useful framework to explore environmental tradeoffs between different technologies that provide a comparable service. However, applying LCA to batteries is challenging for a variety of reasons ranging from methodological choices to scarcity of primary data on battery manufacturing.

To date, there has not been consensus in the field of LCA as to how the environmental impact of batteries should be analyzed, nor how the results should be reported. Studies use a wide variety of system boundaries, functional units, primary data sources (which in turn report data at different levels of granularity), and life-cycle inventory, midpoint, and impact categories. This makes cross-comparisons of different technologies challenging and limits the ability for LCA to provide a feedback loop to early scientific research and technology development. It can also limit our ability to detect and correct errors in the literature; it is common for life-cycle inventory results to vary by one or more orders of magnitude across the literature and most reviews are unable to explain the underlying cause of the differences.

Prior review papers on the LCA of lithium-ion batteries (LIBs) can be categorized into three main groups dependent on their goals: identifying and reducing sources or uncertainty/variability;[7-9] synthesizing results and determining key drivers to inform further research;[10,11] and critical review of literature to improve LCA practices.[12] Sullivan and Gaines[9] reviewed life-cycle inventory estimates for lead-acid, nickel–cadmium, nickel-metal hydride, sodium-sulfur, and Li-ion batteries and calculated their own estimates for comparison; the conclusions focused on the need to fill key data gaps. Ellingsen et al.[7] focused on life-cycle greenhouse gas (GHG) emissions and noted that previously published results differed by an order of magnitude, with differences driven by direct energy demand for cell manufacturing and pack assembly. Pellow et al.[8] focused on gaps in the range of use cases evaluated and the need for additional studies on end-of-life management. Nealer and Hendrickson[10] focused on EVs and summarized prior studies' findings on the energy and GHG advantages of EVs. Nordelöf et al.[12] reviewed 79 LCAs for hybrid, plug-in hybrid, and pure EVs and the study focused more broadly on sources of uncertainty related to light-duty vehicles and their use, as opposed to battery technologies specifically. Peters et al.[11] reviewed a wide array of battery LCAs and offered valuable insights into which studies used primary data and which relied on secondary data sources; the review also provides an in-depth discussion of battery cycle life and round-trip efficiency. Peters et al.[11] did note, as other reviews have, that manufacturing energy use estimates vary across the literature by at least an order of magnitude. However, they did not attempt to offer a detailed explanation and ultimately relied on calculating averages of results from prior studies. Using these calculated averages, combined with 1995 European

normalization factors for each life-cycle impact, Peters et al.[11] suggested that global warming potential (GWP) may not be the most important environmental metric, as abiotic depletion, acidification potential, and human toxicity potential all resulted in larger normalized impacts.

In this paper, we will not revisit all prior LCA studies on life-cycle energy and environmental impacts of batteries. Instead, we will focus on three key issues that have not been adequately explored in the literature to-date: 1) selecting relevant environmental performance metrics and acknowledging their limitations and data requirements, 2) understanding discrepancies in reported battery manufacturing impacts, and 3) defining appropriate functional units. With these key issues in mind, we provide a critical review of recent LCA studies applied to rechargeable batteries produced for grid- and vehicle-based applications and suggest some best practices for the field. We draw from previously published work with a focus on LIBs, although most of the insights in this article can apply to a wide variety of battery technologies.

2.1.1 Lithium-Ion Battery Technologies

LIBs are the most commonly used battery chemistry and, although this paper is not focused on the details of the technologies, it is worthwhile to briefly describe the most common types of LIBs explored in the current literature. Research has continued on the development of non-LIB battery technologies, including sodium-ion batteries, potassium-ion batteries, solid-state batteries (Li-metal, Li-sulfur, and rechargeable zinc alkaline), flow batteries, and multivalent batteries,[13,14] but LIBs are likely to continue to dominate the market in the near-term. LIBs are typically differentiated based on their cathode material: lithium manganese oxide (LMO), lithium nickel manganese cobalt oxide (NMC), lithium iron phosphate (LFP), and lithium nickel cobalt aluminum oxide (NCA). Most batteries explored in prior LCA studies use a graphite carbon anode. As shown in Table 2.1, NMC, NCA, LFP, and LMO batteries with graphite anodes are typically estimated to last for 1000–3000 cycles or more.[15–21] These batteries have specific energy at the cell level ranging from 90 to 250 Wh kg^{-1}.[15] Researchers are exploring other anodes, such as lithium titanate (LTO) and we have included LFP-LTO battery data in Table 2.1 as well; the LFP-LTO battery offers longer cycle life (5000+) at the expense of specific energy, which is lower than all other types of LIBs in Table 2.1.[15,16,19,20,22] NCA-graphite batteries achieve the highest specific energy, but stand out for their relatively poor safety rating, with a far lower thermal runaway temperature than its competitors.[15,23] Other LIB chemistries, such as LCO were intentionally omitted due to their decreasing relevance in vehicle- and grid-scale energy storage systems. “Anode free” configurations, such as Zinc MnO_2 batteries, are in the early stages of development and have the potential to improve energy density relative to batteries with graphite anodes.[24] The remainder of this review will focus on the LIB chemistries outlined in Table 2.1.

Table 2.1. Battery characteristics by common lithium-ion battery chemistries. Price per kWh for each battery chemistry is qualitatively described relative to other battery chemistries.[14,23] Safety rating for each battery chemistry is qualitatively described, primarily dependent on battery stability, thermal behavior, and resiliency to abuse.[15] Data sources: Bloch et al., Mitchel and Waters, Ralon et al., Gantenbein et al., Ecker et al., Battaglia, Srinavasan, Zubi et al., Stewart et al., Buchmann, Grolleau et al., Nelson et al., and Nitta et al.[14-23,25-27]

Li-ion Battery Chemistry	Specific Energy [Wh/kg]	Nominal Voltage [V]	Cycle Life [Cycles]	Shelf Life [Years]	Operating Temperature [°C]	Thermal Runaway [°C]	Price per kWh Rating	Safety Rating	Primary Use Cases	Representative Manufacturers	Common Cathode Compositions
NMC - Graphite	130 - 150	3.7	2000+	8 - 10	0 - 55	210	Med-High	Good	Power Tools, EV	CATL, Sanyo, Panasonic, Samsung, LG Chem, SK Innovation	NMC-111 [a], NMC-532 [b], NMC-622 [c], NMC-811 [d]
NCA [e] - Graphite	200 - 260	3.6	2000+	8 - 10	0 - 55	150	Med	Poor	EV	Tesla/Panasonic	-
LFP [f] - Graphite	90 - 130	3.2	3000+	8 - 12	0 - 55	270	Low	Excellent	EV, Grid-Scale Stationary	BYD, K2, Lishen, Saft, GS Yuasa, A123, Valence, BAK	-
LFP - LTO [g]	50 - 80	2.7	5000+	10+	-40 - 55	270+	Very High	Excellent	Personal Electronics, some EVs	Altairnano, Toshiba, Yabo	-
LMO [h] - Graphite	140 - 180	3.7	1000 - 2000	6 - 10	0 - 55	250	Low	Good	Power tools, EV's (Typ. with NMC blend)	Hitachi, Samsung, LG Chem, Toshiba, NEC	Spinal Layered

[a] $Li_{1.05}(Ni_{0.33}Mn_{0.33}Co_{0.33})_{0.95}O_2$; [b] $Li_{1.05}(Ni_{0.5}Mn_{0.3}Co_{0.2})_{0.95}O_2$; [c] $Li_{1.05}(Ni_{0.6}Mn_{0.2}Co_{0.2})_{0.95}O_2$
[d] $Li_{1.05}(Ni_{0.8}Mn_{0.1}Co_{0.1})_{0.95}O_2$; [e] $LiNi_{0.8}Co_{0.15}Al_{0.05}O_2$; [f] $LiFePO_4$; [g] $Li_4Ti_5O_{12}$; [h] $LiMn_2O_3$.

2.1.2 Life-Cycle Assessment Overview

To compare the environmental impacts of competing battery technologies, or simply understand the full impact of increased battery production and use, the LCA must be designed to answer a well-defined question. LCAs are commonly defined by four key phases, all of which are essential to completing a meaningful study: a) the goal and scope definition phase, b) the inventory analysis phase, c) the impact assessment phase, and d) the interpretation phase.[6] It is during the goal and scope definition phase that researchers must decide what question they seek to answer and let that question guide the definition of system boundaries, environmental metrics, and one or more functional units. In the context of batteries, LCA results can be used to inform battery research and development (R&D) efforts aimed at reducing adverse environmental impacts,[28–30] compare competing battery technology options for a particular use case,[31–39] or estimate the environmental implications of large-scale adoption in grid or vehicle applications.[40]

LCA is most straightforward to apply to a well-defined functional unit; in other words, any environmental impact is simple to normalize per unit of a product or service that is being provided (e.g., g CO_2 emitted per kWh of electricity generated or liters of water withdrawn per bushel of corn produced). However, batteries pose a particular challenge for LCA as it has historically been applied. Batteries are simply storing energy for later use, and how batteries are cycled will impact their longevity and the value of the service they provide in ways that are not straightforward to predict. If a study is comparing multiple battery technologies applied to the same use case, it makes most sense to normalize results in the basis of the service provided. The downside of this approach is that it is very difficult to compare multiple studies, as they inevitably use different assumptions about how the battery is used over the course of its lifetime. In contrast, an assessment of one or more early-stage battery technologies intended to inform further research may not have reliable use-phase performance data. In this case, it may be appropriate to draw a system boundary ending at the factory gate, and simply note any potential difference in cycle life that may ultimately impact the batteries' longevity.

Studies that define system boundaries excluding the use phase and end-of-life are commonly referred to as cradle-to-gate (where "gate" refers to a factory gate). Studies including the use phase and end-of-life are referred to as cradle-to-grave; this can include reuse, recycling, and ultimately disposal.[6] The term cradle-to-cradle has been used to refer to systems that include recycling, but is generally meant to suggest a zero-waste process[41] and thus is not commonly used to refer to battery life cycles, even if they include recycling.

2.2 The Life Cycle of Stationary and Vehicle Li-ion Batteries

Figure 2.1 shows the typical life cycle for LIBs in EV and grid-scale storage applications, beginning with raw material extraction, followed by materials processing, component manufacturing, cell manufacturing, and module assembly.[14] Finished modules may be assembled into packs and placed in vehicles, assembled into racks on-site for shipment to stationary storage facilities, or shipped directly as modules for off-site rack assembly at energy storage sites.[42–45] All LCAs must begin with raw material extraction, regardless of scope. Researchers then decide whether to tie their analysis to a particular use case and, if so, whether to extend the

system boundaries through the use phase and end-of-life (EOL). Even in cradle-to-gate studies, researchers must be careful to indicate the form batteries take at the factory gate; module, pack, or fully assembled rack (in the case of stationary storage).

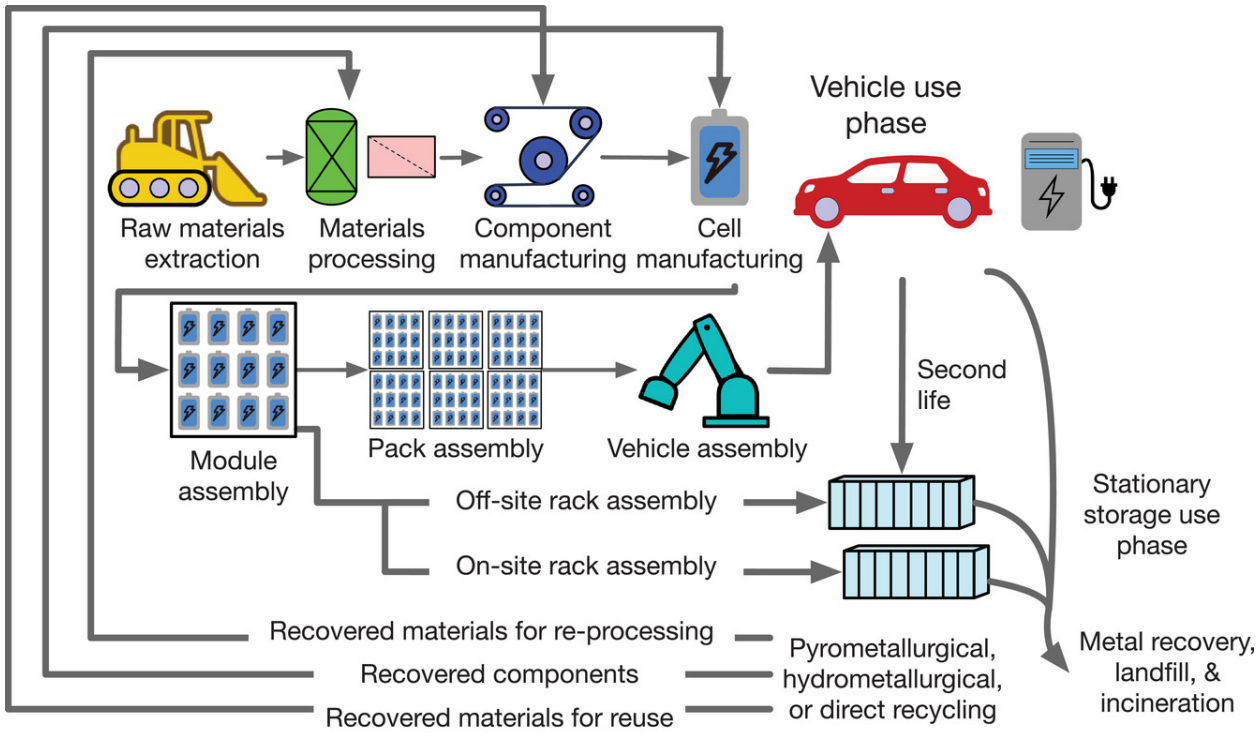

Figure 2.1: Major life-cycle stages for vehicle and stationary batteries.

The majority of battery LCAs are tied to a particular use case, such as EVs, hybrid solar and battery systems, or standalone grid-connected storage.[46–52] This is the preferred approach, where feasible, because performance differences (e.g., round-trip efficiency and cycle life) are important to the definition of a common functional unit across which different alternatives can be compared. However, not all studies include battery use phase for a specific application, nor is this always feasible for more advanced, pre-commercialization battery technologies. Wang et al. (2019)[53] conducted a use-agnostic analysis to compare the environmental impacts of different cathode materials and Wang et al. (2018)[54] conducted a cradle-to-gate analysis of lead acid, LMO, and LFP batteries. For a use-agnostic cradle-to-gate analysis of an LIB, researchers must still select a pack or rack configuration that is tied to a stationary or EV application. In a truly use-agnostic LCA, the system boundary may need to be set at the module assembly stage, since the assembly of the pack or rack (including such components as thermal management and electrical control) will differ substantially depending on how the battery will be used (see Figure 2.1). Cradle-to-grave LCAs consider how batteries will be used and treated at their end of life including collection, recycling and/or disposal. There are multiple options for recycling, ranging from specialized, chemistry-specific direct recycling to hydrometallurgical recycling and pyrometallurgical recycling, which are more flexible and aim to recover only valuable metals from the batteries.[55,56]

2.2.1 Raw Material Extraction and Delivery

LIBs' reliance on finite resources, combined with dramatic growth in production (approximately doubling every 5 years)[21] and uncertain future recycling practices has generated concern over material constraints. Olivetti et al.[57] explored the potential bottlenecks in critical material supplies for LIB manufacturing. The breakdown of material comprising batteries, from active material through individual cells, modules, and packs, is well documented in the literature; breakdowns of elements present in each type of cathode active material are shown in Table 2.2 and mass breakdowns per kWh for modules are shown in Table 2.3. Although the use of critical materials is often discussed as a single challenge, there are three separate issues worth discussing. First, there is the question of resource availability relative to consumption and whether scaling up battery manufacturing will deplete critical material reserves and/or drive up prices. Second, there is the geopolitical risk associated with highly concentrated production, which can lead to conflict, price instability, and artificial shortages. Here, we characterize this concern as supply chain risk, and argue that researchers too often conflate supply chain risk with resource depletion. Traditional LCA methods are not well equipped to capture supply chain risk. Third, there are environmental and social impacts associated with mining operations, which is well within the purview of LCA.

Table 2.2. Element mass ratio per cathode active material. Data sources: Nelson et al. and Nitta et al.[26,27]

Element	NMC-111 [% Mass]	NMC-532 [% Mass]	NMC-622 [% Mass]	NMC-811 [% Mass]	NCA [% Mass]	LFP [% Mass]	LMO [% Mass]
Li	0.078	0.078	0.077	0.077	0.072	0.044	0.038
Ni	0.197	0.297	0.354	0.471	0.489	-	-
Mn	0.184	0.167	0.111	0.055	-	-	0.608
Co	0.198	0.119	0.119	0.059	0.092	-	-
Al	-	-	-	-	0.014	-	-
Fe	-	-	-	-	-	0.354	-
P	-	-	-	-	-	0.196	-
O	0.343	0.338	0.339	0.338	0.333	0.406	0.354

Table 2.3. Module material inventory per kWh. Data source: Nelson et al.[26]

Material	Cell Component	NMC-111	NMC-532	NMC-622	NMC-811	NCA	LFP	LMO
Cathode Active Material [g/kWh]	Cathode	1757.45	1288.79	1481.48	1257.53	1358.70	2031.28	2341.74
Graphite [g/kWh]	Anode	858.02	863.13	840.45	841.18	857.71	956.61	793.59
Carbon Black [g/kWh]	Cathode Additive	36.61	26.85	30.86	26.20	28.31	42.32	48.79
PVFD [g/kWh]	Cathode Binder	36.61	26.85	30.86	26.20	28.31	42.32	48.79
	Anode Binder	17.51	17.61	17.15	17.17	17.50	19.52	16.20
Aluminum [g/kWh]	Cathode Current Collector	104.32	77.24	88.18	75.08	79.12	156.85	149.66
	Positive Terminal Assembly	29.57	27.28	27.06	25.75	27.05	35.88	32.08
	Cell Container	57.55	50.93	51.93	48.85	51.48	73.53	66.51
	Module Heat Conductors	103.34	90.39	93.27	87.34	91.67	133.48	121.61
	Module Enclosure	69.03	64.43	64.03	61.14	63.57	82.09	74.86
Copper [g/kWh]	Anode Current Collector	244.18	182.03	206.82	176.73	186.31	364.82	347.55
	Negative Terminal Assembly	98.13	90.52	89.81	85.46	89.75	119.06	106.47
	Cell Interconnection	29.45	27.17	27.01	25.65	26.85	35.77	31.98
LiPF6 [g/kWh]	Electrolyte Salt	2.79	2.37	2.52	2.31	2.40	3.75	3.42
Ethylene Carbonate [g/kWh]	Electrolyte Fluid	221.14	188.14	199.40	183.43	190.14	297.29	270.79
Dimethyl Carbonate [g/kWh]	Electrolyte Fluid	179.26	152.51	161.63	148.69	154.13	240.98	219.50
Polypropylene [g/kWh]	Separator	16.80	12.40	14.18	12.07	12.73	25.33	24.19
	Cell Container	8.83	7.81	7.96	7.49	7.89	11.28	10.20
Polyethylene [g/kWh]	Separator	16.80	12.40	14.18	12.07	12.73	25.33	24.19
Polyethylene Terephthalate [g/kWh]	Cell Container	3.83	3.39	3.46	3.25	3.43	4.90	4.43
Misc Electronics [g/kWh]	BMS	11.08	11.32	10.28	10.26	11.05	11.81	10.34
Total [kg/kWh]		3.90	3.22	3.46	3.13	3.30	4.71	4.75

2.2.1.1 Resource Depletion and Supply Chain Risk

Olivetti et al.[57] synthesized the available data on consumption rates relative to available reserves for nickel (Ni), manganese (Mn), cobalt (Co), lithium, (Li), and natural graphite. They found that the ratio of known reserves to primary mine production (also known as the static depletion index) has increased for Co, Li, and natural graphite, suggesting that continued demand has

resulted in additional exploration and extraction. Mn and Ni did not show an upward or downward trend, indicating that the ratio of production to known reserves has remained relatively constant. This highlights the challenge of attempting to place a single number on finite resource depletion as part of an LCA; society's understanding of available resources is not static. Increased demand drives advancements in exploration and recovery technologies. Material recovery potential through recycling adds another layer of complexity. As Olivetti et al.[57] rightly point out, there is a time lag between when batteries are manufactured and when they reach the end of their life, so regardless of what can be recovered, recycling is unlikely to address any near-term (10–20 year) material supply constraints. If battery technologies do not evolve away from reliance on these critical materials in coming decades, recycling can be an important long-term strategy. Pyrometallurgical recycling facilities will recover Ni, Co, Mn, and Copper (Cu),[58] while hydrometallurgical recycling facilities will recover all of the aforementioned metals, as well as Li and aluminum (Al). Direct recycling will recover an even larger range of materials, many of which can be reused without further processing. Given this context, it is worth revisiting the assertion by Peters et al.[11] that abiotic depletion (an impact category representing depletion of non-renewable resources, such as minerals and fossil fuels) is the most important impact of batteries on a normalized basis, exceeding the importance of GWP. Many of the nuances in critical material use and supply outlooks are lost in typical LCA practices and reducing these impacts to a single score is more likely to create confusion than generate useful insights, particularly when fossil fuel and critical material depletion are combined in a single score. This is particularly true for materials like Co and Li, for which demand is growing rapidly. In fact, a greater cause for concern is the geographic diversification, or lack thereof, in reserves and supply for some of these materials.

Olivetti et al.[57] note a consensus that Co, Li, and to a lesser extent, natural graphite pose the greatest supply risks. These risks are driven by the concentration of known reserves and current production in a small number of countries. Table 2.4 shows the countries with largest reserves and current production for raw materials used in LIB production. Co, which is required for batteries with NMC and NCA cathodes, is generally regarded as posing the greatest risk because of its geographically-concentrated supply. Batteries are responsible for around 60% of global Co demand, and total demand is expected to double by 2025.[59,60] Over 60% of current supply, and half of estimated reserves are located in the Democratic Republic of the Congo (DRC), where there have been serious environmental and social consequences ranging from child labor to human exposure to heavy metals, particularly from unregulated artisanal and small-scale mining operations.[60–64] Co is largely a co-product of Ni and Cu mining, with 55% of supply coming from Ni mining, while <10% comes from dedicated Co extraction.[57,65] Co processing capacity is even more concentrated; 95% of all Co refining occurs in China.[65]

Table 2.4. 2019 global reserves for materials relevant to Li-ion battery production, 2019 mining production, and distribution of resources. Data source: USGS[61]

Element	Li-ion Battery Component	Global Reserves [tons]	Country with Largest Reserves	Share of Largest Reserves [%]	Global Mining Production [tons]	Country with Largest Mine Production	Share of Largest Mine Production [%]
Aluminum (Al)	Cathode Current Collector, NCA Cathode	30000000[a)]	Australia[a)]	17[a)]	63200[b)]	China[b)]	55[b)]
Iron (Fe)	LFP Cathode	84000[c)]	Australia[c)]	29[c)]	1520000[c)]	Australia[c)]	37[c)]
Phosphorus (P)	LFP Cathode	71000000	MAR and EH[d)]	70	227000	China	42
Manganese (Mn)	LMO, NMC Cathode	1300000	South Africa	40	19600	South Africa	30
Carbon (C)[e]	Graphite Anode	320000000	Turkey	28	1100000	China	64
Nickel (Ni)	NMC, NCA Cathode	94000000	Indonesia	22	2610000	Indonesia	33
Copper (Cu)	Anode Current Collector	870000	Chile	23	20400	Chile	28
Cobalt (Co)	NMC, NCA Cathode	7100000	DRC	51	144000	DRC	69
Lithium (Li)	All cathodes, electrolyte	21000000	Chile	43	86000	Australia	52

[a)]Representative of bauxite reserves; [b)]Representative of smelter production; [c)]Representative of iron content in ore; [d)]Morocco and Western Sahara; [e)]Natural Graphite

Li production is concentrated in Australia, Chile, and Argentina. Combined, Australia, China, Argentina, and Chile make up 90% of global Li supply[59–61] and demand is continuing to increase.[66] Australia produces lithium concentrate from a lithium aluminum inosilicate called spodumene, while Chile and Argentina produce Li_2CO_3 from brine. As Olivetti et al.[57] note, Li supply for battery manufacturing is a controversial topic, discussed at length in the literature, but there are many potential avenues for increasing Li supply. Potential lithium resources exist in the US, DRC, Bolivia, and regions throughout Europe, but these sites are not yet developed for commercial production of Li.[59,61] Two forms of lithium deposits are viable for extraction: hard rock deposits and brine lake deposits.[59,67,68] A majority of reserves are located in brine lakes of South America, while much of the remaining deposits are located in hard rock, predominantly located in Australia.[67,69,70] As of 2016, Li-ion batteries accounted for 34% of global lithium demand.[60] The most likely bottleneck for Li supply will be the ability to ramp up Li production quickly enough to avoid short-term supply constraints and price spikes.[57]

As noted earlier, LCA is ill-equipped to capture the dynamics of demand, reserves, and annual trends in production and distill these factors into a single impact value. LCA is even less well-suited to capturing the supply chain risks associated with geographically-concentrated extraction and processing, as these are all dependent on the location of demand and the perceived political stability and/or friendliness of the region from the perspective of the study's researchers. A study centered in the US may view the China-dominated co processing industry as a source of supply risk, while a study in China would likely not share that perspective. Although it is entirely appropriate to raise these issues as part of an LCA, and perform quantitative analysis to elucidate potential short- and long-term resource depletion, we advise against assigning a single impact value that may be reliant on outdated data or irrelevant assumptions. One approach in LCA that may offer some more useful insights is the notion of average versus marginal and incremental production impacts. For example, if the environmental burden of Li extraction will increase as a result of a shift toward hard rock deposits and brine lake deposits in the future, sensitivity

analyses could contrast the impacts of current average Li production with those of future sources that will supply the next ton (or million tons) of material. Such an approach draws on the strengths of LCA, as a method for quantifying the environmental impact of a product or service, to capture one dimension of the broader concerns around resource depletion.

2.2.1.2 Environmental Impacts of Raw Material Extraction and Processing

For perspective, battery materials are estimated to comprise approximately one third of total primary energy demand to produce an LMO-graphite battery pack, with the remaining energy demand almost entirely owed to battery manufacturing.[46,52] As discussed later in this article, however, this ratio can vary considerably based on the specifics of the manufacturing process and facility scale. Al, Cu, and graphite comprise the largest shares of LIB packs (using graphite anodes) by mass[71] and, in an LMO battery, Al is estimated to be the largest contributor to the materials energy footprint by a fairly wide margin, followed by the cathode, battery management system (BMS), Cu, and graphite.[72] A challenge for conducting the life-cycle inventory for material inputs to LIB manufacturing is that there are not one or two components that dominate the energy use or emissions; the impacts are spread across a wide array of components; Al, for example, is used in the cathode current collector, positive terminal assembly, cell container, module heat conductors, module enclosure.[73–75] Battery designs continue to evolve and detailed material breakdowns are, in many cases, proprietary.

Energy used for raw material mining and processing is typically some combination of diesel fuel to operate mining equipment and transport material, electricity to run mechanical processes, and natural gas for thermal energy during processing. As a general rule, the processing/refining stage is usually what distinguishes materials as being more or less energy intensive. For example, the energy footprint and resulting impacts of Al production are dominated by smelting and refining, which requires large amounts of electricity.[76] The majority of global Al production and refining occurs in China,[61,76] which further increases the impact because China's national average grid mix continues to be coal-dominated.[77] The energy footprint of Cu is dominated by solvent extraction and electrowinning (also known as electroextraction).[78] In the case of Co, researchers must exercise caution in sourcing data from prior studies, as Co is a co-product of Ni or Cu production, meaning some form of allocation is required and the ratios of production will differ by location. In other words, extraction and processing impacts must be attributed appropriately to multiple outputs, which can be done using system expansion (to avoid formal allocation) or mass- or market-value based allocation.

Li, although discussed extensively from a resource depletion standpoint, has so far not proved to be a dominant contributor to the energy and environmental footprint of LIBs. Two thirds of Li is extracted from brine,[68] and the energy footprint of Li_2CO_3 can vary by a factor of two depending on the concentration in the brine.[72] As indicated by Yuan et al.[52] and Dunn et al.[72] for LMO batteries, the LMO cathode itself is the second-largest contributor to energy use (a distant second to Al). However, the single largest driver of this energy footprint is the $LiMn_2O_4$ production, which includes a roasting process.[72] Rock-based Li production has been shown to be far more energy-intensive brine extraction; Jiang et al.[79] estimated that it is an alarming 48 times more GHG-intensive than brine extraction. For most environmental impacts, leaching and roasting seem to be larger contributors.[79] These results strongly suggest that LCA studies must thoroughly

explore the average, marginal, and incremental Li sources and conduct sensitivity analyses to account for different mining and processing alternatives.

Like Li, graphite is an input required across nearly all LIBs as it is the most common anode material. The graphite market is supplied by about half mined natural graphite and half synthetic.[80] China mines roughly 65% of commercial natural graphite globally, followed by Mozambique and Brazil both producing under 10% of natural graphite supply.[61,81] While natural graphite is cheaper and thus the typically preferred option for battery anodes, synthetic graphite is produced through byproducts of fossil fuel industries and is produced in high quantities in the US.[57,82,83] The impacts of graphite are driven by the high thermal energy inputs during processing.[82]

Although energy use can sometimes be the most expeditious proxy for environmental impacts, particularly with some knowledge of what fuels are combusted and in what types of equipment (internal combustion engines, boilers, etc.), it is far from a perfect metric. Nearly all of the articles cited so far have reported energy use without noting what fraction is in the form of primary fuels for thermal energy (e.g., natural gas or coal), how much is satisfied by electricity, and how much is used for operating liquid fuel-powered vehicle and equipment (e.g., diesel). Even if energy use can serve as a proxy for GHG emissions, there are other environmental impacts associated with raw material extraction. As noted by Peters et al.,[11]acidification potential, eutrophication potential, human toxicity, and ozone depletion potential have all been incorporated into prior battery LCAs. The question, however, is what impacts are not directly tied to combustion and how much confidence do we have in the published estimates? Acidification potential, most likely, is tied to SO_2 emissions from combustion sources.

Peters et al.[11] suggests that Ni and Co extraction have significant toxicity impacts. Farjana et al.[84] evaluated Co mining and presented a comparison between Co, Ni, and Cu. Their results indicated that acidification (driven by blasting-related emissions) and, to a lesser extent, particulate matter and non-cancer human toxicity were the most prominent impacts on a normalized basis and Ni mining is responsible for three to four times greater impacts than either Co or Cu on a per-kg output basis. However, that study relies on Australian data and is likely not representative of average global production. There is ample evidence to suggest that artisanal Co mining occurring in the Katanga Copperbelt of the Democratic Republic of Congo (DRC), estimated at 15–20% of total DRC production or 9–12% of global supply, has dramatically increased human exposure to heavy metals in the workers and surrounding population.[63, 64] This case serves as a reminder that local practices and regulations or lack thereof can be as influential to environmental impacts as the specific type of mining activity itself. Although artisanal Co mining makes up a minority of total global supply, its proximity to populated areas combined with unsafe practices are likely to drive an outsized share of the sector's overall health impacts. For this reason, conducting an LCA that relies only on estimated emissions and energy use in formal mining operations[84] may underestimate the average environmental impacts. This concept is analogous to the notion of "superemitters" in natural gas operations,[85] which make up a small fraction of overall sector activity but, if ignored, lead to large underestimates in emissions and impacts. Accurately capturing these impacts, however, can be a challenge if the operations are informal, as most LCAs available on raw material extraction and processing rely on datasets provided by large mining companies.[86]

Amarakoon[87] provided a helpful discussion of the underlying drivers of other less commonly-reported impact categories. For example, they noted that their LFP-graphite battery was modeled based on Canadian production, and at the time of the report, the Canadian grid had substantially higher trichlorofluoromethane (CFC-11) emissions than the U.S. grid. This grid-related CFC-11 emission factor dominated the overall results. However, more recent research has suggested that CFC-11 emissions are steeply declining,[88] which suggests that drawing from older studies that include ozone depletion potential may result in overestimates of this impact.

Estimates of eutrophication potential associated with raw material extraction and processing for LIBs can be particularly difficult to parse. Depending on the impact assessment method used, eutrophication may be separated into freshwater and marine eutrophication or combined into a single metric. These impacts are driven by emissions of ammonia, phosphate, other water-soluble nitrogen and phosphorus-containing compounds to water bodies, as well as biological and chemical oxygen demand. Eutrophication is an impact most commonly associated with agricultural systems or other facilities that result in nutrient runoff or discharge. Amarakoon[87] found that any battery relying on steel for the pack/housing (in their case, LMO) generated net negative eutrophication results because the US Life-Cycle Inventory (LCI) database entry for cold-rolled steel suggested that nutrient concentrations in incoming process water had higher concentrations of phosphate, ammonia, and other nutrients than the effluent, suggesting that the steelmaking process was removing these nutrients from the water. In contrast, Amarakoon[87] found that LFP-graphite batteries resulted in net positive eutrophication potential, presumably owed in part to the diammonium phosphate and phosphoric acid production required to produce the cathode material.[87] Ellingsen et al.[74] indicated that Cu mining, and specifically management/discharge of sulfidic mine tailings, is responsible for 62% of freshwater eutrophication potential and 65% of freshwater ecotoxicity potential. However, it is difficult to find any primary literature data to support the claim that copper mine tailings, which are acidic, are a significant cause of eutrophication. Ellingsen et al.[74] also suggested that the *N*-methyl-2-pyrrolidone (NMP) solvent is a major contributor to marine eutrophication potential, driven by the upstream manufacturing of dimethylamine. Our survey of the literature on eutrophication impacts of raw material extraction and processing suggests that, for the most part, compounds containing nitrogen or phosphorus tend to appear as contributors. In some cases, data on how nutrient-containing wastewater is managed at processing facilities is sparse, making the results difficult to confirm. For perspective, the 8.0 kg P-equivalent for a battery pack provided by Ellingsen et al.[74] would translate to the freshwater eutrophication associated with consuming around 300 kg of beef, based on our simple calculations and data from de Vries et al.[89] It is clear that eutrophication potential, while not entirely irrelevant, must be approached with caution and skepticism about the underlying data inputs.

2.2.2 Battery Manufacturing

Battery manufacturing comprises around two thirds of the cradle-to-gate energy demand for LIBs,[52] although this ratio can vary considerably depending on manufacturing facility scale and utilization.[46] Unlike raw material extraction and processing, most environmental impacts during the battery manufacturing process are directly linked to energy use (on-site combustion and off-site electricity generation),[74] so this section will focus on energy use as the key driver of impacts.

Despite the importance of understanding energy use at manufacturing facilities, prior studies are inconsistent in how individual processes within the manufacturing facility are reported, making harmonization or even basic comparisons difficult. Here, we attempt to demystify the manufacturing process and key drivers of energy use and environmental impacts. This will allow future researchers to focus data gathering and sensitivity analysis efforts on the largest contributors to the environmental impacts of battery manufacturing, and avoid becoming mired in the details of processes that consume minimal energy and do not have other appreciable environmental impacts.

Li-ion cell production is generally divided into three phases: electrode manufacturing, cell assembly, and cell finishing (see Figure 2.2). Electrode manufacturing is largely independent of cell type but may vary by battery chemistry. Cell assembly and cell finishing are typically independent of battery chemistry, but vary by cell configuration. Cylindrical and prismatic cells follow the same manufacturing procedure with some minor differences, while pouch cells deviate from this procedure by requiring the stacking of electrodes and separators instead of winding.[90] While some manufacturing steps do vary by the cell configuration, the main processes contributing to energy consumption and environmental impacts, NMP solvent evaporation and dry room conditioning, are common across all cell configurations. This is not to say that cell configuration is negligible with regards to the environmental impact of the Li-ion battery and its manufacturing. Ciez et al.[91] compare pouch and cylindrical cells for NMC, NCA, and LFP batteries and the results suggest that pouch cells are consistently ≈10% less GHG-intensive than cylindrical cells, enabled by the lower ratio of cell hardware to energy stored per cell. LCAs should clearly identify which cell type(s) are being analyzed and potentially explore multiple cell types to capture this variation in material requirements and environmental impacts.

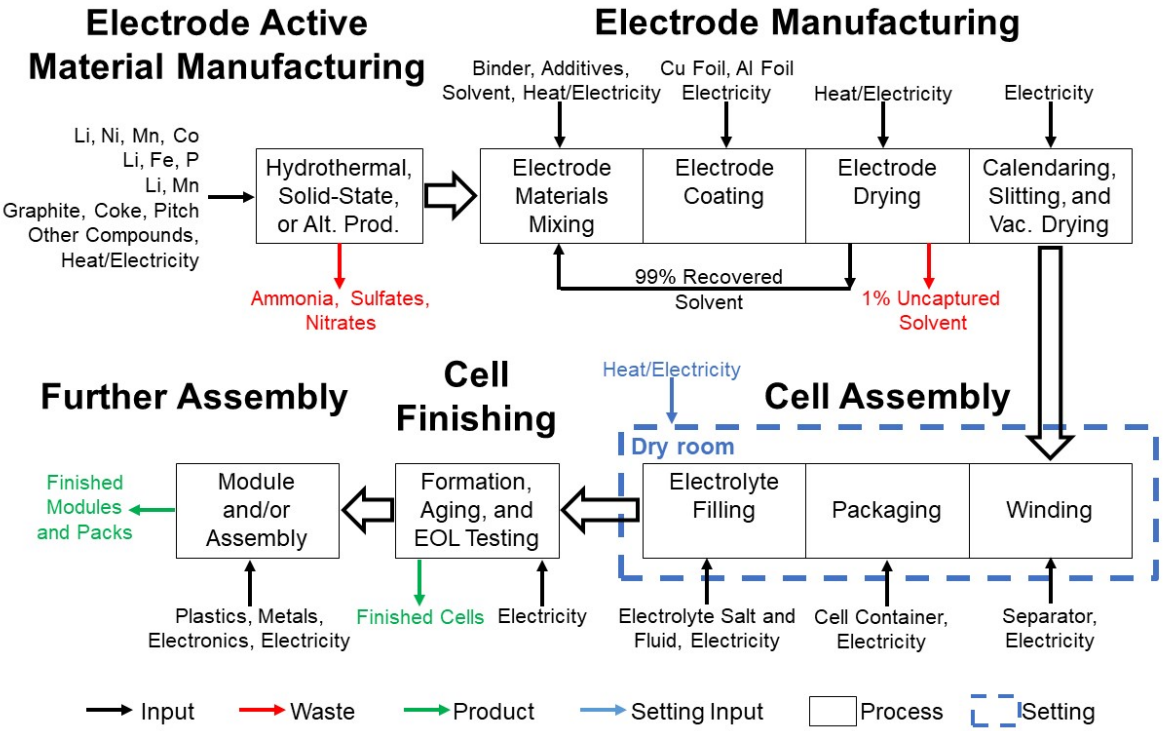

Figure 2.2. Li-ion battery production process flow diagram.[26, 82, 90, 92, 93]

Although battery manufacturing involves many different processes, the majority of energy used in most battery manufacturing plants operating today is dominated by two key activities, namely evaporating the NMP solvent and maintaining the facility's dry room.[52,92] Each of these processes represents around 40% of the total energy use associated with cell manufacturing, together consuming around 80% of the total energy consumed.[52] Evaporating NMP (for eventual condensation and recovery) is energy intensive because of the air flow needed to maintain a safe concentration of the flammable solvent; the result is that facilities use 45 times the minimum thermal energy expended to vaporize NMP for this drying process.[93] This explains why some studies have suggested water-based cathode deposition can save energy and costs,[94,95] although so far the industry continues to rely on NMP. The dominance of NMP evaporation and dry room conditioning also explains why most studies do not provide clear distinctions between electricity needs and primary fuel needs; dehumidification can be achieved through the use of varying amounts of electrical and thermal energy. Dunn et al.[46] have suggested that electrode manufacturing is also an important contributor, and may comprise a larger fraction of energy use than dry room conditioning for large facilities. Beginning with these basic facts, we will discuss the underlying reasons why prior battery LCAs have produced manufacturing energy demand estimates that vary by multiple orders of magnitude, and what can be done to address these discrepancies in future studies.

2.2.2.1 Cathode Material Manufacturing

Dunn et al.[46] suggested that cathode material production can be the largest or second largest contributor to energy use at battery manufacturing facilities under some conditions. Their results suggest that NMC cathode materials are more energy-intensive to make than LFP and LMO by a factor of two to three. For NMC cathode materials, production typically consists of 2 major phases: coprecipitation and calcination.[92] Coprecipitation describes the process of reacting dissolved metal nitrates, metal sulfates, or metal acetates with hydroxide (typically sodium hydroxide) in a solvent to form a mixed metal hydroxide, represented in this paper as $Ni_xMn_yCo_z(OH)_2$ (where the values of x, y, and z vary). This is performed in a continuously stirred tank reactor under a carefully controlled temperature, pH, and speed setting.[46] The $Ni_xMn_yCo_z(OH)_2$ is then isolated and dried via the recovery of the solvent. As a result of coprecipitation, wastewater may be produced containing ammonia and sodium sulfate, which needs to be treated for proper disposal or reuse and could contribute to eutrophication potential. The majority of energy demand associated with coprecipitation is attributable to wastewater treatment (presumably for aeration), with the rest is attributable to the direct production and environmental control of the $Ni_xMn_yCo_z(OH)_2$ in the reactor as well as drying.[46,92] Dai et al.[92] reports that the coprecipitation step consumes 11.8 kWh of heat to produce 1 kg of $Ni_xMn_yCo_z(OH)_2$, but the quantity of energy consumed will vary by specific conditions.

Calcination describes the final production of the NMC active material through a high temperature sintering of the $Ni_xMn_yCo_z(OH)_2$ and a Li compound, typically a hydroxide or carbonate.[46] In theory, this is a two-staged process with the first stage requiring temperatures of 400–500 °C for 4–5 h[82] and the second stage requiring temperatures of 700–900 °C for 8–10 h.[46] In practice, different manufacturers may set different temperatures and durations depending on the capabilities of their equipment (typically a heath roller kiln) and the requirements of their

manufacturing process. Additionally, more stages of calcination may be required, as the priority of the manufacturers is maximizing yields as opposed to reducing energy consumption.[92] The heat required to achieve the high temperatures for long durations represents a majority of the energy demand associated with both coprecipitation and calcination.[46, 92] The heat itself may be sourced through thermal fuel inputs or electricity. Dai et al.[92] reports that the calcination step consumes 7.0 MJ of electricity to produce 1 kg of NMC active material, but the fuel type and quantity of energy consumed will vary by specific conditions.

LFP cathode materials can be produced via a hydrothermal production or a solid state production. The hydrothermal production of the LFP cathode material requires the input of lithium hydroxide, phosphoric acid, and iron sulfate.[96] Iron sulfate is produced as a waste product of the steel industry and can be assumed to have minimal embedded energy or environmental burden if it is indeed sourced from the steel industry. Otherwise, its impacts must still be considered. These materials are coprecipitated to produce LFP with aqueous lithium sulfate as a byproduct to be removed.[46] Dunn et al.[82] reports that the hydrothermal preparation of the LFP cathode active material requires 10.0 kWh per kg of LFP. The solid state production of the LFP cathode material consists of the heating, cooling, and reheating of a Li, Fe, and P compounds, potentially lithium carbonate, iron oxide, and diammonium phosphate.[96] The first heating stage reaches a temperature between 500 and 700 degrees Celsius and is then cooled to room temperature. The second heating stage reaches a temperature between 700 and 900 °C.[82] Dunn et al.[82] reports that the solid state preparation of the LFP cathode active material requires 0.82 kWh per kg of LFP. LFP cathode active material production is not as well documented in the literature from an energy use standpoint, but the production is generally simpler than NMC cathode active material production. The energy demand for heating may be supplied by thermal fuel inputs or electricity depending on individual site conditions.

LMO cathode materials can be produced via multiple methods including solid state, sol-gel, hydrothermal, and combustion procedures. When referring to LMO cathode production, most literature discusses solid state production. This starts with the multi-stage washing of MnO_2 with an H_2SO_4 solution of which up to 98% may be recovered and reused.[97] The cleaned MnO_2 is then mixed with lithium carbonate powder and water to be milled, producing a slurry which is then dried at around 150 °C. This dried, homogeneous mixture is then calcined at around 750 °C for 20 h, producing the LMO cathode material.[97] Once again, the energy demand for heating may be supplied by thermal fuel inputs or electricity depending on the manufacturer. Susarla et al.[97] describes the energy intensity of LMO production as 5.0 kWh per kg of cathode active material.

2.2.2.2 Electrode Manufacturing

During electrode manufacturing, the cathode material (usually Li metal oxide particles) is mixed in dry form with a small quantity of carbon black additive (e.g., acetylene black or graphite).[93] The dry mixture is then combined with a polymeric binder such as polyvinylidene difluoride (PVDF) and the NMP solvent to form a homogenous slurry.[92, 93] This slurry is then intermittently applied to a Cu or Al current collector (Cu for anode, Al for cathode) creating a mother roll and the NMP solvent is evaporated and collected for reuse.[90] NMP is typically used as the solvent for cathode manufacturing and may have a recovery rate of 99%.[93] Water is

generally used as a solvent for anode manufacturing, which is why NMP is only discussed in the context of the cathode. The mother roll of electrodes is then calendared to achieve a specific electrode porosity and improve cell performance.[98] Finally the mother roll is split into several daughter rolls and vacuumed dried.[90] Different battery chemistries may require different types and quantities of active materials, additives, and binders, resulting in unique impacts associated with this phase.[26,96]

Yuan et al.[52] reports that the energy use associated with electrode material mixing and coating are minor with their combined energy consumption representing ≈1% of the energy consumption associated with battery manufacturing. Additionally, Yuan et al.[52] reports that calendaring and slitting represent 2% and 4% of the energy use associated with battery manufacturing, respectively. The main driver of energy use and environmental impacts associated with electrode manufacturing is the NMP evaporation and recovery during cathode drying.

Ahmed et al.[93] explored the process of cathode drying, and energy implications in detail by constructing a process model for a facility producing 100 000 packs per year of 60 kW, 10 kWh LIBs (this translates to 1 GWh per year of battery storage capacity output). In their model, the cathode is sent to a dryer where it is exposed to flowing hot air at 140 °C. NMP concentration in the air must never exceed 1150 parts per million (ppm). After being cooled in a chilled water condenser, NMP, water, and hydrocarbons are condensed and NMP is recovered via distillation and any remaining NMP is recovered using a zeolite wheel to reach total solvent recovery rates around 99%. The resulting energy demand was estimated at 1470 kW of electricity and 4381 kW of thermal energy (5851 kW in total). Based on 300 operating days per year, this translates to 112 MJ of total energy per kWh of battery capacity produced. The question, however, is how sensitive the NMP drying energy is to uncertain parameters, such as facility size and specific chemistries. Ahmed et al.[93] also explored the impact of allowable NMP concentration in the dryer outlet, which varies roughly linearly with the flow rate and total energy demand. However, they did not discuss whether different regulatory frameworks might dictate different caps on NMP concentration or what sorts of safety measures could be taken to enable, for example, a doubling of allowable NMP concentration (which would cut energy demand in half). Yuan et al.[52] suggested that the concentration of the PVDF in the NMP is tied to energy use for NMP recovery, and that reducing PVDF concentration can reduce energy demand for solvent recovery. However, they did not offer a clear explanation as to why this occurs. Yuan et al.[52] also noted that energy demand for NMP recovery at a commercial-scale facility is considerably lower than a pilot-scale facility.

Dunn et al.[46] acknowledged the use of NMP as a solvent but do not mention any energy use associated with NMP recovery, which results in a very small battery assembly energy footprint on par with Notter et al.[50] and these results are likely not representative of the current state of the industry. Dai et al.[92] does an excellent job of noting that some of the energy use differences across prior battery LCAs is driven by solvent assumptions; Notter et al.[50] assume water as the solvent for both cathode and anode, Majeau-Bettez et al.[32] and Ellingsen et al.[74] assume NMP as the cathode and anode solvent. GREET[96] assumes NMP for the cathode and water for the anode, which seems to be the most reasonable choice given current industry practices. Given how significant the energy footprint of NMP recovery is, we suggest that any LIB LCA must devote effort to carefully choosing their solvent use assumptions, and conducting sensitivity analysis as

appropriate. This is an area where some of the most widely-cited studies have not done an adequate job of exploring and highlighting the impacts of solvent recovery on energy and environmental impacts.

2.2.2.3 Cell Assembly

Cell assembly occurs in a dry room, which is essential to battery manufacturing. Per Dunn et al.,[72] this is where electrodes and separators are stacked or wound, current collectors are welded, the cells are enclosed in a container, electrolyte is added, and the cells are closed. While the cell assembly that occurs in a dry room makes up around 5% of the battery manufacturing energy demand according to Yuan et al.,[52] the conditioning of the dry room itself is a major energy consumer. As Dunn et al.[46] point out, energy demand for dry room conditioning is throughput- and scale-dependent. Because primary data, particularly in older (>5 year-old) studies, is most likely to be sourced from small-scale manufacturing facilities, this has resulted in very large energy use estimates. For example, the primary data provided in Yuan et al.[52] indicates that dry room conditioning is the single largest energy consumer, at 43% of total cell manufacturing energy demand. Those results are based on a facility that is operating at full capacity, but only producing 400 cells per day (at 129 cells per pack). Ahmed et al.[99] explore the energy implications of dry room conditioning for a much larger facility in detail using a process simulation approach similar to their approach for estimating NMP drying energy.[99] The model in Ahmed et al.[99] is based on a facility manufacturing 100 000 automotive battery packs annually with a dry room volume of 16 000 cubic meters. In contrast to Yuan et al.,[52] the results from Ahmed et al.[99] indicate energy use for dry room conditioning that is an order of magnitude smaller than the energy required for NMP recovery (400 kW for dry room conditioning, compared with 5851 kW for NMP recovery[93] for a comparably-sized facility). Dunn et al.[46] use a similarly small dry room conditioning estimate, meant to represent a very large facility with high throughput.[99]

From the analysis by Ahmed et al.,[99] it is clear that any battery manufacturing process requiring a dry room is likely to generate widely differing energy demand estimates, depending on scale, as well as local climate (which impacts humidity in the inlet air) and the technological choices that dictate the fraction of electrical versus thermal energy used in the facility. Assembling a small number of scenarios that represent different facility scales, and generating results for each scenario, would provide much-needed clarity in manufacturing energy use results.

2.2.2.4 Cell Finishing and Further Assembly

Cell finishing consists of a variety of processes required for the cell to be ready for use. While the processes included in cell finishing may vary by manufacturer, some form of cycling and precharging are generally required for the formation of the cell. This is associated with a small portion of energy consumption, with Yuan et al. reporting around 1% of the energy used for battery manufacturing is attributable to cell finishing. Additionally, while not a step included in cell manufacturing, the finished cells may be further assembled into modules or packs. This requires the interconnection of individual cells, balance of systems to support the cell in this application, and the addition of structural components. Yuan et al.[52] reports that this additional

assembly is associated with a negligible amount of energy consumption when compared to the energy use associated with cell manufacturing.

2.2.2.5 Variation in Manufacturing Energy Demand Estimates

With the LIB industry in a state of rapid growth and cost reductions, it is not surprising that battery manufacturing energy use estimates have also shifted over time. Figure 2.3 shows a downward trend across most of the studies based on primary data, with Pettinger and Dong[51] as a notable exception. Some of these improvements may be driven by technological advancements, but we hypothesize that much of reductions in energy demand are more likely to be the result of increased facility utilization and scale. If, for example, rapid subsidized growth in LIB manufacturing facilities in China resulted in numerous facilities operating well below their capacity, this would translate to higher energy use estimates, as dry rooms must continue operating regardless of throughput. As larger facilities are built, and begin operating closer to full capacity, we expect that these estimates will stabilize. It is unclear whether they will achieve some of the more ambitious nth plant estimates documented in Notter et al.[50] and Dunn et al.,[46] both of which rely, or appear to rely, on unusual assumptions related to solvent use and recovery that do not reflect current industry practices.

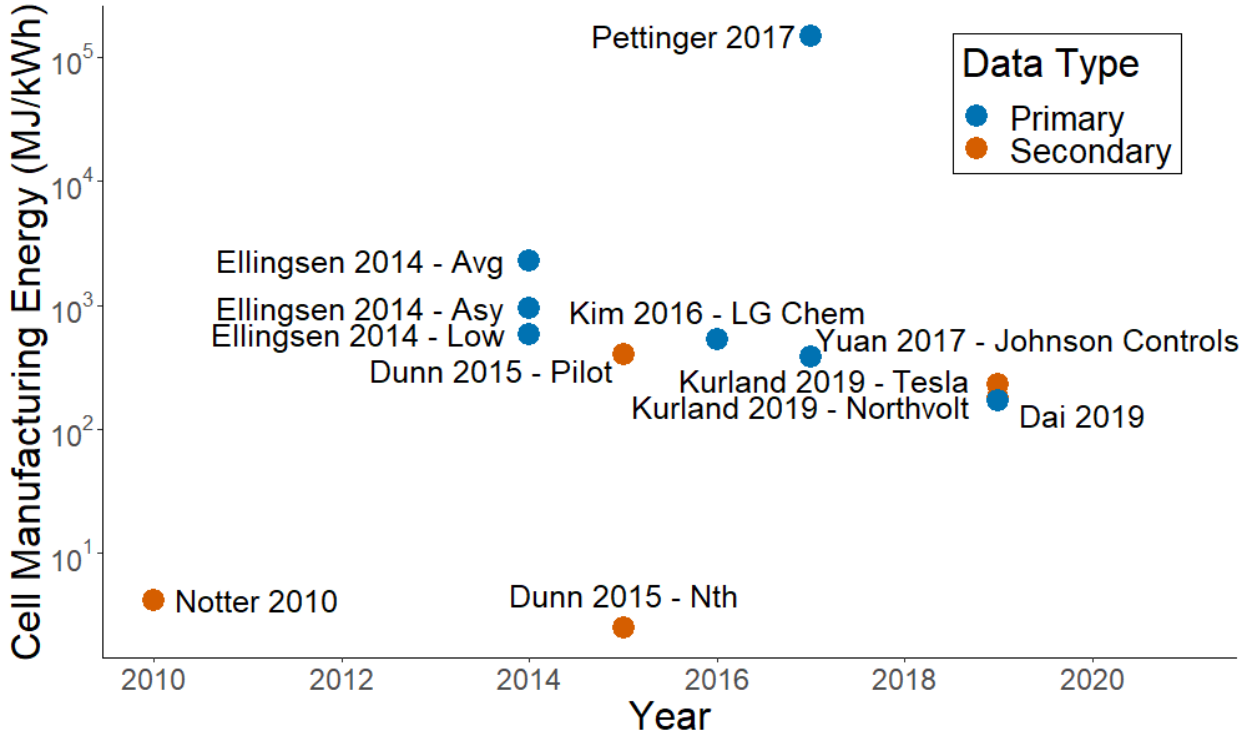

Figure 2.3. Cell manufacturing energy over time. Cell assembly primary energy demand in literature over time. Kurland 2019—Tesla is the estimation of primary energy use at a Tesla, 35 GWh per year manufacturing plant. Kurland 2019—Northvolt is the estimation of primary energy use at a Northvolt, 8 GWh per year manufacturing plant.[100] Dai 2019 is reporting primary energy at an unspecified 2 GWh year manufacturing plant.[92] Ellingsen 2014—Low, Ellingsen 2014—Asy, Ellingsen 2014—Avg are the reported primary energy at an unspecified pilot plant representative of the lowest monthly consumption, stated asymptotic consumption, and average monthly consumption respectively.[74] Notter 2010 is the modeled primary energy use at a pilot scale manufacturing plant.[50] Dunn 2015—Pilot and Dunn 2015—Nth are the modeled primary energy use at a pilot scale and Nth scale plant respectively.[46] Yuan 2017—Johnson Controls is the reported primary energy consumption at a Johnson Controls, 0.018 GWh per year manufacturing plant.[52] Kim 2016—LG Chem is the reported primary energy use at a LG Chem 2 GWh per year manufacturing plant.[49] Pettinger 2017 is the reported primary energy use at an unspecified pilot plant.[51]

Figure 2.4, inspired by a plot provided in Kurland[100] illustrates the impact of facility scale on battery manufacturing energy use estimates. Where plant capacities were not deliberately stated or could not be determined, we used a simple method for approximating the scale: If a plant was described as "pilot," "pioneer," or otherwise novel and small, it was assigned the smallest yearly plant capacity observed in this study, 0.018 GWh yr °C. If a plant was described as "*nth*," it was assigned the largest yearly plant capacity observed in this study or 35 GWh yr^{-1}. The impacts of plant utilization and economies of scale can be observed with the Ellingsen et al.[74] and Dai et al.[92] data points. Ellingsen et al.[74] examined the per unit energy consumption of a cell manufacturing plant for 18 month: their highest data point represents the average per unit energy consumption for this time, their lowest data point represents the lowest monthly per unit energy consumption, and their central point represents a set asymptotic value. The variation of this energy consumption over a relatively short period of time suggests that the cell manufacturer studied had inefficiencies in their cell manufacturing process, potentially arising from varying utilization levels of the plant. In contrast, the manufacturer that worked with Dai et al.[92] claimed

to operate at a high energy efficiency, along with having a greater total capacity and operating during a period of greater cell demand.

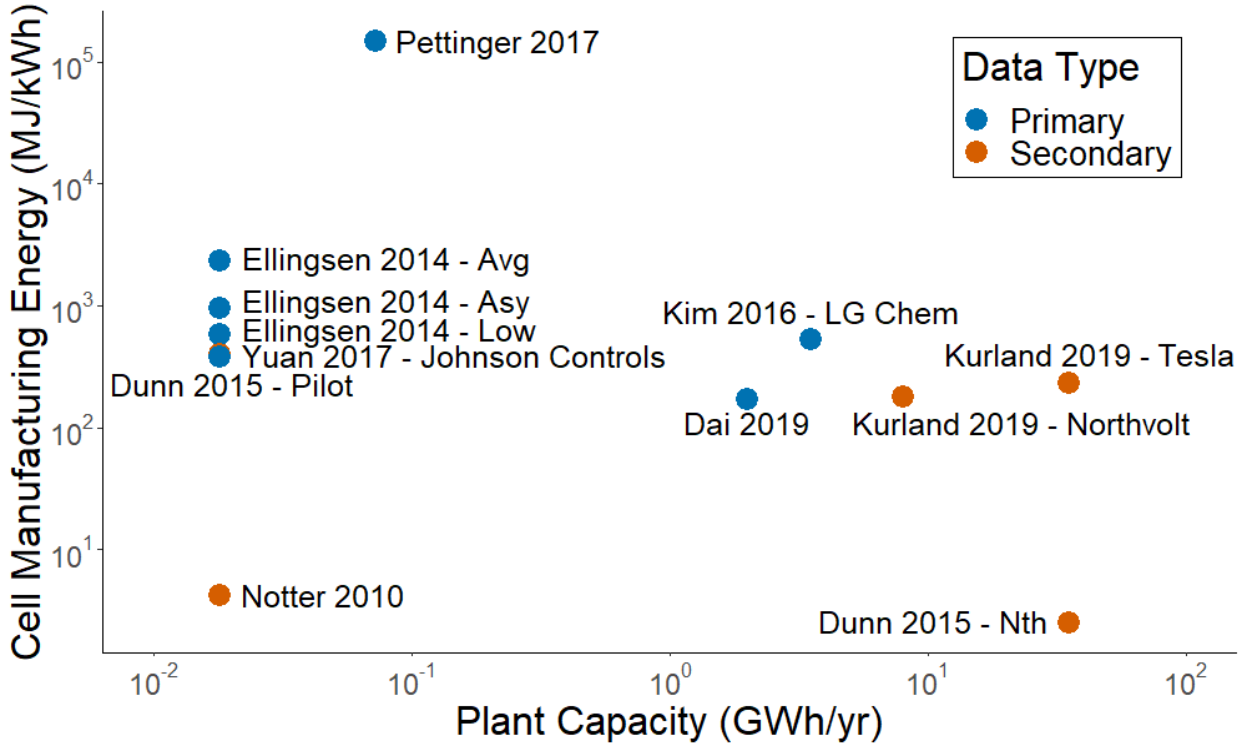

Figure 2.4. Cell manufacturing energy vs plant capacity. Cell assembly primary energy demand in literature versus plant capacity. Kurland 2019 - Tesla is the estimation of primary energy use at a Tesla, 35 GWh/yr manufacturing plant. Kurland 2019 - Northvolt is the estimation of primary energy use at a Northvolt, 8 GWh/yr manufacturing plant.[15] Dai 2019 is the reporting of primary energy at an unspecified 2GWh/yr manufacturing plant.[16] Ellingsen 2014 - Low, Ellingsen 2014 - Asy, Ellingsen 2014 - Avg are the reported primary energy at an unspecified pilot plant representative of the lowest monthly consumption, stated asymptotic consumption, and average monthly consumption respectively.[17] Notter 2010 is the modeled primary energy use at a pilot scale manufacturing plant.[18] Dunn 2015 - Pilot and Dunn 2015 - Nth are the modeled primary energy use at a pilot scale and Nth scale plant respectively.[19] Yuan 2017 - Johnson Controls is the reported primary energy consumption at a Johnson Controls, 0.018 GWh/yr manufacturing plant.[20] Kim 2016 - LG Chem is the reported primary energy use at a LG Chem 2 GWh/yr manufacturing plant.[21] Pettinger 2017 is the reported primary energy use at an unspecified pilot plant.[22]

Most energy demand estimates seem to have fallen in the range of a few hundred MJ per kWh of production. A thorough review of the literature from the perspective of manufacturing energy use and impacts suggests that nearly all LCAs published so far are plagued by unusual assumptions or outright omissions. The question of what a reasonable *nth* plant manufacturing energy footprint should be, and the savings to be had through very large scale production, remains unanswered in the literature. There is a pressing need for a thorough LCA that adequately addresses all the sources of uncertainty associated with battery manufacturing and its energy demands.

2.2.2.6 Geographic Representativeness in Battery Manufacturing

A final critique of battery LCAs is that, while most studies capture the appropriate locations and local grid mixes for raw materials extraction and processing, battery manufacturing has largely been modeled based on grid mixes and primary fuel choices appropriate for the location of the study rather than the most likely manufacturing location. Of the studies we reviewed that included the impacts associate with LIB manufacturing, over 30% used electricity mixes and fuel inputs representative of regions in the European Union, 25% used data representative of North America, and less than 15% used data representative of manufacturers in Asia. The remaining 30% did not provide or clearly state the manufacturing location observed in the study. As of 2019, three quarters of global LIB manufacturing capacity was located in China.[101] The distinction between battery manufacturing in China versus the US or Europe is important for assumptions about the grid mix as well as the primary fuel(s) likely to be combusted on-site. Coal remains the single largest source of primary energy in the Chinese industrial sector; 39% total coal demand comes from the industrial sector. Direct coal use (excluding coke and coal gas) for industrial facilities exceeds natural gas use by about a factor of four.[77] The grid mix in China is coal-dominated, with 70% of total generation from fossil fuel-fired power plants, and of that fraction, 91% is coal. However, a consequential LCA may require a more nuanced look at the source of the marginal kWh across the country, as recent capacity investments in solar, wind, nuclear, and hydroelectricity comprise more than half of all new generating capacity.[77]

The degree to which any given LCA should reflect current manufacturing practices and locations depends on the type of question it is seeking to answer. If the analysis is meant to provide insight into an early-stage battery technology, establishing clear, simple assumptions (e.g., natural gas as the sole source of primary fuel consumption and an average US grid mix) may be sufficient. Varying grid mixes and on-site primary fuels can always be explored through sensitivity analysis. However, for LCAs that seek to offer insights into how EVs broadly compare with other technologies or information on the net impact of widespread adoption of grid-connected stationary batteries, future studies must consider scenarios that reflect the supply chains currently in place. This means incorporating typical practices at Chinese facilities, at least as one of a set of scenarios.

2.2.3 Use Phase and End-of-Life

2.2.3.1 Use Phase

Many papers do not consider the use phase of an LIB when performing and LCA, often citing the uncertainty and complexity of battery performance and lifetime (see Table 2.5). However, accounting for different roundtrip efficiencies and lifetimes is essential when comparing different battery technologies.[10, 31, 34, 51, 102–104] Other characteristics may be more or less relevant, depending on the specific application. For example, pack weight will impact vehicle efficiency in an electric car, truck, or aircraft, while weight is far less relevant for stationary applications. Table 2.1 presents several metrics used to describe an LIBs performance as it varies by battery chemistry, namely the battery's cycle life and shelf life.

Table 2.5: Life-cycle assessment studies sorted by system boundary and application area

Scope						
	Sub-phase/Component	Cradle-to-gate	Cradle-to-gate (w/ use)	Cradle-to-grave	Cradle-to-grave (w/o use)	Review Papers
Application						
Automotive	Hendrickson et al. 2015 Golroudbary et al. 2019	Wu and Kong 2018 Jiang et al. 2020 Ellingsen et al. 2014 Kim et al. 2016 Cobas-Flores et al. 1996	Majeau-Bettez et al. 2011 Bekel and Pauliuk 2019	Dunn et al. 2015 Notter et al. 2010 Wang et al. 2020 Zhao and You 2019 Zackrisson et al. 2010 Deng et al. 2017* Deng et al. 2019 Zackrisson et al. 2016** Li et al. 2014 Longo et al. 2014**	Sun et al. 2020 Wang and Yu 2020 Raugei and Winfield 2019 Dunn et al. 2012 Ciez and Whitacre 2019	Nealer and Hendrickson 2015 Ellingsen et al. 2017 Nordelöf et al. 2014
Stationary		Le Varlet et al. 2020	Hiremath et al 2015	Ryan et al. 2018 Jenu et al. 2020 Weber et al. 2018* Vandepaera et al. 2017 Jones et al. 2020 Chowhurdy et al. 2020 Spanos et al. 2014		Pellow et al. 2020
Unspecified/General/ Other	Wang et al. 2019 Cusenza et al. 2019 Sathre et al. 2015 Kamath et al. 2020	Peters and Weil 2017 Kallitsis et al. 2020	Peters et al. 2016 Casals et al. 2015 Ioakimidis et al. 2019	Lankey and McMichael 2000	Ahmadi et al. 2015 Cicconi et al. 2012 Bobba et al. 2018	Peters et al. 2017 Sullivan and Gaines 2012

Cycle life is defined as the number of charge/discharge cycles a battery can perform under defined conditions before its storage capacity degrades to a specified condition, typically 80% of its original capacity for EVs and 60% for stationary storage. A battery's actual cycle life will be impacted by its operating conditions, and when data is available, should be adjusted based on the expected use case before calculating lifetime energy throughput. Battery operations at extreme temperatures contribute to battery aging. Higher temperatures result in more efficient and faster reactions, but the aging reactions are also enhanced at high temperatures. Low operating temperatures may cause electrode materials to contract, reducing the available space for Li-ion insertion on the anode and potentially contributing to lithium plating, a major contributor to capacity fade.[18, 25, 105, 106] Battery operations at high or low state of charge (SOC) also contribute to accelerate battery aging. At the extreme ends of the SOC, active material loss in the positive electrode is a main driver of increased battery aging.[18, 25, 105, 107, 108] The shelf life metric is defined as the number of years before a battery degrades to a specified condition while remaining inactive (e.g., in very underutilized batteries). These high-level metrics capture the combined effects of multiple battery degradation mechanisms on capacity fade[105, 109, 110] and can be useful in estimating the total energy discharged over a battery's lifetime as a useful functional unit for LCAs.

Focusing exclusively on throughput (kWh discharged over a battery's lifetime) as a functional unit in LCA fails to account for another crucial dimension of the use phase: battery efficiency. A small fraction of energy in batteries cannot be recovered due to irreversible side reactions. Coulombic efficiency represents idealized slow charging and discharging, and is ≈99% for LIBs, but in practice, the ratio of total charge extracted from the battery to total energy put into the battery during charging depends on the charge and discharge C-rate and temperature, and is generally closer to 90%.[111] Frequent use of ultra-fast charging, for example, will decrease battery efficiency, as will rapid discharging. This means that the manner in which a battery is cycled will impact total throughput and energy losses over its lifetime. Round-trip efficiency can refer to the efficiency of a pack or system, as opposed to individual cells, but this terminology is used inconsistently. When incorporating energy losses during charging/discharging, researchers must be careful to avoid omitting or double-counting energy lost in the battery itself in addition to losses at inverters or in parasitic loads, such as thermal management systems. To further complicate matters, battery efficiency decreases over time, although capacity fade is generally the determining factor in deciding to decommission a battery.[105, 112] Impedance is often used as an indicator of LIB health because it can capture the effects of many of the mechanisms that drive capacity fade, power fade, and reduced efficiency,[105, 112, 113] but this metric cannot be easily converted to any of the practical measures of efficiency and lifetime throughput that are needed to account for use-phase performance in an LCA.

Given the complexity of modeling battery behavior, and the lack of performance data from real-world applications, it is not surprising that many battery LCAs do not incorporate the use phase and most ignore battery aging. Sathre et al.,[114] which focused on second life applications for LIBs from EVs, performed a sensitivity analysis to identify the battery parameters and their influence cumulative energy balance and cumulative greenhouse gas emissions. They noted considerable uncertainty in the timing at which LIBs reach an inflection point, when capacity fade accelerates. Hiremath et al.[31] portrayed the different life-cycle impacts associated with LIBs used in different stationary storage applications. Their analysis provided the power rating,

discharge duration, energy rating, and cycle frequency for multiple stationary storage applications, finding that use phase greenhouse gas emissions per MWh delivered can vary by nearly two orders of magnitude between applications. Longo et al.[115] compared two theoretical EV batteries with one having a cycle life of 3000 cycles and a cycling frequency of 2 cycles per day, and the other having a cycle life of 3500 cycles and a cycling frequency of 1.6 cycles per day. This resulted in a 5% difference in global warming potential during the use phase of these two battery scenarios. Although a more thorough accounting of use-phase cycling and its impact on lifetime and efficiency would be ideal, reliable data for use in LCAs is rare. Future studies would benefit greatly from a set of standardized scenarios that capture variations in C-rate, operating temperatures, SOC, and the expected impacts on capacity fade, battery lifetime, and efficiency.

2.2.3.2 Battery End-of-Life and Recycling

Once a battery has reached its EOL, it must be safely disposed of or recycled. Incorporating reuse and recycling has long been a methodological challenge in LCA, raising questions of how credits for recovered materials, and the resulting avoided impacts of virgin material production, should be allocated.[116] Recycling is categorized as closed-loop, meaning materials are recycled within the same production system (e.g., cathode materials recovered for use in new cathodes), or open-loop, where materials are recovered for use in other production systems. For batteries, most studies take a closed-loop approach to recycling and they explore one or more of the three main recycling approaches: pyrometallurgical, hydrometallurgical, and direct recycling.[46, 50, 72, 91, 117, 118]

Pyrometallurgical recycling is a smelting process capable of recovering transition metals, namely Co, Ni, and Cu, and is used to recycle LIBs as well as Ni Metal-Hydride (NiMH) batteries.[119] Other materials are oxidized in the process to provide process heat and are not generally recovered; this includes Li and Al. Hydrometallurgical and direct recycling, which are based on leaching and physical separation processes, respectively, recover a greater fraction of battery materials by mass. Both processes are designed to recover the cathode (including Li, in addition to metals like Co or Mn), Al, and the anode, while only direct recycling can recover the electrolyte (through flushing of cells).[119] With the exception of water use, hydrometallurgical recycling achieves greater savings across a wide range of life-cycle inventory metrics relative to pyrometallurgical recycling.[117] Direct recycling is more challenging to compare because it is less commonly used and the process configuration and materials recovered vary. However, as Gaines points out, there is more of a continuum than a clear distinction between hydrometallurgical and direct recycling; as the Co content of LIBs declines, a hybrid direct/hydrometallurgical approach may become preferable to a pyrometallurgical process.[119] Although not the focus of this study, EV batteries have the potential to be tested, refurbished as needed, and extend their service life in stationary storage applications.[47, 48, 114, 120–123] As noted in Sathre et al.,[114] there are additional impacts associated with configuring vehicle batteries for use in stationary applications, including the installation and use of cell cooling systems, and capacity can decline rapidly once the battery reaches its inflection point.

The attractiveness of these recycling processes is ultimately contingent upon good use-phase performance of the recovered materials, and this is perhaps most uncertain with direct recycling

processes. If recovered cathode materials cause a decrease in cycle life or round-trip efficiency, such impacts could easily negate the benefits of offsetting raw material production. LCA studies focused on battery recycling to-date have relied in the assumption that recycled materials are functionally equivalent to new materials. This is understandable, as empirical data to support any other assumption is scarce or non-existent. An additional challenge is the establishment of a clear business-as-usual case for use as a baseline for comparison. The quantity of stationary and EV LIBs reaching their EOL remains small and recycling and disposal practices vary by country. Globally, it is estimated that 95% of LIBs are not recycled.[124] As demand for energy storage in EV and stationary energy storage applications grows and batteries continue to reach their EOL, additional studies will be needed to track the date of these batteries and establish a clearer understanding of what processes are being used and what materials are ultimately recovered.

2.3 Recommendations for Battery LCA

It is surprising that, despite the publication of LIB LCAs dating back more than a decade, we are unable to point to a single study that sets the standard for best practices in battery LCAs. This is not meant to suggest that prior studies have not offered value and insight to the research community; the most widely-cited studies often perform well in one or more dimensions, but each has its own drawbacks. Most of the published LCAs have provided detailed data on the environmental impacts of raw materials extraction and processing.[32, 46, 50, 72, 74] The shortcomings in our understanding of raw material extraction and processing are twofold. First, the studies we surveyed did not adequately account for geographic variation in mining practices and variations in the exposure risk for nearby populations. Some mining operations that comprise a minority share of production are likely to drive an outsized fraction of overall environmental impacts because of local conditions and practices. We liken these operations, which may be informal or loosely regulated, to the concept of "superemitters" in the natural gas industry.[85] Second, there are inherent limitations in the underlying midpoint and impact methodologies; it is impossible for any LCA to conduct detailed fate and transport modeling for every emission to air, soil, and water, so studies rely on regional or global average factors that are likely to be one or more orders of magnitude different from the actual values. These uncertainties are compounded by the fact that documentation of where specific waste streams are discharged from mining and material processing operations is sparse. Moreover, we have yet to find any study that explores the differences between average, marginal, and incremental sources of key material inputs, and the implications for mining and processing-related energy use and emissions. This seems to be an obvious gap in the literature, and one that could be filled with data and market projections that are available today.

Achieving consensus and clarity in battery manufacturing energy use and impacts is where prior studies largely fall short. Because there is little evidence to suggest appreciable non-combustion emissions to air, water, or soil during manufacturing, nearly all direct environmental impacts from this stage are expected to be tied directly to on-site combustion of fuels and emissions from electricity generation. Dunn et al.[46] provided the first clear and compelling discussion of dry room conditioning in an LCA context, and the reasons behind large differences in reported energy use, but did not provide a similarly detailed exploration of energy used for NMP recovery. Although its scope was more limited, focusing only on NMC-graphite LIBs, Dai

et al.[92] did provide a more thorough exploration of both dry room conditioning and NMP recovery. Battery recycling, by comparison to battery manufacturing, is relatively well studied and there is better agreement across the literature, although battery recycling LCAs must rely largely on estimated or simulated mass and energy balances because of the limited number of LIBs being recycled.[46, 72, 117] It is possible that, when primary data becomes more widely available, it will reveal inconsistencies between simulations and primary data similar to those found in battery manufacturing. Although battery technologies will continue to evolve, and there will continue to be disagreements between primary and secondary data sources, we hope to provide recommendations for approaching these uncertainties in a manner that makes each study more interpretable, and simpler to replicate and update as battery technologies and the infrastructure supporting their production continues to develop.

2.3.1 Defining Appropriate System Boundaries

Defining the system boundaries requires researchers to weigh the value of comprehensiveness against the downsides of incorporating more assumptions that are not central to the battery technology itself. Expansive system boundaries that include the use- and end-of-life phases will result in the most complete assessment of the net environmental impacts. Inclusion of these phases can alter the conclusions of battery technology (or recycling technology) comparisons; if a less resource-intensive batter technology or directly-recycled cathode material results in reduced battery cycle life, a cradle-to-grave analysis captures these important differences. A cradle-to-gate analysis using only kWh of battery capacity as the functional unit, in this case, would be misleading. Similarly, a battery that relies on a larger quantity of Co may appear to be at a greater disadvantage in a cradle-to-gate analysis, but Co also has a higher likelihood of being recovered and this recovered material can offset the impacts of raw Co extraction and processing.

One can make a similarly compelling argument that cradle-to-grave LCAs carry, in some cases, considerable downsides. Tying results to a specific use case, can make results nearly impossible to compare across studies. This is especially true for stationary energy storage applications, where specific configurations and services provided vary. The layers of assumptions and uncertainty introduced while incorporating the use and EOL phases can dilute what might otherwise be a rigorous and clearly defined analysis of battery production impacts. For example, in analyses conducted based on novel battery technologies, the most viable use case may not be known and use phase performance is uncertain. For the purposes of cross-study comparisons and improving reproducibility of results, reporting cradle-to-gate results separately is valuable regardless of the study's overall system boundaries. In cases where use-phase performance is not known, the development of alternative functional units and scenario analysis can ameliorate some of the drawbacks of the constrained system boundaries, as discussed further in Section 3.3 below.

2.3.2 Selecting Relevant Environmental Metrics

Above all, we recommend that future studies consider the goal and scope of the study, in addition to the availability of adequate quality data when selecting environmental metrics (inventory, midpoints, and endpoints). Presenting a long list of impacts without context or

uncertainty analysis is likely to generate confusion and offer limited value to the broader research community. Omitting an impact category may lead readers to believe it is not important, but producing results that are inaccurate and/or convey false precision may lead to the same outcome. Making additional efforts to highlight the key drivers of each impact is also critical. There is an important distinction between environmental impacts tied to energy use (and combustion to generate that thermal or electrical energy) and impacts tied to other activities, such as non-combustion pollutant releases to water, air, or soil or depletion of finite resources through mining activities. GHG emissions and 100-year GWP for LIB production are dominated by combustion-related CO_2.[11] The same is true for human health impacts from other air pollutant emissions, including particulate matter (PM), SO_x, and NO_x, and terrestrial acidification potential, which is driven by SO_x emissions.[11] We strongly recommend that future LCAs make an attempt to separate impacts tied to energy use with those tied to other activities. If facilities shift their fuel use to lower-emission alternatives (e.g., from coal to natural gas, or natural gas to renewable fuels), making this distinction in published LCAs will make it easier to adjust the results accordingly. Furthermore, denoting which impacts are dependent on assumed grid mixes will make the use of LCA data for future studies considerably simpler; future researchers may wish to update underlying grid mixes or select mixes that are more representative of where production occurs. Emissions may also evolve depending on the tightening or loosening of emissions regulations in the location selected for analysis. Given the rapid decarbonization of electricity occurring in many countries, it is imperative that researchers be given the opportunity to update our understanding of battery production impacts in the context of current and future grid mixes.

As discussed previously, most of the non-energy-related environmental impacts in the life cycle of LIBs are tied to mining and material processing operations. There are various midpoint and endpoint metrics aimed at characterizing depletion of non-renewable resources. We argue that these multipliers fail to capture the nuances of some of the key inputs to battery production, where availability itself may be a secondary or tertiary concern and the more likely outcome is a long-term shift toward more costly and energy-intensive extraction methods. Rather than attempting to quantify resource depletion in a single metric, we recommend that future LCAs develop a set of current average, marginal, and incremental scenarios for the recovery and processing of a few key material inputs (including Li, for example) and use these scenarios to illustrate the long-term implications of continuing to extract these materials without recovering and recycling them at the battery end-of-life. The other impact most relevant to raw material extraction we have discussed here is eutrophication potential. We hesitate to recommend that this metric be included in future studies, in part because the required data on relevant waste stream discharges may not be of sufficient quality to draw meaningful conclusions from the results. Ozone depletion potential, which we briefly touch on, is not likely to be a useful metric to quantify given the ongoing phase-out of ozone-depleting substances such as CFC-11.[88] Human toxicity does not feature prominently in non-energy-related impacts within the studies we surveyed, but as noted earlier, published values regularly rely on data provided by large mining companies[86] and those datasets likely reflect best industry practices and fail to account for the impact of outliers, particularly in artisanal and small mining operations. Omitting such outliers is a known problem in emissions and environmental impact accounting[85] and must be mitigated in future LCAs, particularly in the context of material extraction and processing.

Water consumption and withdrawals associated with battery production can be substantial, yet it is often overlooked in LCAs.[68] Battery electric vehicles are associated with over 50% more water use relative to internal combustion engine vehicles over the course of their lifetime. This is mostly associated with the electricity use associated with vehicle charging, but a large contribution of water consumption is attributable to the LIB itself, consisting of 5–10% of the total water consumption depending on the battery chemistry.[125] It estimated that 752 liters of water are consumed per kWh of Li-ion battery pack produced, with roughly 50% of this attributable to aluminum used as housing and 30% attributable to the cathode active material for NMC-111 cathodes.[92] Electrolysis during aluminum production is responsible for 65% of the water use attributable to aluminum production if produced through thermal power,[126] and mineral extraction is responsible for a large majority of water use attributable to the cathode active material. In particular, Co production consumes the most water, representing 50% of the embedded water consumption in NMC-111 cathode active materials.[92] Water use, while not the central focus of most battery LCAs, is worthy of further exploration for studies seeking to broaden their scope beyond energy use and GHG emissions, particularly if the values can be weighted based on a water stress index or similar metric aimed at capturing local water scarcity impacts.[127]

2.3.3 Defining Functional Units for Analysis

Defining functional units for battery LCA presents a challenge; the closer the functional unit is to representing the actual service a battery provides (e.g., powering a vehicle to travel one km), the more underlying assumptions, none of which are standardized, must be made. This makes cross-comparisons in the literature labor-intensive or impossible. Conversely, it is common for studies to report results per kg of battery mass,[32, 46, 74] which has no direct relationship to the service a battery provides but it does provide for straightforward comparison across multiple studies. Functional units used in prior studies include battery or material mass (kg), individual battery pack, energy capacity (kWh of battery capacity), energy throughput (kWh passed through the system over the battery lifetime), and distance driven (km) for battery electric vehicles. Ellingsen et al.[74] set a useful precedent in reporting their results across multiple functional units (per pack, per kWh, and per kg of battery mass).

We suggest that the time has come to phase out the use of kg of battery mass as a functional unit in LCAs. Normalizing results per kWh of battery capacity offers similar potential for cross-comparison while also serving as a more logical functional unit because storage capacity is tied to the core service provided by rechargeable batteries. Normalizing LCA results in terms of lifetime energy throughput is another compelling alternative because it incorporates differences in cycle life and round-trip efficiency that a per unit-capacity analysis does not. One can imagine fascinating assessments of the tradeoffs between, for example, a shift from NMP to aqueous solvents and the resulting impact on lifetime kWh throughput if phasing out NMP negatively impacts cycle life. As long as underlying assumptions about cycle life are clearly documented, we suggest that studies would be well served to report results in these two formats (per kWh of capacity and per kWh of lifetime throughput). This being said, studies aimed at capturing the contribution of battery-related impacts in the context of a larger system may justifiably choose to report their results differently, including per-km traveled or at the individual pack level.

2.3.4 Recommendations for Future Work

Although we are not the first to highlight the difficulties in achieving consensus on methods for conducting battery LCAs,[7–11] we hope this review provides the most comprehensive exploration of the underlying reasons behind inconsistent battery LCA results. Quantifying the environmental impacts of battery production can seem enormously complicated and we recommend that future studies simplify and prioritize their efforts based on the processes and materials that are the largest contributors. Comprehensiveness has value, but it must be acknowledged that it also comes at a cost; selecting a large number of inventory, midpoint, or endpoint categories increases the likelihood that researchers will rely on inventory data and characterization factors that are not technologically, temporally, and/or geographically correlated with the details of the study. Selecting life-cycle inventory, midpoint, and/or endpoint metrics that are likely to yield the greatest insights (and have sufficiently high quality data to support those conclusions) will make future battery LCAs more interpretable and impactful. We also urge researchers go beyond representation of industry best practices and develop datasets that capture outliers or "superemitters," particularly in mining and material processing. Disaggregating environmental impacts by location and type of operation can provide better transparency and accuracy, and also establish a framework by which companies that carefully manage their supply chains to avoid such suppliers are able to be recognized in their estimated environmental footprints.

Improving the interpretability and impact of future battery LCAs will also require that every study conduct a sensitivity analysis across a range of manufacturing facility scales. It is clear from our review of the literature that this point, and the resulting deviations in estimated manufacturing energy use, causes more confusion than any other parameter. We recommend that future LCAs define two or three facilities scales, on the order of 0.1, 1, and 10 GWh per year of battery capacity output and generate results across these different scales. Specific facility scale scenarios could be chosen based on economic "tipping points" for a change in design of, for example, the NMP recovery system or dry room conditioning equipment. Clearly indicating the likely breakdowns of thermal energy use versus electrical energy will also provide enormous value, as many studies do not differentiate between the two. An LCA that makes use of market reports to estimate global-average energy use for battery manufacturing, and ideally projects potential trends, is also sorely needed to illustrate the gap between the current literature and current/future practices in industry.

A final conclusion from this review is that a rigorous, complete cradle-to-grave LCA of multiple battery technologies can be made more tractable by the production of consensus-based scenarios to address some of the major sources of uncertainty for these analyses. Specifically, scenarios that capture critical raw material availability, the geographic distribution of near- and long-term sources, and any expected shifts in extraction/processing methods would reduce reliance on sub-standard data sources and enable easier cross-comparisons between different battery studies. The same is true for the battery use-phase; most LCA researchers and practitioners do not have the resources and subject matter expertise to develop detailed scenarios for battery cycling, operating temperatures, and SOC, nor can such a scenario easily be translated to expected shifts in capacity fade, efficiency, and lifetime. However, if a collection of experts were able to devise a set of scenarios that reflect the most likely use cases for batteries in transportation and stationary

applications, these would be widely used and further improve the ability to compare studies and externally validate results. Ambitious harmonization projects are not unheard of[128]and, through a partnership between systems analysis experts and technology experts, the community can ensure that future analyses of battery technologies further our understanding of their impacts on the environment.

References

1. Scown, C. D., Taptich, M., Horvath, A., McKone, T. E. & Nazaroff, W. W. Achieving deep cuts in the carbon intensity of U.S. automobile transportation by 2050: complementary roles for electricity and biofuels. *Environ. Sci. Technol.* **47,** 9044–9052 (2013).

2. Ziegler, M. S. *et al.* Storage requirements and costs of shaping renewable energy toward grid decarbonization. *Joule* **3,** 2134–2153 (2019).

3. Schill, W.-P. Electricity storage and the renewable energy transition. *Joule* **4,** 2059–2064 (2020).

4. Oliveira, L. *et al.* Key issues of lithium-ion batteries – from resource depletion to environmental performance indicators. *J. Clean. Prod.* **108,** 354–362 (2015).

5. Peters, J. & Weil, M. A Critical Assessment of the Resource Depletion Potential of Current and Future Lithium-Ion Batteries. *Resources* **5,** 46 (2016).

6. Finkbeiner, M., Inaba, A., Tan, R., Christiansen, K. & Klüppel, H.-J. The new international standards for life cycle assessment: ISO 14040 and ISO 14044. *Int. J. Life Cycle Assess.* **11,** 80–85 (2006).

7. Ellingsen, L. A.-W., Hung, C. R. & Strømman, A. H. Identifying key assumptions and differences in life cycle assessment studies of lithium-ion traction batteries with focus on greenhouse gas emissions. *Transportation Research Part D: Transport and Environment* **55,** 82–90 (2017).

8. Pellow, M. A., Ambrose, H., Mulvaney, D., Betita, R. & Shaw, S. Research gaps in environmental life cycle assessments of lithium ion batteries for grid-scale stationary energy storage systems: End-of-life options and other issues. *Sustainable Materials and Technologies* **23,** e00120 (2020).

9. Sullivan, J. L. & Gaines, L. Status of life cycle inventories for batteries. *Energy Conversion and Management* **58,** 134–148 (2012).

10. Nealer, R. & Hendrickson, T. P. Review of recent lifecycle assessments of energy and greenhouse gas emissions for electric vehicles. *Curr. Sustainable Renewable Energy Rep.* **2,** 66–73 (2015).

11. Peters, J. F., Baumann, M., Zimmermann, B., Braun, J. & Weil, M. The environmental impact of Li-Ion batteries and the role of key parameters – A review. *Renewable and Sustainable Energy Reviews* **67,** 491–506 (2017).

12. Nordelöf, A., Messagie, M., Tillman, A.-M., Ljunggren Söderman, M. & Van Mierlo, J. Environmental impacts of hybrid, plug-in hybrid, and battery electric vehicles—what can we learn from life cycle assessment? *Int. J. Life Cycle Assess.* **19,** 1866–1890 (2014).

13. Tian, Y. *et al.* Promises and Challenges of Next-Generation "Beyond Li-ion" Batteries for Electric Vehicles and Grid Decarbonization. *Chem. Rev.* (2020). doi:10.1021/acs.chemrev.0c00767

14. Bloch, C., Newcomb, J., Shiledar, S. & Tyson, M. *Breakthrough Batteries: Powering the Era of Clean Electrification*. (Rocky Mountain Institute, 2020).

15. Mitchel, P. & Waters, J. *Energy Storage Roadmap Report*. (Energy Systems Network, 2017).

16. Ralon, P., Taylor, M., Ilas, A., Diaz-Bone, H. & Kairies, K.-P. *Electricity Storage and Renewables: Costs and Markets to 2030*. (IRENA, 2017).

17. Gantenbein, S., Schönleber, M., Weiss, M. & Ivers-Tiffée, E. Capacity Fade in Lithium-Ion Batteries and Cyclic Aging over Various State-of-Charge Ranges. *Sustainability* **11,** 6697 (2019).

18. Ecker, M. *et al.* Calendar and cycle life study of Li(NiMnCo)O2-based 18650 lithium-ion batteries. *J. Power Sources* **248,** 839–851 (2014).

19. Battaglia, V. Lithium Ion Battery Performance by Chemistry Interview. (2020).

20. Srinavasan, V. Lithium Ion Battery Performance by Chemistry Interview. (2020).

21. Zubi, G., Dufo-López, R., Carvalho, M. & Pasaoglu, G. The lithium-ion battery: State of the art and future perspectives. *Renewable and Sustainable Energy Reviews* **89,** 292–308 (2018).

22. Stewart, S. *et al.* Optimizing the Performance of Lithium Titanate Spinel Paired with Activated Carbon or Iron Phosphate. *J. Electrochem. Soc.* **155,** A253 (2008).

23. Buchmann, I. Types of Lithium-Ion. (2021). At <https://batteryuniversity.com/learn/article/types_of_lithium_ion>

24. Zhu, Y., Cui, Y. & Alshareef, H. N. An Anode-Free Zn-MnO2 Battery. *Nano Lett.* (2021). doi:10.1021/acs.nanolett.0c04519

25. Grolleau, S. *et al.* Calendar aging of commercial graphite/LiFePO4 cell – Predicting capacity fade under time dependent storage conditions. *J. Power Sources* **255,** 450–458 (2014).
26. Nelson, P. *et al. BatPaC*. (Argonne National Laboratory, 2019).

27. Nitta, N., Wu, F., Lee, J. T. & Yushin, G. Li-ion battery materials: present and future. *Materials Today* **18,** 252–264 (2015).

28. Li, B., Gao, X., Li, J. & Yuan, C. Life cycle environmental impact of high-capacity lithium ion battery with silicon nanowires anode for electric vehicles. *Environ. Sci. Technol.* **48,** 3047–3055 (2014).

29. Morrow, H. in *Used battery collection and recycling* **10,** 1–34 (Elsevier, 2001).

30. Raugei, M. & Winfield, P. Prospective LCA of the production and EoL recycling of a novel type of Li-ion battery for electric vehicles. *J. Clean. Prod.* **213,** 926–932 (2019).

31. Hiremath, M., Derendorf, K. & Vogt, T. Comparative life cycle assessment of battery storage systems for stationary applications. *Environ. Sci. Technol.* **49,** 4825–4833 (2015).

32. Majeau-Bettez, G., Hawkins, T. R. & Strømman, A. H. Life cycle environmental assessment of lithium-ion and nickel metal hydride batteries for plug-in hybrid and battery electric vehicles. *Environ. Sci. Technol.* **45,** 4548–4554 (2011).

33. Yu, Y. *et al.* Environmental characteristics comparison of Li-ion batteries and Ni-MH batteries under the uncertainty of cycle performance. *J. Hazard. Mater.* **229–230,** 455–460 (2012).

34. Zhao, S. & You, F. Comparative Life-Cycle Assessment of Li-Ion Batteries through Process-Based and Integrated Hybrid Approaches. *ACS Sustain. Chem. Eng.* **7,** 5082–5094 (2019).

35. Deng, Y., Li, J., Li, T., Gao, X. & Yuan, C. Life cycle assessment of lithium sulfur battery for electric vehicles. *J. Power Sources* **343,** 284–295 (2017).

36. Deng, Y., Ma, L., Li, T., Li, J. & Yuan, C. Life Cycle Assessment of Silicon-Nanotube-Based Lithium Ion Battery for Electric Vehicles. *ACS Sustain. Chem. Eng.* **7,** 599–610 (2019).

37. Weber, S., Peters, J. F., Baumann, M. & Weil, M. Life cycle assessment of a vanadium redox flow battery. *Environ. Sci. Technol.* **52,** 10864–10873 (2018).

38. Vandepaer, L., Cloutier, J. & Amor, B. Environmental impacts of Lithium Metal Polymer and Lithium-ion stationary batteries. *Renewable and Sustainable Energy Reviews* **78,** 46–60 (2017).

39. Bekel, K. & Pauliuk, S. Prospective cost and environmental impact assessment of battery and fuel cell electric vehicles in Germany. *Int. J. Life Cycle Assess.* **24,** 2220–2237 (2019).

40. Chowdhury, J. I. *et al.* Techno-environmental analysis of battery storage for grid level energy services. *Renewable and Sustainable Energy Reviews* **131,** 110018 (2020).

41. Bjørn, A. & Hauschild, M. Z. in *Life Cycle Assessment* (eds. Hauschild, M. Z., Rosenbaum, R. K. & Olsen, S. I.) 605–631 (Springer International Publishing, 2018). doi:10.1007/978-3-319-56475-3_25

42. Fu, R., Remo, T. & Margolis, R. *2018 U.S. Utility-Scale Photovoltaics-Plus-Energy Storage System Costs Benchmark*. (National Renewable Energy Laboratory, 2018).

43. Ramasamy, V. LIB Stationary Storage Cost Modeling Interview. (2020).

44. Leggett, G. LIB Stationary Storage Cost Modeling Interview. (2020).

45. Shriver, J. LIB Stationary Storage Cost Modeling Interview. (2020).

46. Dunn, J. B., Gaines, L., Kelly, J. C., James, C. & Gallagher, K. G. The significance of Li-ion batteries in electric vehicle life-cycle energy and emissions and recycling's role in its reduction. *Energy Environ. Sci.* **8,** 158–168 (2015).

47. Ioakimidis, C. S., Murillo-Marrodán, A., Bagheri, A., Thomas, D. & Genikomsakis, K. N. Life cycle assessment of a lithium iron phosphate (LFP) electric vehicle battery in second life application scenarios. *Sustainability* **11,** 2527 (2019).

48. Kamath, D., Arsenault, R., Kim, H. C. & Anctil, A. Economic and Environmental Feasibility of Second-Life Lithium-Ion Batteries as Fast-Charging Energy Storage. *Environ. Sci. Technol.* **54,** 6878–6887 (2020).

49. Kim, H. C. *et al.* Cradle-to-Gate Emissions from a Commercial Electric Vehicle Li-Ion Battery: A Comparative Analysis. *Environ. Sci. Technol.* **50,** 7715–7722 (2016).

50. Notter, D. A. *et al.* Contribution of Li-ion batteries to the environmental impact of electric vehicles. *Environ. Sci. Technol.* **44,** 6550–6556 (2010).

51. Pettinger, K.-H. & Dong, W. When does the operation of a battery become environmentally positive? *J. Electrochem. Soc.* **164,** A6274–A6277 (2017).

52. Yuan, C., Deng, Y., Li, T. & Yang, F. Manufacturing energy analysis of lithium ion battery pack for electric vehicles. *CIRP Annals - Manufacturing Technology* **66,** 53–56 (2017).

53. Wang, L., Wu, H., Hu, Y., Yu, Y. & Huang, K. Environmental Sustainability Assessment of Typical Cathode Materials of Lithium-Ion Battery Based on Three LCA Approaches. *Processes* **7,** 83 (2019).

54. Wang, Q. *et al.* Environmental impact analysis and process optimization of batteries based on life cycle assessment. *J. Clean. Prod.* **174,** 1262–1273 (2018).
55. Recycle spent batteries. *Nat. Energy* **4,** 253–253 (2019).

56. Yao, Y. *et al.* Hydrometallurgical Processes for Recycling Spent Lithium-Ion Batteries: A Critical Review. *ACS Sustain. Chem. Eng.* **6,** 13611–13627 (2018).

57. Olivetti, E. A., Ceder, G., Gaustad, G. G. & Fu, X. Lithium-Ion Battery Supply Chain Considerations: Analysis of Potential Bottlenecks in Critical Metals. *Joule* **1,** 229–243 (2017).

58. Zheng, X. *et al.* A Mini-Review on Metal Recycling from Spent Lithium Ion Batteries. *Engineering* **4,** 361–370 (2018).

59. Elkind, E., Heller, P. & Lamm, T. *Sustainable Drive, Sustainable Supply: Priorities to Improve the Electric Vehicle Battery Supply Chain*. (Berkeley Law, 2020).

60. Igogo, T., Sandor, D., Mayyas, A. & Engel-Cox, J. *Supply Chain of Raw Materials Used in the Manufacturing of Light-Duty Vehicle Lithim-Ion Batteries*. (Clean Energy Manufacturing Analysis Center, 2019).

61. U.S. Geological Survey. *Mineral Commodity Summaries 2021*. (U.S. Geological Survey, 2021).

62. Steward, D., Mayyas, A. & Mann, M. Economics and Challenges of Li-Ion Battery Recycling from End-of-Life Vehicles. *Procedia Manufacturing* **33,** 272–279 (2019).

63. Banza Lubaba Nkulu, C. *et al.* Sustainability of artisanal mining of cobalt in DR Congo. *Nat. Sustain.* **1,** 495–504 (2018).

64. Banza, C. L. N. *et al.* High human exposure to cobalt and other metals in Katanga, a mining area of the Democratic Republic of Congo. *Environ. Res.* **109,** 745–752 (2009).

65. Cobalt Development Institute. Cobalt supply & demand. Cobalt Facts. (2020). at <https://www.cobaltinstitute.org/about-cobalt.html>

66. Hund, K., La Porta, A., Fabregas, T., Laing, T. & Drexhage, J. *Minerals for Climate Action: The Mineral Intensity of the Clean Energy Transition*. (World Bank Group, 2020).

67. Agusdinata, D. B., Liu, W., Eakin, H. & Romero, H. Socio-environmental impacts of lithium mineral extraction: towards a research agenda. *Environmental Research Letters* **13,** 123001 (2018).

68. Flexer, V., Baspineiro, C. F. & Galli, C. I. Lithium recovery from brines: A vital raw material for green energies with a potential environmental impact in its mining and processing. *Sci. Total Environ.* **639,** 1188–1204 (2018).

69. Stamp, A., Lang, D. J. & Wäger, P. A. Environmental impacts of a transition toward e-mobility: the present and future role of lithium carbonate production. *J. Clean. Prod.* **23,** 104–112 (2012).

70. Kesler, S. E. *et al.* Global lithium resources: Relative importance of pegmatite, brine and other deposits. *Ore Geology Reviews* **48,** 55–69 (2012).

71. Diekmann, J. *et al.* Ecological Recycling of Lithium-Ion Batteries from Electric Vehicles with Focus on Mechanical Processes. *J. Electrochem. Soc.* **164,** A6184–A6191 (2017).

72. Dunn, J. B., Gaines, L., Sullivan, J. & Wang, M. Q. Impact of recycling on cradle-to-gate energy consumption and greenhouse gas emissions of automotive lithium-ion batteries. *Environ. Sci. Technol.* **46,** 12704–12710 (2012).

73. Wu, Z. & Kong, D. Comparative life cycle assessment of lithium-ion batteries with lithium metal, silicon nanowire, and graphite anodes. *Clean Techn. Environ. Policy* **20,** 1233–1244 (2018).

74. Ellingsen, L. A.-W. *et al.* Life Cycle Assessment of a Lithium-Ion Battery Vehicle Pack. *J. Ind. Ecol.* **18,** 113–124 (2014).

75. Kallitsis, E., Korre, A., Kelsall, G., Kupfersberger, M. & Nie, Z. Environmental life cycle assessment of the production in China of lithium-ion batteries with nickel-cobalt-manganese cathodes utilising novel electrode chemistries. *J. Clean. Prod.* **254,** 120067 (2020).

76. Farjana, S. H., Huda, N. & Mahmud, M. A. P. Impacts of aluminum production: A cradle to gate investigation using life-cycle assessment. *Sci. Total Environ.* **663,** 958–970 (2019).

77. LBNL. *China Energy Outlook*. (Lawrence Berkeley National Laboratory, 2020).

78. Mahmud, M., Huda, N., Farjana, S. & Lang, C. Comparative Life Cycle Environmental Impact Analysis of Lithium-Ion (LiIo) and Nickel-Metal Hydride (NiMH) Batteries. *Batteries* **5,** 22 (2019).

79. Jiang, S. *et al.* Environmental impacts of lithium production showing the importance of primary data of upstream process in life-cycle assessment. *J. Environ. Manage.* **262,** 110253 (2020).

80. Whiteside, J. & Finn-Foley, D. Supply Chain Looms as Serious Threat to Batteries' Green Reputation. *Green Tech Media* (2019).

81. Jara, A. D., Betemariam, A., Woldetinsae, G. & Kim, J. Y. Purification, application and current market trend of natural graphite: A review. *International Journal of Mining Science and Technology* (2019). doi:10.1016/j.ijmst.2019.04.003

82. Dunn, J. B., James, C., Gaines, L. & Gallagher, K. *Material and Energy Flows in the Production of Cathode and Anode Materials for Lithium Ion Batteries*. (Argonne National Laboratory, 2015).

83. Song, J. *et al.* Material flow analysis on critical raw materials of lithium-ion batteries in China. *J. Clean. Prod.* **215,** 570–581 (2019).

84. Farjana, S. H., Huda, N. & Mahmud, M. A. P. Life cycle assessment of cobalt extraction process. *Journal of Sustainable Mining* (2019). doi:10.1016/j.jsm.2019.03.002

85. Alvarez, R. A. *et al.* Assessment of methane emissions from the U.S. oil and gas supply chain. *Science* **361,** 186–188 (2018).

86. Farjana, S. H., Huda, N., Parvez Mahmud, M. A. & Saidur, R. A review on the impact of mining and mineral processing industries through life cycle assessment. *J. Clean. Prod.* **231,** 1200–1217 (2019).

87. Amarakoon, S. *Application of Life-Cycle Assessment to Nanoscale Technology: Lithium-ion Batteries for Electric Vehicles* . (U.S. Environmental Protection Agency, 2013).

88. Montzka, S. A. *et al.* A decline in global CFC-11 emissions during 2018-2019. *Nature* **590,** 428–432 (2021).

89. de Vries, M., van Middelaar, C. E. & de Boer, I. J. M. Comparing environmental impacts of beef production systems: A review of life cycle assessments. *Livest. Sci.* **178,** 279–288 (2015).

90. Heimes, H. *et al. Lithium-ion Battery Cell Production Process*. (PEM of RWTH Aachen University, 2018).

91. Ciez, R. E. & Whitacre, J. F. Examining different recycling processes for lithium-ion batteries. *Nat. Sustain.* **2,** 148–156 (2019).

92. Dai, Q., Kelly, J. C., Gaines, L. & Wang, M. Life Cycle Analysis of Lithium-Ion Batteries for Automotive Applications. *Batteries* **5,** 48 (2019).

93. Ahmed, S., Nelson, P. A., Gallagher, K. G. & Dees, D. W. Energy impact of cathode drying and solvent recovery during lithium-ion battery manufacturing. *J. Power Sources* **322,** 169–178 (2016).

94. Wood, D. L. *et al.* Technical and economic analysis of solvent-based lithium-ion electrode drying with water and NMP. *Drying Technology* **36,** 234–244 (2018).

95. Wood, D. L., Li, J. & Daniel, C. Prospects for reducing the processing cost of lithium ion batteries. *J. Power Sources* **275,** 234–242 (2015).

96. Wang, M. *GREET2 2020*. (Argonne National Laboratory, 2020).

97. Susarla, N. & Ahmed, S. *Estimating the Cost and Energy Demand of Producing Lithium Manganese Oxide for Li-ion Batteries*. (Argonne National Laboratory, 2020).

98. Meyer, C., Bockholt, H., Haselrieder, W. & Kwade, A. Characterization of the calendering process for compaction of electrodes for lithium-ion batteries. *Journal of Materials Processing Technology* **249,** 172–178 (2017).

99. Ahmed, S., Nelson, P. A. & Dees, D. W. Study of a dry room in a battery manufacturing plant using a process model. *J. Power Sources* **326,** 490–497 (2016).

100. Kurland, S. D. Energy use for GWh-scale lithium-ion battery production. *Environ. Res. Commun.* **2,** 012001 (2019).

101. Frith, J. & Goldie-Scot, L. *2019 Lithium Ion Battery Price Survey*. (Bloomberg Finance, 2019).

102. Ryan, N. A., Lin, Y., Mitchell-Ward, N., Mathieu, J. L. & Johnson, J. X. Use-Phase Drives Lithium-Ion Battery Life Cycle Environmental Impacts When Used for Frequency Regulation. *Environ. Sci. Technol.* **52,** 10163–10174 (2018).

103. Jenu, S. *et al.* Reducing the climate change impacts of lithium-ion batteries by their cautious management through integration of stress factors and life cycle assessment. *Journal of Energy Storage* **27,** 101023 (2020).

104. Jones, C., Gilbert, P. & Stamford, L. Assessing the climate change mitigation potential of stationary energy storage for electricity grid services. *Environ. Sci. Technol.* **54,** 67–75 (2020).

105. Kabir, M. M. & Demirocak, D. E. Degradation mechanisms in Li-ion batteries: a state-of-the-art review. *Int. J. Energy Res.* **41,** 1963–1986 (2017).

106. Nazari, A., Esmaeeli, R., Hashemi, S. R., Aliniagerdroudbari, H. & Farhad, S. The Effect of Temperature on Lithium-Ion Battery Energy Efficiency With Graphite/LiFePO4 Electrodes at Different Nominal Capacities. in *Volume 2: Heat Exchanger Technologies; Plant Performance; Thermal Hydraulics and Computational Fluid Dynamics; Water Management for Power Systems; Student Competition* (American Society of Mechanical Engineers, 2018). doi:10.1115/POWER2018-7375

107. Gao, Y., Jiang, J., Zhang, C., Zhang, W. & Jiang, Y. Aging mechanisms under different state-of- charge ranges and the multi-indicators system of state-of-health for lithium-ion battery with Li(NiMnCo)O2 cathode. *J. Power Sources* **400,** 641–651 (2018).

108. Kang, J., Yan, F., Zhang, P. & Du, C. Comparison of comprehensive properties of Ni-MH (nickel- metal hydride) and Li-ion (lithium-ion) batteries in terms of energy efficiency. *Energy* **70,** 618–625 (2014).

109. Spotnitz, R. Simulation of capacity fade in lithium-ion batteries. *J. Power Sources* **113,** 72–80 (2003).

110. Ashwin, T. R., Chung, Y. M. & Wang, J. Capacity fade modelling of lithium-ion battery under cyclic loading conditions. *J. Power Sources* **328,** 586–598 (2016).

111. Yang, F., Wang, D., Zhao, Y., Tsui, K.-L. & Bae, S. J. A study of the relationship between coulombic efficiency and capacity degradation of commercial lithium-ion batteries. *Energy* **145,** 486–495 (2018).

112. Waag, W., Käbitz, S. & Sauer, D. U. Experimental investigation of the lithium-ion battery impedance characteristic at various conditions and aging states and its influence on the application. *Appl. Energy* **102,** 885–897 (2013).

113. Osaka, T., Nakade, S., Rajamäki, M. & Momma, T. Influence of capacity fading on commercial lithium-ion battery impedance. *J. Power Sources* **119–121,** 929–933 (2003).

114. Sathre, R., Scown, C. D., Kavvada, O. & Hendrickson, T. P. Energy and climate effects of second- life use of electric vehicle batteries in California through 2050. *J. Power Sources* **288,** 82–91 (2015).

115. Longo, S., Antonucci, V., Cellura, M. & Ferraro, M. Life cycle assessment of storage systems: the case study of a sodium/nickel chloride battery. *J. Clean. Prod.* **85,** 337–346 (2014).

116. Johnson, J. X., McMillan, C. A. & Keoleian, G. A. Evaluation of life cycle assessment recycling allocation methods. *J. Ind. Ecol.* **17,** 700–711 (2013).

117. Hendrickson, T. P., Kavvada, O., Shah, N., Sathre, R. & D Scown, C. Life-cycle implications and supply chain logistics of electric vehicle battery recycling in California. *Environmental Research Letters* **10,** 014011 (2015).

118. Sun, X., Luo, X., Zhang, Z., Meng, F. & Yang, J. Life cycle assessment of lithium nickel cobalt manganese oxide (NCM) batteries for electric passenger vehicles. *J. Clean. Prod.* **273,** 123006 (2020).

119. Gaines, L. Lithium-ion battery recycling processes: Research towards a sustainable course. *Sustainable Materials and Technologies* **17,** e00068 (2018).

120. Casals, L. C., García, B. A., Aguesse, F. & Iturrondobeitia, A. Second life of electric vehicle batteries: relation between materials degradation and environmental impact. *Int. J. Life Cycle Assess.* **22,** 82–93 (2017).

121. Cicconi, P., Landi, D., Morbidoni, A. & Germani, M. Feasibility analysis of second life applications for Li-Ion cells used in electric powertrain using environmental indicators. in *2012 IEEE International Energy Conference and Exhibition (ENERGYCON)* 985–990 (IEEE, 2012). doi:10.1109/EnergyCon.2012.6348293

122. Bobba, S. *et al.* Life Cycle Assessment of repurposed electric vehicle batteries: an adapted method based on modelling energy flows. *Journal of Energy Storage* **19,** 213–225 (2018).

123. Cusenza, M. A., Guarino, F., Longo, S., Mistretta, M. & Cellura, M. Reuse of electric vehicle batteries in buildings: An integrated load match analysis and life cycle assessment approach. *Energy and Buildings* **186,** 339–354 (2019).

124. V elázquez-Martínez, V alio, Santasalo-Aarnio, Reuter & Serna-Guerrero. A Critical Review of Lithium-Ion Battery Recycling Processes from a Circular Economy Perspective. *Batteries* **5,** 68 (2019).

125. Lattanzio, R. & Clark, C. *Environmental Effects of Battery Electric and Internal Combustion Engine Vehicles*. (Congressional Research Service, 2020).

126. Yang, Y., Guo, Y., Zhu, W. & Huang, J. Environmental impact assessment of China's primary aluminum based on life cycle assessment. *Transactions of Nonferrous Metals Society of China* **29,** 1784–1792 (2019).

127. Schomberg, A. C., Bringezu, S. & Flörke, M. Extended life cycle assessment reveals the spatially- explicit water scarcity footprint of a lithium-ion battery storage. *Commun. Earth Environ.* **2,** 11 (2021).

128. Heath, G. A. & Mann, M. K. Background and reflections on the life cycle assessment harmonization project. *J. Ind. Ecol.* **16,** S8–S11 (2012).

Chapter 3

Temporal Variations in Learning Rates of Li-ion Technologies: Insights for Price Forecasting and Policy through Segmented Regression Analysis

3.1 Introduction

3.1.1 Motivation

Over the last three decades, lithium ion (Li-ion) batteries have revolutionized multiple sectors of the global economy, beginning with the proliferation of portable electronics, and now helping achieve environmental goals through vehicle electrification and grid decarbonization. The normalized price ($/kWh) of Li-ion cells has declined rapidly, dropping over 97% since their initial commercial availability in 1991.[1] Li-ion modules, which consist of several cells combined into a single unit, and total installed costs for stationary storage systems have also seen substantial price decreases since their introduction in more recent years.[2–7] Despite these substantial declines, further cost reductions are needed to meet policy goals. In 2022, the average Li-ion battery module was estimated to be $138/kWh,[8] whereas the U.S. Department of Energy has an official manufactured cost target of $80/kWh for electric vehicle batteries and a 90% cost reduction from 2020-2030 for long-duration (over 10 hours) energy storage systems.[9,10] In order to meet these policy goals and continue sustainable development and deployment of Li-ion batteries, it is critical to understand the drivers and patterns of historical cost reductions and how they inform the potential future costs of the technology. More specifically, we must improve our understanding of technology learning rates, which are widely used in system dynamics models, policy analyses, and forecasting activities that inform technology research and investment decisions. Though learning rates are typically calculated as a single historical value, this study is the first to apply a segmented regression approach to traditional experience curve analysis for Li-ion batteries with the goal of exploring how and why learning rates for Li-ion batteries change over time, providing insights to better inform the uncertainty in future Li-ion technology price forecasting and policy development.

3.1.2 Review of the Li-ion Technologies Learning Rates in Literature

Past literature on Li-ion technologies assume that learning rates remain constant over the entire history of the technology. However, research on a variety of energy technologies has considered segmented experience curves and found statistically significant changes in the rate over time.[11–14] Research on the costs of Li-ion technologies typically focuses on costs at the cell level, though costs of higher-level “tiers" of systems, namely modules and installed costs, may be more relevant to certain analyses. Table 3.1 presents the learning rates of a variety of Li-ion technologies from relevant literature and time period examined for each study.

Table 3.1. Li-ion technology learning rates in literature.[1–3,15–17]

Learning Rate	Li-ion Technology	Time Period	Source
30	Cells - Electronics	1995 - 2011	Schmidt et al 2017
16.3 - 17	Cells	1993 - 2004	Gerssen-Gondelach and Faij 2012
24	Cells - Cylindrical	1992 - 2016	Ziegler and Trancik 2021
20.4	Cells - All	1992 - 2016	Ziegler and Trancik 2021
16	Pack - EV	2010 - 2016	Schmidt et al 2017
9	Packs - EV	2011 - 2015	Nykvist and Nilsson 2015
16.6	Packs - EV	2010 - 2019	Hsieh et al. 2019
25.28	Packs - Unspecified	2007 - 2019	Penisa et al. 2020
12	Stationary - Residential	2013 - 2016	Ziegler and Trancik 2021
12	Stationary - Utility	2010 - 2015	Ziegler and Trancik 2021

From Table 3.1 we can see that the learning rate for Li-ion cells in literature ranges between 16.3% and 30.0%. All analyses assume this learning rate is constant over time. Literature on Li-ion battery packs shows learning rates ranging from 9% to 20.8%. Only one source has constructed experience curves on total installed costs of stationary storage, finding a learning rate of 12%. Only one source, Nykvist and Nilson,[3] performed an experience curve analysis using cost instead of price.

In contrast with these prior studies, we apply segmented regression to experience curves for Li-ion technologies to describe the historical variations in learning rates. We employ the methodology outlined in Smith et al.[13] to identify time periods with statistically distinct learning rates. We propose that understanding the relationship between these periods in a segmented experience curve and the development of Li-ion markets can explain the variance of Li-ion learning rates in literature. Additionally, we propose that the multiple learning rates from a segmented experience curve can be used to better inform the uncertainty in the future prices of Li-ion technologies, leading to improved price forecasting and policy development.

3.2 Theoretical Framework, Methods, and Data

3.2.1 Theoretical Framework

This work aims to build on the foundational learning curve analysis that typically follows Wright's law, while also better accounting for temporal variations and cost patterns in technology learning analysis. This improvement is accomplished by applying the segmented regression approach and utilizing price data instead of cost data.

Segmented regression analysis has proven valuable in diverse research fields for exploring and comprehending relationships between variables that may display distinct patterns within different segments of the data. This statistical method is especially advantageous when examining cases with abrupt changes or shifts in the relationship between variables. In learning curve analysis, the literature[18] suggests that projecting the learning rate beyond 3-4 doublings of cumulative

production may lead to significant under or overestimation of costs. This indicates that the relationship between the cost of a technology and the cumulative production volume can change over time, resulting in temporary variations in learning rates.

Wright's law[19] proposes that an increase in the cumulative production of a good results in an increased efficiency in production, observable as a decrease in a good's cost. The rate at which the cost declines is often expressed as a learning rate, which is quantified as the percent cost decrease for every doubling in cumulative production. Equations 1 and 2 outline Wright's law and the mathematical representation of a learning rate, where Y represents the cost of a product over time, X represents the cumulative production of the product over time, a and b are coefficients derived by regression, and LR represents the learning rate.

Equation 1. $Y=aX^b$
Equation 2. $LR = 1 - 2^b$

This formulation is useful for describing overall cost reductions (either sector-wide or at a specific facility) but developing true learning curves via Wright's Law's often poses a challenge for analysts, in that actual *cost* data is difficult to obtain due to the confidential nature of the manufacturing industry. Thus, *price* data is often used instead; when prices are used as the Y values in Equation 1, the result is referred to as an experience curve rather than a learning curve. The learning rate developed from this experience curve therefore captures cost reductions that come from multiple factors beyond the technological "learning" that Wright set out to describe. Though multiple drivers of cost reduction are captured, the formulation is unable to provide insight on individual mechanisms affecting cost reductions. More information on individual cost reduction factors and their modeling through learning rates can be found in Appendix A1.

The differences between price and underlying cost will cause learning rates based on experience curves to differ from those based on learning curves. Further, the price vs. cost relationship is thought to evolve as a technology matures, as described originally by Boston Consulting Group (BCG).[20] The BCG model separates the price dynamics of a technology into three main phases: (1) "Development," (2) "Shakeout," and (3) "Stability." "Development" describes the period when a technology is novel on a market and typically has relatively constant prices (less than 10% learning rate, according to IEA[21] even as costs initially fall. This is followed by a "Shakeout" period in which price reduction accelerates (typical learning rate of 60%). The Shakeout phase is considered a correction period, where inflated prices (due to limited market competition and a holdover from early creators recouping their losses from the development phase) are brought down to be better aligned with costs, as expected in a competitive market. Finally, a "Stability" phase occurs as technological knowledge of a good depreciates and its market matures, causing price reductions to mimic the underlying cost reductions and observed learning continues, though at a slower rate than in the "Shakeout" period.

3.2.2 Methods

This study aims to describe the variance in learning rates of Li-ion technologies attributable to the behavior documented by BCG by applying segmented regression to an experience curve analysis. Experience curves are constructed by graphing a representative price in a given year

against the cumulative production of a technology (in this case, GWh of Li-ion cells, modules, or installed systems) that had been produced up until that year. Cumulative production data from multiple sources was aggregated into representative series for each Li-ion system tier studied here. The uncertainty behind these series was explored in low, medium and high scenarios, though learning rate results were not found to be sensitive to this underlying assumption.

Segmented experience curves were developed using the methodology described in Smith et al.,[13] where learning curves are iteratively generated for an increasing number of change points and evaluated for best fit and statistical justification. For a given number of change points, the location of the breakpoints that lead to the lowest mean squared error (MSE) are chosen. We tested models with up to three breakpoints for cells and up to two breakpoints for modules and installed costs (due to the shorter time period those datasets cover). Model selection between different numbers of breakpoints (i.e. a constant learning rate compared to ones that change once or twice over time) is based on the Akaike Information Criterion (AIC), which evaluates the justification of the additional degree of freedom that an additional breakpoint provides. The results from the segmented experience curve are compared against constant learning rates from literature. A discussion on the behavior described by the segmented experience curve and its implications on forecasting is also presented.

3.2.2 Data

3.2.2.1 Li-ion Battery Prices

Data on the price of Li-ion technologies at all tiers (cells, modules, and total installed costs for consumer, EV, and stationary batteries) was collected from literature. In total, over 9,000 data points were collected globally. The vast majority of these (8,000) are for installed stationary systems, mostly coming from the California SGIP database. Otherwise, data points are split relatively evenly across cells (330), modules (350), BOS (310), soft costs (260) and unspecified (110). Representative series were generated from the collected data in order to perform experience curve analysis. Descriptions of the methods used to produce the representative series are available in the Appendix A2. Figure 3.1 displays the price data points and the representative series used in this study.

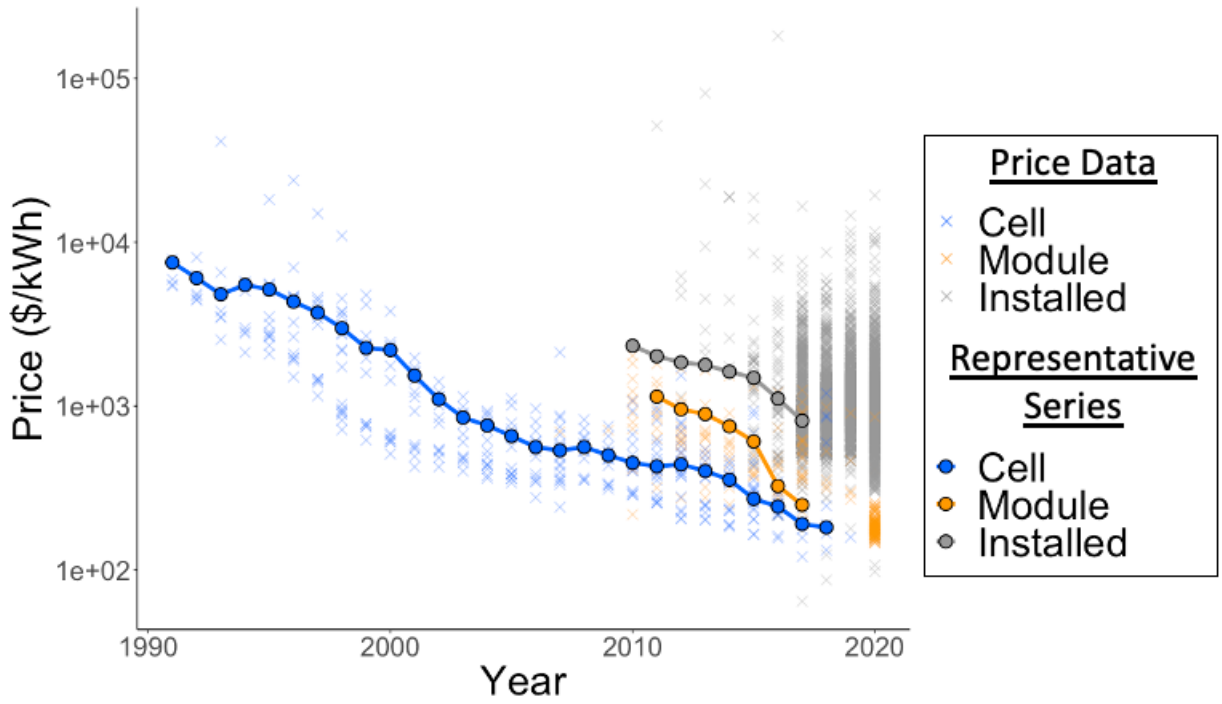

Figure 3.1. Individual price data points and representative price series overtime.

3.2.2.2 Cumulative Production of Li-ion Batteries

Representative series for the cumulative production of Li-ion technologies was determined from a number of different sources.[1,2,22–29] Appendix A2 outlines the procedure for creating these representative series, visualized in Figure 3.2a. Additionally, to aid in analyses, the cumulative storage capacity of all Li-ion technologies distinguished their market applications (consumer, EV, or stationary) visualized in Figure 3.2b. This was done by assuming the remainder of modules when stationary storage is removed are used for EV applications, and the remainder of cells when module capacity is removed are used for general consumer applications

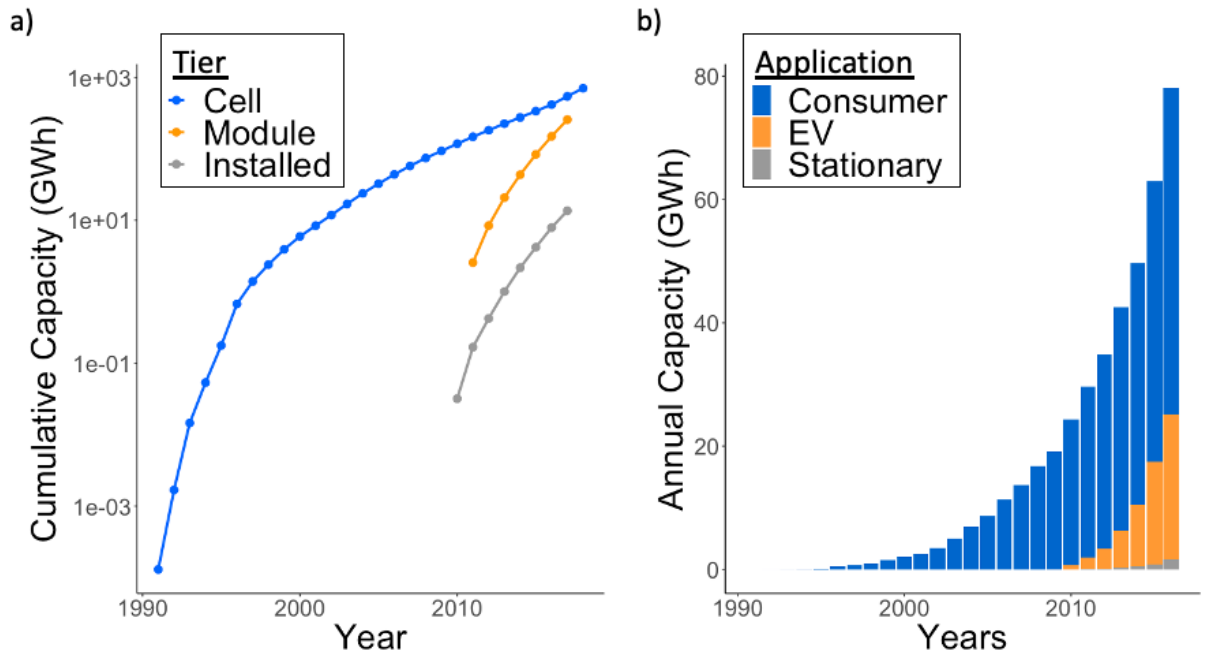

Figure 3.2. a) Cumulative capacity of Li-ion technology tiers overtime. b) Annual capacity of Li-ion technology applications overtime.

3.3 Results

3.3.1 Historical Variations in Learning Curves

The results of the segmented experience curve analysis are presented in Figure 3.3. The red solid lines show the curve with the maximum statistically-justified breakpoints, while the gray dashed lines results for additional numbers of breakpoints. Additionally, Table 3.2 summarizes the learning rates, uncertainty, AICs, and MSEs from all relevant segmented experience curve analyses.

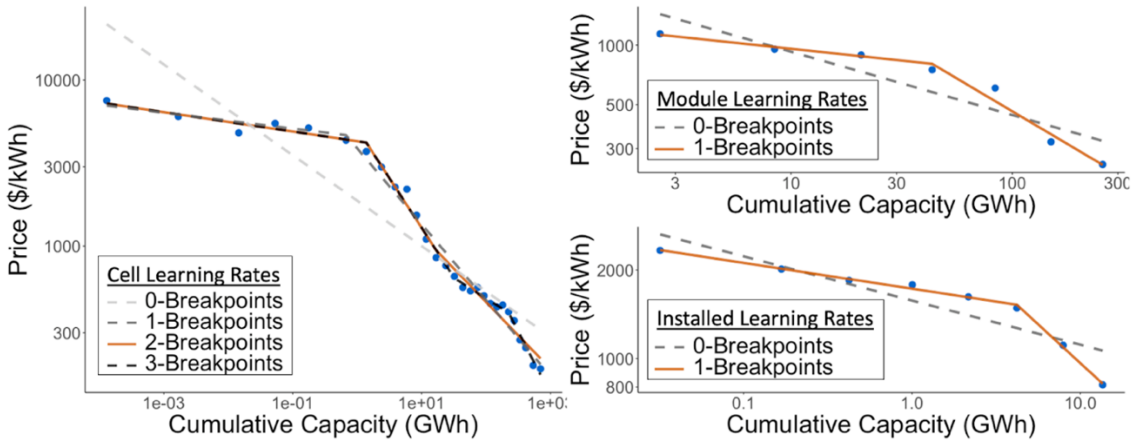

Figure 3.3. Learning rates for Li-ion technology tiers.

Table 3.2. Learning rates for Li-ion technology tiers over time.

Tier	Breakpoints	Learning Rates (%)							AIC	MSE
		1991	1995	2000	2005	2010	2015	2018		
Cell	0	17.3 +/- 1.3							39.3	0.46
	1	3.3 +/- 1.1		27.2 +/- 1.5					-22.5	0.14
	2	4.0 +/- 0.9		34.0 +/- 2.1		24.4 +/- 3.8			-24.4	0.12
	3	4.0 +/- 0.9		34.0 +/- 2.1		15.7 +/- 3.2		40.9 +/- 4.5	-19.4	0.08
Modules	0					19.9 +/- 3.7			4.6	0.26
	1					7.9 +/- 2.8	36.8 +/-4.8		-4.8	0.10
Installed	0					9.9 +/- 1.8			-3.0	0.02
	1					5.9 +/-3.2	30.6 +/- 1.1		-31.4	0.02

For Li-ion cells, the traditional experience curve (0 breakpoints) shows a learning rate of 17.3%. However, the statistically significant 2-breakpoint model found that the learning rate was much lower from 1991-1997 (4.0%) before increasing significantly from 1997 through 2003 (34.0%), then declining through 2018 (24.4%). The 3-breakpoint cell model showed that the 2003-2018 time period is perhaps more accurately split into two, with a learning rate of 15.7% from 2003-2013 and 40.8% from 2013-2018. This breakpoint was not statistically justified (via the AIC), though future analysis with more data collection from recent years may show with more certainty that a second acceleration in the learning rate has occurred.

A 1-breakpoint model is most representative for Li-ion modules, with a modest learning rate in the first few years (7.9%) before significant acceleration after 2014 (36.8%); the installed cost experience curve shows a similar pattern, but with a slightly lower learning rate (5.9% 2010-2015, 30.6% 2015-2017). The constant learning rate model for modules installed costs are 19.9% and 9.9%, respectively. Learning rate values and trends for both modules and installed costs mimic the early years (1991-2003) of the cell learning curve. While our analysis finds the 1 breakpoint model to be statistically significant for modules and installed systems, one can qualitatively observe that the number of data points in each segment are small, potentially indicating statistically insignificance. Therefore, learning rate results for modules and installed systems are more likely to change as additional years of data are observed.

3.3.2 Comparison with Prior Works

When employing traditional learning curve techniques, the results of the learning rate are frequently heavily influenced by the time during which the research was conducted. Figure 3.4 shows the learning rates found in this study in comparison to previously published values. The length of a given line in the figure represents the years over which the study assessed the learning rate. As shown in Figure 3.4a, where we compare our cell learning rates to four results from three other publications,[1,2,15] studies that assess earlier years of data tend to have lower learning rates. This is consistent with our finding that the cell learning rate was much lower in the first six years of the technology than afterwards. Schmidt et al.'s analysis produced the highest learning rate previously published, utilizing data from 1995-2011.[2] This value is aligned with this study's post-1997 results, which sit slightly above and then slightly below their finding. However, it is still significantly lower than the 2013-2018 learning rate from our 3-breakpoint model.

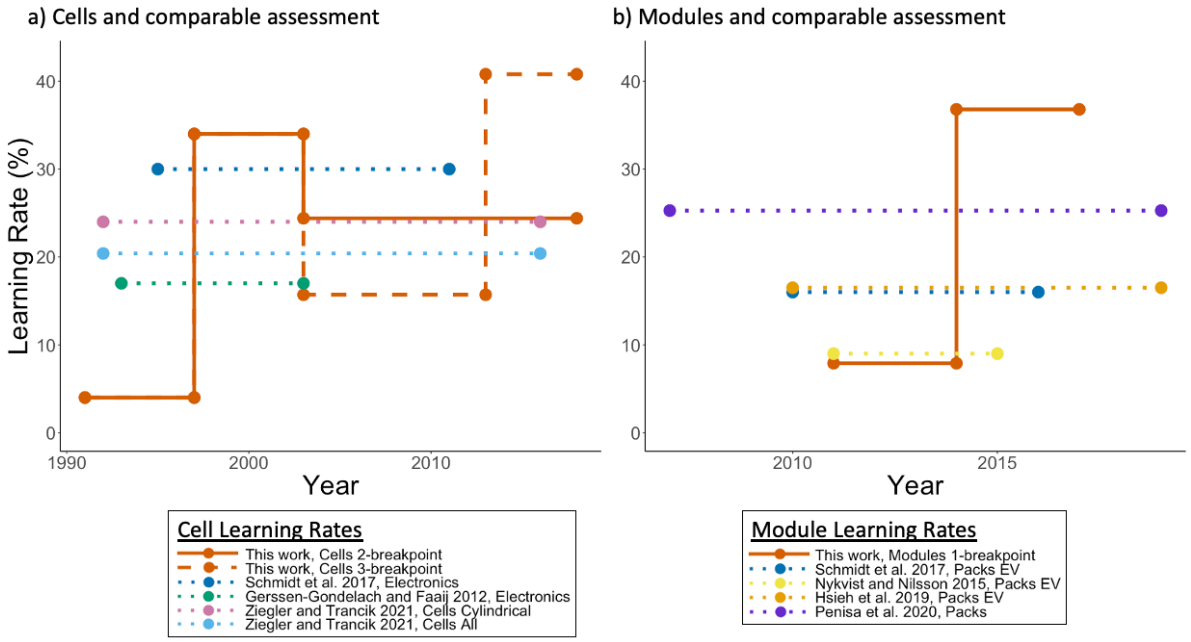

Figure 3.4. Comparison of learning rate results to previously published values, for (a) cells and (b) modules. [1–3,15–17]

The impact of study timeline on results is even more pronounced in literature on Li-ion modules and packs, shown in Figure 3.4b. Nykvist and Nilsson's[3] 2011-2015 learning rate is nearly identical to this study's 2011-2014 result, while other studies that included later years of data found higher learning rates. But again, even the highest value previously published, 25.5% in Pensia et al.,[17] is much lower than the recent learning rate observed in this study. Comparison for installed costs is not visualized, as only one prior study[2] had a comparable value (12% for 2010-2015), which was higher than our rate over that same time period (5.9%), but much lower than later years in our analysis.

3.4 Discussion

3.4.1 Learning Rates and Market Behavior

The 2 breakpoint learning rate model for Li-ion cells shows a clear agreement with the price phases identified by BCG,[20] further supported by the cumulative capacity of Li-ion technologies presented in Figure 3.2. Between 1991 and 1997, the low learning rate of 4.0%, as well as the small cumulative capacity of Li-ion technology indicates that the technology was in a "Development" and "Price Umbrella" resulting from its novel commercialization. From 1997 through 2003, the high learning rate of 34.0% indicates a "Shakeout" period where price reduction occurs at a rapid rate. This is supported by the increasing cumulative capacity during this period, indicating greater sales of Li-ion technology. Between 2003 and 2018, the learning rate of 24.4% indicates a "Stabilization" period, indicating a maturity of the technology. However, it is noteworthy that this learning rate is slightly higher than those typically associated with mature technologies.[21]

This anomaly can be explained if we consider the 3-breakpoint model and examine the time period of 2003 to 2013 and 2013 to 2018 as separate. From 2003 to 2013, the learning rate of 15.7% indicates a "Stabilization" period and agrees with the learning rates of mature technologies.[21] Additionally, the relatively consistent rate of growth of the cumulative capacity of Li-ion technologies indicates a stable market for Li-ion technologies. In this period, the majority of battery capacity is still dominated by the consumer portable applications and the technology is relatively more mature compared EV batteries. Based on international patent analysis,[30] the number of patents targeting electric vehicles overtook consumer electronics in 2011 and, while patents for portable electronic battery pack designs levelled off after this time, electric vehicle patents continued to grow with even more vigorously, primarily dominated by Japanese companies. Interestingly, between 2013 and 2018, the high learning rate of 40.8% indicates a second "Shakeout" period. At first glance, this secondary "Shakeout" appears to contradict the idea of knowledge depreciation and market maturity that occurs during the "Stability" phase. However, we observe that the EV market experienced rapid growth during this time period, as visualized by Figure 3.2, spurring the additional cost reduction mechanisms that offset knowledge depreciation. This may be attributable to more aggressive EV and renewable energy targets and incentives issued in different parts of the world since 2010,[31] in tandem with the rapid growing EV batteries patenting activities since 2009.[30] The effects of knowledge depreciation may also be mitigated by reduction in labor requirements, changes in raw materials costs, or new manufacturing and engineering advancements, and therefore the learning rate may even rise as knowledge depreciation occurs.[32] Additionally, discontinuities in the learning curve may occur from "technology structural change", "a new variant of the technology or a major change in the way the technology is produced."[33] These factors, along with more competition emerging as the global market developed[34,35] all contributed to a this secondary "Shakeout," suggesting a pathway where the growth of new market applications of a good can provoke technological change and competition, leading to another "Shakeout" of a good. The preliminary results from the module and installed experience curve analysis indicate that these Li-ion technologies are undergoing similar stages of development to the early phases of Li-ion cell development that was dominated by the consumer portable applications. Further discussions can be made on these technologies as more data points become available with time. However, all models explored have a lower AIC than a generic experience curve (0-breakpoint model), indicating greater statistical significance than traditional methods.

3.4.2 Learning Scenarios for Uncertainty in Forecasting

Many modeling tools and analyses forecast technology prices using (1) an assumed, constant learning rate and (2) a demand forecast. Often uncertainty in these forecasts only arises from the standard errors associated with a learning curve analysis and potential demand scenarios. We propose that incorporating scenarios that correspond to different historical learning rates may allow for a greater understanding of likely scenarios in price forecasting. To demonstrate this, we performed an uncertainty analysis on the future price of Li-ion cells, starting from 2021 (sample year 0). We forecast cell prices 14 years forward using three global Li-ion demand forecasts and four different learning rates. The medium demand forecast comes from Bloomberg,[36] and the high and low forecasts are then generated by raising and lowering annual demand by 20% before summing up the series to the cumulative production (Appendix A3).

Four different learning rates are applied based on historical data for Li-ion cells as well as other mature technologies. The "Average Learning" rate of 17.3% represents the constant Li-ion cell learning rate from 1991 to 2018, while "Stability Learning" rate of 24.4% and the "Shakeout Learning" rate of 40.5% represent the final segments of our 2- and 3-breakpoint cell learning curves, respectively. The fourth learning rate modeled represents the potential learning rate of Li-ion cells once the technology is considered fully mature, meaning no more significant technological advancements are occurring. This scenario is included because even the modest learning rates seen in the Li-ion cell analysis are quite high relative to mature technologies. An aggregation of 108 energy technology learning rates (representing both mature and developing technologies) found an average value of 18%, with 10% of cases having learning rate less than 10.5%.[37] Additionally, technologies in earlier stages of development (less cumulative production) are found to have higher learning rates than more mature technologies.[37] Therefore, the "Mature Learning" rate of 10.5% is selected to demonstrate this potential future.

The resulting twelve price scenarios are presented in Figure 3.5. Within a learning scenario, adjusting demand has a modest effect on forecasted Li-ion cell prices, at most causing a 17.6% difference by year 14. However, price forecasts vary significantly between learning scenarios, at most causing a 79.0% - 83.3% difference between demand scenarios by the end of the observed period. With a medium demand scenario, the Mature Learning scenario sees a price reduction of 36.4%, the Average Learning scenario sees a price reduction of 53.8%, the Stability Learning scenario sees a price reduction of 67.9%, and the Shakeout Learning scenario sees a price reduction of 88.2% by the end of the observed period. Knowing which learning and demand scenarios (or combination of scenarios) are most likely to occur is impossible to predict with certainty. However, the high variation in potential prices among scenarios highlights the importance of performing a thorough uncertainty analysis, since using a single learning rate may vastly mischaracterize the uncertainty in forecasted prices. Understanding the differences in prices among these scenarios and what market behaviors may lead to potential scenarios is crucial for informed decision making.

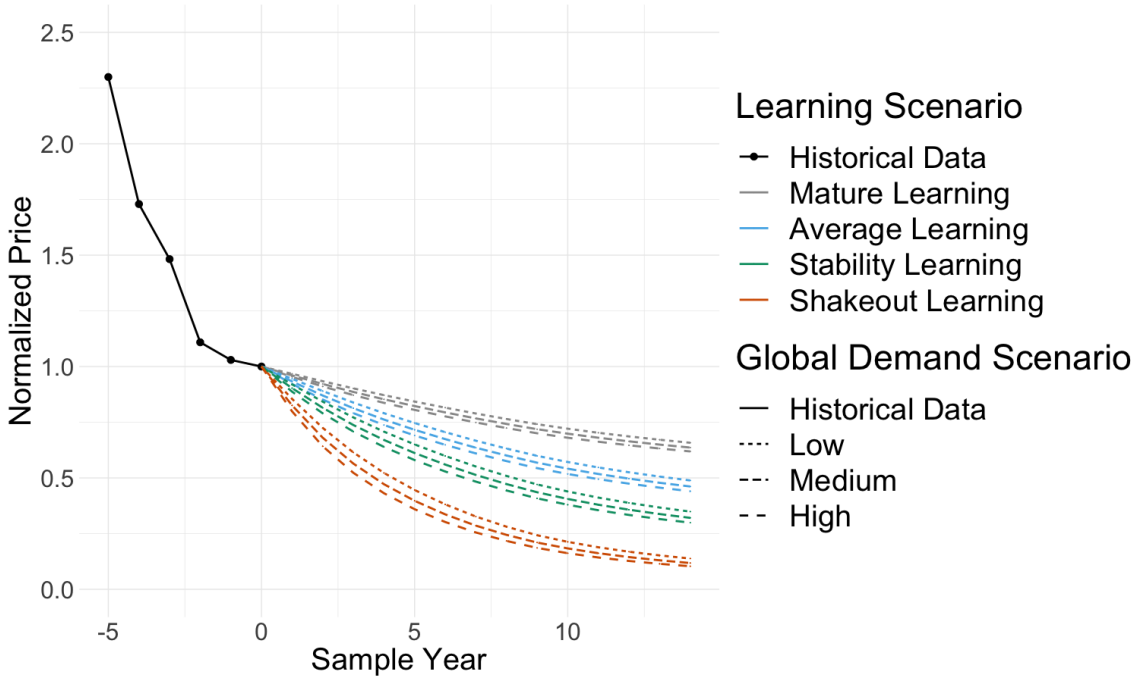

Figure 3.5. Forecasted Li-ion cell prices in different demand and learning scenarios

3.5 Conclusions

Our segmented experience curve analysis shows both a greater conceptual agreement and statistical justification with existing price behavioral analyses than studies that perform traditional experience curves with Li-ion technology prices. A segmented experience curve analysis should be performed when using price instead of cost in order to gain greater insight and a more accurate description of the price reductions over time. Our novel application of these methods to Li-ion technologies exemplifies the importance of using segmented experience curves to better understand the temporal patterns of Li-ion technology changes. For instance, we identified different learning rates for lithium-ion cells: the learning rate was 4% through 1997, 34% through 2003, and 24.4% onward. Additionally, by allowing greater flexibility in the experience curve, a secondary period of increased learning (40.9%) emerges from 2013 onward. This secondary "Shakeout" aligns well with Li-ion market behavior but is slightly less statistically significant than the previous model; however, this model may emerge as significant with the availability of more price and market size data.

Using a segmented experience curve may have significant implications on the modeling of uncertainty for price forecasting. Traditional forecasting approaches use a limited number of learning rates, typically centered around the average learning rate across the lifespan of the technology. This modeling approach does not account for the effects of market emergence and technological change that may still occur, a consideration especially important for batteries given the ongoing growth of the EV market and the emergence of stationary applications.[26,34,38] Excluding these considerations from price forecasting of Li-ion technologies may lead to artificially diminish uncertainties since the learning rates may deviate significantly from the average learning rate as they have in the past. Examining historical learning rates through the

segmented regression experience curve model employed in this study allows for greater consideration of these price dynamics into the future.

References

1. Ziegler, M. S. & Trancik, J. E. Re-examining rates of lithium-ion battery technology improvement and cost decline. Energy Environ. Sci. (2021) doi:10.1039/D0EE02681F.

2. Schmidt, O., Hawkes, A., Gambhir, A. & Staffell, I. The future cost of electrical energy storage based on experience rates. Nat. Energy **6**, 17110 (2017).

3. Nykvist, B. & Nilsson, M. Rapidly falling costs of battery packs for electric vehicles. Nat. Clim. Chang. **5**, 329–332 (2015).

4. Cole, W. & Karmakar, A. Cost Projections for Utility-Scale Battery Storage: 2023 Update. (2023).

5. Viswanathan, V. et al. 2022 Grid Energy Storage Technology Cost and Performance Assessment. (2022).

6. U.S. Energy Information Administration. Battery Storage in the United States: An Update on Market Trends. (2021).

7. Ramasamy, V., Feldman, D., Desai, J. & Margolis, R. U.S. Solar Photovoltaic System and Energy Storage Cost Benchmarks: Q1 2021. (2021).

8. Henze, V. Lithium-ion Battery Pack Prices Rise for First Time to an Average of $151/kWh. BloombergNEF https://about.bnef.com/blog/lithium-ion-battery-pack-prices-rise-for-first-time-to-an-average-of-151-kwh/ (2022).

9. U.S. DOE. Energy Storage Grand Challenge Roadmap. https://www.energy.gov/energy-storage-grand-challenge/downloads/energy-storage-grand-challenge-roadmap (2020).

10. U.S. DOE. Long Duration Storage Shot. U.S. Department of Energy Office of Energy Efficiency and Renewable Energy https://www.energy.gov/eere/long-duration-storage-shot (2021).

11. Van Buskirk, R. D., Kantner, C. L. S., Gerke, B. F. & Chu, S. A retrospective investigation of energy efficiency standards: policies may have accelerated long term declines in appliance costs. Environmental Research Letters **9**, 114010 (2014).

12. Bolinger, M., Wiser, R. & O'Shaughnessy, E. Levelized cost-based learning analysis of utility-scale wind and solar in the United States. iScience **25**, 104378 (2022).

13. Smith, S. J., Wei, M. & Sohn, M. D. A retrospective analysis of compact fluorescent lamp experience curves and their correlations to deployment programs. Energy Policy **98**, 505–512 (2016).

14. Wei, M., Smith, S. J. & Sohn, M. D. Non-constant learning rates in retrospective experience curve analyses and their correlation to deployment programs. Energy Policy **107**, 356–369 (2017).

15. Gerssen-Gondelach, S. J. & Faaij, A. P. C. Performance of batteries for electric vehicles on short and longer term. J. Power Sources **212**, 111–129 (2012).

16. Hsieh, I.-Y. L., Pan, M. S., Chiang, Y.-M. & Green, W. H. Learning only buys you so much: Practical limits on battery price reduction. Appl. Energy **239**, 218–224 (2019).

17. Penisa, X. N. et al. Projecting the Price of Lithium-Ion NMC Battery Packs Using a Multifactor Learning Curve Model. Energies **13**, 5276 (2020).

18. Taylor, M. & Fujita, K. S. Accounting for Technological Change in Regulatory Impact Analyses: The Learning Curve Technique. (2013).

19. Wright, T. P. Factors affecting the cost of airplanes. Journal of the Aeronautical Sciences **3**, 122–128 (1936).

20. Henderson, B. The Experience Curve. https://www.bcg.com/publications/1968/business-unit-strategy-growth-experience-curve (1968).

21. International Energy Agency. Experience Curves for Energy Technology Policy. (2000).

22. Kittner, N., Lill, F. & Kammen, D. M. Energy storage deployment and innovation for the clean energy transition. Nat. Energy **2**, 17125 (2017).

23. Pillot, C. Current Status and Future Trends of the Global Li-ion Battery Market. Avicenne report (2018).

24. Beuse, M., Steffen, B. & Schmidt, T. S. Projecting the Competition between Energy-Storage Technologies in the Electricity Sector. Joule (2020) doi:10.1016/j.joule.2020.07.017.

25. Chalamala, B., Sandia National Laboratories, DOE Office of Electricity & Pacific Northwest National Laboratory. DOE Global Energy Storage Database. Energy Storage Systems Program https://www.sandia.gov/ess-ssl/global-energy-storage-database-home/ (2020).

26. Tsiropoulos, I., Tarvydas, D. & Lebedeva, N. Li-ion Batteries for Mobility and Stationary Storage Applications. (2018).

27. Hocking, M., Kan, J., Young, P., Terry, C. & Begleiter, D. Lithium 101. (2016).

28. Curry, C. Lithium-ion Battery Costs and Market. https://data.bloomberglp.com/bnef/sites/14/2017/07/BNEF-Lithium-ion-battery-costs-and-market.pdf (2017).

29. Lazard. Lazard's Levelized Cost of Storage Analysis - Version 6.0. (2020).

30. Gregori, G. et al. Innovation in batteries andelectricity storage: A global analysis based on patent data. (2020).

31. Smith, S. J., Porzio, J. & Zhang, J. Unveiling historical Li-ion cost trends and opportunities for domestic manufacturing: Development of a technology learning framework and analysis ofimplications for the future. (2022).

32. Junginger, M., Faaij, A. & Turkenburg, W. C. Global experience curves for wind farms. Energy Policy **33**, 133–150 (2005).

33. Seegbregts, A. J. Gas-Fired Power. http://www.etsap.org (2010).

34. International Energy Agency. Global EV Outlook 2023. (2023).

35. Bridge, G. & Faigen, E. Towards the lithium-ion battery production network: Thinking beyond mineral supply chains. Energy Research & Social Science **89**, 102659 (2022).

36. BNEF. Lithium-Ion Batteries: State of the Industry 2021. (2021).

37. International Energy Agency. Experience curves for energy technology policy. (OECD, 2000). doi:10.1787/9789264182165-en.

38. U.S. Department of Energy. Energy Storage Grand Challenge: Energy Storage Market Report. (2020).

Chapter 4

Private and External Costs and Benefits of Replacing High-Emitting Peaker Plants with Batteries

The text and research in this chapter was published in *Environmental Science & Technology*. The citation for the published article is as follows:

> Porzio, J., Wolfson, D., Auffhammer, M., & Scown, C. D. (2023). Private and External Costs and Benefits of Replacing High-Emitting Peaker Plants with Batteries. *Environmental Science & Technology*, *57*(12), 4992–5002.

4.1 Introduction

The cost of lithium-ion (Li-ion) batteries has dropped dramatically in the last three decades, making them a competitive option for deployment in electric vehicles, household power management, and grid-scale energy storage.[1–5] These battery energy storage systems (BESS) can help address the intermittency of renewable generation and the need for frequency regulation on the grid.[6-8] Because Li-ion batteries offer fast ramping, they are well suited to mitigate the grid impacts of the "duck curve" in typical summer-peaking regions where renewable energy is plentiful during midday but less available during some of the highest-demand times (e.g., evening and early morning, although this timing may change with the emergence of new technologies like heat pumps).[9-12] Properly operating Li-ion batteries do not emit local or global pollutants at the point of installation, which makes them an attractive replacement for high-emitting "peaker plants," which are often located in disadvantaged communities and operate on hot days when ambient ozone concentrations are high.[13] The practice of decommissioning peaker plants and installing BESS in their place has been hypothesized to generate significant benefits by reducing onsite air pollutant emissions and providing other revenue-generating grid services (e.g., grid stabilization).[14-17]

In California and New York, there are active requests for proposals to replace peaker plants with Li-ion BESS, and the first battery storage installations have already come online (Table B4).[18-22] These facilities aim to earn revenue while avoiding peaker plant generation and its associated emissions. What remains unanswered is how total social costs (private and external) compare to total social benefits for these peaker replacement projects. In other words, if the goal is to reduce greenhouse gas (GHG) emissions and decrease the burden on human health, can these peaker plant replacement projects deliver on their promise? If so, what conditions are required to make the BESS installations economically attractive for profit-maximizing firms and society as a whole? To answer these questions, we evaluate the full life-cycle costs and air quality impacts of replacing California's highest-emitting natural gas peaker plants with BESS. We explore how the net present value (NPV) is impacted by incorporating monetized human health benefits from avoided air emissions as well as revenue from arbitrage and grid services that BESS can provide.

4.2 Materials and Methods

4.2.1 Selection of Natural Gas Peaker Plants

We focused our analysis on California because the state is home to the only completed peaker plant replacement project to-date, in addition to several BESS installations designed to reduce (but not eliminate) peaker activity, with large amounts of energy storage projects that are planned.[19-21] Additionally, due to the high penetration of solar photovoltaics (PV) in California, the state is facing near-term grid impacts associated with the "duck curve" that must be mitigated through energy storage investments and/or fast-ramping power plants.[10-11] To understand the economic attractiveness of BESS replacements for peakers, we selected a set of peaker plants currently operating across California and then modeled their hypothetical replacement. We began the process of selecting peaker plants by considering California's 228 natural gas-fired power plants included in the EPA's Continuous Emissions Monitoring Systems (CEMS); although

California does have oil and diesel-fired generators, these plants are not large enough to be included in CEMS.[23] Peakers were chosen for further analysis if they are in the top quintile of total air emission-related damages (monetized, including climate change and human health) per unit of energy output, have a maximum continuous output (a single generation event) under 1200 MWh, and are not a cogeneration facility. Climate damages were estimated based on the social cost of carbon, and human health damages were modeled using the Estimating Air pollution Social Impact Using Regression (EASIUR) model, as described in Procedure B7. The selection criteria yielded 19 generation facilities for hypothetical replacement. Figure 4.1 displays the location of all plants (selected and not selected) with maximum continuous output under 1200 MWh, their normalized climate and human health damages from stack emissions (CO_2, NO_X, SO_X, and $PM_{2.5}$), and rated power in MW. Upstream/life-cycle emissions were not included in the screening criteria used to select peaker plants for replacement. Operational data and stack emissions for natural gas combusting generators in California are from 2018 through 2020 and were obtained through CEMS.[23] We assume that all modeled BESS are sited as close as possible to the corresponding offset peaker plants in order to reduce uncertainty with geographical market variance and infrastructure requirements. Additionally, each BESS is modeled independently, so the model does not consider any interactions that might occur if multiple peakers were simultaneously replaced with BESS.

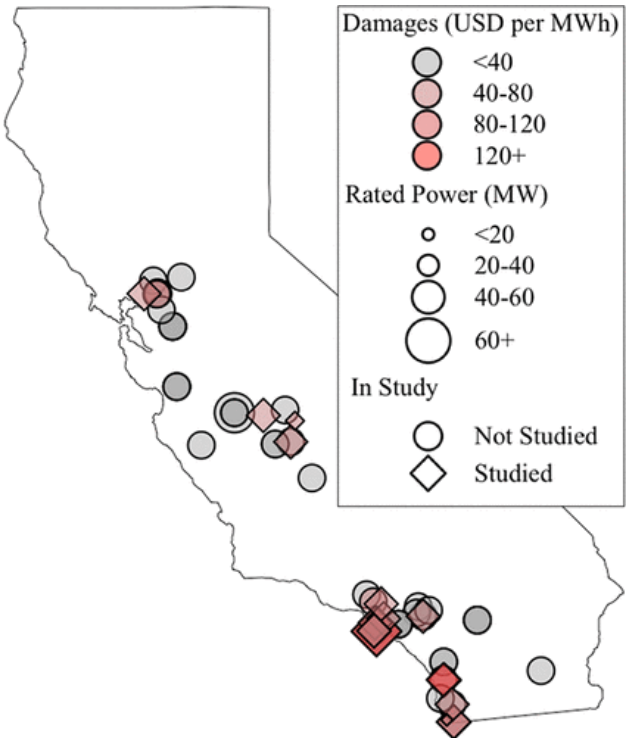

Figure 4.1. Map of natural gas peaker power plants in California. Each natural gas peaker plant is represented by one icon on the map. Color represents the monetized damages per MWh in USD caused by emissions from that plant between 2018 and 2020. Size represents the rated power of a power plant in MW. A circle indicates that replacement by BESS may be feasible but is not studied in the paper. An oblique square indicates that the impacts of replacement by BESS are studied for the natural gas peaker plant.

4.2.2 Battery Energy Storage System Sizing, Operation, and Upfront Costs

To understand the costs and net air pollutant emission impacts of installing BESS in place of peaker plants, we needed to identify locations, size each system appropriately based on the peaker it is replacing, and then simulate how the battery would be charged and discharged throughout each day. We assumed each new BESS will be located at the same site as the corresponding peaker plant it replaces and will not exceed the peaker's maximum power output during charging or discharging. This avoids having to model additional potential costs associated with upgrading transmission and distribution infrastructure, which are outside the scope of this study. Additionally, we assumed that the BESS will have a four-hour discharge duration; while this represents the higher end of durations for front-of-the-meter BESS in the US,[24] a four-hour duration is frequently used when studying peaker replacement capabilities and in rulemaking for California and New York.[25-27] This assumption dictates that the power-to-energy ratios of all modeled BESS will be 0.25.

We used optimization to determine the minimum necessary rated energy storage capacity of the BESS based on how each peaker plant has historically operated. Unlike peaker plants, the BESS must be charged, and those charging decisions will impact the optimal sizing, facility economics, and emissions. The optimization program developed for this study considers the historical output of each natural gas peaker plant and local hourly electricity prices from 2018 through 2020, obtained through California Independent System Operator (CAISO) Open Access Same-time Information System (OASIS) and CEMS,[23,28] to minimize the rated energy storage capacity of the BESS while simultaneously determining the charging decisions that minimize the cost of purchasing electricity. Several previously published studies used optimization to estimate profits earned during the operation of BESS;[29-32] we used an approach most similar to the linear method outlined by Nguyen et al.,[33] which reduces the computational requirements. The optimization model is described in greater detail in Procedure B1.

After determining the minimum necessary rated energy storage capacity, we determined the capacity fade (referred to here as degradation) that the Li-ion cells will experience during their operation. Battery systems for each BESS were then over-sized to ensure they could deliver a consistent level of service after compensating for this loss. Degradation is accounted for based on two separate mechanisms: degradation from cycling, and degradation from maintaining a state-of-charge over time (shelf-life degradation). Increasing the number of times the system is cycled and extending the length of time before the battery is replaced will both increase the required size of the battery system. We assume that all BESS will have a scheduled battery replacement midway through the facility's lifespan. This assumption reflects expected market behavior, given the longer lifetimes of many system components relative to the Li-ion batteries themselves.[34-36] The simulated charging and discharging behavior for peaker replacement and arbitrage behavior is used to determine the expected degradation. Further details of battery oversizing and degradation are presented in Procedure B8, B9, Tables B5, B6, and Figure B2.

Figure 4.2 visualizes the optimized charging behavior of three example BESS for peaker replacement only, each replacing a different natural gas peaker plant representing the minimum (Chula Vista Energy Center Unit 1A), median (Long Beach Generating Station Unit 1), and maximum (Larkspur Energy Facility Unit 1) annual electrical generation of all peaker plants

included in this study. The number of full charge–discharge cycle-equivalents required for peaker replacement varies widely by facility, with a high of approximately 62 cycles/year, a low of around 8, and an average across all facilities of 27 (Table B7). The charging times and loads determined by the optimization align with the expected behavior of an energy storage system, charging mostly during the day and early morning when electricity is cheapest. Exceptions to this expected behavior are due to daily variation in electricity price and peaker output. Large periods of continuous output may require charging at nonideal hours in order to store enough electricity to fully meet the required load. This is more common in plants with greater energy throughput, such as the Larkspur facility.

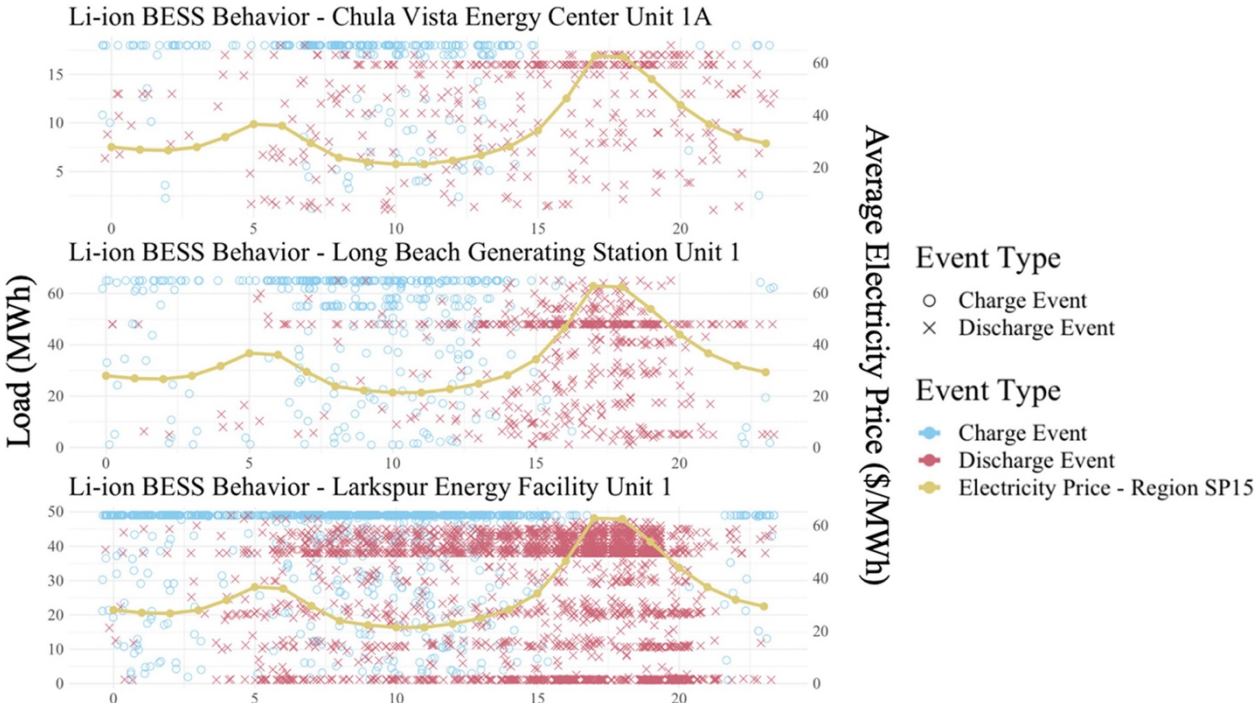

Figure 4.2. Charging behavior of selected BESS in 2018–2020 for peaker replacement considering electricity prices. The time of day and load (MWh) of each charge and discharge event from 2018 through 2020 is illustrated for three natural gas peaker plants. The optimized charging events are represented as blue circles. The fixed discharging events are represented as red x's. Chula Vista Energy Center Unit 1A is the peaker plant with the least output of the studied peaker plants; Long Beach Generating Station Unit 1 has the median output; and Larkspur Energy Facility Unit 1 has the maximum output. The average electricity price at each time of day from 2018 to 2020 is plotted on the second axis to visualize the relationship between charging/discharging events and electricity price. Figure A3 visualizes the state of charge of the BESS offsetting Long Beach Generating Station 1 for two example weeks to further visualize behavior.

Using the optimal BESS sizing for each peaker replacement system as an input, we constructed a detailed technoeconomic model to quantify the private costs associated with the installation and operation of each BESS, using a bottom-up method similar to that of Feldman et al.,[37] which is further documented in Procedure B4, Figure B4, Tables B8, B10, and B11. The initial cost results suggest that sizing BESS to fully replace natural gas peaker plants would require rated capacities well beyond what could be considered economically feasible. A first, albeit somewhat obvious, finding of this research is that building BESS to fully replace peaker plants will result in

massive capital expenditures (CapEx) and insufficient revenue to compensate for those costs. However, if a BESS is instead sized to meet the 95th percentile load event for each peaker plant (by hours of continuous generation), the required rated capacity decreases by nearly 80% in some cases. Other strategies or infrastructure will be required to supply the energy otherwise provided during the largest fifth percentile of load events served by natural gas peaker plants (roughly 19% of the current peaker output on average), such as demand response measures.[38-40] For example, a cell phone alert from the California Governor's Office of Emergency Services sent during a recent heat wave prompted a 1.2 GW drop in demand in a span of just 5 min.[41] The relationship between BESS sizing and the fraction of peaker plant activity avoided is further explored in Procedure B2 which illustrates the BESS size required to offset varying percentiles of natural gas peaker plant activity.

4.2.3 Potential for Arbitrage and Grid Services

While the hypothetical BESS studied here are sized and operated based on the need for peaker replacement, operators would be free to take advantage of other revenue-generating activities through arbitrage and the provision of grid services. BESS can engage in a variety of revenue-generating activities, and based on available information on the size and value of these markets, we identified arbitrage and frequency regulation as the most attractive options in the near term.[6,42-45] We determined the revenue and emission impacts associated with arbitrage using a similar optimization approach to that previously described for predicting charging and discharging behavior (described in Procedure B3). In addition to arbitrage, providing grid services can serve as a source of substantial revenue for BESS.

Within the grid services that BESS are well positioned to provide, participation in frequency regulation markets offers a particularly large potential source of revenue for BESS.[46,47] We model the revenue from frequency regulation as three main components in accordance with Xu et al.:[48] capacity revenue, mileage revenue, and fast regulation revenue. Each component is further broken into an individual component for upward and downward mileage. Capacity revenue is modeled as the BESS available capacity for frequency regulation multiplied by the hourly frequency regulation capacity clearing price. Mileage revenue is modeled as the BESS available capacity for frequency regulation, multiplied by the hourly percentage of that capacity that is called on by CAISO, the hourly accuracy score, and the hourly mileage clearing price. The hourly frequency regulation capacity clearing price, the hourly percentage of called capacity, the hourly accuracy score, and the hourly mileage clearing price are sourced from CAISO for the years 2018 through 2020 modeled in this study. Additionally, while some independent system operators have an additional market minute regulation activity (referred to as fast regulation in this study), CAISO does not have a market for this service, so this component is omitted from modeling. Furthermore, we assume that frequency regulation and mileage cannot occur during arbitrage or peaker replacement to avoid conflicts with available capacity. Additional modeling details are available in Procedure B4.

In many instances, profits from frequency regulation exceed the profits from arbitrage in the same period (Table B12), yet our analysis prioritizes arbitrage over frequency regulation. This choice is based on the small size of the frequency regulation market and high likelihood that arbitrage will be more common in the future as the frequency regulation market becomes

saturated.[43,46,47,49] Table B13 illustrates this point by comparing total electricity charged and discharged by batteries in California with the total frequency regulation market sizes (up and down).

4.3 Results and Discussion

4.3.1 Net Present Value of Battery energy Storage Systems

To understand whether replacing peaker plants in California with BESS is profitable, we explored a range of scenarios and calculated the NPV for each. To capture differences among Li-ion cathode materials, we explored three alternatives: $LiFePO_4$ (LFP), $LiNi_xCo_yAl_zO_2$ (NCA), and $LiNi_xMn_yCo_zO_2$ (NMC). We assigned a normalized price per kWh and set of degradation characteristics to each battery type, representing current prices and performance. Each battery is sized for a four-hour discharge duration. The system lifetime was varied between 15 and 20 years, with battery replacement occurring at 7.5 and 10 years, respectively (conservatively assuming battery prices remain constant). We performed upfront system sizing with respect to the battery replacement timeline through the methods outlined in Procedure B1 as well as the details outlined in Procedure B8, B9, Table B5, B6, and Figure B2. We used the federally mandated social cost of carbon of 51 USD per metric ton of CO_{2eq} emitted in 2020[50] as well as a higher social cost of carbon of 185 USD per metric ton of CO_{2eq} from Rennert et al.[51] and included monetized human health damages from pollutants that form secondary fine particulate matter: primarily NO_X. We explored three different discount rates: 3, 5, and 7% and applied these rates to both private costs/revenues and changes to monetized climate and human health damages. Additionally, the analysis includes operations and maintenance (O&M) costs, which entail replacement of heating, ventilation, and air conditioning (HVAC) equipment and other components with limited lifespans. Separate from the scenarios discussed here, we capture uncertainty in all other cost and design parameters using probability distributions (Table B8) and Monte Carlo simulations. The NPV of all BESS across all scenarios is presented in Figures B5–B10.

Figure 4.3 presents the NPV and net 100-year global warming potential (GWP) for each of the BESS replacing the 19 natural gas peaker plants considered in the study. These results include a LFP cathode with a replacement battery at 10 years, a total project lifespan of 20 years, and a discount rate of 3%. A more detailed breakdown of life-cycle GWP for the Long Beach 1 facility (a representative average case) is presented in Figures B11a and B11b, and the impact of changing design parameters and discount rates is discussed in the Sensitivity Analysis section. In 14 of the 19 hypothetical peaker replacements shown in Figure 4.3a, the expected total NPV falls below zero, while 5 have expected NPVs above zero. In 10 of the total projects presented, the uncertainty around the total NPV spans both negative and positive values, indicating that some of these BESS could be viable, particularly if Li-ion battery costs continue to fall. However, these results rely on current market values for frequency regulation, which may also fall as more BESS come online and saturate the market.

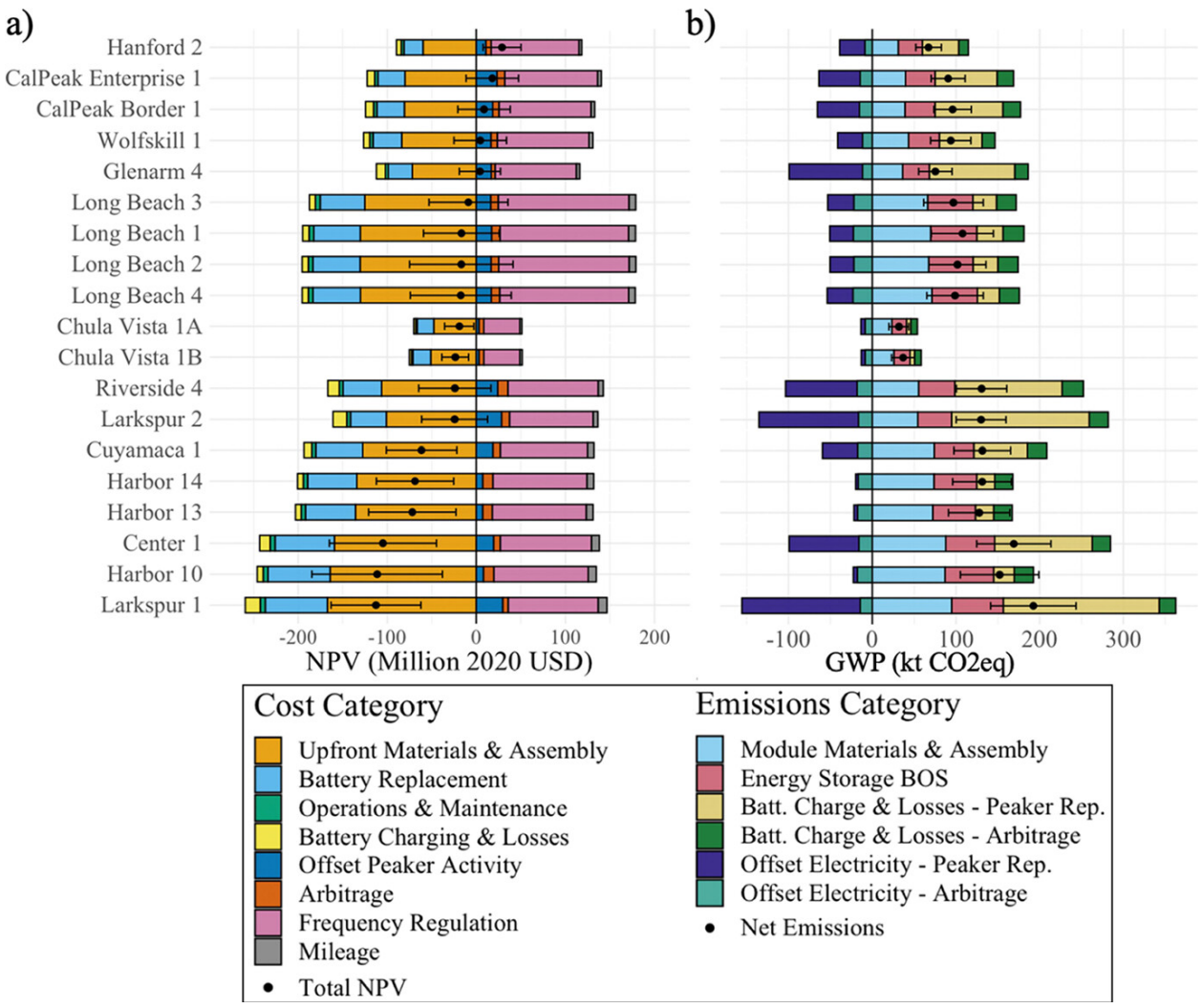

Figure 4.3. Net present value and global warming potential of BESS replacing natural gas peaker plants. Figure 4.3 illustrates the (a) NPV and (b) global warming potential of all the BESS explored for the scenario described, and breaks down the sources of costs and revenues by category. The NPVs and emissions are presented, as well as the uncertainty at two standard deviations, determined through Monte Carlo Simulation with 500 model runs. These results represent an LFP cathode with a battery replacement occurring after 10 years, a total facility lifetime of 20 years, and discount rate of 3%.

Figure 4.4 provides a more detailed breakdown of the NPV for a single BESS, distinguishing between the private costs and revenue, as well as the monetized emissions impacts. The bars labeled "monetary" represent the private revenues and costs associated with building and operating the BESS. The emissions cost bars represent the monetized human health damages and climate damages resulting from the induced electricity generation due to battery charging. Emission offsets are modeled as the avoided damages to human health and the climate from electrical generation that the battery displaces when it is discharging. The remaining peaker plant activity that cannot be economically replaced with the BESS (any event with a greater energy demand than the 95th percentile peaker event) is not included as either a cost or benefit. Further details are provided in Procedure B7.

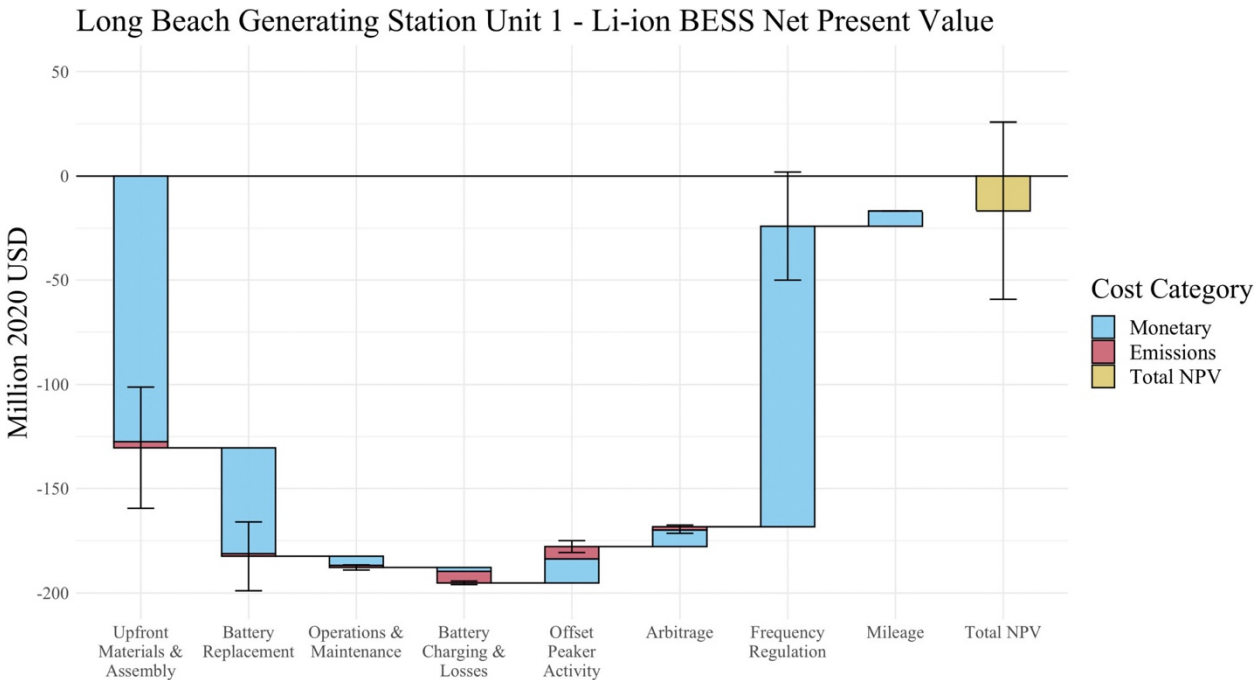

Figure 4.4. Net present value of BESS replacing Long Beach Generation Station Unit 1. Figure 4.4 illustrates the NPV of the BESS replacing Long Beach Generating Station Unit 1 and breaks down the sources of costs and revenues by category, additionally specifying the impact from monetary and environmental sources per category. Error bars represent two standard deviations.

As shown in Figures 3a and 4, the monetary upfront and battery replacement costs represent the two largest costs across all BESS. The costs associated with both O&M and battery charging and losses are near negligible in comparison. Frequency regulation is the dominant source of revenue, despite the fact that we model the BESS to prioritize arbitrage whenever it is profitable. The other revenue-generating activities offsetting peaker activity, arbitrage, and mileage offer relatively small economic revenue streams compared to the total system cost. Prior studies have also emphasized the near-term profitability of ancillary service markets relative to arbitrage when choosing how to operate energy storage systems.[43,44,52] The results in Figure 4.3a highlight that, while the key cost and revenue drivers remain consistent across all facility designs, the relative breakdown of costs and revenues for each BESS do vary. This variation suggests that some peaker plant replacement projects can be prioritized based on system characteristics that lead to more profitable BESS.

The two largest costs (upfront materials and assembly and battery replacement) are dictated by the BESS storage capacity required to meet the 95th percentile load event of the natural gas peaker plant being replaced (see Figure B1 and Table B9). Plants that historically have required frequent extended, continuous generation must be replaced with larger BESS, often with a rated power much greater than that of the peaker plant (Table B7), in part because of the degradation the batteries will experience over their lifetime. In contrast, the potential revenue from frequency regulation is dictated by the maximum power output of the BESS. In this study, the maximum power output for each BESS when it is operating is capped at the rated power of the replaced natural gas peaker plant. This prevents the model from inadvertently exceeding the capacity of the local grid infrastructure. However, the BESS can have a rated power greater than this if needed to ensure adequate storage capacity while maintaining a power-to-energy ratio of 0.25.

Ultimately, a BESS will have a higher total NPV if the natural gas peaker plant being replaced has a relatively high rated power, yet is rarely called upon for extended, continuous generation.

While frequency regulation represents the greatest near-term source of revenue for all BESS, the future of this revenue stream is uncertain. Frequency regulation represents a small, fairly localized market.[43,46,47,49] Given the forecasted growth of grid-connected energy storage in California,[19] the value of frequency regulation will likely decrease over time. A key question is how this may be counterbalanced by anticipated reductions in battery costs.

In this study, the prices of replaced Li-ion cells are held constant at current market prices. However, many forecasts suggest that Li-ion cell prices will decrease,[1,53-55] meaning the cost of battery replacements may be lower than what is modeled here. The degree of this potential price reduction is highly variable on how the Li-ion technology develops, especially since constant learning is not guaranteed.[56] Technological learning for Li-ion batteries can drive prices lower, while material shortages and supply chain challenges for Li-ion cells may counterbalance some of these improvements.[57-59] If the US Department of Energy's $60/kWh target for Li-ion modules[60] is reached in advance of when battery replacement occurs for the facilities in Figure 4.3, nine of the 19 BESS explored will have a positive NPV (as opposed to 5, based on current Li-ion battery prices).

4.3.2 Global Warming Potential of Battery Energy Storage Systems

Figure 4.3b presents the life-cycle GWP of BESS in the previously described scenario. We conservatively assumed no recycling of Li-ion cells given the current challenges with Li-ion recycling supply chains.[61-62] For perspective, a prior study estimated that recycling could save approximately one quarter of the Li-ion batteries' GHG footprint, although results vary by the cathode material and recycling process.[63] Future uncertainty in cell manufacturing and other energy storage components were captured in a Monte Carlo analysis. Probability distributions for input parameters are provided in Table B14. The life-cycle GWP for all plants across all scenarios is presented in Figures B12–B14.

The GWP for all BESS examined is net positive (based on the current grid mix), as illustrated in Figure 4.3b, meaning that system-wide life-cycle GHG emissions increase relative to the counterfactual case in which the peaker plant continues to operate and no BESS is installed. There are two reasons for this: first, the embedded emissions associated with the BESS and its eventual replacement are substantial and second, the replacement of peaker plant activity and engagement in arbitrage induce more GHG emissions at power plants elsewhere on the grid during BESS charging than what is saved during discharging. This result is not without precedent; Craig et al.[64] found that grid-scale electricity storage would increase system-wide CO_2 emissions for Electricity Reliability Council of Texas (ERCOT) in the very near-term, based on the outputs of their economic dispatch model. Our results for California echo this finding: with the current grid, charging can induce additional fossil-based generation, particularly when excess solar capacity is not available. Our modeling approach, described in Procedure B7, captures this behavior and estimates the impact on GWP from this induced thermal generation. Our modeling does not consider how the availability of storage may impact capacity expansion in the long run. As demonstrated by Bistline and Young,[65] the availability of grid-scale battery

systems can influence future investments in generating capacity and infrastructure, although the effects may increase or decrease emissions. Finally, energy losses attributable to the Li-ion cells and the balance-of-systems components such as HVAC translate to a round-trip efficiency ranging from 80 to 95%, meaning the battery consumes more electricity during charging than it supplies during discharging.

One may reasonably expect the impact of battery charging and discharging on GWP to be larger than what is shown in Figure 4.3b. When not replacing peaker plant activity, the optimization model allows each BESS to engage in arbitrage whenever it is profitable (accounting for electricity prices and battery degradation). However, as shown in Table B7, this occurs infrequently (an average of 8 cycles per year for LFP BESS). Replacing peaker plant activity requires more cycles (average of 27 across all BESS in this study). From our analysis, we determined that each BESS would likely spend the majority of the year participating in frequency regulation, which is the most profitable strategy but adds a negligible number of cycles and little to no emissions benefits. However, BESS installed for different use cases are reported to cycle more frequently. For example, a 2020 IHS report that sampled eight projects, with an average rated power of under 20 MW (considerably smaller than the BESS modeled here which have an average rated power of 97 MW) over a period of 1 to 5 years reported that the BESS cycled an equivalent of 251 times per year on average, with a minimum of around 75 and a maximum over 450.[66]

While it may be possible to achieve greater avoided emissions from offset electricity─and potentially a negative net GWP─through intentional system behavior and arbitrage,[34,67-69] this behavior is not achievable in any profit-maximizing peaker replacement scenarios explored (in the context of the 2018–2020 grid) and may lead to significantly reduced revenues and increased costs associated with battery sizing due to higher degradation from cycling.

4.3.3 Sensitivity Analysis

BESS design and input parameters for the cash flow analysis are likely to change as technology and market conditions evolve. The LFP cathode chemistry (shown in Figures 3 and 4) results in the most profitable BESS due to its reduced cell price, and it also results in lower life-cycle GWP because it avoids the need for cobalt, nickel, and manganese. Five of 19 BESS had a positive expected NPV when modeled with an LFP cathode, a 3% discount rate, 20-year lifespan, and social cost of carbon of 51 USD per metric ton of CO_{2eq}. Similarly, five of the 19 BESS also had a positive expected NPV when modeled with an NCA cathode but had a lower average NPV across all 19 plants (−33 million 2020 USD versus −31 million 2020 USD for LFP cathodes). Only one BESS had a positive expected NPV with the NMC cathode. The impact of different cathode materials on NPV is provided in Figures B5–B10.

Altering the lifespan of the entire BESS facility can also substantially impact the NPV. Our modeling approach assumes a single battery replacement will occur midway through the lifespan of the BESS. The battery system is sized to deliver a consistent level of service, accounting for capacity fade from cycling and shelf-life degradation that will occur over half of the total BESS facility's lifespan. Shortening the battery replacement time from 10 to 7.5 years (total BESS lifespan from 20 to 15 years) will require a smaller battery system to maintain a consistent level

of service and, thus, CapEx decreases. However, decreasing the lifespan of the BESS also reduces the revenue earned while it is in service. In all scenarios explored, the revenue earned during a longer battery lifetime (replacement at 10 years, total BESS lifetime of 20 years) outweighed the increased CapEx. Specifically, at a 3% discount rate and a social cost of carbon of 51 USD per metric ton of CO_{2eq}, going from a BESS lifespan of 15 to 20 years, the number of BESS with a positive NPV increased from 2 to 5 for the LFP and NCA cathode and 0 to 1 for the NMC cathode chemistry. The impact of different lifespans on NPV is demonstrated in Figures B5–B10. However, increasing lifespan is also associated with increasing life-cycle GWP, as more materials are required for the larger battery capacity, as shown in Figures B12–B14.

Varying discount rates also affects the NPV. While increasing the discount rate will lower the present value of the future battery replacement cost, it will also lower the value of future revenues. In the scenarios explored, increasing the discount rates slightly decreased the NPV of all BESS. For example, when modeled with an LFP cathode chemistry, a 20-year lifespan, and a social cost of carbon of 51 USD per metric ton of CO_{2eq}, increasing the discount rate from 3 to 7% decreased the number of BESS with a positive NPV from 5 to 2. Figures B5–B10 visualize the impacts of changing discount rates on NPV.

To understand the impact of an elevated social cost of carbon, scenarios were performed with a cost of 185 USD per metric ton of CO_{2eq} emitted in 2020. This increased the upfront environmental costs associated with battery production as well as increasing the costs and benefits of battery operation. The cumulative impact is a net decrease in NPV across all scenarios because all BESS evaluated resulted in net positive life-cycle GWP. For example, when modeled with an LFP cathode chemistry, a 20-year lifespan, and a 3% discount rate, increasing the social cost of carbon from 51 to 185 USD per metric ton of CO_{2eq} caused the number of BESS with positive NPV to remain the same, but the average NPV decreased from −31 million 2020 USD to −36 million 2020 USD. Figures B5–B10 visualize the increasing the social cost of carbon on NPV.

4.4 Discussion

Analyzing Li-ion BESS as replacements for natural gas peaker plants reveals several insights, some of which have implications for all front-of-the-meter battery storage. First, sizing BESS to fully replace the service provided by natural gas-fired peaker plants is unlikely to be economically viable. Instead, sizing each BESS to serve all but approximately the top fifth percentile of load events (appropriate threshold may vary by facility) dramatically reduces the required storage capacity and, thus, CapEx, while still meeting 81% of load on average (Table B9). This result highlights the continued need for demand-response[38-40] and potentially mobile battery storage that can be called upon during extreme heat and other exceptional circumstances.[70]

Based on California's current electricity market, BESS sized to meet the 95th percentile of loads served by natural gas peaker plants can achieve a positive NPV, but only if the value of frequency regulation does not decline. The BESS most likely to be profitable are those with LFP cathodes replacing large natural gas peaker plants that do not output large quantities of energy

frequently and continuously, since most profits come from slack capacity sold in the frequency regulation market. Arbitrage, in contrast, is only a small contributor to total revenue. These findings are consistent with prior studies.[43,44,71] However, given the limited size of the frequency regulation market and the forecasted growth of energy storage in California, the value of frequency regulation may decrease in the future.[43,46,47,49] A remaining question is whether the social benefits of energy storage can compensate for the declining value of frequency regulation. Additionally, peaker plants can place a disproportionate environmental burden on historically marginalized groups.[72-74] For example, the Hanford 2 peaker plant sits in a census tract where the $PM_{2.5}$ concentrations are in the 99th percentile for the United States and nearly half of the population is Hispanic or Latino.[75] Based on our analysis, this plant is potentially the most profitable target for replacement with a BESS. The community around the Wolfskill 1 facility averages $PM_{2.5}$ concentrations in the top 95th percentile for the nation and is also approximately half Hispanic or Latino.[75] Combining an understanding of the economics of replacement, alongside data on the distributional impacts of each plant's emissions, can be a compelling strategy for replacing high-emitting plants.

The BESS scenarios evaluated in this study yielded small monetized climate and human health impacts relative to the private costs and benefits. While replacing peaker power plants does reduce air quality-related health damages in surrounding communities, the profit-maximizing behavior for the BESS we modeled also increased life-cycle GHG emissions once the embodied emissions in the BESS were accounted for. It may be possible to achieve a net zero or negative GWP through an intentional arbitrage strategy to reduce emissions[68,69] and the installation of additional renewable resources on the grid can increase the likelihood that BESS will offer net environmental benefits.[34,67] In the near-term, optimizing for emissions reductions would be less profitable due to increased cycling and reduced availability for frequency regulation.

Future prices of Li-ion cells and the evolution of electricity markets are critical to increasing the NPVs of BESS. If the value of frequency regulation does indeed decrease over time, battery costs must decrease and revenue from arbitrage must increase to maintain or increase NPVs. If the US Department of Energy target price for Li-ion modules, \$60/kWh,[60] is reached as battery replacement occurs for the scenario in Figure 4.3a, then nine of the 19 BESS explored will have a positive NPV, instead of 5. However, achieving this price reduction in 7.5 to 10 years will require learning rates much higher than the recent average learning rates for Li-ion cells.[1] The rate at which Li-ion battery prices will decrease in the future is highly uncertain.[76] Additionally, we modeled the future operation of BESS assuming electricity prices will remain at 2018 to 2020 prices over the next 15 to 20. This will almost certainly not be the case. In reality, transmission investments, new generation capacity, shifting demand, and changes in utility rate structures will influence the NPVs of BESS.

While we modeled realistic conditions for Li-ion energy storage aimed at replacing peaker plants in California, there may be a greater monetary value of storage technologies in other scenarios. In particular, some regions rely on coal combustion to meet peak demand, and combining BESS with renewable generation resources may further increase profitability while avoiding emissions associated with electricity generation.[34,67,77-79] Other energy storage technologies like redox flow batteries or hydrogen storage may ultimately prove to be better suited for peaker replacement as they mature.[80-85] Additionally, uncertainty in near-term energy supply may cause variation in

market sizes and structure, altering future revenues.[86,87] Finally, the modeled NPVs also do not capture the monetized human health impacts tied to rolling blackouts or prolonged outages,[88-90] as well as the nonhealth community impacts associated with the removal of natural gas combustion peaker plants.[91] Including these considerations may increase the value of BESS, especially since greater renewable integration and worsening effects from climate change increase the variability of electricity supply and demand.[92-96]

References

1. Ziegler, M. S. & Trancik, J. E. Re-examining rates of lithium-ion battery technology improvement and cost decline. *Energy Environ. Sci.* (2021) doi:10.1039/D0EE02681F.

2. Nykvist, B. & Nilsson, M. Rapidly falling costs of battery packs for electric vehicles. *Nat. Clim. Chang.* **5**, 329–332 (2015).

3. Zheng, M., Meinrenken, C. J. & Lackner, K. S. Smart households: Dispatch strategies and economic analysis of distributed energy storage for residential peak shaving. *Appl. Energy* **147**, 246–257 (2015).

4. Mongird, K., Viswanathan, V., Alam, J., Vartanian, C., Sprenkle, V. & Baxter, R. *2020 Grid Energy Storage Technology Cost and Performance Assessment*. (2020).

5. Obi, M., Jensen, S. M., Ferris, J. B. & Bass, R. B. Calculation of levelized costs of electricity for various electrical energy storage systems. *Renew. Sustain. Energy Rev* **67**, 908–920 (2017).

6. Chen, T., Jin, Y., Lv, H., Yang, A., Liu, M., Chen, B., Xie, Y. & Chen, Q. Applications of Lithium-Ion Batteries in Grid-Scale Energy Storage Systems. *Trans. Tianjin Univ.* **26**, 208–217 (2020).

7. Solomon, A. A., Child, M., Caldera, U. & Breyer, C. How much energy storage is needed to incorporate very large intermittent renewables? *Energy Procedia* **135**, 283–293 (2017).

8. Stroe, D.-I., Knap, V., Swierczynski, M., Stroe, A.-I. & Teodorescu, R. Operation of a Grid-Connected Lithium-Ion Battery Energy Storage System for Primary Frequency Regulation: A Battery Lifetime Perspective. *IEEE Trans. Ind. Appl.* **53**, 430–438 (2017).

9. Fan, X., Liu, B., Liu, J., Ding, J., Han, X., Deng, Y., Lv, X., Xie, Y., Chen, B., Hu, W. & Zhong, C. Battery Technologies for Grid-Level Large-Scale Electrical Energy Storage. *Trans. Tianjin Univ.* **26**, 92–103 (2020).

10. Kosowatz, J. Energy storage smooths the duck curve. *Mechanical Engineering* **140**, 30–35 (2018).

11. California ISO. *What the duck curve tells us about managing a green grid*. https://www.caiso.com/documents/flexibleresourceshelprenewables_fastfacts.pdf (2016).

12. Keskar, A., Galik, C. & Johnson, J. X. Planning for winter peaking power systems in the United States. *Energy Policy* **173**, 113376 (2023).

13. PSE Healthy Energy. *California Peaker Power Plants: Energy Storage Replacement Opportunities*. https://www.psehealthyenergy.org/wp-content/uploads/2020/05/California.pdf (2020).

14. Tarekegne, B., O'Neil, R. & Michener, S. *Energy Storage and Power Plant Decommissioning*. PNNL-32214. https://www.pnnl.gov/main/publications/external/technical_reports/PNNL-32214.pdf (2021).

15. Childs, E., Animas, E., Jones, D., Gorman, J. & Maciey, A. *The Fossil Fuel End Game: A Frontline Vision to Retire New York City's Peaker Plans by 2030*. (2021).

16. Krieger, E. M., Casey, J. A. & Shonkoff, S. B. C. A framework for siting and dispatch of emerging energy resources to realize environmental and health benefits: Case study on peaker power plant displacement. *Energy Policy* **96**, 302–313 (2016).

17. Martinez-Bolanos, J. R., Udaeta, M. E. M., Gimenes, A. L. V. & Silva, V. O. da. Economic feasibility of battery energy storage systems for replacing peak power plants for commercial consumers under energy time of use tariffs. *Journal of Energy Storage* **29**, 101373 (2020).

18. Energy and Environmental Economics Inc. *Small Clean Power Plant Adaptation Study*. https://www.geenergyconsulting.com/content/dam/Energy_Consulting/global/en_US/pdfs/NYPA-SCPP-Adaptation-Study.pdf (2022).

19. Pacific Gas and Electric Company. The Next Giant Leap for Electric System Reliability: PG&E Proposes Nearly 1,600 MW of New Battery Energy Storage Capacity. *PG&E* https://www.pge.com/en_US/about-pge/media-newsroom/news-details.page?pageID=38883b6b-8597-4734-b85a-104a9f6e8af3&ts=1643133870903 (2022). [Accessed August 15, 2022].

20. The Energy Mix. Oxnard, California Declares Environmental Justice Win as Batteries Replace Gas Peaker Plant. *The Energy Mix* https://www.theenergymix.com/2021/07/07/oxnard-california-declares-environmental-justice-win-as-batteries-replace-gas-peaker-plant/ (2021). [Accessed August 15, 2022].

21. Fordney, J. A Tale of Two Natural Gas Plants. *California Energy Markets* https://www.newsdata.com/california_energy_markets/bottom_lines/a-tale-of-two-natural-gas-plants/article_954761d8-e6cb-11e9-9784-9ffbd37b02b2.html (2019). [Accessed August 15, 2022].

22. California Public Utility Comission. Energy Storage. *California Public Utility Comission* https://www.cpuc.ca.gov/industries-and-topics/electrical-energy/energy-storage. [Accessed August 15, 2022].

23. United States EPA. EMC: Continuous Emission Monitoring Systems. *United State Environmental Protection Agency* https://www.epa.gov/emc/emc-continuous-emission-monitoring-systems (2021). [Accessed August 15, 2022].

24. U.S. Energy Information Administration. Form EIA-860 detailed data with previous form data (EIA-860A/860B). *Independent Statistics and Analysis: U.S. Energy Information Administration* https://www.eia.gov/electricity/data/eia860/ (2021). [Accessed August 15, 2022].

25. Denholm, P., Nunemaker, J., Gagnon, P. & Cole, W. The potential for battery energy storage to provide peaking capacity in the United States. *Renew. Energy* **151**, 1269–1277 (2020).

26. New York Independent System Operator. *The State of Energy Storage: Energy Storage Resources in New York's Wholesale Electricity Markets*. https://www.nyiso.com/documents/20142/2225293/2017-State-Of-Storage-Report.pdf/c80da6ff-b239-3464-3b6d-f191bf62c597 (2017).

27. California Public Utilities Commission. *2022 Filing Guide for System, Local and Flexible Resource Adequacy (RA) Compliance Filings*. R.19-11-009. https://www.cpuc.ca.gov/-/media/cpuc-website/divisions/energy-division/documents/resource-adequacy-homepage/resource-adequacy-compliance-materials/final-2022-ra-guide-clean-101821.pdf (2021).

28. California ISO. California ISO Oasis. *Oasis Prod* http://oasis.caiso.com/mrioasis/logon.do. [Accessed August 15, 2022].

29. Bansal, R. K., You, P., Gayme, D. F. & Mallada, E. Storage degradation aware economic dispatch. in *2021 American Control Conference (ACC)* 589–595 (IEEE, 2021). doi:10.23919/ACC50511.2021.9482838.

30. Maheshwari, A., Paterakis, N. G., Santarelli, M. & Gibescu, M. Optimizing the operation of energy storage using a non-linear lithium-ion battery degradation model. *Appl. Energy* **261**, 114360 (2020).

31. Xu, B., Shi, Y., Kirschen, D. S. & Zhang, B. Optimal battery participation in frequency regulation markets. *IEEE Trans. Power Syst.* **33**, 6715–6725 (2018).

32. Davies, D.M., Verde, M.G., Mnyshenko, O., Chen, Y.R., Rajeev, R., Meng, Y.S. & Elliott, G. Combined economic and technological evaluation of battery energy storage for grid applications. *Nat. Energy* (2018) doi:10.1038/s41560-018-0290-1.

33. Nguyen, T. A., Byrne, R. H., Chalamala, B. R. & Gyuk, I. Maximizing the revenue of energy storage systems in market areas considering nonlinear storage efficiencies. in *2018 International Symposium on Power Electronics, Electrical Drives, Automation and Motion (SPEEDAM)* 55–62 (IEEE, 2018). doi:10.1109/SPEEDAM.2018.8445321.

34. Rahman, M. M., Gemechu, E., Oni, A. O. & Kumar, A. The greenhouse gas emissions' footprint and net energy ratio of utility-scale electro-chemical energy storage systems. *Energy Conversion and Management* **244**, 114497 (2021).

35. Burger Mansilha, M., Brondani, M., Farret, F. A., Cantorski da Rosa, L. & Hoffmann, R. Life cycle assessment of electrical distribution transformers: comparative study between aluminum and copper coils. *Environ. Eng. Sci.* **36**, 114–135 (2019).

36. Bessede, J.-L. & Krondorfer, W. *Impact of High-voltage SF6 Circuit Breakers on Global Warming - Relative Contribution of SF6 Losses*. https://www.epa.gov/sites/default/files/2016-02/documents/conf00_krondorfer.pdf (2017).

37. Feldman, D., Ramasamy, V., Fu, R., Ramdas, A., Desai, J. & Margolis, R. *U.S. solar photovoltaic system and energy storage cost benchmark: Q1 2020*. (2021) doi:10.2172/1764908.

38. Palensky, P. & Dietrich, D. Demand Side Management: Demand Response, Intelligent Energy Systems, and Smart Loads. *IEEE Trans. Ind. Inf.* **7**, 381–388 (2011).

39. Uddin, M., Romlie, M.F., Abdullah, M.F., Abd Halim, S. & Kwang, T.C. A review on peak load shaving strategies. *Renew. Sustain. Energy Rev* **82**, 3323–3332 (2018).

40. Shirazi, E. & Jadid, S. Cost reduction and peak shaving through domestic load shifting and DERs. *Energy* **124**, 146–159 (2017).

41. Calma, J. Why a text alert might have helped California keep the lights on. *The Verge* https://www.theverge.com/2022/9/7/23340821/california-electricity-grid-power-outage-text-phone-alert (2022). [Accessed August 15, 2022].

42. Biggins, F. A. V., Homan, S., Roberts, D. & Brown, S. Exploring the economics of large scale lithium ion and lead acid batteries performing frequency response. *Energy Reports* **7**, 34–41 (2021).

43. Preskill, A. & Callaway, D. How much energy storage do modern power systems need? *arXiv* (2018). [Accessed August 15, 2022].

44. Elshurafa, A. M. The value of storage in electricity generation: A qualitative and quantitative review. *Journal of Energy Storage* **32**, 101872 (2020).

45. Wüllner, J., Reiners, N., Millet, L., Salibi, M., Stortz, F. & Vetter, M. Review of Stationary Energy Storage Systems Applications, Their Placement, and Techno-Economic Potential. *Curr. Sustainable Renewable Energy Rep.* **8**, 263–273 (2021).

46. Brooks, A. E. & Lesieutre, B. C. A review of frequency regulation markets in three U.S. ISO/RTOs. *The Electricity Journal* **32**, 106668 (2019).

47. Frew, B., Gallo, G., Brinkman, G., Miligan, M., Clark, K., Bloom, A. *Impact of Market Behavior, Fleet Composition, and Ancillary Services on Revenue Sufficiency*. NREL/TP-5D00-66076. https://www.nrel.gov/docs/fy16osti/66076.pdf (2016).

48. Bolun Xu, Dvorkin, Y., Kirschen, D. S., Silva-Monroy, C. A. & Watson, J.-P. A comparison of policies on the participation of storage in U.S. frequency regulation markets. in *2016 IEEE Power and Energy Society General Meeting (PESGM)* 1–5 (IEEE, 2016). doi:10.1109/PESGM.2016.7741531.

49. California ISO. *2020 Annual Report on Market Issues & Performance*. http://www.caiso.com/Documents/2020-Annual-Report-on-Market-Issues-and-Performance.pdf (2021).

50. Interagency Working Group on Social Cost of Greenhouse Gases, United States Government. *Technical Support Document: Social Cost of Carbon, Methane, and Nitrous Oxide Interim Estimates under Executive Order 13990*. (2021).

51. Rennert, K., Errickson, F., Prest, B.C., Rennels, L., Newell, R.G., Pizer, W., Kingdon, C., Wingenroth, J., Cooke, R., Parthum, B. & Smith, D. Comprehensive evidence implies a higher social cost of CO2. *Nature* (2022) doi:10.1038/s41586-022-05224-9.

52. Zhang, X., Qin, C.C., Loth, E., Xu, Y., Zhou, X. & Chen, H. Arbitrage analysis for different energy storage technologies and strategies. *Energy Reports* (2021) doi:10.1016/j.egyr.2021.09.009.

53. Schmidt, O., Melchior, S., Hawkes, A. & Staffell, I. Update 2018 - The future cost of electrical energy storage based on experience rates. *Figshare* (2018) doi:10.6084/m9.figshare.7012202.v1.

54. Frith, J. & Goldie-Scot, L. *2019 Lithium-Ion Battery Price Survey*. Reference Number 31379202003260441431. bnef.com. (2019).

55. Cole, W. & Frazier, W. *Cost Projections for Utility-Scale Battery Storage: 2020 Update*. NREL/TP-6A20-75385. https://www.nrel.gov/docs/fy20osti/75385.pdf (2020).

56. Ziegler, M. S., Song, J. & Trancik, J. E. Determinants of lithium-ion battery technology cost decline. *Energy Environ. Sci.* (2021) doi:10.1039/D1EE01313K.

57. Helbig, C., Bradshaw, A. M., Wietschel, L., Thorenz, A. & Tuma, A. Supply risks associated with lithium-ion battery materials. *J. Clean. Prod.* **172**, 274–286 (2018).

58. International Energy Agency. *Global EV Outlook 2021: Accelerating ambitions despite the pandemic*. https://www.iea.org/reports/global-ev-outlook-2021 (2021).

59. Lee, A. The Trouble With Lithium. *Bloomberg* https://www.bloomberg.com/news/features/2022-05-25/lithium-the-hunt-for-the-wonder-metal-fueling-evs (2022). [Accessed August 15, 2022].

60. LeVine, S. The Goalposts Move: The New Lithium-Ion Standard is An Astonishing $60 per kWh. *The Mobolist* https://themobilist.medium.com/the-goalposts-move-the-new-lithium-ion-standard-is-an-astonishing-60-per-kwh-7153fa8ec328 (2021). [Accessed August 15, 2022].

61. Bird, R., Baum, Z. J., Yu, X. & Ma, J. The Regulatory Environment for Lithium-Ion Battery Recycling. *ACS Energy Lett.* **7**, 736–740 (2022).

62. Golmohammadzadeh, R., Faraji, F., Jong, B., Pozo-Gonzalo, C. & Banerjee, P. C. Current challenges and future opportunities toward recycling of spent lithium-ion batteries. *Renew. Sustain. Energy Rev* **159**, 112202 (2022).

63. Hendrickson, T. P., Kavvada, O., Shah, N., Sathre, R. & D Scown, C. Life-cycle implications and supply chain logistics of electric vehicle battery recycling in California. *Environmental Research Letters* **10**, 014011 (2015).

64. Craig, M. T., Jaramillo, P. & Hodge, B.-M. Carbon dioxide emissions effects of grid-scale electricity storage in a decarbonizing power system. *Environmental Research Letters* **13**, 014004 (2018).

65. Bistline, J. E. T. & Young, D. T. Emissions impacts of future battery storage deployment on regional power systems. *Appl. Energy* **264**, 114678 (2020).

66. Forsyth, O. & Huntington, S. *How Do Batteries Make Money in the US Power Market*. https://www.spglobal.com/commodityinsights/en/ci/research-analysis/how-do-batteries-make-money-in-us-power-markets.html (2020).

67. Virguez, E., Wang, X. & Patiño-Echeverri, D. Utility-scale photovoltaics and storage: Decarbonizing and reducing greenhouse gases abatement costs. *Appl. Energy* **282**, 116120 (2021).

68. Lipu, M.H., Ansari, S., Miah, M.S., Hasan, K., Meraj, S.T., Faisal, M., Jamal, T., Ali, S.H., Hussain, A., Muttaqi, K.M. & Hannan, M.A. A review of controllers and optimizations based scheduling operation for battery energy storage system towards decarbonization in microgrid: Challenges and future directions. *J. Clean. Prod.* **360**, 132188 (2022).

69. Sun, S., Crossland, A., Chipperfield, A. & Wills, R. An Emissions Arbitrage Algorithm to Improve the Environmental Performance of Domestic PV-Battery Systems. *Energies* **12**, 560 (2019).

70. He, G., Michalek, J., Kar, S., Chen, Q., Zhang, D. & Whitacre, J.F. Utility-Scale Portable Energy Storage Systems. *Joule* (2021) doi:10.1016/j.joule.2020.12.005.

71. de Sisternes, F. J., Jenkins, J. D. & Botterud, A. The value of energy storage in decarbonizing the electricity sector. *Appl. Energy* **175**, 368–379 (2016).

72. Thind, M. P. S., Tessum, C. W., Azevedo, I. L. & Marshall, J. D. Fine Particulate Air Pollution from Electricity Generation in the US: Health Impacts by Race, Income, and Geography. *Environ. Sci. Technol.* **53**, 14010–14019 (2019).

73. Cushing, L. J., Li, S., Steiger, B. B. & Casey, J. A. Historical red-lining is associated with fossil fuel power plant siting and present-day inequalities in air pollutant emissions. *Nat. Energy* **8**, 52–61 (2022).

74. Daouda, M., Henneman, L., Kioumourtzoglou, M.A., Gemmill, A., Zigler, C. & Casey, J.A. Association between county-level coal-fired power plant pollution and racial disparities in preterm births from 2000 to 2018. *Environ. Res. Lett.* **16**, (2021).

75. Council on Environmental Quality. Climate and Economic Justice Screening Tool. *Explore the Map - Climate and Economic Justice Screening Tool* https://screeningtool.geoplatform.gov/en/#3/33.47/-97.5 (2022). [Accessed August 15, 2022].

76. Hsieh, I.-Y. L., Pan, M. S., Chiang, Y.-M. & Green, W. H. Learning only buys you so much: Practical limits on battery price reduction. *Appl. Energy* **239**, 218–224 (2019).

77. Hendryx, M., Zullig, K. J. & Luo, J. Impacts of coal use on health. *Annu. Rev. Public Health* **41**, 397–415 (2020).

78. Munawer, M. E. Human health and environmental impacts of coal combustion and post-combustion wastes. *Journal of Sustainable Mining* **17**, 87–96 (2018).

79. Burt, E., Orris, P. & Buchanan, S. *Scientific Evidence of Health Effects from Coal Use in Energy Generation*. (2013).

80. Ye, R., Henkensmeier, D., Yoon, S.J., Huang, Z., Kim, D.K., Chang, Z., Kim, S. & Chen, R. Redox flow batteries for energy storage: A technology review. *J. Electrochem. En. Conv. Stor.* **15**, (2018).

81. Arenas, L. F., Ponce de León, C. & Walsh, F. C. Redox flow batteries for energy storage: their promise, achievements and challenges. *Curr. Opin. Electrochem.* **16**, 117–126 (2019).

82. Sánchez-Díez, E., Ventosa, E., Guarnieri, M., Trovò, A., Flox, C., Marcilla, R., Soavi, F., Mazur, P., Aranzabe, E. & Ferret, R. Redox flow batteries: Status and perspective towards sustainable stationary energy storage. *J. Power Sources* **481**, 228804 (2021).

83. Luo, J., Hu, B., Hu, M., Zhao, Y. & Liu, T. L. Status and Prospects of Organic Redox Flow Batteries toward Sustainable Energy Storage. *ACS Energy Lett.* **4**, 2220–2240 (2019).

84. Wolf, E. Large-Scale Hydrogen Energy Storage. in *Electrochemical energy storage for renewable sources and grid balancing* 129–142 (Elsevier, 2015). doi:10.1016/B978-0-444-62616-5.00009-7.

85. Mayyas, A., Wei, M. & Levis, G. Hydrogen as a long-term, large-scale energy storage solution when coupled with renewable energy sources or grids with dynamic electricity pricing schemes. *Int. J. Hydrogen Energy* **45**, 16311–16325 (2020).

86. Notton, G., Nivet, M.L., Voyant, C., Paoli, C., Darras, C., Motte, F. & Fouilloy, A. Intermittent and stochastic character of renewable energy sources: Consequences, cost of intermittence and benefit of forecasting. *Renew. Sustain. Energy Rev* **87**, 96–105 (2018).

87. Koh, L. H., Yong, G. Z., Peng, W. & Tseng, K. J. Impact of energy storage and variability of PV on power system reliability. *Energy Procedia* **33**, 302–310 (2013).

88. Casey, J. A., Fukurai, M., Hernández, D., Balsari, S. & Kiang, M. V. Power outages and community health: a narrative review. *Curr. Environ. Health Rep.* **7**, 371–383 (2020).

89. Busby, J.W., Baker, K., Bazilian, M.D., Gilbert, A.Q., Grubert, E., Rai, V., Rhodes, J.D., Shidore, S., Smith, C.A. & Webber, M.E. Cascading risks: Understanding the 2021 winter blackout in Texas. *Energy Research & Social Science* **77**, 102106 (2021).

90. Stone Jr, B., Mallen, E., Rajput, M., Broadbent, A., Krayenhoff, E.S., Augenbroe, G. & Georgescu, M. Climate change and infrastructure risk: Indoor heat exposure during a concurrent heat wave and blackout event in Phoenix, Arizona. *Urban Climate* **36**, 100787 (2021).

91. Pacific Northwest National Laboratory. *Energy Storage for Social Equity: Capturing Benefits from Power Plant Decommissioning*. (2021).

92. Beyza, J. & Yusta, J. M. The effects of the high penetration of renewable energies on the reliability and vulnerability of interconnected electric power systems. *Reliability Engineering & System Safety* **215**, 107881 (2021).

93. Harker Steele, A. J., Burnett, J. W. & Bergstrom, J. C. The impact of variable renewable energy resources on power system reliability. *Energy Policy* **151**, 111947 (2021).

94. Denholm, P., Ela, E., Kirby, B. & Milligan, M. *Role of Energy Storage with Renewable Electricity Generation*. (2010) doi:10.2172/972169.

95. Bartos, M. D. & Chester, M. V. Impacts of climate change on electric power supply in the Western United States. *Nat. Clim. Chang.* **5**, 748–752 (2015).

96. Panteli, M. & Mancarella, P. Influence of extreme weather and climate change on the resilience of power systems: Impacts and possible mitigation strategies. *Electric Power Systems Research* **127**, 259–270 (2015).

Chapter 5

Private and External Impacts of Electrifying Heavy-Duty Long-Haul Trucking with Li-ion Batteries

5.1 Introduction

The transportation sector is the greatest emitter of greenhouse gases (GHGs) in the US, representing nearly 29% of domestic GHG emissions in 2022.[1] Heavy-duty vehicles (HDVs) are responsible for a disproportionate amount of these emissions, accounting for 27% of on-road GHG emissions despite only representing 1% of on road vehicles.[2] Diesel combustion in the internal combustion engine (ICE) of HDVs is also associated with high burdens to human health, responsible for 50% of PM2.5 emissions from on-road vehicles, often in highly populated urban corridors resulting in disproportionate impacts to disadvantaged communities.[2–5] While there are several mandates and legislation at the state and national level to electrify, decarbonize, and reduce the human health impacts of HDVs, the technological pathway to achieving these changes remains unclear.[6–8]

Lithium-ion (Li-ion) batteries are a popular candidate when exploring options to electrify HDVs, largely due to the rapidly growing popularity of Li-ion battery passenger electric vehicles (EVs) and decreasing Li-ion battery prices. Since 2010, the size of the US passenger EV fleet has increased by nearly two orders of magnitude, all while the price of Li-ion batteries has decreased by nearly 90%.[9,10] Despite this, there are relatively few options for Li-ion battery electric HDVs, particularly for those designed for long-haul freight (trips over 250 miles). When reviewing the HDV market (Figure C1), we found only three makes of Li-ion battery electric heavy-duty trucks with a range greater than 250 miles, all with limited commercial availability. However, long-haul trips over 250 miles are responsible for 68% of GHG emissions from HDVs.[11]

Several studies report that the limited range, along with other factors like increased refueling time and less available weight for cargo, make current Li-ion HDVs uneconomical in long-haul freight applications when compared to diesel HDVs.[12–14] However, other studies frequently report the social and environmental benefits of using Li-ion HDVs in long-haul settings, primarily due to reduced GHG and particulate matter (PM2.5) emissions.[15–19] Yet no study to-date examines both the private and social impacts from the life-cycle of Li-ion HDVs operating in long-haul freight.

This study aims to determine if the electrification of long-haul HDVs with Li-ion batteries can reduce greenhouse gas (GHG) emissions and decrease the burden on human health while being economically feasible for the truck operator. If not, what are the conditions required to make Li-ion battery long-haul HDVs attractive economically and societally from a life-cycle perspective? To answer this, we compare the total lifetime costs (TLCs) of Li-ion battery electric Class 8 trucks operating in a long-haul capacity relative to diesel internal combustion engine Class 8 trucks performing the same trips. Included in the TLCs are the private monetary costs to the owner as well as contributions to global warming potential and human health burdens due to air pollution across the lifetime of the vehicles. We model the TLC for trucks operating in 2024 and 2035 while accounting for changes in vehicle design, battery technology, and electricity generation. Additionally, we compare the differences in TLC that arise when using different Li-ion battery chemistries.

5.2 Materials and Methods

5.2.1 Class 8 Truck Life-cycle and Study Boundaries

The life-cycle of a Class 8 truck is nonlinear and variable between individual trucks.[20] Figure 5.1 outlines common life-cycles of a Class 8 truck and the boundaries set for this study. Included in this study are the impacts associated with the material extraction, manufacturing and assembly, and long-haul freight use phase of a Class 8 truck. The long-haul fright use phase is often the first phase of life for a Class 8 truck. The average Class 8 truck spends around 4 years in this use phase, accruing around 110,000 vehicle miles traveled (VMT) per year.[13,20,21] This use phase concludes when the truck has depreciated to around 40% its intital value or major engine rebuilds are required.[20] The long-haul freight operator then sells the truck to a regional freight operator or a local freight operator.

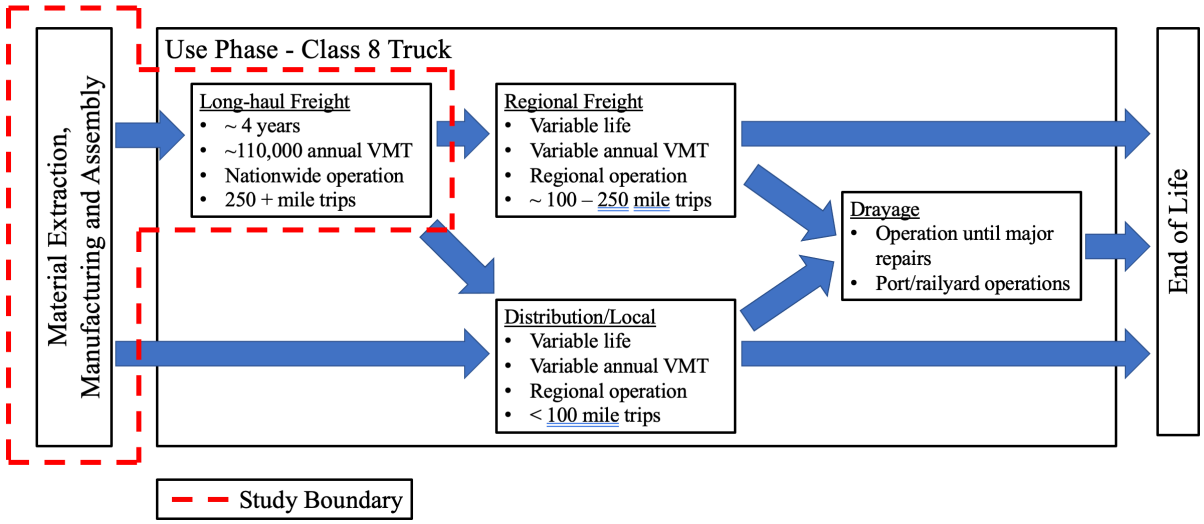

Figure 5.1. Class 8 truck life-cycle and study boundaries.

In our TLCs, we include the costs of ownership during the long-haul freight use phase, the contributions to global warming potential (GWP) and human health burdens during this use phase, and the contributions to GWP from the material extraction, manufacturing and assembly phases. Monetary costs and societal impacts outside of these phases are assumed to be attributable to other life-cycle phases. Human health burdens arising from material extraction, manufacturing and assembly are excluded due to high levels of uncertainty and limited data availability.

5.2.2 Truck Power Model and Design Parameters

A model of battery electric truck power demand and performance is required to determine costs of ownership and impacts to society. Equations 5.1 through 5.8 make up the standard model for the instantaneous power demand of a vehicle used in this study. [22]

Eq 5.1: $P_{Tot} = \left(\lambda * \left(\frac{1}{\eta_{BW}}\right) * P_{Mech} + (1 - \lambda) * (\eta_{BW} * \eta_{Br}) * P_{Mech} + P_{Ac}\right) * (1 - R_{Br})$

Eq 5.2: $\lambda = 1 \; if \; P_{Mech} \geq 0; \; \lambda = 0 \; if \; P_{Mech} < 0$

Eq 5.3: $P_{Mech} = P_{AR} + P_F + P_G + P_I$

Eq 5.4: $P_{AR} = 0.5 * \rho * C_D * A * v^3$

Eq 5.5: $P_F = C_{RR} * m * g * v$

Eq 5.6: $P_G = m * g * v * Z$

Eq 5.7: $P_I = 0.5 * m * v * a$

Eq 5.8: $m = \min(m_B + m_V + m_P, GVWR)$

A time resolution of a minute was used in Equations 5.1 through 5.8. All variables represent the average value over this resolution. In these equations P_{Tot} represents the total battery power demand, P_{AR} represents the power contribution due to air resistance, P_F represent the power contribution due to friction, P_G represents the power contribution due to gravity, P_I represents the power contribution due to inertia, and P_{Ac} represents the power contribution from accessory loads. Since the impacts from regenerative braking typically occur at a time resolution less than a minute, we instead model describe the energy recovered as reduction to power demand. The value of this reduction (R_{Br}) is determined via review of reported regenerative braking performance of electric Class 8 trucks commercially available today. Variables η_{BW} and η_{Br} represent the battery-to-wheels efficiency and brake efficiency respectively. Parameters ρ represents air density, C_D represents the vehicle's drag coefficient, A represents the frontal area of the truck, v represents the velocity of the truck, C_{rr} represents the coefficient of rolling resistance between the truck tires and the road, g represent the gravitational coefficient, Z represents the current grade of the road, and a represents the acceleration. Additionally, m represents the total weight of the vehicle is comprised of the weight of battery (m_B), the weight of the tractor and trailer excluding the battery weight (m_V), and the weight of the payload (m_P). The maximum total weight of the vehicle is set at the maximum federal gross vehicle weight rating (GVWR) of 82,000 lbs for Li-ion Class 8 trucks and 80,000 for diesel Class 8 trucks.[21,23]

Table 5.1 shows the parameter values and battery size, as well as the resulting range of the vehicles included in this study. Uncertainties for all these parameters is presented in Table C1. Battery weight varies by the battery chemistry chosen and is determined by multiplying the chemistry-specific pack specific energy by the battery size. The pack specific energies for each chemistry are provided in Table C2.[24]

Table 5.1. Truck design parameters by performance scenario.

Parameter	Li-ion Class 8 Truck	Diesel Class 8 Truck
R_{Br} [%]	7.5	-
η_{BW} [%]	0.85	-
η_{Br} [%]	0.97	0.97
η_{GB} [%]	0.95	-
η_{E} [%]	-	0.42
η_{TW} [%]	-	0.9
C_D	0.63	0.63
A [m^2]	5.4	5.4
C_{rr}	0.0055725	0.0055725
m_B [kg]	Var. by Chem.	0
m_V [kg]	8,767	13,267
GVWR [lbs]	82,000	80,000
P_{AC} [kW]	If ref.* 8 kW Else 2 kW	If ref.* 8 kW Else 2 kW
Full Rated Capacity [kWh]	1000	-
Available Capacity [kWh]	85	-
Range [mi]	560	-

* Refrigerated trailer

The design parameters and power demand model of diesel Class 8 trucks are similar to Li-ion Class 8 trucks with η_{BW} being replaced by the product of the diesel engine efficiency (η_E) and the transmission-to-wheels efficiency (η_{TW}). The parameters for the diesel truck design scenario are also displayed in Table 5.1.[15,22,25]

5.2.3 Trip Generation and Behavioral Model

We constructed a model to describe the trips performed by a truck and how it would complete them over a year of operating in long-haul freight. To determine the routing of a Class 8 truck, we referenced the 2017 Commodity Flow Survey (CFS)[26] and only observed trips that were over 250 miles and performed by Class 8 trucks. The CFS provides origin-destination (OD) pairs between all major metropolitan areas and describes characteristics for typical trips along these OD pairs. These characteristics include payload weight, whether the trailer was refrigerated, and a statistical-weight parameter that describes how frequently trips had these characteristics and how frequently trips occurred between OD pairs. These statistical weight parameters were used to construct discrete probability density functions (PDFs) describing the likelihood of going to specifics destination from different origins, the likelihood common payload weights, and the likelihood a trailer was refrigerated.

We assigned the major metropolitan areas from the CFS as nodes in a network of all major US trucking corridors and set the corridors as links.[27] Additionally, nodes where charging could occur were placed at every major metropolitan area and every 250 miles along corridors. The length of corridors and road grade were stored in these links. The constructed PDFS were then used to determine an OD pair, a payload weight, and whether the trailer was refrigerated. A standard shortest path algorithm was used to determine the specific routing a truck would follow within the corridor network. This procedure was repeated, using the previous destination as the origin for the next trip. If chosen payload weight for a trip causes the total vehicle weight to exceed the federal GVWR limit, we assume that the excess weight is removed from payload and must be shipped by taking up a portion of another vehicle's cargo space. These excess tonne-miles are considered when calculating ownership costs.

A behavioral model of Li-ion and diesel Class 8 trucks was constructed to determine dispatch times, vehicle speeds, when and how charging occurs, and when to rest while completing the routes determined from the trip generation model for a year of operation. The outputs of this model included the VMTs and power demand along every kilometer driven in the network, the hourly electricity power demand at every node where charging occurs, time spent driving, time spent simultaneously resting and charging, and time spent solely charging over the course of a year.

Initial trip dispatching from a location was decided via a discrete probability density function presented in Figure C2.[28] We assumed truck velocity and acceleration followed the California Air Resource Board Heavy Heavy-Duty Diesel Truck Cruise Segment drive cycle when driving.[29] This drive cycle is visualized in Figure C3. Using the power model outlined in Equations 5.1 through 5.8 while assuming a max payload, no accessory power demand, and no elevation change results in a energy efficiency of 1.52 kWh per mile along this drive cycle. Additionally, our model employed logic to ensure that the state-of-charge of a Li-ion battery on a Class 8 truck remained between zero and one, and that the labor regulations for truck drivers in the US were followed.[30] We assumed there was no preference on the time of day when charging occurred. Similar logic was used to determine diesel trucking behavior. Charging speeds as a function of state-of-charge and infrastructure type are presented Figure C4.[31–33]

5.2.4 Grid Emissions Modeling, Global Warming Potential, and Human Health

The hourly electricity power demand at charging nodes is used to determine the use phase contributions to GWP and human health burden from Li-ion Class 8 truck operation. We employ the electricity grid model outlined in McNeil et al.[19] to determine marginal generator type and location responding to the hourly electricity demand at each node. Procedure C1 describes the methodology for determining the hourly marginal generator responding to the electricity demand at each node. The emitted GHGs and criteria air pollutants at the responding marginal generators is then estimated using emission factors from the Grid Optimized Operation Dispatch Model.[34] GHG emissions are then converted to tonnes of CO_2-equivalents (CO_{2eq}) to determine contributions to GWP. Emissions of primary and secondary fine particulate matter (PM2.5) are used to determine resulting human health damages using the InMAP source–receptor matrix (ISRM).[35–38] Two scenarios of renewable energy adoption are used to determine responding

marginal generators: one where renewable energy costs are high and one where renewable energy costs are low. These scenarios are outlined in NREL's Standard Scenarios.[39,40]

For diesel Class 8 truck operation, we use the modeled VMT and power demand along each kilometer segment of all trucking corridors to determine contributions to GWP and human health burden following procedure outlined in McNeil et al.[19] Emission factors from GREET[41] and Preble et al.[42] are used to determine GHG and PM2.5 emissions at each kilometer segment. GHG emissions are then converted to tonnes of CO_2-equivalents (CO_{2eq}) to determine contributions to GWP. Two sets of emission factors are used: one representing current the performance of pollution control technologies (diesel particulate filter and selective catalytic reduction), and one representing the performance of potentially improved pollution control technologies.[15,41–43] Table C3 contains the specific emission factors used. Emissions of PM2.5 are used to determine resulting human health damages using the InMAP source–receptor matrix (ISRM).[35–38] For TLCs in 2024, we assume emission factors match those of model year 2010 through 2018 diesel Class 8 trucks. For TLCs in 2035, we assume incremental improvements to 2024 emission factors.

5.2.5 Battery and Truck Material Extraction and Manufacturing Emissions

The contributions from battery material extraction and manufacturing are modeled using the procedure used in Porzio et al.[44] The inputs, outputs, and emissions associated with the material extraction and manufacturing of truck materials are added to the framework used to determine life-cycle emissions,[44,45] and presented in Tables C4 and C5.

5.2.6 Ownership Costs

Ownership costs are broken into six major categories: general operations (general ops), fuel, battery, standing, payload, and tax credits. We calculate the costs ownerships cost after modeling truck behavior for a year and assuming four years a spent performing long-haul freight. The annual VMT, age, and other statistics are used to model the categories of ownerships. Discount rates of 3%, 5% and 7% are used for determining costs into the future.

General ops costs consist of vehicle depreciation, insurance, taxes, additional fees, maintenance, and driving labor. Vehicle depreciation is modeled as a percentage of the initial manufacturer suggested retail price of a vehicle. This percentage is determined by a function of the VMT and age of a vehicle and is assigned to occur at the end of the long-haul freight use phase.[12,13] The cost of the battery for Li-ion Class 8 trucks is excluded from this calculation given that no significant second-life battery market currently exists.[46] Insurance is modeled as an annual cost per annual VMT.[13] Taxes consist of an upfront component due to the federal excise tax and a fixed annual component due to the Heavy Vehicle Use Tax.[47,48] Fees consist of a variable annual component dependent on vehicle weight representing registration fees and a variable annual component dependent on VMT due to tolls and miscellaneous permits.[13] Maintenance consists of a variable annual component determined by a function of vehicle miles traveled and vehicle age. Additionally, maintenance costs are high for diesel Class 8 trucks due to the increased complexity of their powertrain.[12,13] Driving labor is modeled as an annual cost per annual VMT. Table C6 describes the calculation and uncertainties of the values used to calculate general ops costs.

Fuel costs for Li-ion battery Class 8 trucks consist of two components: one representing the cost of purchasing electricity, and one representing the cost of utilizing provided charging infrastructure. The cost of purchasing electricity is set at a forecasted national average and varies by the future renewable cost scenario and years of operation modeled.[49] For 2024, electricity prices are set at $0.141/kWh and $0.142/kWh in the low and high renewable cost scenarios respectively. For 2035, electricity prices are set at $0.141/kWh and $0.146/kWh in the low and high renewable cost scenarios respectively. These prices represent the averages over the years of vehicle operation. The cost of utilizing charging infrastructure is estimated at $0.114/kWh in 2024 by Burnham et al.[50] and primarily considers equipment costs, installation costs, infrastructure lifetime, and infrastructure provider margins. For diesel Class 8 trucks, the cost of fuel consists of the national average diesel prices. Figure C5 visualizes forecasted electricity and diesel costs under high and low renewable cost scenarios.

Battery costs are only present for Li-ion Class 8 trucks and assigned as an upfront cost. Current battery pack prices for each cathode chemistry are used when modeling 2024 costs of ownership. A learning rate of 17% and a forecast of Li-ion battery demand as used to model 2035 costs. Figure C6 and Tables C7 and C8 visualize the modeled future battery prices, battery demand, and uncertainty. The procedure used in Porzio et al.[44] is employed to size truck batteries such that they can maintain their rated power over the entire time spent operating in long-haul freight even as they degrade due to cycling and calendar aging.

Standing costs for Li-ion Class 8 trucks represents the additional cost of labor accrued while the truck is charging. This is modeled by multiplying the annual time spent charging (excluding time simultaneously used to rest for the driver) by the hourly cost of labor and supporting operations incurred from this additional time.[13]

Payload costs for Li-ion Class 8 trucks represent the cost of performing the excess tonne-miles due to the offset cargo from the additional battery weight relative to diesel Class 8 trucks. The average excess tonne-miles is normalized by the payload capacity of an additional Li-ion Class 8 truck and multiplied by the total cost of ownership excluding payload costs.[13,51]

Tax credits represent an upfront federal tax credit due to the Commercial Clean Vehicle Credit.[52] Table C9 contains the values and uncertainties used to calculate standing, payload costs, and tax credits.

5.3 Results

5.3.1 Total Lifetime Costs

A Monte Carlo simulation consisting of simulating a fleet of 25 trucks was used to determine the average TLCs for each Class 8 truck type in each scenario. Figure 5.2 visualizes the TLCs of Li-ion and diesel Class 8 trucks over the four-year average lifetime of a Class 8 truck in long-haul freight. Figure 5.2a and b visualize the TLCs of truck operation starting in 2024 under high and low renewable cost scenarios respectively. Figure 5.2c and d visualize the TLCs of truck

operation starting in 2035 under high and low renewable cost scenarios respectively. A social cost of carbon (SCC) of \$190/tonne CO_{2eq}[53] and a 5% discount rate are used. Error bars represent two standard deviations.

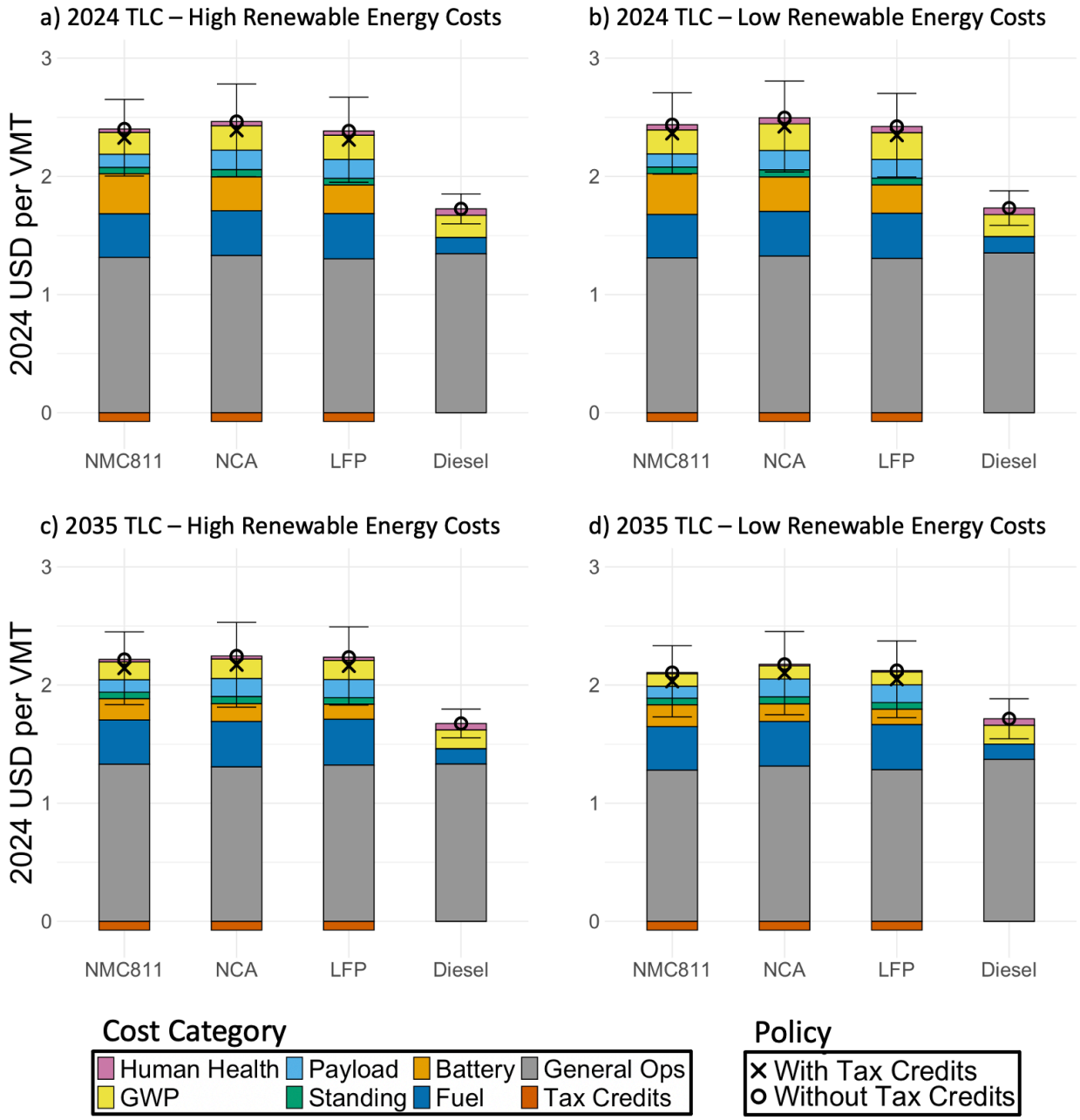

Figure 5.2. TLC of Li-ion and diesel Class 8 trucks in 2024 and 2035 under high and low renewable cost scenarios. Tax credits are representative of values from the Commercial Clean Vehicle Credit.

5.3.2 GWP and Human Health Impacts

Figure 5.3 visualizes the contributions to GWP and human health from Li-ion and diesel Class 8 trucks in 2024 and 2035 under high and low renewable cost scenarios. Figure 5.3a and b visualize contributions of truck operation starting in 2024 under high and low renewable cost scenarios respectively. Figure 5.3c and d visualize the contributions of truck operation starting in 2035 under high and low renewable cost scenarios respectively. A social cost of carbon (SCC) of \$190/tonne CO_{2eq}[1] and a 5% discount rate are used. Error bars represent two standard deviations.

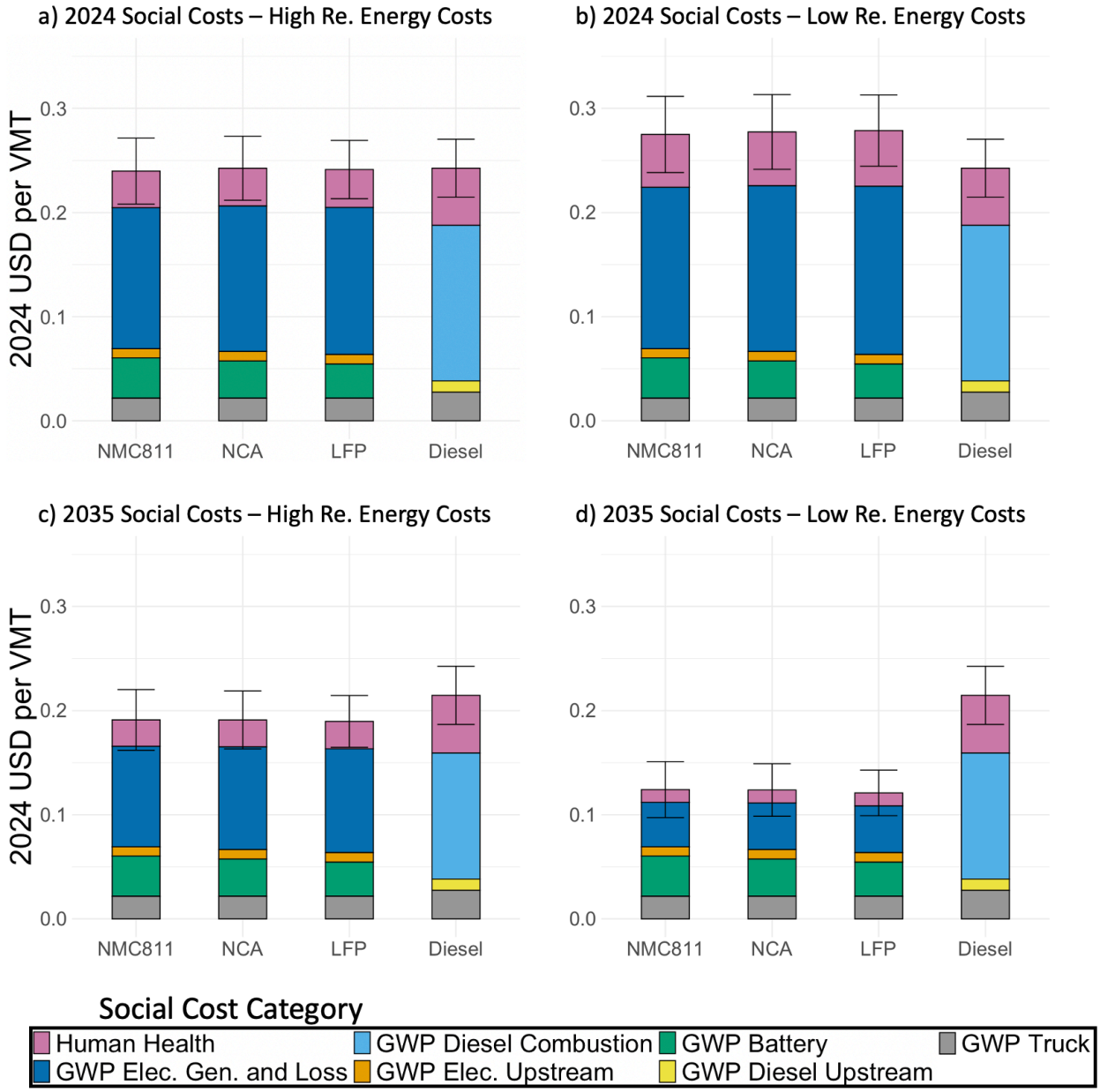

Figure 5.3. Contributions to GWP and human health burden from Li-ion and diesel Class 8 trucks in 2024 and 2035 under high and low renewable cost scenarios.

5.3.3 Sensitivity Analysis

The value of the SCC is continually evolving as modeling continues to climate improve and societal understanding of the impacts associated with global warming grows.[53,54] Additionally, methodologies for determining human health burdens resulting from emitted air pollutants continue to improve due to developments in meteorology, environmental sciences, biology, public health, and environmental justice.[35–38] Battery prices and the cost of utilizing charging infrastructure are added sources of high unpredictability in our TLC model.
A sensitivity analysis was performed to determine how the TLC costs to society would vary given changes to the SCC, methods of determining human health burden, battery prices, and infrastructure utilization costs. The Figure 5.4 visualizes the TLC and the total percent change for a Li-ion NMC811 Class 8 truck compared to a diesel Class 8 truck under 4 sensitivity scenarios relative to the 2035 low renewable cost TLC.

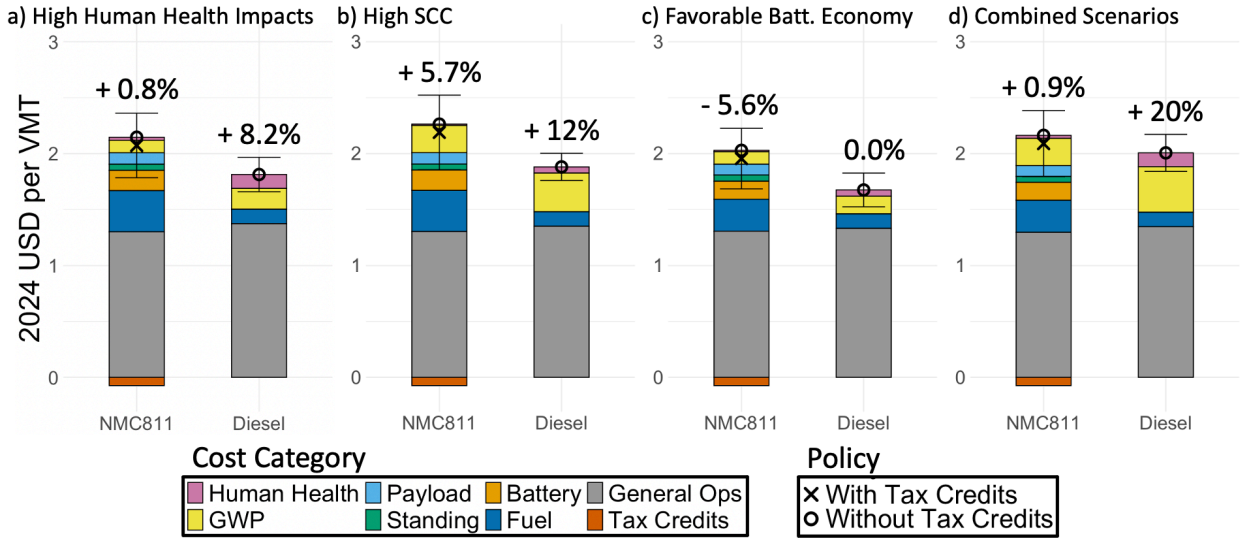

Figure 5.4. TLC and percent change from sensitivity scenarios relative to 2035 low renewable cost scenario.

Under the *High Human Health Impacts* scenario, the burden to human health is determined using the methods outlined by Krewski et al.,[38] resulting in higher damages from PM2.5 emissions. In the *High SCC* scenario, the social cost of carbon is set to the 95th percentile estimate of 413 $/tonne modeled by Rennert et al.[54] In the *Favorable Batt. Economy* scenario, the learning rate for battery prices is increase by 2% to 19% and the cost of utilizing charging infrastructure is decreased by 50%. [24,50] All these changes are present in the *Combined Scenarios* figure, showing the stacked effects of the sensitivity scenarios.. Additionally, the impacts of varying discount rates are presented in Figures C7 and C8.

5.4 Discussion

As seen in Figure 5.2, the TLC across all scenarios is higher for Li-ion Class 8 trucks relative to diesel Class 8 trucks. Other than the cost from general ops, the greatest contributors to TLC for Li-ion Class 8 trucks are the fuel costs from charging, battery costs, payload costs from offset cargo, and in some scenarios the contributions to GWP from induced electricity generation. TLC contributions from standing costs due to labor associated with the additional time of charging, burdens to human health, and tax credits are lesser but still significant. The TLC of diesel Class 8 trucks is lower than the TLC of Li-ion Class 8 trucks in all scenarios due to reduced fuel costs and the absence of battery, payload, and standing costs.

In three of the four scenarios modeled, the TLC of LFP Li-ion Class 8 truck is the lowest of the battery electric trucks. This is attributable to the lower price of Li-ion batteries with the LFP cathode chemistry. The reduced battery costs are enough to overcome effects of the lower energy density associated with the LFP cathode chemistry (increased fuel and payload costs). In all scenarios modeled, the TLC of the NCA Li-ion Class 8 truck is the highest due to its middling energy density but relatively high price.

The social costs of Li-ion Class 8 trucks relative to diesel Class 8 trucks fluctuates by scenario, illustrated in Figure 5.3. In 2024 under a high renewable energy cost scenario, the social impacts of Li-ion Class 8 trucks are marginally less than impacts from diesel Class 8 trucks. However, under the low renewable energy cost scenario, the 2024 social impacts of Li-ion Class 8 trucks are greater than those from diesel Class 8 trucks. More fossil fuel combusting generators are responding to the marginal load under the low renewable energy cost scenario than the high renewable energy cost scenario, resulting in greater contributions to GWP and human health burden.

In 2035, the social impacts from Li-ion Class 8 trucks are lower than diesel Class 8 trucks under both renewable energy cost scenarios since both assume that less fossil fuel combusting generator are responding to marginal electricity demand. Less fossil fuel combustion is assumed to occur in the low renewable energy cost scenario, resulting in significantly lower contributions to GWP and human health burden. These reductions to social costs highlight the importance of offsetting fossil fuel combustion from responding to marginal electricity demand.

Figure 5.4a and b visualize how the magnitudes and relative differences of the TLC and social impacts associated with Class 8 trucking fluctuates with the value of the SCC and how we model human health burden. In 2035, increasing the SCC or contributions to human health burden both raise the TLC diesel Class 8 trucks by a greater magnitude than the TLC Li-ion Class 8 trucks. Additionally, Figure 5.4c shows how favorable economic development can lower the future TLC of Li-ion Class 8 trucks relative to the diesel alternative. Combining these impacts in Figure 5.4d illustrate how the future difference between the TLC of diesel and Li-ion Class 8 trucks is largely dependent on highly unpredictable factors like how we model the SCC and human health burdens, as well as how the battery economy develops.

5.5 Conclusions and Future Work

Our analysis reveals several insights on the TLC and social impacts associated with Li-ion Class 8 trucks relative to diesel. First, without major improvements to battery technology, it is unlikely that the TLC of Li-ion Class 8 trucks operating in long-haul freight ever falls below the TLC of diesel trucks. As shown in Figure 5.4c, Reductions in Li-ion battery prices and the costs of charging are essential in improving the TLC of Li-ion Class 8 trucks in long-haul freight. Improved specific energy into the future can result in lower standing and fuel costs, visualized by comparing these cost categories between NMC811 and NCA Li-ion Class 8 trucks. However, the future TLC of both Li-ion and diesel Class 8 trucks is largely dependent on highly unpredictable factors, like society's valuation of contributions to climate change and human health burdens, as well as the economic development of batteries.

Additionally, the current use of Li-ion Class 8 trucks does not result in clear improvements to social impacts relative to diesel Class 8 trucks when studied at a national level. However, regional variations in the value of social impacts are likely due to differences in electricity generation portfolios and the amount of renewable generation available by region.[55] Continued integration of renewable energy, particularly low-cost renewable energy, is required to offset fossil fuel combustion from responding to marginal electricity demand and achieve improved social impacts of Li-ion Class 8 trucks in the future.

Future works will examine the impacts of different driving behaviors and regulations on the social and economic costs Li-ion Class 8 trucks in long-haul freight. The impacts of incentivizing versus requiring charging to occur at night on the TLC of Li-ion Class 8 trucks will be studied. A more thorough sensitivity analysis on the impacts of improved Li-ion Class 8 truck performance will be modeled as well. This analysis will account for the forecasted technological improvements associated with Li-ion Class 8 trucking to determine if an of the expected technological improvements can significantly change the TLC relative to the diesel alternative. Finally, the impacts of increasing the lifetime of a Li-ion Class 8 truck relative to diesel will be examined.

References

1. US EPA. *Draft Inventory of U.S. Greenhouse Gas Emissions and Sinks: 1990-2022*. (2024).

2. Davis, S. C. *Transportation Energy Data Book Edition 40*. (2022).

3. Choma, E. F. *et al.* Health benefits of decreases in on-road transportation emissions in the United States from 2008 to 2017. *Proc Natl Acad Sci USA* **118**, (2021).

4. Lathwal, P., Vaishnav, P. & Morgan, M. G. Environmental injustice in America: Racial disparities in exposure to air pollution health damages from freight trucking. *arXiv* (2022) doi:10.48550/arxiv.2204.06588.

5. Laden, F., Neas, L. M., Dockery, D. W. & Schwartz, J. Association of fine particulate matter from different sources with daily mortality in six U.S. cities. *Environ. Health Perspect.* **108**, 941–947 (2000).

6. US DOE. *The U.S. National Blueprint for Transportation Decarbonization: A Joint Stratedy to Transform Transportation*. (2023).

7. US EPA. *Greenhouse Gas Emissions Standards for Heavy-Duty Vehicles - Phase 3*. (2023).

8. Executive Department State of California. *Executive Order N-79-20*. (2020).

9. BloombergNEF. *Long-Term Electric Vehicle Outlook 2023*. (2023).

10. BloombergNEF. *Lithium-Ion Batteries: State of the Industry 2023*. (2023).

11. Ledna, C., Mueratori, M., Yip, A., Jadun, P. & Hoehne, C. *Decarbonizing Medium- & Heavy-Duty On-Road Vehicles: Zero-Emissions Vehicles Cost Analysis*. (2022).

12. Hunter, C. *et al. Spatial and Temporal Analysis of the Total Cost of Ownership for Class 8 Tractors and Class 4 Parcel Delivery Trucks*. (2021).

13. Burnham, A. *et al. Comprehensive Total Cost of Ownership Quantification for Vehicles with Different Size Classes and Powertrains*. (2021).

14. Wang, Z. *et al.* A total cost of ownership analysis of zero emission powertrain solutions for the heavy goods vehicle sector. *J. Clean. Prod.* **434**, 139910 (2024).

15. Tong, F., Jenn, A., Wolfson, D., Scown, C. D. & Auffhammer, M. Health and Climate Impacts from Long-Haul Truck Electrification. *Environ. Sci. Technol.* **55**, 8514–8523 (2021).

16. Camilleri, S. F. *et al.* Air quality, health and equity implications of electrifying heavy-duty vehicles. *Nat. Sustain.* (2023) doi:10.1038/s41893-023-01219-0.

17. Lin, Z. Mostly positive implications of long-haul truck electrification. *Joule* **5**, 2548–2550 (2021).

18. Phadke, A., Khandekar, A., Abhyankar, N., Wooley, D. & Rajagopal, D. *Why Regional and Long-Haul Trucks are Primed for Electrification Now*. (2021).

19. McNeil, W. H., Tong, F., Harley, R. A., Auffhammer, M. & Scown, C. D. Corridor-Level Impacts of Battery-Electric Heavy-Duty Trucks and the Effects of Policy in the United States. *Environ. Sci. Technol.* **58**, 33–42 (2024).

20. Wall, J. Interview with John Wall, Former CTO of Cummins. (2023).

21. Hunter, C. A. *et al.* Techno-economic analysis of long-duration energy storage and flexible power generation technologies to support high-variable renewable energy grids. *Joule* (2021) doi:10.1016/j.joule.2021.06.018.

22. Sripad, S. & Viswanathan, V. Performance Metrics Required of Next-Generation Batteries to Make a Practical Electric Semi Truck. *ACS Energy Lett.* **2**, 1669–1673 (2017).

23. Burnham, A. *et al. Comprehensive Total Cost of Ownership Quantification for Vehicles with Different Size Classes and Powertrains*. (2021).

24. BloombergNEF. *2022 Lithium-Ion Battery Price Survey*. (2022).

25. Tong, F., Wolfson, D., Jenn, A., Scown, C. D. & Auffhammer, M. Energy consumption and charging load profiles from long-haul truck electrification in the United States. *Environmental Research: Infrastructure and Sustainability* (2021) doi:10.1088/2634-4505/ac186a.

26. US Department of Transportation, Bureau of Transportation Statistics, US Department of Commerce & US Census Bureau. 2017 Commodity Flow Survey Datasets. https://www.census.gov/data/datasets/2017/econ/cfs/historical-datasets.html (2020).

27. ESRI, Bureau of Transportation Statistics, Federal Highway Administration & GeoSystems Global Corporation. USA Interstate Highway and Freeway System. *ArcGIS* https://www.arcgis.com/home/item.html?id=1bca8077671b4089b28436fd2dbe2611 (2010).

28. Boriboonsomsin, K. *et al. Collection of Activity Data from On-Road Heavy-Duty Diesel Vehicles*. (2017).

29. National Renewable Energy Laboratory. NREL DriveCAT - Chassis Dynamometer Drive Cycles. https://www.nrel.gov/transportation/drive-cycle-tool/ (2023).

30. Federal Motor Carrier Safety Administration. *Interstate Truck Driver's Guide to Hours of Service*. (2015).

31. Andrenacci, N., Karagulian, F. & Genovese, A. Modelling charge profiles of electric vehicles based on charges data. *Open Res. Europe* **1**, 156 (2021).

32. Hackmann, M. *P3 Charging Index Report 07/22 – Comparison of the Fast Charging Capability of Various Electric Vehicles*. (2022).

33. Moura, S. Interview with Prof. Scott Moura. (2023).

34. Jenn, A., Clark-Sutton, K., Gallaher, M. & Petrusa, J. Environmental impacts of extreme fast charging. *Environmental Research Letters* **15**, 094060 (2020).

35. Thind, M. P. S., Tessum, C. W., Azevedo, I. L. & Marshall, J. D. Fine Particulate Air Pollution from Electricity Generation in the US: Health Impacts by Race, Income, and Geography. *Environ. Sci. Technol.* **53**, 14010–14019 (2019).

36. Goodkind, A. L., Tessum, C. W., Coggins, J. S., Hill, J. D. & Marshall, J. D. Fine-scale damage estimates of particulate matter air pollution reveal opportunities for location-specific mitigation of emissions. *Proc Natl Acad Sci USA* **116**, 8775–8780 (2019).

37. Tessum, C. W., Hill, J. D. & Marshall, J. D. InMAP: A model for air pollution interventions. *PLoS ONE* **12**, e0176131 (2017).

38. Krewski, D. *et al.* Extended follow-up and spatial analysis of the American Cancer Society study linking particulate air pollution and mortality. *Res Rep Health Eff Inst* 5–114; discussion 115 (2009).

39. Gagnon, P. *et al. 2022 Standard Scenarios Report: A U.S. Electricity Sector Outlook*. (2022).

40. National Renewable Energy Laboratory. Scenario Viewer: Data Downloader. https://scenarioviewer.nrel.gov.

41. Wang, M. *GREET (Greenhouse Gases, Regulated Emissions, and Energy Use in Transportation) Model*. (Argonne National Laboratory, 2023).

42. Preble, C. V., Harley, R. A. & Kirchstetter, T. W. Control Technology-Driven Changes to In-Use Heavy-Duty Diesel Truck Emissions of Nitrogenous Species and Related Environmental Impacts. *Environ. Sci. Technol.* **53**, 14568–14576 (2019).

43. Tong, F., Jaramillo, P. & Azevedo, I. M. L. Comparison of life cycle greenhouse gases from natural gas pathways for medium and heavy-duty vehicles. *Environ. Sci. Technol.* **49**, 7123–7133 (2015).

44. Porzio, J., Wolfson, D., Auffhammer, M. & Scown, C. D. Private and External Costs and Benefits of Replacing High-Emitting Peaker Plants with Batteries. *Environ. Sci. Technol.* **57**, 4992–5002 (2023).

45. Scown, C. D., Gokhale, A. A., Willems, P. A., Horvath, A. & McKone, T. E. Role of lignin in reducing life-cycle carbon emissions, water use, and cost for United States cellulosic biofuels. *Environ. Sci. Technol.* **48**, 8446–8455 (2014).

46. Zhao, Y. *et al.* A Review on Battery Market Trends, Second-Life Reuse, and Recycling. *Sustainable Chemistry* **2**, 167–205 (2021).

47. US EPA. Learn About Federal Excise Tax Exemption. https://www.epa.gov/verified-diesel-tech/learn-about-federal-excise-tax-exemption (2023).

48. US Department of Transportation. Heavy Vehicle Use Tax. *Policy and Governmental Affairs Office of Highway Policy Information* https://www.fhwa.dot.gov/policyinformation/hvut/mod1/whatishvut.cfm (2020).

49. US Energy Information Administration. *Annual Energy Outlook 2023*. (2023).

50. Burnham, A. *et al.* Enabling fast charging – Infrastructure and economic considerations. *J. Power Sources* **367**, 237–249 (2017).

51. Hunter, C. *et al. Spatial and Temporal Analysis of the Total Cost of Ownership for Class 8 Tractors and Class 4 Parcel Delivery Trucks*. (2021).

52. Internal Revenue Service. Commercial Clean Vehicle Credit. *Commercial Clean Vehicle Credit* https://www.irs.gov/credits-deductions/commercial-clean-vehicle-credit (2024).

53. US EPA. *Supplementary Material for the Regulatory Impact Analysis for the Final Rulemaking, "Standards of Performance for New,Reconstructed, and Modified Sources and Emissions Guidelines for Existing Sources: Oil and Natural Gas Sector Climate Review"*. (2023).

54. Rennert, K. *et al.* Comprehensive evidence implies a higher social cost of CO2. *Nature* (2022)

55. Dong, K. *et al.* CO2 emissions, economic and population growth, and renewable energy: Empirical evidence across regions. *Energy Economics* **75**, 180–192 (2018).

Chapter 6

Conclusions

6.1 Summary of Major Findings

6.1.1 Life-cycle assessment considerations for batteries and battery materials

To date, we are unable to find studies that set the standard for best practices in battery LCAs. While many studies perform well in one or more dimensions, they often still have their own drawbacks. Most of the published LCAs have provided detailed data on the environmental impacts of raw materials extraction and processing. The shortcomings in our understanding of raw material extraction and processing are twofold. First, the studies we surveyed did not adequately account for geographic variation in mining practices and variations in the exposure risk for nearby populations. Some mining operations that comprise a minority share of production are likely to drive an outsized fraction of overall environmental impacts because of local conditions and practices. Second, there are inherent limitations in the underlying midpoint and impact methodologies; it is impossible for any LCA to conduct detailed fate and transport modeling for every emission to air, soil, and water, so studies rely on regional or global average factors that are likely to be one or more orders of magnitude different from the actual values. These uncertainties are compounded by the fact that documentation of where specific waste streams are discharged from mining and material processing operations is sparse. Moreover, we have yet to find any study that explores the differences between average, marginal, and incremental sources of key material inputs, and the implications for mining and processing-related energy use and emissions. This seems to be an obvious gap in the literature, and one that could be filled with data and market projections that are available today.

Achieving consensus and clarity in battery manufacturing energy use and impacts is where prior studies largely fall short. Because there is little evidence to suggest appreciable non-combustion emissions to air, water, or soil during manufacturing, nearly all direct environmental impacts from this stage are expected to be tied directly to on-site combustion of fuels and emissions from electricity generation. Battery recycling, by comparison to battery manufacturing, is relatively well studied and there is better agreement across the literature, although battery recycling LCAs must rely largely on estimated or simulated mass and energy balances because of the limited number of LIBs being recycled. It is possible that, when primary data becomes more widely available, it will reveal inconsistencies between simulations and primary data similar to those found in battery manufacturing. Although battery technologies will continue to evolve, and there will continue to be disagreements between primary and secondary data sources, we hope to provide recommendations for approaching these uncertainties in a manner that makes each study

more interpretable, and simpler to replicate and update as battery technologies and the infrastructure supporting their production continues to develop. These suggestions are provided in the *Recommendations for Future Works* section.

6.1.2 Temporal Variations in Learning Rates of Li-ion Technologies

Our segmented experience curve analysis shows both a greater conceptual agreement and statistical justification with existing price behavioral analyses than studies that perform traditional experience curves with Li-ion technology prices. A segmented experience curve analysis should be performed when using price instead of cost to gain greater insight and a more accurate description of the price reductions over time. Our novel application of these methods to Li-ion technologies exemplifies the importance of using segmented experience curves to better understand the temporal patterns of Li-ion technology changes. For instance, we identified different learning rates for lithium-ion cells: the learning rate was 4% through 1997, 34% through 2003, and 24.4% onward. Additionally, by allowing greater flexibility in the experience curve, a secondary period of increased learning (40.9%) emerges from 2013 onward. This secondary "Shakeout" aligns well with Li-ion market behavior but is slightly less statistically significant than the previous model; however, this model may emerge as significant with the availability of more price and market size data. Understanding these historical changes to Li-ion technology prices is essential for informing the methods used to project future Li-ion prices.

6.1.3 Private and External Costs and Benefits of Replacing High-Emitting Peaker Plants with Batteries

Our results show that sizing BESS to fully replace the service provided by natural gas-fired peaker plants is unlikely to be economically viable. Instead, sizing each BESS to serve all but approximately the top fifth percentile of load events (appropriate threshold may vary by facility) dramatically reduces the required storage capacity and, thus, CapEx, while still meeting 81% of load on average. Based on California's current electricity market, BESS sized to meet the 95th percentile of loads served by natural gas peaker plants can achieve a positive NPV, but only if the value of frequency regulation does not decline. The BESS most likely to be profitable are those with LFP cathodes replacing large natural gas peaker plants that do not output large quantities of energy frequently and continuously, since most profits come from slack capacity sold in the frequency regulation market. Arbitrage, in contrast, is only a small contributor to total revenue. Given the limited size of the frequency regulation market and the forecasted growth of energy storage in California, the value of frequency regulation may decrease in the future. A remaining question is whether the social benefits of energy storage can compensate for the declining value of frequency regulation.

The BESS scenarios evaluated in this study yielded small monetized climate and human health impacts relative to the private costs and benefits. While replacing peaker power plants does reduce air quality-related health damages in surrounding communities, the profit-maximizing behavior for the BESS we modeled also increased life-cycle GHG emissions once the embodied emissions in the BESS were accounted for. Future prices of Li-ion cells and the evolution of electricity markets are critical to increasing the NPVs of BESS. If the value of frequency regulation does indeed decrease over time, battery costs must decrease and revenue from

arbitrage must increase to maintain or increase NPVs. Additionally, transmission investments, new generation capacity, shifting demand, and changes in utility rate structures will influence the NPVs of BESS.

6.1.4 Private and External Impacts of Electrified Heavy-Duty Long-Haul Trucking with Li-ion Batteries

Our analysis reveals several insights on the TLC and social impacts associated with Li-ion Class 8 trucks relative to diesel. First, without major improvements to battery technology, it is unlikely that the TLC of Li-ion Class 8 trucks operating in long-haul freight ever falls below the TLC of diesel trucks. Reductions in Li-ion battery prices and the costs of charging are essential in improving the TLC of Li-ion Class 8 trucks in long-haul freight. Improved specific energy into the future can result in lower standing and fuel costs, visualized by comparing these cost categories between NMC811 and NCA Li-ion Class 8 trucks. However, the future TLC of both Li-ion and diesel Class 8 trucks is largely dependent on highly unpredictable factors, like society's valuation of contributions to climate change and human health burdens, as well as the economic development of batteries.

Our study also highlights how the aggregated social impacts of Li-ion Class 8 trucks operating across the nation is not clearly lower than the aggregated social impacts of diesel Class 8 trucks. However, our study does not capture the potential for substantial regional differences in social impact to variations in local generation capacity, population density, and meteorology. But regardless of regional variations, the ongoing integration of low-cost renewable energy will aid in achieving improved future social impacts of Li-ion Class 8 trucks at a national level.

6.2 Limitations

We identify limitations for our chapters where we perform novel analyses. When performing segmented regression, temporally varied learning rates can only be statistically justified if enough data points are included. However, the historic price of Li-ion technologies is often not publicly available, especially in more recent years. As a result, conclusions about the current behavior of learning rates are limited to several years prior to the date of a study, when Li-ion price data is made available. Additionally, learning rates are inherently poor at extrapolation due to the unpredictability of future markets and their dependence on events outside the bounds of their interpolation. For example, no learning scenario in any study predicted the impact of the global COVD19 pandemic on battery prices.

Data availability in electricity markets is a major limitation when modeling the impacts associated with replacing peaker plants with large-scale Li-ion BESS. This is especially true when modeling the value of resource adequacy (RA), or the monetary value a Li-ion BESS may receive for providing "large-scale, stand-by, backup" power for operational generators, which was excluded from our study due to a lack of data availability and marginal importance. In CAISO, generators must self-provide or outsource an amount of standby power relative to their generation capacity, known as RA. In recent years, this outsourced RA component has represented a significant portion of revenue for large-scale Li-ion BESS. However, contracts for

RA are entirely private and only reported once every two years with a two year delay. This delay causes major uncertainty in the current value of providing RA due to changes in the CAISO energy generation market. The rapid addition of solar and other renewable generation in CIASO has resulted in high demand for the provision of RA, raising its price. However, this change in value was unreported to the public until 2024.

Additionally, the rapid state of change of current electricity markets poses a significant challenge to TEA modelers. Between 2020 and 2022, the BESS generation capacity reported on the CAISO increased over five-fold from 500 MW to over 2500 MW. This unprecedented growth was associated with the saturation of the frequency regulation market and a decreased value for providing said service. Our study examined the BESS market in 2020, and while our conclusions were not incorrect at the time, they were already out of date for BESS in 2022. Modelers should be forward looking in their efforts in order to better capture expected changes to electricity markets.

When modeling the TLC of Li-ion Class 8 trucks, the high uncertainty in DCFC and extremely fast charging (XFC) infrastructure limits the overall certainty of our study. We assumed that charging infrastructure will be readily available for utilization throughout the United States aat a fixed price. In realty, this utilization price and the availability of the infrastructure is unknown since the development of this charging infrastructure for electrified Class 8 trucks has yet to occur at a large-scale. How and where this infrastructure is developed can change the cost of charging, while also limiting the viability of these Li-ion Class 8 trucks to certain routes, inducing additional costs when trying to perform long-haul freight. Additionally, this may impact how a Li-ion Class 8 truck passes through its use-phases in its overall lifetime. The value of depreciation may be substantially impacted if charging infrastructure is not available to support Li-ion Class 8 trucks in regional or distributional/local freight. This may increase the general ops cost incurred by the owner if a Li-ion Class 8 truck cannot be resold at a comparable value to diesel Class 8 trucks due to infrastructure limitations.

Finally, the modeling of human health impacts is associated with high uncertainty attributable to several sources of potential error. One source of potential error stems from our estimations of which marginal generators are responding to induced electrical loads. It is an impossibility to model the electrical grid response to additional demand with absolute certainty. Therefore, the quantity and location of pollutant emissions associate with electricity generation will be inherently flawed. Additionally, our understanding of pollution transport and the interactions between pollutants and humans is constantly improving. While our current modeling of contributions to human health burdens is highly detailed, future models will be able to assess impacts to human health with less uncertainty.

6.3 Policy Implications

LCA studies are frequently used to inform government policy and decision making, particularly given the recent importance placed on environmental justice. The standards for the depth and quality of LCA should be improved to inform better decision making related to Li-ion batteries.

Suggestions for achieving these improvements are provided in the *Recommendations for Future Works* section.
Additionally, policy based on the future prices of Li-ion batteries should use a wide range of learning rates to forecast short-term prices. Our results show that the "instantaneous" learning rate of Li-ion batteries is highly variable and dependent on market developments. Using a learning rate based on the complete history of Li-ion prices may result in widely inaccurate price forecasts. Instead, different learning scenarios based on potential market growth should be used to better understand the different pathways future Li-ion prices may follow.

The fourth chapter of this dissertation highlights how Li-ion BESS replacing peaker plants are not inherently a win-win for advocacy groups and electricity providers. Replacing many peaker plants may result in net negative impacts when considering the monetized impacts of GWP and human health burden contributions. Additionally, all Li-ion BESS replacing peaker plants are a positive carbon emission technology due to the high emissions associated with material extraction, refining, and assembly, as well as the frequency in which thermal generators respond to the charging loads of the Li-ion BESS. While local human health benefits are observed, it is important that decision makers perform thorough analysis to determine where the highest value peaker replacements can occur and have an accurate understanding of the climate impacts associated with the technology.

Finally, policy makers should emphasize the continued integration of low-cost renewable electricity in order to achieve higher social benefits associated with Li-ion Class 8 trucks performing long-haul freight. This will help in reducing the TLC of L-ion Class 8 trucks performing long-haul freight, but ultimately their TLC will remain higher than diesel under all modeled scenarios unless major technological improvements occur, cheap charging is made available, or higher tax credits are provided.

6.4 Recommendations for Future Works

This dissertation puts forth several recommendations to improve the quality and depth of LCA for Li-ion batteries. First, LCAs should focus analyses of resource depletion on long-term trends toward more energy and resource-intensive material extraction and processing rather than treating known reserves as a fixed quantity being depleted. Second, future studies should account for extraction and processing operations that deviate from industry best-practices and may be responsible for an outsized share of sector-wide impacts, such as artisanal cobalt mining. Third, LCAs should explore at least 2–3 battery manufacturing facility scales to capture size- and throughput-dependent impacts such as dry room conditioning and solvent recovery. Finally, future LCAs must transition away from kg of battery mass as a functional unit and instead make use of kWh of storage capacity and kWh of lifetime energy throughput.

On the topic of learning rates for Li-ion batteries, understanding the historical changes in Li-ion battery prices provides insight on price forecasting into the future. All the studies examined in this study simplify the decades of Li-ion price history into a single learning rate and continue this trend into the future. Our study highlights how significantly the learning has changed since its development and how much this deviates from the single learning rate model. Future analysis

should consider a wider range of learning rates when projecting costs into the future to better account for the variation that occurs at a smaller temporal resolution.

With regards to modeling the impacts associated with replacing peaker plants with Li-ion BESS, future works should account for how electricity markets and regulation will evolve overtime, affecting the source and quantity of revenue earned by the BESS. This is particularly important in regions like CAISO where the rapid growth of Li-ion BESS capacity is capitalizing on high resource adequacy prices while simultaneously saturating the frequency regulation market and forcing more involvement in arbitrage. Capturing these market dynamics may significantly alter the modeled net impact associated with these facilities, especially over a longer lifetime.

Future works should examine the impacts of different driving behaviors and regulations on the social and economic costs Li-ion Class 8 trucks in long-haul freight. The impacts of incentivizing versus requiring charging to occur at night on the TLC of Li-ion Class 8 trucks should be studied. Future analyses should consider the forecasted technological improvements associated with Li-ion Class 8 trucking to determine if an of the expected technological improvements can significantly change the TLC relative to the diesel alternative. The potential impacts of increasing the lifetime of a Li-ion Class 8 truck relative to diesel should be examined as well. Additionally, there is a high level of uncertainty on future electricity prices and costs associated with utilizing charging infrastructure. A more in-depth sensitivity analysis on the relationship between TLC and these costs should be performed to understand how these factors will affect the relative TLCs of Li-ion and diesel Class 8 trucks. Variations by regionality should also be considered since electricity prices and generation portfolios may differ substantially by geography. Future analysis should consider comparing advanced technologies that may further alter Li-ion Class 8 truck behavior, like battery swapping instead of recharging and self-driving fleets. Finally, comparisons to alternative powertrains like fuel-cell and hybrid-electric Class 8 trucks will be modeled to better understand what niche Li-ion Class 8 trucks might occupy in the near future.

Appendix A

Supplemental Information

Temporal Variations in Learning Rates of Li-ion Technologies: Insights for Price Forecasting and Policy through Segmented Regression Analysis

.

A1 Cost reduction mechanisms

Literature on economics and manufacturing generalizes the mechanisms that contribute to a product's cost reductions across an entire sector to four main factors: (1) learning by doing, (2) economies of scale, (3) innovation, and (4) cost reduction of material inputs.[1] These factors and their relationships to costs can be briefly defined as follows:

(1) Learning by doing is the well established concept that cost reductions are achieved through increased productivity as individuals passively self improve and innovate through practice. These effects may extend beyond an individual facility to an entire sector as knowledge is shared and individuals move. Cost impacts are most often characterized as varying with the cumulative production of a product.[2–4]

(2) Economies of scale states that as the production capacity of a facility increases, the fixed costs of said production are subsequently spread across a great number of units, decreasing the per unit cost of production. Cost impacts are characterized in relation to facility capacity or output.[5,6]

(3) Innovation is a complex process in which a product, its means of production, or its market are improved upon and altered through technological advancements. Innovation's impacts on costs are often described as varying with the quantity and quality of research being conducted in a sector or tangential sector. The number of patents or amount of spending on research and development are common proxies for research quantity and quality.[7–10]

(4) Variations in the cost of material inputs directly impact production costs.[1]

Other factors, such as regulations and supply chain constraints, can also influence the pace and trajectory of technology progress. For instance, over the past decade, the learning rates of nuclear power have accelerated, partly attributable to enhanced safety regulations.[11]

Multi-factor regressions are often performed in an attempt to characterize and distinguish the impacts of two or more factors on the cost of a product. These analysis frequently the generic form:

Equation 1. $$\log(Y) = a + \Sigma c_i \log(X_i)$$

Where Y represents the cost of a product over time, X_i represents the proxy data series used to describe a factor over time, and c_i represents the regression coefficients that characterize the effect of each factor. In practice distinguishing the effects of these factors may be difficult since these factors may be highly correlated and there is often a lack of data available at a high enough level of detail to support statistically significant analyses.[12]

A2 Representative Series Construction

Cell Capacity (GWh)
The representative series for annual cell capacity was constructed by taking an average of reported cell annual capacities from Kittner et al.,(Kittner et al. 2017) Pillot et al.,[13] and Ziegler and Tancik.[8] These sources perform robust searches for market data, often with overlapping sources themselves. While the reported values for capacity are all similar between sources, taking the average between them may capture any variances in excluded or included datapoints. Cumulative capacity was determined from the annual capacity series.

Module Capacity (GWh)
The representative series for annual module capacity was determined by summing the reported EV and stationary capacity from Beuse et al.[14] Cumulative capacity was determined from the annual capacity series.

Installed Systems Capacity (GWh)
The representative series for annual installed system capacity was determined by summing all relevant entries in the GESDB[15] (as of 2021) for each year and averaging this with the Beuse et al. stationary series. This combination was performed in order to compensate for the possibility of a time delay for uploading energy storage entries into the GESDB,[15] which may result in an artificially low global storage capacity. Cumulative capacity was determined from the annual capacity series.

Cell Price ($/kWh)
The representative series for annual cell price constructed by Ziegler and Trancik[8] was used in this study. Ziegler and Trancik[8] performed an exhaustive survey of market data points to construct this series, and any adjustments from us would likely result in the double counting of primary sources.

Module Price ($/kWh)
The representative series for annual cell price was constructed from the average of nine different cost series across five different sources.[16–20] Six of these series represented EV module costs, two represented modules in unspecified applications, and one represented modules in utility scale energy storage applications. This representative series is not weighted by the size of market applications due to uncertainty in primary sources for these series, as well as uncertainty in the accuracy of the size of market applications for Li-ion modules. Thus this representative series is associated with high levels of uncertainty itself.

Installed Price ($/kWh)
The representative series for installed system prices was constructed from the average of the cost of utility stationary storage from Schmidt et al.,[21] the mean cost of utility stationary storage from the EIA,[22] and the cost of utility stationary storage from Lazard et al.[23] Each of these sources cover different time periods, but averaging the three series is done in an attempt to create a smooth, representative series for analysis.

A3 Scenarios of forecasted demand for Li-ion cells by sector

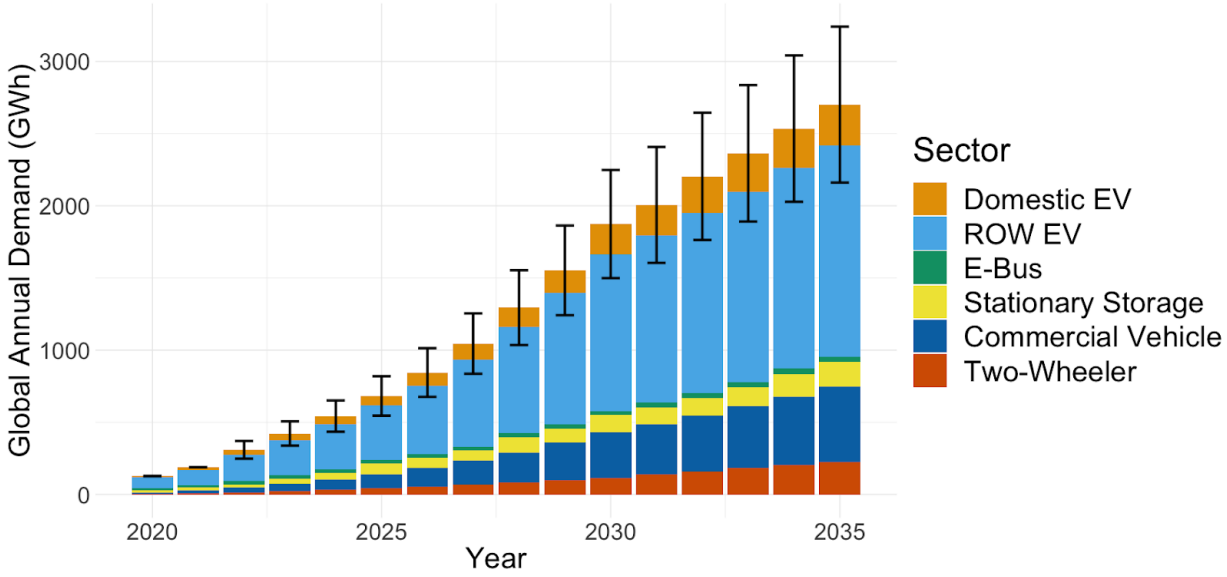

Scenarios of forecasted global demand for Li-ion cells by sector

Three representative forecasts of global cumulative production of Li-ion capacity are generated from the historic cumulative market described by Ziegler and Trancik,[8] and the historic and forecasted demand from BNEF[24] as well as FCAB.[25] The global cumulative production forecasts represent three different scenarios for US Li-ion demand growth out to 2035. The first scenario assumes a moderate amount of domestic EV integration, with EVs representing 62% of domestic passenger car sales by 2035. The second scenario assumes a low amount of domestic EV integration, with EVs representing only 25% of domestic passenger car sales by 2035. The final scenario assumes a high amount of domestic EV integration, with EVs representing 95% of domestic passenger car sales by 2035. The forecasted Li-ion cell demand in other sectors and other countries is identical between the three scenarios in order to isolate the effects of increasing EV domestic EV demand. The cumulative production forecasts corresponding to these different domestic EV adoption scenarios will be referred to as the "Medium", "Low", and "High" forecasts, corresponding to moderate, low, and high EV integration. Error bars represent the low and high demand scenarios. Medium forecasts are represented by the barplots.

References

1. Rubin, E., Azevedo, I., Jaramillo, P. & Yeh, S. A review of learning rates for electricity supply technologies.pdf. Energy Policy (2015).

2. Thompson, P. Learning by Doing. in Handbook of the economics of innovation, vol. 1 vol. 1 429–476 (Elsevier, 2010).

3. Schank, R., Berman, T. & Macpherson, K. Learning by Doing. in Instrucional-Desing Theories and Models: A New Paradigm of Instructional Theory vol. 2 (1999).

4. Arrow, K. J. The economic implications of learning by doing. Rev. Econ. Stud. **29**, 155 (1962).

5. Silberston, A. Economies of scale in theory and practice. The Economic Journal **82**, 369 (1972).

6. Haldi, J. & Whitcomb, D. Economies of Scale in Industrial Plants. Journal of Political Economy (1967).

7. The Economics of Innovation. (1990).

8. Ziegler, M. & Trancik, J. Re-examining Rates of Lithium-ion Battery Technology Improvement and Cost Declines. (2020).

9. Kittner, N., Lill, F. & Kammen, D. M. Energy storage deployment and innovation for the clean energy transition. Nat. Energy **2**, 17125 (2017).

10. Penisa, X. N. et al. Projecting the Price of Lithium-Ion NMC Battery Packs Using a Multifactor Learning Curve Model. Energies **13**, 5276 (2020).

11. Roser, M. Why did renewables become so cheap so fast? Our World in Data https://ourworldindata.org/cheap-renewables-growth (2020).

12. Wooldridge, J. M. Introductory Econometrics: A Modern Approach (Upper Level Economics Titles). (2015).

13. Pillot, C. The Rechargeable Battery Market and Main Trends 2018-2030. (2019).

14. Steffen, B., Beuse, M., Tautorat, P. & Schmidt, T. Experience Curves for Operations and Maintenance Costs of Renewable Energy Technologies. Joule (2020).

15. Chalamala, B., Sandia National Laboratories, DOE Office of Electricity & Pacific Northwest National Laboratory. DOE Global Energy Storage Database. Energy Storage Systems Program https://www.sandia.gov/ess-ssl/global-energy-storage-database-home/ (2020).

16. Beuse, M., Steffen, B. & Schmidt, T. S. Projecting the Competition between Energy-Storage Technologies in the Electricity Sector. Joule (2020) doi:10.1016/j.joule.2020.07.017.

17. Nykvist, B. & Nilsson, M. Rapidly falling costs of battery packs for electric vehicles. Nat. Clim. Chang. **5**, 329–332 (2015).

18. Kleinberg, M. Battery Energy Storage Study for the 2017 IRP. (2016).

19. Tsiropoulos, I., Tarvydas, D. & Lebedeva, N. Li-ion Batteries for Mobility and Stationary Storage Applications. (2018).

20. Hsieh, I.-Y. L., Pan, M. S., Chiang, Y.-M. & Green, W. H. Learning only buys you so much: Practical limits on battery price reduction. Appl. Energy **239**, 218–224 (2019).

21. Schmidt, O., Melchior, S., Hawkes, A. & Staffell, I. Update 2018 - The future cost of electrical energy storage based on experience rates. Figshare (2018) doi:10.6084/m9.figshare.7012202.v1.

22. U.S. Energy Information Administration. Form EIA-860 detailed data with previous form data (EIA-860A/860B). Independent Statistics and Analysis: U.S. Energy Information Administration https://www.eia.gov/electricity/data/eia860/ (2021).

23. Lazard. Lazard's Levelized Cost of Storage Analysis - Version 6.0. (2020).

24. Frith, J. & Li, D. 2021 Lithium-Ion Battery Price Survey. (2021).

25. FCAB. National Blueprint Lithium Batteries. (2021).

Appendix B

Supplemental Information

Private and External Costs and Benefits of Replacing High-Emitting Peaker Plants with Batteries

Procedure B1 Peaker Replacement Behavior and Sizing Optimization

The following optimization formulation is used to determine the charging behavior and rated power of the BESS when operating to offset natural gas combustion at peaker plants. The formulations represent the optimization for a single 24-hour period, repeated for everyday from 2018 through 2020. The maximum rated power observed over the entire three-year span is set as the rated power for the BESS.

(1) $$\min(R * P_{Batt} + \sum_{i}^{n} P_{Elec,i} * r_i)$$

Such that:

(2) $$0 \leq r_i \leq R \leq R_{Cap}$$

(3) $$z_i = z_{i-1} + \eta * r_{i-1} - \frac{Q_{i-1}}{\eta}$$

(4) $$0 \leq z_i \leq R * D$$

(5) $$z_0 = z_p$$

(6) $$r_i * Q_i = 0$$

(7) $$R \geq Q_i$$

Table S1 defines the variables and scripts. For the first optimization period observed from 2018 through 2020, z_p is set to zero. Negative prices are artificially set to near-zero positive values during optimization in order to avoid unrealistic charging behavior – when calculating costs and revenues, negative prices are allowed. 24 hour segments are optimized at a time to mimic the day-ahead market structure. When optimization is infeasible for 24 hour periods (generally if discharging events occur too near the beginning of these periods and/or if the discharge event is very large), the period is expanded earlier by an additional 24 hours until feasible. The largest R solved from the optimization of the all the periods in the three-year span considered is set as the rated power of the BESS. Our methods ensure that R remains less than r_{cap} (the rated power of the existing peaker plant) for all optimization periods to minimize impacts associated with upgrading transmission and distribution infrastructure while still meeting the historic output of the peaker plant, Q_i. The price for increasing energy storage is set artificially high to minimize battery size while simultaneously minimizing the cost of purchasing electricity while still requiring that the BESS have sufficient energy storage capacity to displace all considered discharge periods from purchased electricity. The largest energy capacity from all 24 hour segments optimized and the annual number of cycles, are used to size the BESS such that it maintains its rated energy capacity despite calendar and cycling capacity fade.

Table B1 Natural Gas Peaker Replacement Optimization Definitions

Variable/Script	Definition
i	Hour timestep
n	Maximum hour observed, set to 24
p	Final timestep from prior optimization period
R	Required rated power (kW) for the optimization period
P_{Batt}	BESS price per kW, set artificially high to dissuade increasing rated power
$P_{Elec,\ i}$	Historical electricity price per kW from 2018 through 2020
r_i	BESS charging in kW
R_{Cap}	Maximum allowed charging per period in kW, set to the rated power of the peaker plant
z_i	State of charge of the BESS in kWh
η	One way efficiency of the BESS, set to square root of 0.85
Q_i	Fixed BESS discharging in kW from historical peaker output from 2018 through 2020
D	Duration of BESS, set to 4

Variables and scripts used in the optimization along with their associated definitions.

Procedure B2 Additional Peaker Replacement Characteristics

The initial optimization indicated that a BESS must have a large rated power and energy capacity to fully offset a natural gas peaker plant. In order to reduce the potential sizing and CapEx of a BESS, we performed an analysis in which the top n^{th} percentile load events from the historical activity of a natural gas peaker plant are excluded from the optimization above. Figure S1a, S1b, and S1c illustrate the results of the performed analysis. Figure S1a plots the required rated power of the BESS against the percentile of load events excluded. Figure S1b plots the annual load passing through the BESS against the percentile of load events excluded. Figure S1c plots the annual load passing through the BESS against the normalized required rated power of the BESS.

Figure S1a illustrates how excluding the top 5^{th} percentile of load events from the optimization allows for a significantly reduced rated power for all BESS explored, in some cases even reducing the required rated power by around 80%. In Figure S1b, the impact of excluding the top n^{th} percentile of load events on the annual load passing through the BESS can be observed. In Figure S1c, the effect of reducing the required rated power of a BESS on the annual load passing through the system can be observed. Significant size reductions can be achieved by excluding the 5^{th} percentile of load events while still meeting over 75% of the total annual load that would otherwise be offset by a fully sized BESS. Therefore, all BESS are optimized to meet the 95^{th} percentile load event for natural gas peaker replacement – a decision that will significantly reduce CapEx and increase the feasibility of BESS for natural gas peaker replacement.

Figure B1 Relationship Between Percentile of Load Events Excluded, BESS Rated Power, and Offset Annual Load by BESS.

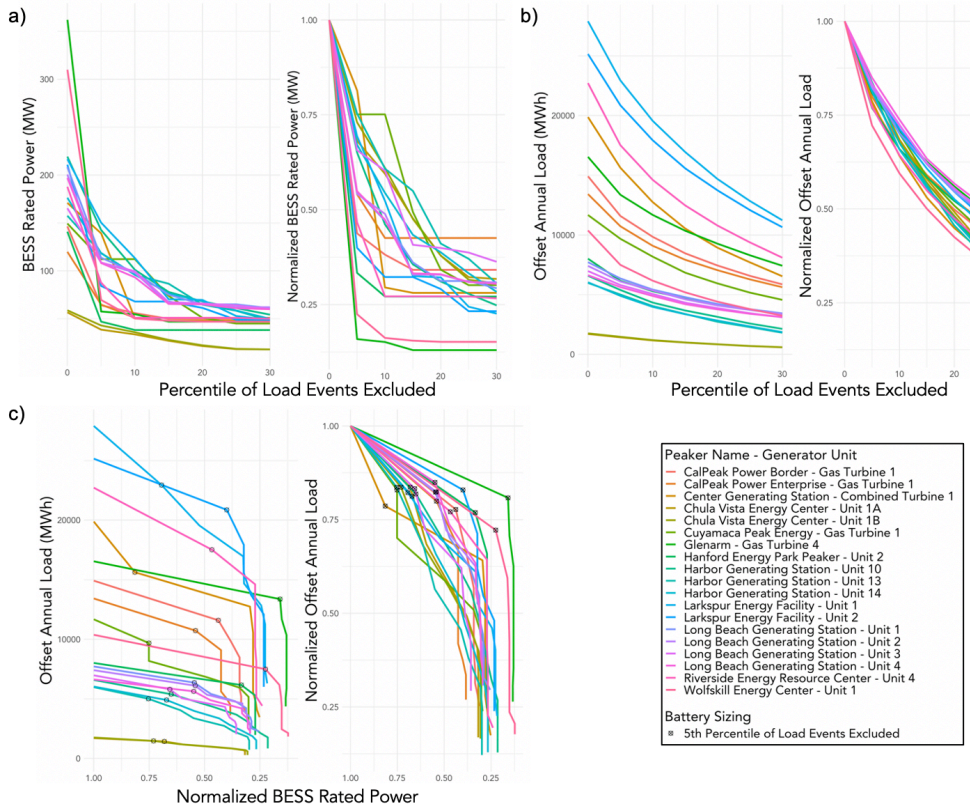

Each color represents the characteristics of each peaker studied and each line represents an individual BESS offsetting peaker plant activity. The "Percentile of Load Events Excluded" refers to the omission of discharge events by the events' sizes. For example, at the 5th percentile of load events excluded, any discharge event from 2018 to 2020 that is in the top 5th percentile by size (MWh) has been omitted from the study. As a result, the required rated power of the BESS to offset all considered peaker activity is reduced, since less storage capacity is required. (A) The plot visualizes the relationship between the required BESS rated power and the percentile of load events excluded when sizing through optimization. (B) The plot visualizes the relationship between the offset annual load by the BESS and the percentile of load events excluded when sizing through optimization. (C) The plot visualizes the relationship between the offset annual load by the BESS and the BESS rated power, with an additional point indicating where the BESS are sized for this study, excluding the 5th percentile of load events.

Procedure B3 Arbitrage Behavior Optimization

The following optimization formulation is used to determine the charging and discharging behavior of the BESS when performing arbitrage. The formulations represent the optimization for a single 24 hour period, repeated for everyday from 2018 through 2020.

(8) $$\min \sum_{i}^{n}\{(Q_i - r_i) * P_{Elec,i} - \frac{Q_i}{R*D} * P_{Cycle}\}$$

Such that:

(9) $$0 \leq r_i \leq R \leq R_{Cap}$$

(10) $$z_i = z_{i-1} + \eta * r_{i-1} - \frac{Q_{i-1}}{\eta}$$

(11) $$0 \leq z_i \leq R * D$$

(12) $$z_0 = z_p$$

(13) $$r_i * Q_i = 0$$

For the first optimization period observed from 2018 through 2020, z_p is set to zero. Negative prices are artificially set to near-zero positive values. When optimization is infeasible for 24 hour periods, the period is expanded early by an additional 24 hours until feasible. The optimization skips periods when the BESS is participating in natural gas peaker replacement. A cost penalty equivalent to the fractional cost of the battery degraded from cycling (Table S15) is incurred with discharging. The price of electricity controls the revenues from selling electricity and the costs of purchasing electricity. Table S2 outlines the variables used for modeling.

In order to perform the optimization on a convex set, we artificially set the discharging event of maximum power at the hour with the highest electricity price during the period. If arbitrage is found to be profitable, we set a second maximum discharge event at the hour with the next highest hour and perform the optimization again. We repeat this until profits decrease; after that we use the prior discharge scenario. If we find the initial optimization scenario unprofitable, then no arbitrage occurs over the period.

After the number of cycles associated with arbitrage is determined, the upfront size of the BESS is increased to ensure it can maintain its rated power despite the additional degradation from cycling for arbitrage.

Table B2 Natural gas peaker replacement optimization definitions.

Variable/Script	Definition
i	Hour timestep
n	Maximum hour observed, set to 24
p	Final timestep from prior optimization period
R	Required rated power (kW) for the optimization period, set to results from peaker replacement optimization
$P_{Elec, i}$	Historical electricity price per kW from 2018 through 2020
P_{Cycle}	Incurred cost per cycle attributable to additional upfront sizing to compensate for degradation from battery cycling. See Table S12 for description of P_{Cycle} as it varies by battery chemistry.
r_i	BESS charging in kW
R_{Cap}	Maximum allowed charging per period in kW, set to the rated power of the peaker plant
z_i	State of charge of the BESS in kWh
η	One way efficiency of the BESS, set to square root of 0.85
Q_i	BESS discharging in kW, set iteratively
D	Duration of BESS, set to 4

Variables and scripts used in the optimization along with their associated definitions.

Procedure B4 Frequency Regulation and Mileage Revenue Modeling

The following modeling approach is modified from the description of frequency regulation markets in Xu 2016[1] and is used to estimate revenues from participation in frequency regulation and mileage. Generally, total revenue can be broken into three main components, Capacity, Mileage, and Fast Response:

$$Total\ Revenue = Capacity\ Rev. + Mileage\ Rev. + Fast\ Response\ Rev.$$

Capacity revenue represents the revenue earned from bidding a capacity available for charging or discharging (regulation up or regulation down). It takes the following form:

$$Capacity\ Rev. = \sum_{i=1}^{n} Ci * P_{Ci}$$

Where C_i represents the bid capacity (kW) for each hour i, and P_{Ci} represents the clearing price ($/kW) for capacity for each hour i.

Mileage revenue represents the revenue earned from charging or discharging a portion of a system's bid capacity and takes the following form:

$$Mileage\ Rev. = \sum_{i=1}^{n} Ci * M_i * P_{Mi} * \rho_i$$

Where C_i represents the bid capacity (kW) for each hour i, M_i represents the proportion of that capacity that is actually called upon for regulation up or down, P_{Mi} represents the clearing price ($/kW) for mileage for each hour i, and ρi represents an accuracy score from 0 to 1 that varies based on the performance of the system.

Fast response revenue is an additional stream of revenue that is employed by some independent system operators but is not used by CAISO. Thus, it is excluded from this study. More information on this revenue stream and all other revenue components can be found with Xu 2016.[1] Additionally, environmental impacts associated with frequency response are not included in NPV results due to their minor contributions and complexity of modeling relative to other emission categories.

Procedure B5 BESS CapEx Modeling

The CapEx of the BESS can be categorized into 8 primary components: the battery, the inverter, the container balance of systems (BOS), the electrical BOS, the structural BOS, installation and labor sales tax, and developer costs. These primary cost components align with categories specified by NREL in past works[2,3] with some modifications to allow for a greater level of granularity inspired by PNNL modeling.[4] These primary components are made up of secondary components that generally represent a single type of equipment, material, or soft cost. Table S3 shows the 8 primary cost components and their associated secondary components.

The battery primary component consists of the Li-ion battery module itself and the systems contained within it. This generally includes the Li-ion cells, miscellaneous electronics associated with module level controls, and housing/cooling elements. We determine the sizing of this component by the required rated power determined from optimization for natural gas peaker replacement, the amount of annual cycles determined from optimization for natural gas peaker replacement and arbitrage, and the scenario specific system lifetime and battery replacement timeframe. We provide additional details on the sizing of the battery system and all other primary components in the Procedures S8 and S9.

Table B3 Primary and secondary components of BESS.

Primary Component	Secondary Component
Battery System	Battery Module
Inverter	Inverter
Container BOS	Thermal Regulation, Fire Suppression, Gas/Fire Detection
Electrical BOS	Transformer, Switchgear, Substation*, Conductors, Conduits, Communications
Structural BOS	Battery Housing, Battery Racks, Inverter Housing, Foundations
Installation and Labor	Battery Module Installation, Inverter Installation, Electrical BOS Installation, Structural BOS Installation, Site and Misc. Labor
Sales Tax	State Taxes, Local Taxes
Developer Costs	Developer Overhead, EPC Overhead, Permitting, Inspection, Interconnection, Contingency, Net Profit, Environmental Study and Mitigation, Land Acquisition

* Substation only included if certain model conditions met, i.e. rated power exceeds 100 MW[2–4]

Procedure B6 Life-Cycle Assessment

A hybrid process-based/physical units-based input-output method was used to calculate the life-cycle GHG footprint of each BESS using an approach described in prior studies.[5–7] LCA generally considers four phases of a product's lifecycle: material extraction and processing, assembly, use, and end-of-life. For a BESS and its subcomponents, values pertaining to the impacts associated with material extraction and processing are generally sourced from GREET2 as well as other bodies of literature or first order estimations, all of which are presented in Table S13. For the assembly of BESS and its subcomponents, distributions and ranges are assembled from literature values to best reflect the many possibilities in cell manufacturing. These distributions are presented in Table S11. The local environmental damages associated with Li-ion cell manufacturing are excluded due to the unavailability of data on foreign energy mixes, generation dynamics, and on site fuel consumption. However, as illustrated in Figure 4, environmental damages are minor relative to monetary considerations, and the exclusion of these damages will likely not significantly alter the final NPV. Use phase impacts are determined through the analyses Experimental Procedure previously outlined for each potential revenue stream. Additionally, the impacts associated with induced and offset electricity demand are outlined in the following section. A BESS is assumed to be landfilled at its end-of-life, with the partial recovery of certain high value materials like the HVAC refrigerant and fire suppressant. No battery recycling is assumed due to the current, limited state of the battery recycling supply chain.[8,9] Impacts associated with material transportation and onsite BESS construction are considered negligible, excluding the emissions associated with concrete. Future extraction and processing, manufacturing, and end-of-life conditions are assumed to mimic current conditions. Additionally material breakdowns and assumptions are presented in Table S13 and S14.

Procedure B7 Induced and Offset Electricity Demand

In order to understand the impacts of battery charging and discharging behavior – we must know something about the electricity and emissions associated with charging a battery and the electricity that the battery offsets. We use a regression-based reduced form approach to this problem based on widely used Experimental Procedure in the economics literature.[10–12] We build a model to predict individual plant behavior based on the aggregate demand for electricity in a plant's region. This model allows us to statistically estimate which plants respond to the increased electricity load from battery charging.

We conducted this analysis by leveraging EPA's Continuous Emissions Monitoring Systems (CEMS) data—which allows us to observe hour-by-hour power output and emissions for nearly all of the plants in the Western Interconnection. The EPA reports CEMS data for each generating unit within a plant separately. The data we use consists of hourly measures of generation in MWh, CO_2, SO_2, NO_X and $PM_{2.5}$ for 574 unique generating units contained within 224 power plants. CEMS data are highly accurate given the requirement of these data for regulatory purposes and because the methodology used to impute missing data creates a disincentive for firms to skirt regulations by turning off their monitoring equipment.[13]

In order to relate emissions to system load, we merged these CEMS data with aggregate demand (or load) data for the relevant North American Electric Reliability (NERC) regions servicing California. Since California operates a fairly distinct wholesale market from the rest of the Western Interconnection, we tabulated loads via Federal Energy Regulatory Commission (FERC) Form 714 data for California and the remainder of WECC separately.

With these two datasets, we estimated a model of how each generating unit responds to additional electricity load, which allows us to measure the explicit impacts from increased demand for electricity derived from battery charging. Specifically, we ran a set of generator-specific regressions that relate a generator's power output and emissions to aggregate electricity demand for the two NERC regions separately. As such, the dependent variable in each of our regressions is an hourly measure of generator i's hourly generation or emissions (CO_2, SO_2, NO_X, PM_{25}). We regress each dependent variable on a set of variables constructed from the aggregate demand for each NERC region. We allow for heterogeneity in the responsiveness of generators by hour-of-day since it is likely a plant responds to increased demand at 5AM differently than 3PM. Functionally, we estimate the following equation to determine how plants respond to additional system load:

$$Y_{it} = \sum_{h=1}^{24} \sum_{n \in \{CA, West\}} \beta_{int} * HOUR_h LOAD_{jt} + \sum_{h=1}^{24} \sum_{m=1}^{36} \gamma_{ihm} HOUR_h MONTH_m + \varepsilon_{it}$$

Here Y_{it} represents hourly generation or emissions for generator i in hour t. The set of $\boldsymbol{\beta}$int coefficients measure the marginal effect of additional (or decreased) load from NERC region n in hour-of-day h on that generator's emissions or generation. Allowing these changes to vary by NERC region n, allows, for example, a generator in California to respond to increased electricity demand in California in a different manner than it responds to increased electricity load in

Nevada. This is an important feature of the market given that NERC regions are interconnected– but remain separate entities when it comes to market-based generation behavior. We also note the $\boldsymbol{\beta}_{int}$ coefficients are specific to generator i, allowing for these marginal effects to differ by generator. The set of γ_{ihm} coefficients act as high-dimensional fixed effects that net out any fixed shifts in behavior for generator i at the sample-month-by-hour-of-day level. These fixed effects soak up any seasonal or hour-of-day variation that may be related to trends in electricity demand. Hence, our $\boldsymbol{\beta}_{int}$ coefficients measure the impact of additional load net of any of this hour-of-day-by-sample month variation. We used these coefficients to calculate generator-specific power output and emissions responses to additional system load induced by battery charging in region n and hour h.

We next converted these changes in emissions into monetary damages. For CO_2, we simply multiplied each generator's emissions by the social cost of carbon since these damages do not vary across location. Air pollution damages (i.e. SO_2, NO_X and $PM_{2.5}$), however, vary depending on where they are emitted, so we use generator-specific marginal damage estimates from the EASIUR model to convert these damages into monetary units for each plant separately. The EASIUR model provides marginal damage estimates for 16,576 cells from a 148x112 grid representing the United States. For each generator, we determined the relevant grid cell based on the generator's GPS coordinates and apply marginal damage estimates from EASIUR to the induced emissions from charging for that generator. Since EASIUR reports monetized damages for three different emission altitudes (0M, 150M and 300M), we matched generators to the nearest altitude based on the generator or plant smokestack height. We report damages in 2020 USD throughout the paper.

Accounting for the impacts of offset generation from the peaker generator we replace with a battery storage facility presents an easier task. Since we model the battery storage facility to replace a given amount of observed generation for a specific generator, we can simply calculate the offset emissions associated with that replaced generation directly based on the observed hourly data in the EPA CEMS data. We do not replace all generation hours for each generator in our final model, so we only remove the emissions associated with the hours our model selects to offset with the battery storage facility. For hours where we only partially offset generation, we remove emissions in proportion to the ratio of offset generation and total generation for that hour. We convert these reductions in emissions to monetary units using the same procedure outlined above for induced emissions from charging.

Table B4 Connected or under contract large-scale battery energy storage systems in CA.[14]

Name	Location	Rated Power (MW)	Commissioned Date
Gateway BESS	San Diego, CA	50	August 2020
NextEra Blythe BESS	Riverside, CA	63	August 2021
Vistra Moss Landing BESS	Moss Landing, CA	400	August 2021
Coso BESS	Little Lake, CA	60	August 2021
Diablo BESS	Contra Costa County, CA	200	August 2021
Elkhorn BESS	Moss Landing, CA	182.5	April 2022
Beaumont BESS	Beaumont, CA	100	August 2023
Edwards Sanborn BESS	Mojave, CA	169	August 2023
Canyon Country BESS	Santa Clarita, CA	80	October 2023
MOSS350 BESS	Moss Landing, CA	350	August 2023
Inland Empire BESS	Rialto, CA	100	April 2024
Corby BESS	Vacaville, CA	125	June 2024
Kola BESS	Tracy, CA	275	June 2024
Nighthawk BESS	Poway, CA	300	June 2024
Caballero BESS	Nipomo, CA	100	June 2024

Procedure B8 Additional details on battery sizing.

The battery system of the Li-ion BESS is sized to ensure that the whole system can output its rated power and energy capacity over the entire lifespan of the battery, either 7.5 years or 10 years, before the battery is replaced. The following equations are used to perform this sizing.

(14) $$r_{Cal}\left[\frac{\%}{Cycle}\right] = \left(1 - EOL^{1/T_{Life}}\right) * \left(\frac{1}{Cycles\ Per\ Year}\right)$$

(15). $$r_{Cyc}\left[\frac{\%}{Cycle}\right] = \left(1 - EOL^{1/C_{Life}}\right)$$

(16) $$r_{Tot} = r_{Cal} + r_{Cyc}$$

(17) $$D_n = D_0 * \prod_1^{i=n}(1 + r_{Tot} * D_{i-1})$$

(18) $$R_{Adj} = \frac{R}{D_n * RTE}$$

Table B5 Battery sizing definition.

Variable/Script	Definition
r_{Cal}	Battery degradation attributable to calendar aging, converted to % per cycle
r_{Cyc}	Battery degradation attributable to cycling, converted to % per cycle
T_{Life}	Shelf life in years, varies by cathode chemistry, collected from literature. See Table S6
C_{Life}	Cycle life in number of cycles, varies by cathode chemistry, collected from literature. See Table S6
EOL	Battery state of health (%) at end of life. Set to uniform distribution of 70% to 80% to reflect uncertainty in reporting in literature
Cycles Per Year	Equivalent cycles per year from peaker replacement and arbitrage
r_{Tot}	Total battery degradation attributed to each cycle
D_n	Required initial depth of discharge
D_0	Maximum allowable depth of discharge, set to 95% [15]
R_{Adj}	Adjusted battery capacity to achieve rated power over entire battery lifespan
R	Rated power
RTE	Round trip efficiency calculated from battery efficiency, transformer efficiency, inverter efficiency, HVAC power draw, and miscellaneous power draw.

Table S5 defines variables used for sizing. This formulation does not mimic the real behavior of battery degradation but rather estimates the required battery capacity to maintain a rated power throughout its lifetime using high level properties. Additionally, other options exist for maintaining a rated power, but the oversizing approach has the least uncertainty with battery pricing and is frequently used for projects this size.[16,17]

Table B6 Battery shelf and cycle life definitions by chemistry.[18–26]

Chem	T_{Life}	C_{Life}
NCA	8 – 10	2000 – 3500
NMC	8 – 10	2000 – 3000
LFP	8 – 12	3000 – 5000

Procedure B9 Additional details on other primary component sizing.

The container BOS primary component consists of the controls and balance of systems that support battery modules. This includes equipment associated with thermal regulation (i.e. HVAC or cell cooling) , fire suppression, and gas detection.[27–30] Each containerized group of battery modules has its own container BOS.[4]

The inverter primary component consists of the bidirectional inverters used to convert the energy from AC to DC while the system is charging and from DC to AC while the system is discharging. In utility scale BESS, multiple bidirectional inverters may be used, each one connected to a single or set of containers housing battery modules.[16,27,28,31,32]

The electrical BOS primary component consists of the transformers, switchgear and breakers, conductors, conduits, and communications required to transfer energy within the system and onto the grid infrastructure. The quantity and properties of transformers in the system can vary by grid properties such as voltage and interconnection limits. The configuration of conductors and conduits is highly variable and dependent on-site constraints, system design, and grid interactions. Additional equipment may be required for site integration, such as a substation, depending on the size of the energy storage system and the characteristics of the grid.[27,28,30,32]

The structural BOS primary component includes the racks and housing for the batteries, the inverter housing, and foundations required for the equipment in the system.[27,28]

The installation and labor primary component is made up of the costs associated with the wages of workers and the time spent installing the equipment tied to each of the previous primary components, as well as any other miscellaneous work that must be performed. This miscellaneous work may include grading, trenching, and hauling among others.[27 28]

Developer costs are generally defined as the soft costs that are passed onto the project developer and include developer overhead, permitting, inspection, interconnection, contingency, net profit, environmental study, and environmental mitigation. Developer overhead is defined as the fees required for the developers to maintain their operations. EPC overhead is defined as the fees required for the EPC company to maintain their operations. Permitting is defined as the administrative review and permits required to construct a battery energy storage project. Interconnection is defined as all the grid upgrades required to integrate the battery energy storage system to the grid. Inspection is defined as the testing that must occur before the BESS is fully integrated into the grid. Contingency is defined as a factor to account for any unforeseen events that may occur during development of the BESS. The environmental study is defined as the study that must be performed to determine if further environmental mitigation is required, while environmental mitigation is defined as the additional site work that may be required to minimize damage to impacted ecosystems in our surrounding the site.[16,17,27,28,33]

Sales tax consists of both local and state taxes that are applied as a factor to the total cost of materials required.[34]

These primary components and the secondary components they include are visualized in Figure S2.

Figure B2 Primary components, secondary components, and interactions of a BESS.[4,27]

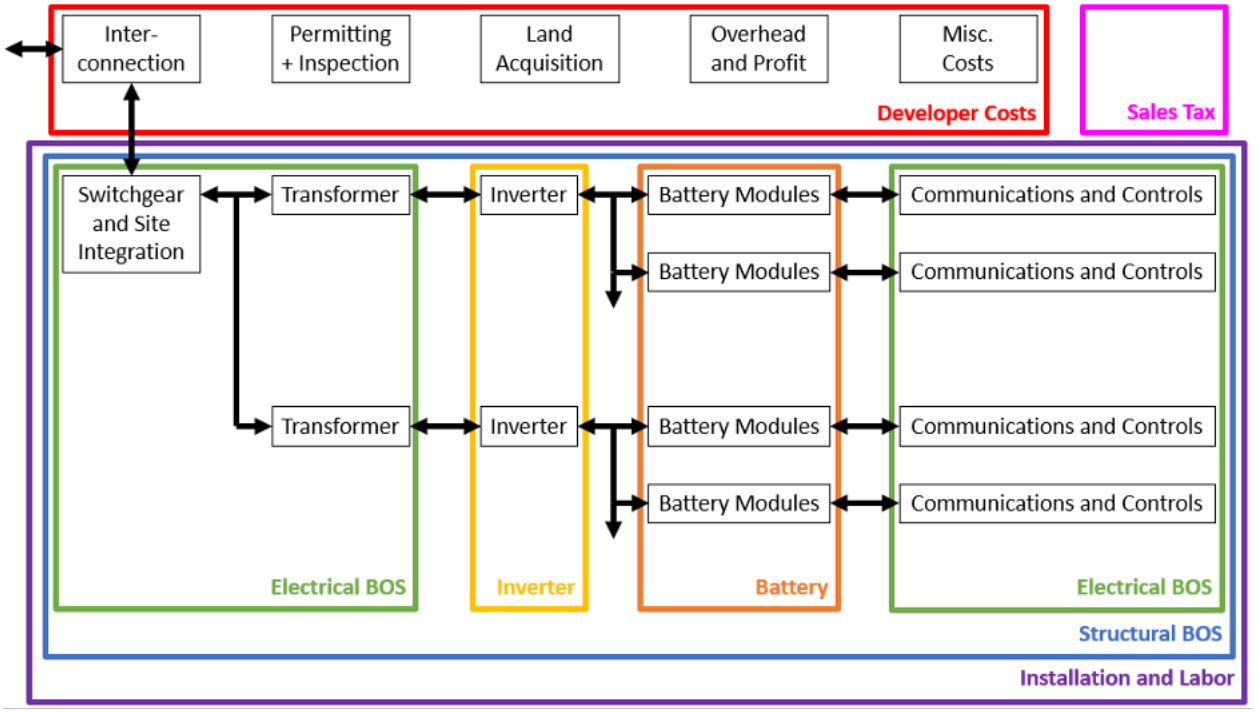

Schematic representation showing the secondary components included in each primary component and their interactions of the BESS when discussing CapEx.

Table B7 Characteristics of natural gas peaker plants in CA and optimized characteristics of BESS.

Replaced Peaker Plant	CAISO Region	Peaker Rated Power (MW)	Opt. BESS Rated Power (MW)	Annual Eq. Cycles - Peaker Rep.	Annual Eq. Cycles - LFP Arbitrage	Annual Eq. Cycles - NCA Arbitrage	Annual Eq. Cycles - NMC Arbitrage
Long Beach Generating Station - Unit 1	SP15	65	113.72	13.89	9.62	4.43	1.19
Long Beach Generating Station - Unit 2	SP15	66	108.67	13.94	9.82	4.30	0.86
Long Beach Generating Station - Unit 3	SP15	66	108.62	13.24	9.67	4.20	0.86
Long Beach Generating Station - Unit 4	SP15	65	108.11	12.92	10.27	4.66	1.00
Harbor Generating Station - Unit 10	SP15	47	142.65	9.32	7.47	4.20	1.92
Harbor Generating Station - Unit 13	SP15	47	118.69	10.48	8.98	4.88	1.95
Harbor Generating Station - Unit 14	SP15	47	118.37	10.20	8.87	4.90	2.28
Glenarm - Gas Turbine 4	SP15	47	57.55	58.07	7.69	3.95	1.29
CalPeak Power Border	SP15	51	64.06	45.24	9.75	5.31	2.39

- Gas Turbine 1							
Cuyamaca Peak Energy - Gas Turbine 1	SP15	45	112.24	21.51	6.62	3.57	1.47
CalPeak Power Enterprise - Gas Turbine 1	SP15	51	64.81	41.38	9.05	5.25	3.02
Chula Vista Energy Center - Unit 1A	SP15	18	38.62	9.08	11.53	6.64	3.22
Chula Vista Energy Center - Unit 1B	SP15	18	42.98	8.42	10.51	5.97	2.90
Larkspur Energy Facility - Unit 1	SP15	49	150.29	38.16	3.56	1.85	0.76
Larkspur Energy Facility - Unit 2	SP15	49	84.20	61.94	7.37	4.22	2.04
Hanford Energy Park Peaker - Unit 2	NP15	47	47.00	32.77	7.33	4.42	2.92
Wolfskill Energy Center - Unit 1	NP15	48	69.60	26.91	6.90	4.31	2.76
Riverside Energy Resource Center - Unit 4	SP15	51	87.64	49.98	7.86	5.24	3.15
Center Generating Station - Combined Turbine 1	SP15	48	139.21	28.07	4.52	2.20	0.91

Figure B3 Example State-of-Charge for BESS Offsetting Long Beach Generator Unit 1

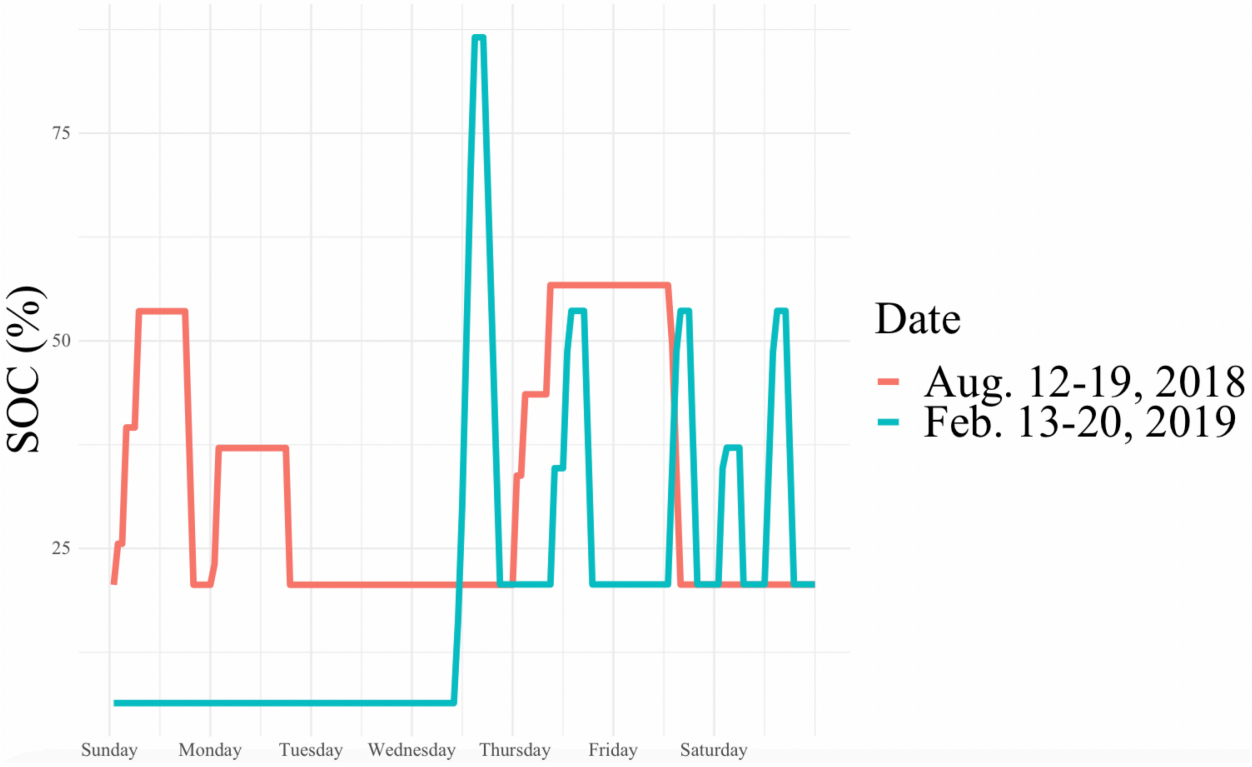

Figure B4 Example CapEx of BESS

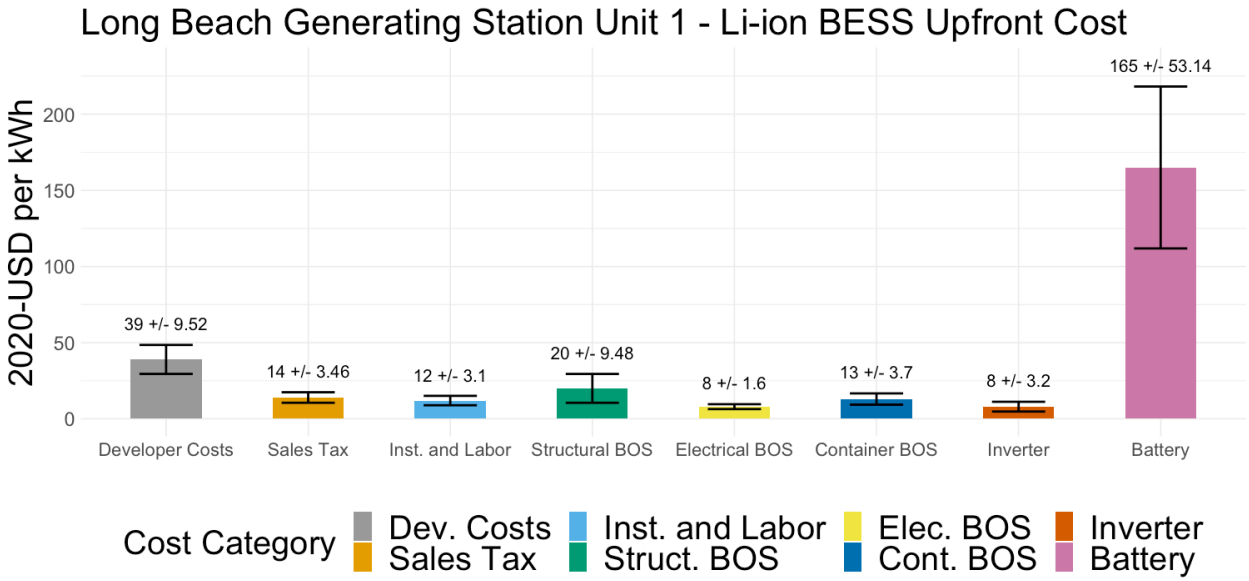

The CapEx for the BESS replacing the Long Beach Generating Station Unit 1 peaker plant is presented by category. An LFP cathode chemistry is assumed, with a 15 year lifespan and battery replacement at 7.5 years. Error bars represent two standard deviations with 500 runs in the Monte Carlo analysis.

Table B8 Distributions and values for design and cost parameters of BESS.

Component/Parameter	Distribution/equation/description	Source
LFP Module	Price ($/kWh): lognormal distribution; alpha = 99, beta = 1.25, mu = 0, sd = 5, min = 99, max = 225 Additional rack multiplier of 1.07 on price to account for additional structural components due to reduced energy density Labor: labor hours = 1 hr/module; labor rate = 50.70 $/hr One way efficiency: Uniform distribution; min = 98%, max = 99%	[16,28,35–37]
NCA Module	Price ($/kWh): lognormal distribution; alpha = 115, beta = 5*10^-6, mu = 0, sd = 20, min = 115, max = 415 Labor: labor hours = 1 hr/module; labor rate = 50.70 $/hr One way efficiency: Uniform distribution; min = 98%, max = 99%	[16,28,35,37]
NMC Module	Price ($/kWh): lognormal distribution; alpha = 115, beta = 100, mu = 0, sd = 5, min = 115, max = 525 Labor: labor hours = 1 hr/module; labor rate = 50.70 $/hr One way efficiency: Uniform distribution; min = 98%, max = 99%	[16,28,35,37]
Inverter	Price ($/W): Triangular distribution; min = 0.04. mode = 0.06, max = 0.08 Labor: modeled as transformer Losses: Normal distribution; mean = 1.83%, sd = 0.599%	[16,28,36,38] Sampled from available products

Transformer	Price ($): Mode interpolated by size, see Table S10. Triangular distribution; max/min = mode +/- 12.5%*mode Labor: Labor hours interpolated by size, see Table S10; labor rate = $60.07/hr Losses: Normal distribution; mean = 0.47 %, sd = 12.5% * mean	16,28,39
Switchgear	Price ($/MW): Triangular distribution; If under electrical BOS size is less than 25 MW, mode = 100,000 USD. If electrical BOS is greater than 25 MW, mode = 100,000 USD + 1,333.33 $/MW. max/min = mode +/- 12.5%*mode Labor: modeled as transformer	16,28
Interconnection	Price ($/MW): Uniform distribution; min = 1,000,000 USD, max = 3,000,000 USD	16,17,36
Conductors	Price ($/ft): Uniform distribution: min = 2.5, max = 7.5 Labor: labor hours = 5.5 hrs per 100 ft; labor rate = $54.24/hr	16,28,36
Conduits	Price ($/ft): Normal distribution; mean = 18.9, sd = 3.4 Labor: labor hours = 0.16 hrs per foot; labor rate = $54.24/hr	16,28
BMS	Price ($): Uniform distribution; min = 200,000, max = 600,000 Labor: labor hours = 13.33 hrs/MW_rated_power; labor rate = $54.20/hr	16,17,28,36

Fire Suppression	Price ($/Battery container): Normal distribution; mean = 1975 + 1.76 * container_volume_ft^3, sd = 12.5% * mode Labor: labor hours = (2 + 0.1 * container_length_ft + containter_length/30) hours per container ; labor rate = $52.12/hr	[28–30,32]
HVAC	Price ($/Battery container): Uniform distributuion; min = $5,000/battery_container, max = $15,000/battery_container Labor: labor hours = 6.67 hours per MW_rated_power, Labor rate = $53.31/hr Losses (%): min = 0.5%, max = 2.5%	[28,36,40–42]
Battery Housing	Price ($/container): Normal distribution; mean is variable by container size (30,000 for 40 ft container, 15,000 for 20 ft container, 5,000 for cabinet), sd = 25% * mean Labor: modeled as transformer	[16,28,36]
Inverter Housing	Price ($/container): Normal distribution; mean is variable by container size (15,000 for 20 ft container, 5,000 for cabinet, 0 for in battery), sd = 25% * mean Labor: Installed with inverter	[16,28] Sampled from available products
Foundation	Price ($/cubic yard): normal distribution; mean = $140/cubic yard, sd = 12.5% * mean Labor: labor hours = 0.957 hrs/cubic yard, labor rate = 46.00	[28]
Grading	Labor: labor hours and rates variable by site size, see Table S11	[28]
Trenching	Labor: Labor hours = 4 hrs/cubic_yard, labor rate = $46/hr	[28]
Backfill	Labor: Labor hours = 0.691 hrs/cubic yard, labor rate = $50.69/hr	[28]

Communications	Price ($): Uniform distribution; min = 100,000 USD, max = 300,000 USD Labor: labor hours modeled as transformer, labor rate = $54.24/hr	16,28,36
Gas Detection Probes	Price ($/Battery Container): 630 Labor: Labor hours = 1 hr/battery_container, labor rates = $54.24/hr	16,28,30
Gas Detection Controllers	Price ($/Battery Container): 2925 Labor: Labor hours = 1 hr/battery_container, labor rates = $54.24/hr	16,28,30
Fire Detection	Price ($/Battery Container): 51.50 Labor: Labor hours = 1 hr/battery_container, labor rates = $54.24/hr	16,28,30
Misc. Power Loss	Losses (%): Uniform distribution; min = 1%, max = 5%	16
Total Labor	Normal distribution; mean = total labor cost, sd = 12.5% * mean	Assumed
EPC Overhead	25% total labor cost + 8.67% material cost	16,27,28,36
Sales Tax	National average = 6.5696%	34
Dev Overhead	(12% +.0315%/MW_rated_power) * (Total labor cost + material cost)	27,28,36
Permits	Varies by state, national set to 0	16,27,36
Inspection	Uniform distribution; min = 5,000 USD, max = 15,000 USD	16,27,36
Contingency	Uniform distribution; min = 0.03% * (Total labor cost + material cost), max = 0.05% * (Total labor cost + material cost)	16,27,28,36
Net profit	Normal distribution; mean = 5% * (Total labor cost + material cost), sd = 12.5% * mean	16,27,28,36

Environmental Study	Uniform distribution; min = 5,000 USD, max = 15,000 USD	[16]
Environmental Mitigation	Uniform distribution; min = 0 USD, max = 100,000 USD	[16]
Land	Uniform distribution; min = 125,000 USD, max = 375,000 USD	[16]

Table B9 Annual Output and Omitted Load by Peaker Sized for the 95th Percentile Load Event

Replaced Peaker	Rated Power (MW)	Avg. Annual Peaker Replacement Output (MWh)	Avg. Annual Omitted Load (MWh)
Long Beach Generating Station - Unit 1	114	6,360	1,360
Long Beach Generating Station - Unit 2	109	6,100	1,300
Long Beach Generating Station - Unit 3	109	5,810	1,170
Long Beach Generating Station - Unit 4	108	5,630	1,000
Harbor Generating Station - Unit 10	143	5,390	1,200
Harbor Generating Station - Unit 13	119	5,000	980
Harbor Generating Station - Unit 14	118	4,900	1,130
Glenarm - Gas Turbine 4	58	13,370	3,170
CalPeak Power Border - Gas Turbine 1	64	11,590	3,330
Cuyamaca Peak Energy - Gas Turbine 1	112	9,680	1,990
CalPeak Power Enterprise - Gas Turbine 1	65	10,730	2,700
Chula Vista Energy Center - Unit 1A	39	1,430	280
Chula Vista Energy Center - Unit 1B	43	1,470	290
Larkspur Energy Facility - Unit 1	150	22,940	4,960
Larkspur Energy Facility - Unit 2	84	20,860	4,290
Hanford Energy Park Peaker - Unit 2	47	6,160	1,850

Wolfskill Energy Center - Unit 1	70	7,490	2,880
Riverside Energy Resource Center - Unit 4	88	17,520	5,200
Center Generating Station - Combined Turbine 1	139	15,630	4,250

Table B10 Transformer price and labor hours by size.[28]

Size (MW)	Labor Hours	Price (USD)
0.15	30.769	9750
0.3	44.444	13900
0.05	50	19700
0.75	52.632	25000
1	76.923	29600
1.5	86.957	35200
2	100	44400
3.75	125	83500

Table B11 Grading labor hours and rates.[28]

Size Area (SF)	Labor hours	Labor Rate ($/hrs)
0 - 400	12	37.76
400 - 1,000	24	37.76
1,000 – 3,000	16	47.46
3,000 – 5,000	24	47.46
5,000 – 8,000	40	43.33
8,000 – 10,000	12	81.85
10,000 – 20,000	9	81.12
20,000 – 25,000	11.5	81.12
25,000 – 30,000	13.33	81.12
30,000 – 35,000	16	81.12
35,000 – 40,000	18	81.12
40,000 – 45,000	20	81.12
45,000 – 50,000	22	81.12
50,000 – 75,000	32	81.12
75,000 – 100,000	44	81.12

Table B12 Frequency regulation and arbitrage profit comparison.[43]

Peaker Plant	Instances where FR profits exceed Arbitrage profits	Potential Annual FR Profits Change	Potential Annual Arbitrage Profits Change
Long Beach Generating Station - Unit 1	99 of 128	$589,547	-$255,285
Long Beach Generating Station - Unit 2	101 of 128	$618,180	-$265,720
Long Beach Generating Station - Unit 3	101 of 128	$611,610	-$261,342
Long Beach Generating Station - Unit 4	103 of 133	$620,101	-$269,646
Harbor Generating Station - Unit 10	95 of 149	$421,873	-$186,109
Harbor Generating Station - Unit 13	101 of 155	$455,235	-$201,492
Harbor Generating Station - Unit 14	96 of 152	$439,535	-$193,935
Glenarm - Gas Turbine 4	52 of 70	$206,180	-$99,168
CalPeak Power Border - Gas Turbine 1	55 of 85	$290,338	-$116,934
Cuyamaca Peak Energy - Gas Turbine 1	76 of 114	$302,456	-$133,897
CalPeak Power Enterprise - Gas Turbine 1	51 of 79	$285,913	-$113,591
Chula Vista Energy Center - Unit 1A	108 of 164	$179,922	-$81,687

Chula Vista Energy Center - Unit 1B	109 of 165	$181,276	-$82,188
Larkspur Energy Facility - Unit 1	53 of 76	$241,310	-$105,043
Larkspur Energy Facility - Unit 2	57 of 84	$251,139	-$115,036
Hanford Energy Park Peaker - Unit 2	44 of 61	$228,193	-$77,197
Wolfskill Energy Center - Unit 1	52 of 73	$246,754	-$83,121
Riverside Energy Resource Center - Unit 4	46 of 71	$247,419	-$111,019
Center Generating Station - Combined Turbine 1	70 of 90	$310,380	-$140,728

Instances in 2018 to 2020 where frequency regulation (FR) activity profits exceed arbitrage profits in the same time period, as well as the potential annual change in FR and arbitrage profits from these instances; determined from CAISO AS clearing prices and CAISO hour ahead markets.[43]

Table B13 Monthly energy for frequency regulation markets and monthly energy discharged and charged by batteries in CAISO.[43,44]

Month	Regulation Up (MWh)	Regulation Down (MWh)	Battery Discharge (MWh)	Battery Charge (MWh)
January 2022	368,820	538,900	102,520	140,010
February 2022	309,070	468,660	101,090	166,390
March 2022	338,650	558,430	76,270	155,490
April 2022	325,630	580,410	88,280	188,050
May 2022	312,240	551,580	94,140	210,510
June 2022	254,840	552,790	159,390	238,720

Figure B5 Net present values of BESS with LFP cathode chemistry and a social cost of carbon of $51/tonne CO_{2eq}.

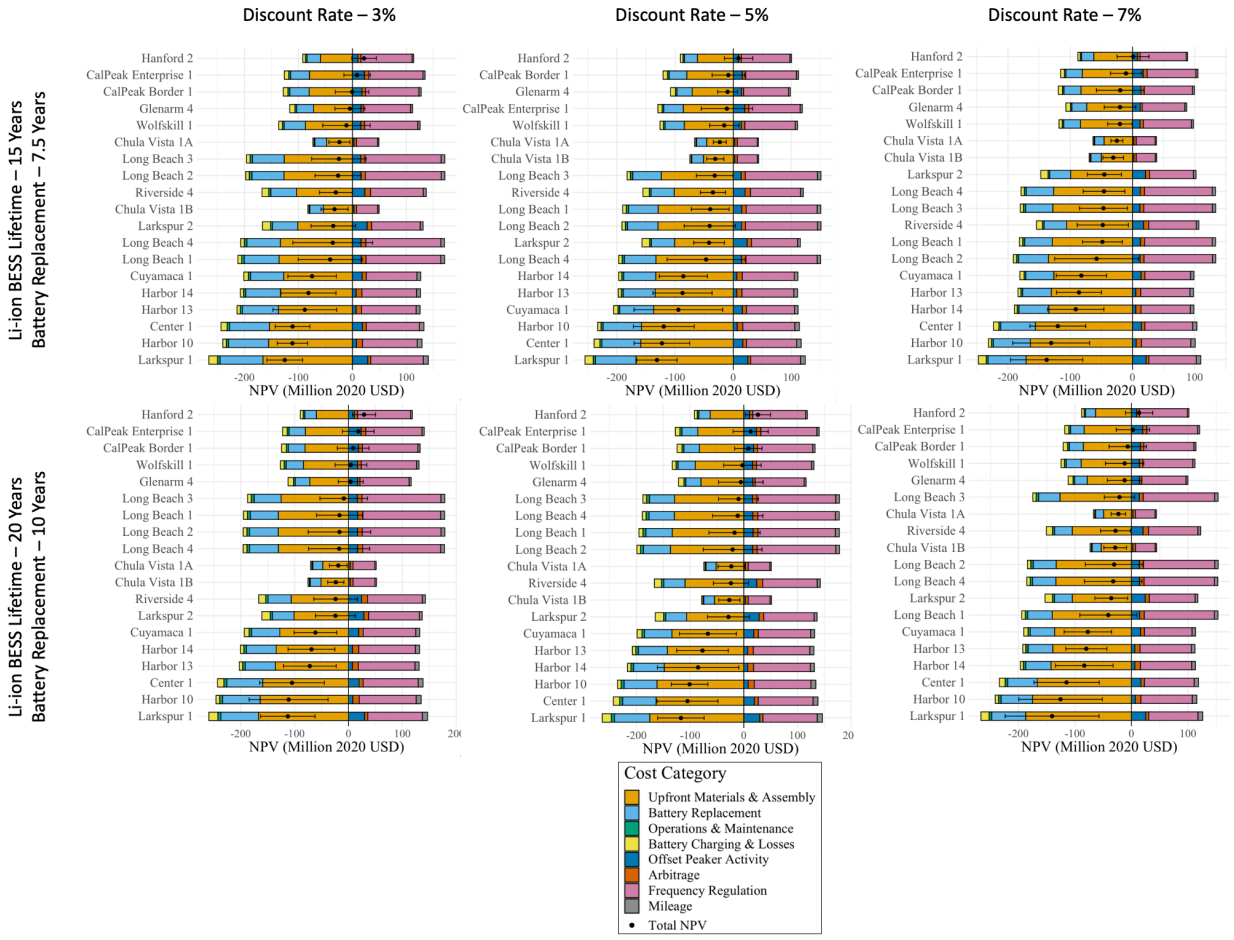

Figure B6 Net present values of BESS with LFP cathode chemistry and a social cost of carbon of $185/tonne CO_{2eq}.

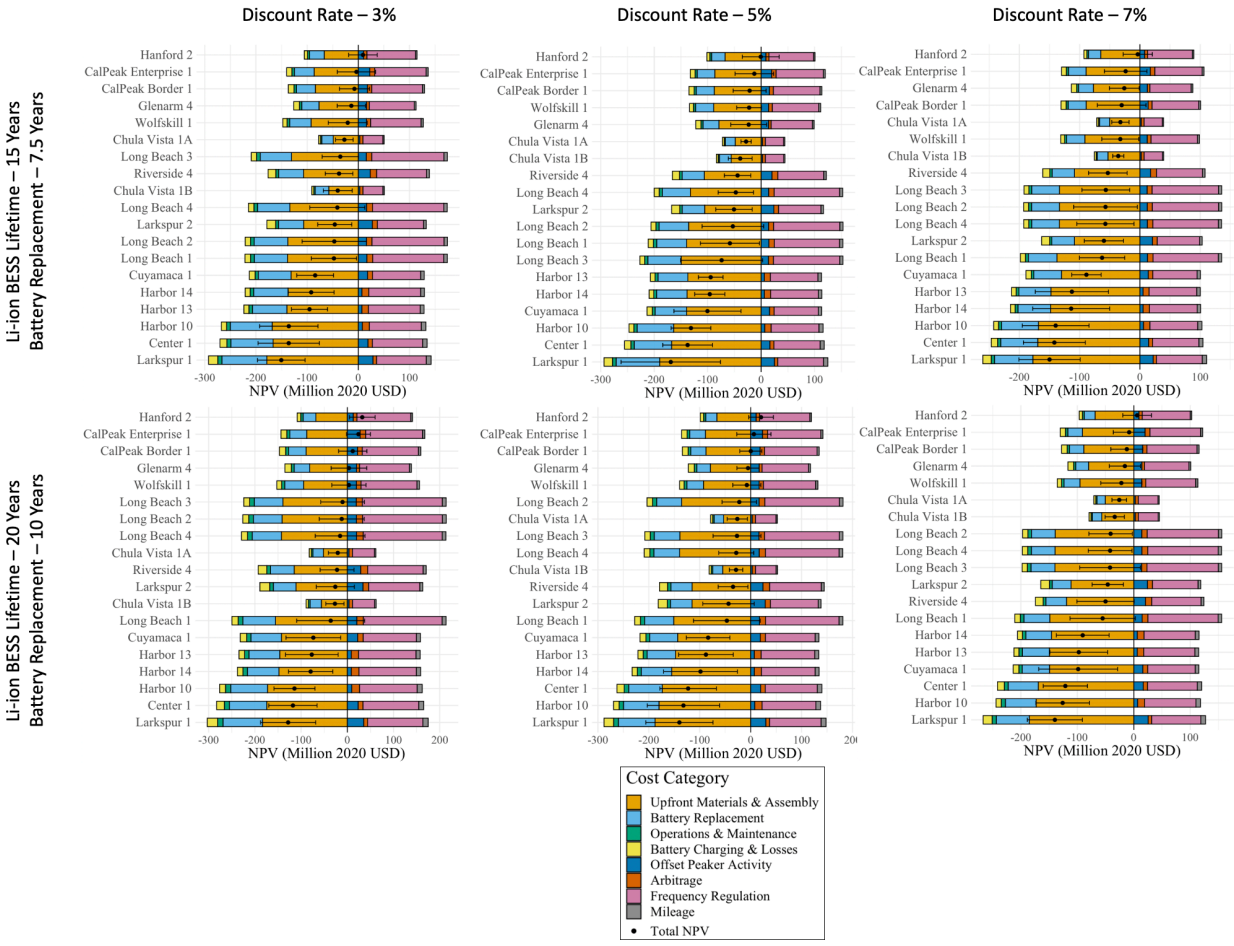

Figure B7 Net present values of BESS with NCA cathode chemistry and a social cost of carbon of $51/tonne CO_{2eq}.

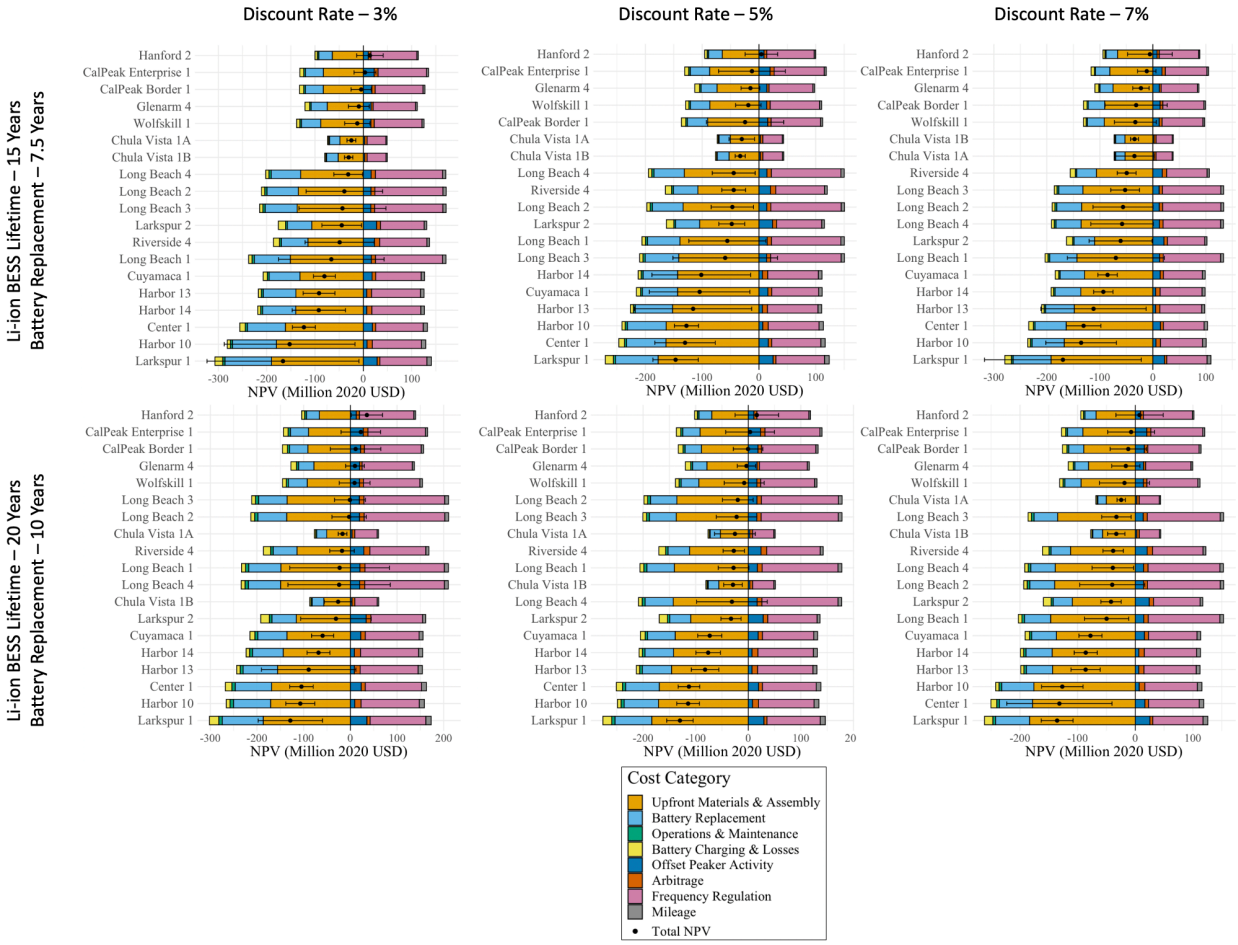

Figure B8 Net present values of BESS with NCA cathode chemistry and a social cost of carbon of $185/tonne CO_{2eq}.

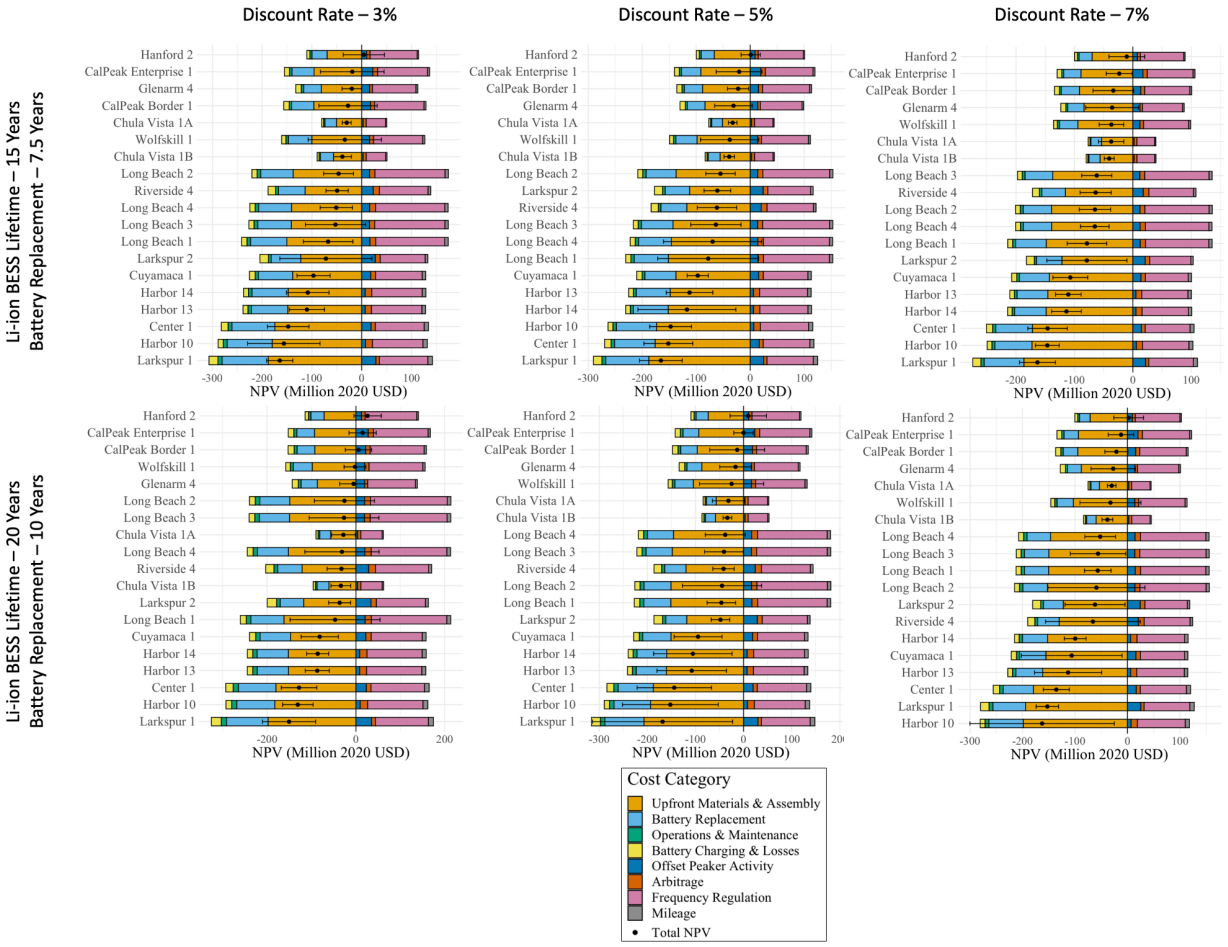

Figure B9 Net present values of BESS with NMC cathode chemistry and a social cost of carbon of $51/tonne CO_{2eq}.

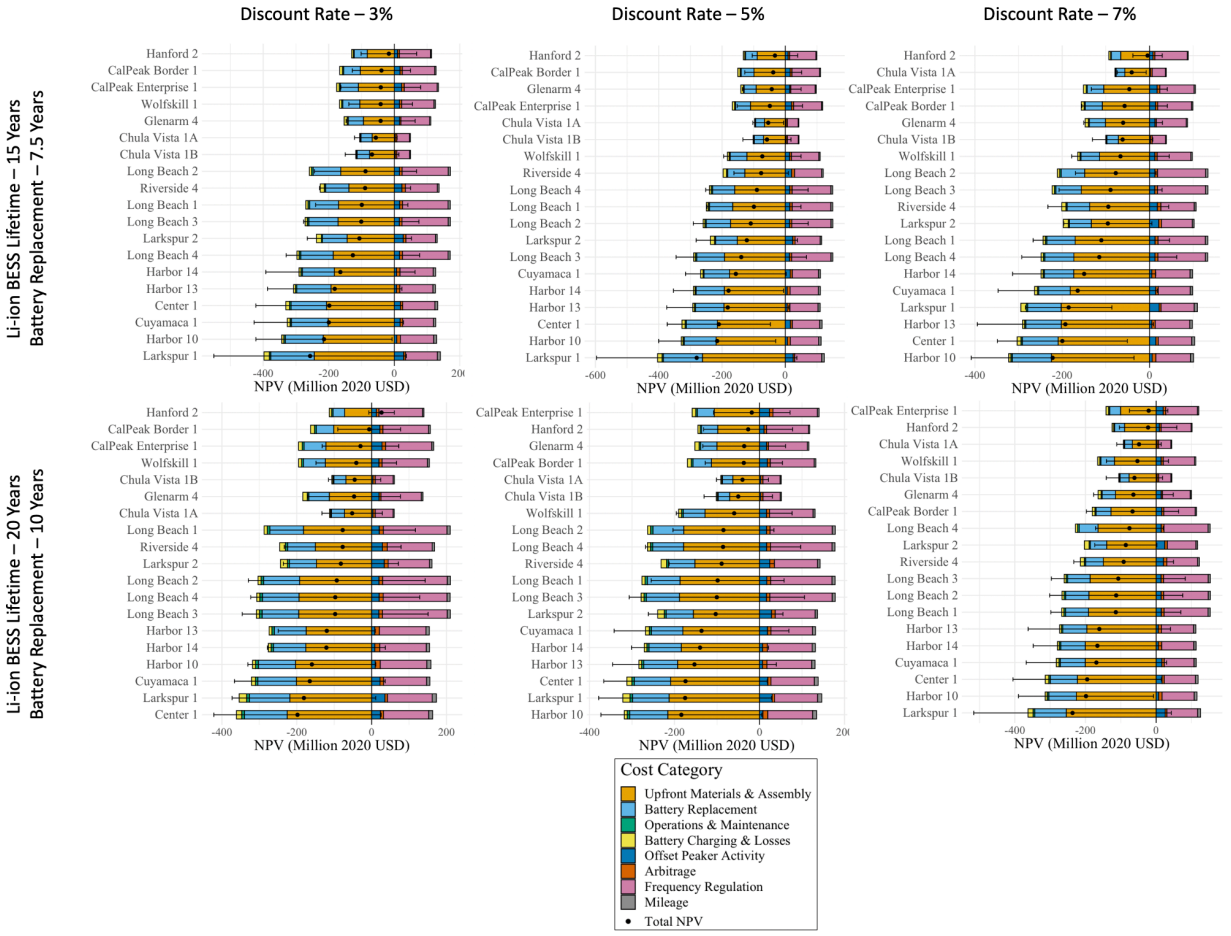

Figure B10 Net present values of BESS with NMC cathode chemistry and a social cost of carbon of $185/tonne CO_{2eq}.

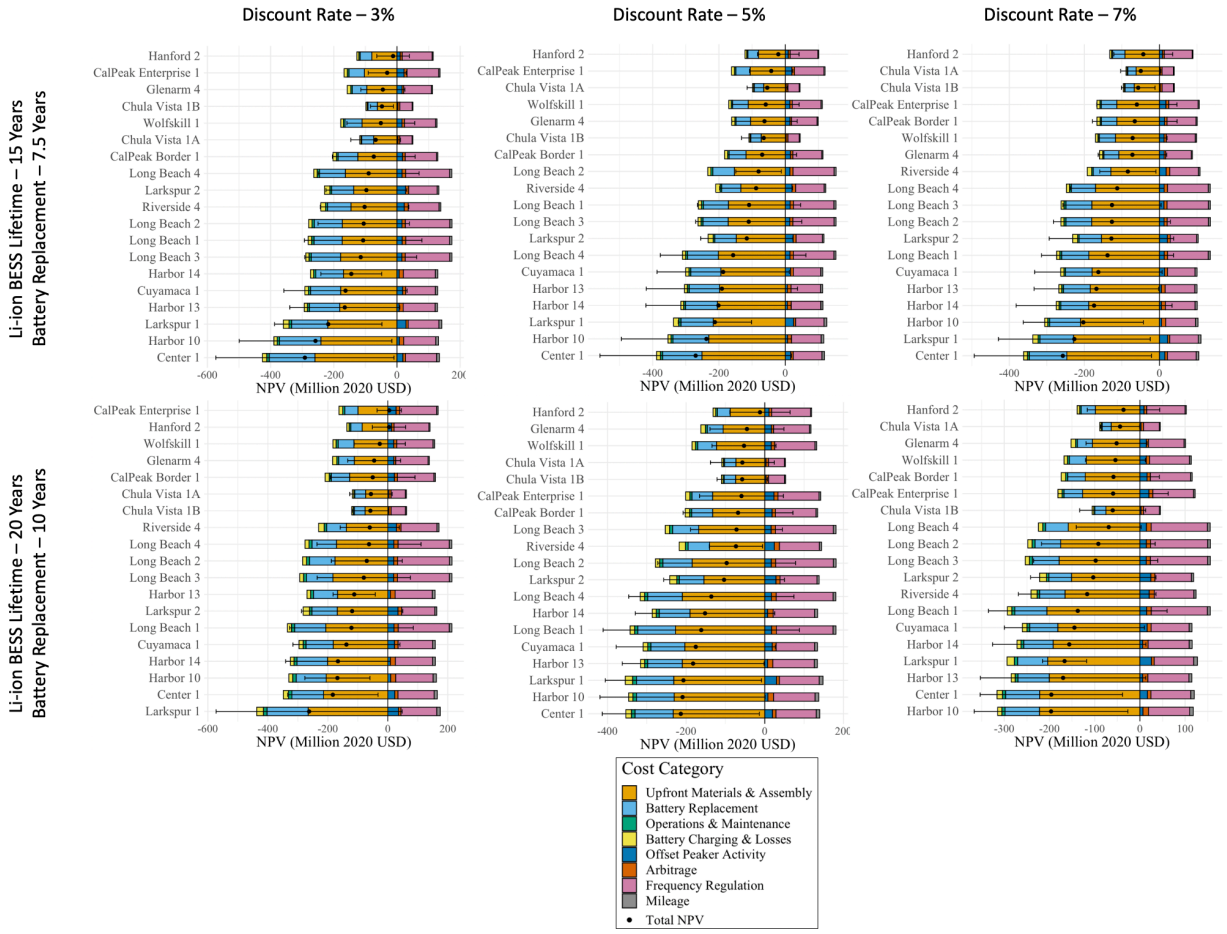

Figure B11a Example LCA GWP of BESS replacing long beach generating station unit 1.

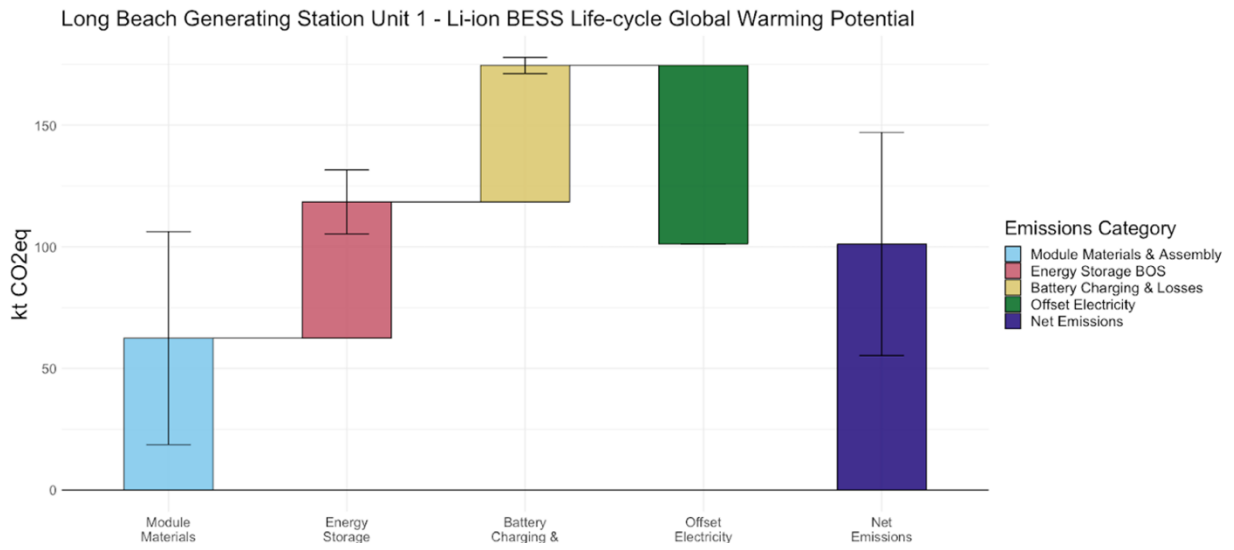

Figure B11b Example LCA GWP breakdown of BESS replacing long beach generating station unit 1.

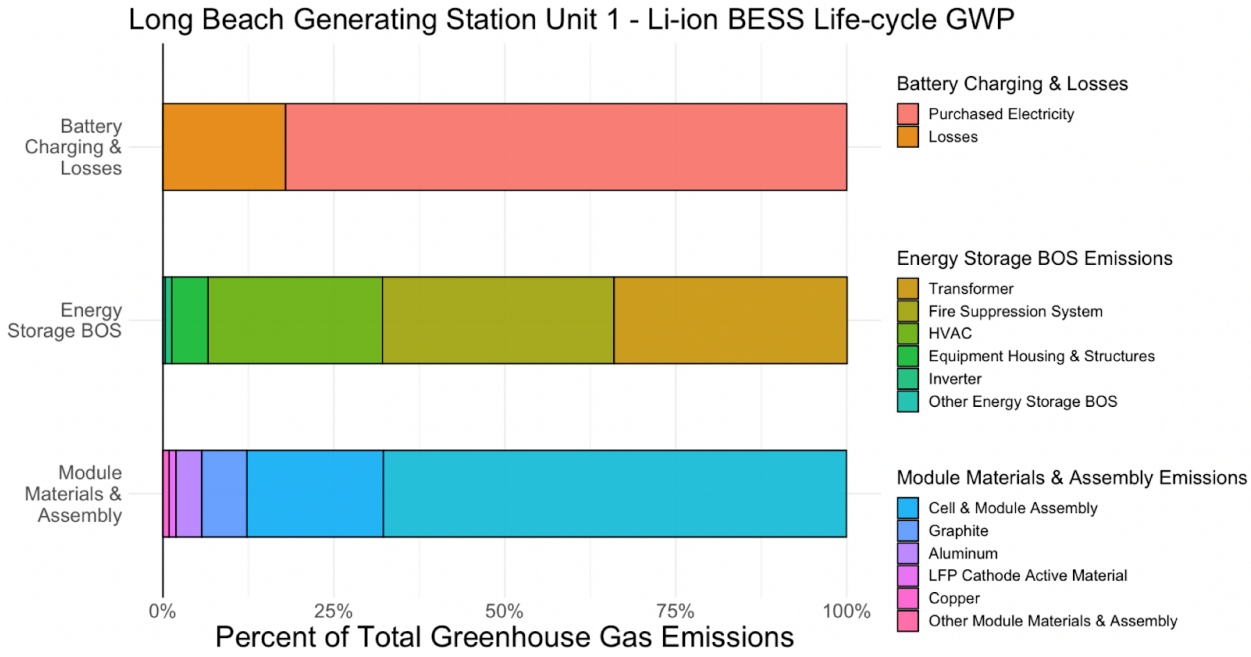

Exemplary graphical representation of the GWP of BESS replacing Long Beach Generating Station Unit 1. Emissions are categorized into "Battery Charging & Losses", "Energy Storage BOS Emissions", and "Module Materials & Assembly Emissions." A percent breakdown of the components contributing to each category are also presented.

Table B14 Distributions and assumptions for cell assembly and BOS of BESS.[18,45–47]

Component/Parameter	Distribution/equation/description (prices and efficiencies)
Battery Assembly Energy Demand (MJ/kWh) – Pilot Scale	Triangular distribution; mode = 1,000; min = 100; max = 10,000
Battery Assembly Energy Demand (MJ/kWh) – Nth Scale	Uniform distribution; min = 100; max = 1,000
Battery Assembly Energy Demand (MJ/kWh) - Unspecified	Triangular distribution; mode = 101; min = 100; max = 10,000
Battery Assembly Energy Supply – Max Thermal	Thermal energy percent of total energy = 80% Electrical energy percent of total energy = 20%
Battery Assembly Energy Supply – Min Thermal	Thermal energy percent of total energy = 0% Electrical energy percent of total energy = 100%
Battery Assembly Energy Supply – Unspecified Thermal	Thermal energy percent of total energy: uniform distribution; min = 0%, max = 80% Electrical energy percent of total energy = 100% - thermal energy percent
Battery Assembly Thermal Source – Natural Gas	Thermal energy provided by natural gas = 100%
Battery Assembly Thermal Source – Coal	Thermal energy provided by coal = 100%
Battery Assembly Thermal Source – Unspecified	Thermal energy provided by natural gas: uniform distribution; min = 0%, max = 100% Thermal energy provided by coal = 100% - natural gas percent

For all runs presented in the main body of literature, the “unspecified” distributions for battery assembly energy demand, battery energy supply, and battery assembly thermal source are selected to include all possible scenarios for cell assembly.

Figure B12 Lifecycle greenhouse gas emissions of BESS with LFP cathode chemistry. Plants listed in order of highest to lowest expected NPV with a 3% discount rate and a social cost of carbon of $51/tonne CO_{2eq}.

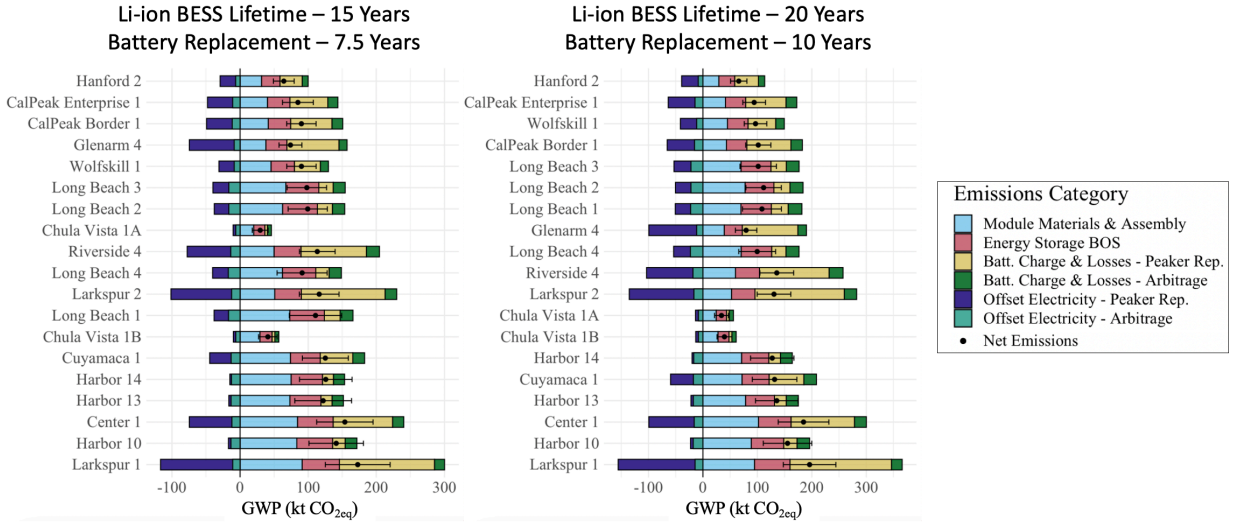

Figure B13 Lifecycle greenhouse gas emissions of BESS with NCA cathode chemistry. Plants listed in order of highest to lowest expected NPV with a 3% discount rate and a social cost of carbon of $51/tonne CO_{2eq}.

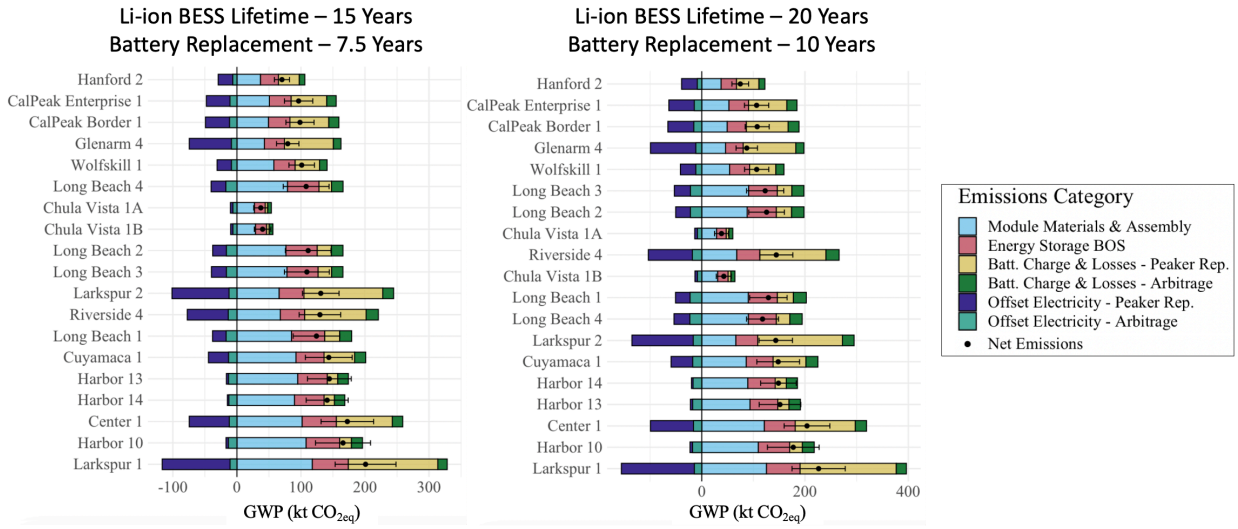

Figure B14 Lifecycle greenhouse gas emissions of BESS with NMC cathode chemistry. Plants listed in order of highest to lowest expected NPV with a 3% discount rate and a social cost of carbon of $51/tonne CO_{2eq}.

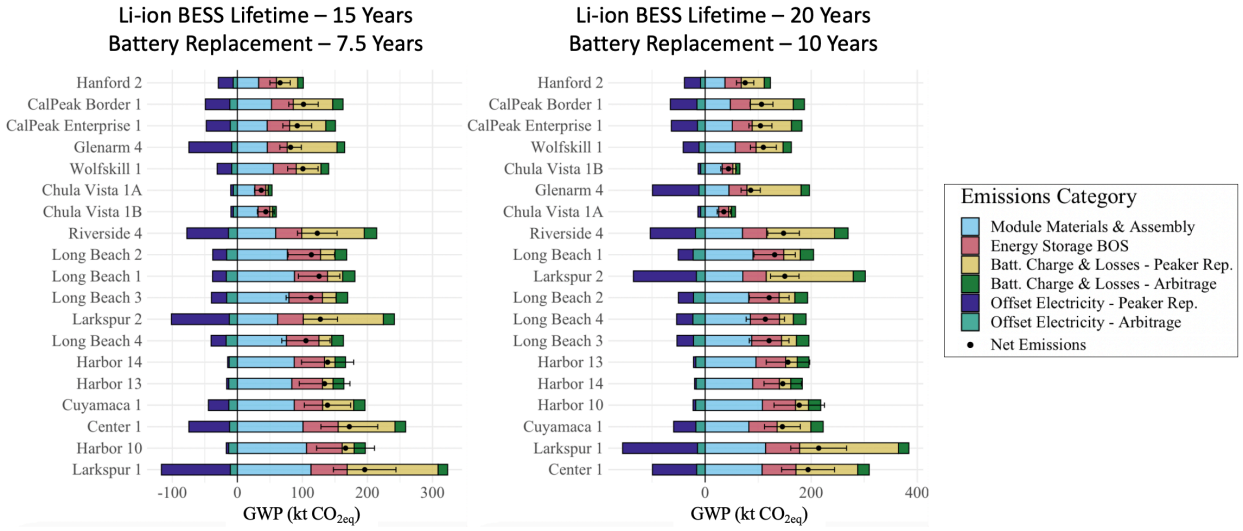

Table B15 Cost per cycle by Li-ion cathode chemistry derived from Monte Carlo Assessment.

Cathode Chemistry	Average Cost per Cycle [$/(MWh*Cycle)]	Standard Deviation
NMC	149.6	27.9
NCA	89.58	11.3
LFP	65.27	5.18

Cost per cycle is representative of the additional upfront cost associated with the increasing upfront battery capacity in order to compensate for the degradation that will occur from performing a cycle during the lifetime of a BESS. The impacts of non-cycle degradation are excluded from the cost per cycle. It is derived through a Monte Carlo simulation with 1000 runs that considers the degradation mechanisms and battery prices used throughout this study.

Table B16 Distributions and assumptions for BESS component LCAs.

Component/Parameter	Distributions and characteristics	Source
Li-ion Modules	Material Breakdown: Module material breakdown by chemistry taken from Porzio and Scown 2021 Table 3.	[18,48]
Inverters	Mass Equation: Mass [kg] = 1987.3 * Size [MW] ^ 0.7484 Material Breakdown by Mass: Steel = 60.24% Aluminum = 17.74% Copper = 12.40% Plastics = 9.62% Energy Consumption: Electricity [kWh] = 5.6856 * Size [MW] ^ 0.68 Refined Oil [MJ] = 0.1211 * Size [MW] ^ 0.68 Natural Gas [MJ] = 1.9131 * Size [MW] ^ 0.68 Heatwaste [MJ] = 4.9277 * Size [MW] ^ 0.68 Additional Characteristics: Lifetime = 10 years	[49]

Transformers (Medium Voltage)	Mass Equation: Mass [kg] = 2780.7 * Size [MW] ^ 0.8674 Material Breakdown by Mass: Transformer oil = 24% Steel = 56% Copper = 12% Pressboard = 3% Paper = 1% Other = 4% Energy Consumption: Electricity [kWh] = 1993.3 * Size [kW] Natural Gas [kWh] = 3865.2 * Size [kW] Additional Characteristics: Lifetime = 40 years	49,50

Switchgears	Mass: Mass[kg] = 2400 Material Breakdown by Mass: Aluminum = 15% Steel = 31.67% Stainless steel = 1.7917% Copper = 1.0833% SF_6 = 0.4167% EPDM = 0.05% Copper tungsten = 0.125% PTFE = 0.0625% Epoxy resin = 0.1667% Molecular sieve = 0.070833% Porcelain = 44.1667% Other = 5.4% Energy Consumption (Modeled as inverter): Electricity [kWh] = 1993.3 * Size [kW] Natural Gas [kWh] = 3865.2 * Size [kW] Additional Characteristics: SF_6 annual leak rate = 2% Lifetime = 40 years	[49,51]
Conductors	Mass Breakdown: XLPE [kg/ft] = 0.1643 (XLPE modeled as HDPE) Copper [kg/ft] = 0.887	[28] Sampled from available products
Conduits	Mass Breakdown: Galvanized steel [kg/ft] = 2.1098	[28] Sampled from available products

Battery Management System (BMS)	<u>Mass Breakdown:</u> Copper = 8.79% Glass fiber = 9.99% Epoxy resin = 3.03% Steel = 43.0% Aluminum = 4.53% Nylon = 4.21% HDPE = 4.57% PC = 8.39% Other = 13.5% <u>Energy Consumption:</u> Electricity [kWh] = 1.0275 Natural gas [MJ] = 0.03661	[52]
Fire Suppression	<u>Mass Breakdown (40 ft Container):</u> Galvanized steel = 635.81 [kg per container] HFC227ea = 193.09 [kg per container] <u>Mass Breakdown (20 ft Container):</u> Galvanized steel = 408.74 [kg per container] HFC227ea = 96.55 [kg per container] <u>Mass Breakdown (Cabinet):</u> Galvanized steel = 100 [kg per container] HFC227ea = 25 [kg per container] <u>Additional Characteristics:</u> HFC227ea recovery leak rate: uniform distribution; min = 2.5%, max = 7.5% HFC227ea lifetime = 10 years	[28,29,53–55] Sampled from available products

HVAC	<u>Mass Breakdown (40 ft Container):</u> Steel = 156 [kg per container] Galvanized steel = 70 [kg per container] Aluminum = 34 [kg per container] Copper = 34 [kg per container] R410a: uniform distribution; min = 6; max = 9 [kg per container] <u>Mass Breakdown (20 ft Container):</u> Steel = 78 [kg per container] Galvanized steel = 35 [kg per container] Aluminum = 17 [kg per container] Copper = 17 [kg per container] R410a: uniform distribution; min = 3; max = 4.5 [kg per container] <u>Mass Breakdown (Cabinet):</u> (Assumed glycol cell cooling with negligible mass) <u>Additional Characteristics:</u> R410a annual leak rate: Triangular distribution; min = 2%; max = 20%, mode = 10% R410a recovery leak rate: Triangular distribution; min = 15%; max = 100%; mode = 0.56% HVAC lifetime = 15 R410a to R32 conversion = 1 to uniform distribution; min = 0.7; max = 0.8	[40–42,56] See Table S17

Battery Container	Mass Breakdown (40 ft Container): Steel = 3563 [kg per container] Wood = 637.1 [kg per container] Mass Breakdown (20 ft Container): Steel = 1881 [kg per container] Wood = 318.6 [kg per container] Mass Breakdown (Cabinet): Steel = 212.7 [kg per container]	Sampled from available products
Inverter Housing	Mass Breakdown (20 ft Container): Steel = 1881 [kg per container] Wood = 318.6 [kg per container] Mass Breakdown (Cabinet): Steel = 212.7 [kg per container] Mass Breakdown (In Module): No additional inverter housing	Sampled from available products

Foundation	<u>Energy Consumption</u>: Electricity [MJ/cu-yard] = 0.01543 Residual Oil [MJ/cu-yard] = 0.0004071 Diesel [MJ/cu-yard] = 0.001750 Petcoke [MJ/cu-yard] = 0.01847 Natural Gas [MJ/cu-yard] = 0.01805 Coal [MJ/cu-yard] = 0.04213 Waste heat [MJ/cu-yard] = 0.004776 Tire [MJ/cu-yard] = 0.004776 Waste Oil [MJ/cu-yard] = 0.000742866 Renewables [MJ/cu-yard] = 0.0007428 <u>Process Emissions</u>: CO2 [kg/cu-yard] = 0.07925 CH4 [kg/cu-yard] = $4.496 * 10^{-6}$ N2O [kg/cu-yard] = $4.62*10^{-7}$ VOC [kg/cu-yard] = $7.782*10^{-5}$ CO [kg/cu-yard] = $1.246*10^{-4}$ NOx [kg/cu-yard] = $1.415*10^{-4}$ PM10 [kg/cu-yard] = $7.408*10^{-5}$ PM25 [kg/cu-yard] = $2.566*10^{-5}$ SOx [kg/cu-yard] = $3.114*10^{-5}$	[48]
Battery Racks	<u>Mass Breakdown (40 ft Container):</u> Steel: Uniform distribution; min = 1,200; max = 4,800 [kg per container] <u>Mass Breakdown (20 ft Container):</u> Steel: Uniform distribution; min = 600; max = 2,400 [kg per container] <u>Mass Breakdown (Cabinet):</u> Steel = 0 [kg per container]	Sampled from available products

Impacts from electricity consumption as associated with the US national average generation mix.

Table B17 HVAC Properties, Assumptions, and Calculations for BESS Cooling Load and Refrigerant Quantities.[40–42,57]

Design Parameter/Assumptions	**20 ft Container**	**40 ft Container**
Internal Thermal Load	9 kW 2.6 tons cooling 30,857 btu/hr	18 kW 5.1 tons cooling 61,714 btu/hr
Footprint	12 x 20 ft	12 x 40 ft
Height	10 ft	10 ft
U Value	0.1	0.1
Indoor Temp	70	70
Design Day Outdoor Temp	85	85
Datacenter Modeling Approach		
Oversizing factor	30%	30%
Environmental Thermal Load [btu/hr] (Roof & Wall Area * U Value * DT)	1320	2280
Total Load [btu/hr] (100% + Oversize Factor) * Internal Thermal Load + Environmental Thermal Load	41,194	82,509
Total Load [tons]	~3.33	~6.66
lbs of r410a per ton	Uniform distribution: min = 2 lbs per ton; max = 3 lbs per ton	Uniform distribution: min = 2 lbs; max = 3 lbs
Total r410a	Min = 6.66 lbs; max = 10 lbs	Min = 13.33 lbs; max = 20 lbs

References:

1. Bolun Xu, Dvorkin, Y., Kirschen, D. S., Silva-Monroy, C. A. & Watson, J.-P. A comparison of policies on the participation of storage in U.S. frequency regulation markets. in 2016 IEEE Power and Energy Society General Meeting (PESGM) 1–5 (IEEE, 2016). doi:10.1109/PESGM.2016.7741531.

2. Fu, R., Remo, T. & Margolis, R. 2018 U.S. Utility-Scale Photovoltaics Plus-Energy Storage System Costs Benchmark. (2018).

3. Ardani, K., O'Shaughnessy, E., Fu, R., McClurg, C., Huneycutt, J., Margolis, R. Installed Cost Benchmarks and Deployment Barriers for Residential Solar Photovoltaics with Energy Storage: Q1 2016. (2017).

4. Mongird, K., Viswanathan, V., Alam, J., Vartanian, C., Sprenkle, V., Baxter, R. 2020 Grid Energy Storage Technology Cost and Performance Assessment. (2020).

5. Scown, C. D., Gokhale, A. A., Willems, P. A., Horvath, A. & McKone, T. E. Role of lignin in reducing life-cycle carbon emissions, water use, and cost for United States cellulosic biofuels. Environ. Sci. Technol. **48**, 8446–8455 (2014).

6. Yang, M., Baral, N. R., Anastasopoulou, A., Breunig, H. M. & Scown, C. D. Cost and life-cycle greenhouse gas implications of integrating biogas upgrading and carbon capture technologies in cellulosic biorefineries. Environ. Sci. Technol. **54**, 12810–12819 (2020).

7. Nordahl, S. L., Devkota, J. P., Amirebrahimi, J., Smith, S. J., Breunig, H. M., Preble, C. V., Satchwell, A. J., Jin, L., Brown, N. J, Kirchstetter T. W., Scown, C. D. Life-cycle greenhouse gas emissions and human health trade-offs of organic waste management strategies. Environ. Sci. Technol. **54**, 9200–9209 (2020).

8. Bird, R., Baum, Z. J., Yu, X. & Ma, J. The Regulatory Environment for Lithium-Ion Battery Recycling. ACS Energy Lett. **7**, 736–740 (2022).

9. Golmohammadzadeh, R., Faraji, F., Jong, B., Pozo-Gonzalo, C. & Banerjee, P. C. Current challenges and future opportunities toward recycling of spent lithium-ion batteries. Renew. Sustain. Energy Rev **159**, 112202 (2022).

10. Holland, S. P., Mansur, E. T., Muller, N. Z. & Yates, A. J. Are There Environmental Benefits from Driving Electric Vehicles? The Importance of Local Factors. American Economic Review **106**, 3700–3729 (2016).

11. Borenstein, S. & Bushnell, J. Do two electricity pricing wrongs make a right? cost recovery, externalities, and efficiency. (2018) doi:10.3386/w24756.

12. Graff Zivin, J. S., Kotchen, M. J. & Mansur, E. T. Spatial and temporal heterogeneity of marginal emissions: Implications for electric cars and other electricity-shifting policies. J. Econ. Behav. Organ. **107**, 248–268 (2014).

13. Davis, L. & Hausman, C. Market impacts of a nuclear power plant closure. American Economic Journal: Applied Economics **8**, 92–122 (2016).

14. Pacific Gas and Electric Company. The Next Giant Leap for Electric System Reliability: PG&E Proposes Nearly 1,600 MW of New Battery Energy Storage Capacity. PG&E https://www.pge.com/en_US/about-pge/media-newsroom/news-details.page?pageID=38883b6b-8597-4734-b85a-104a9f6e8af3&ts=1643133870903 (2022).

15. Wei, J. Interview on Utility-Scale Lithium-Ion Battery Energy Storage Cost Modeling. (2020).

16. Leggett, G. Interview on Lithium-Ion Utility-Scale Battery Energy Storage Cost Modeling. (2020).

17. Shriver, J. Interview on Lithium-Ion Utility-Scale Battery Energy Storage Cost Modeling. (2020).

18. Porzio, J. & Scown, C. D. Life-cycle assessment considerations for batteries and battery materials. Adv. Energy Mater. 2100771 (2021) doi:10.1002/aenm.202100771.

19. Bloch, C., Newcomb, J., Shiledar, S. & Tyson, M. Breakthrough Batteries: Powering the Era of Clean Electrification. (2020).

20. Mitchell, P. J. & Waters, J. E. Energy Storage Roadmap Report. (2017).

21. Ralon, P., Taylor, M., Ilas, A., Diaz-Bone, H. & Kairies, K.-P. Electricity Storage and Renewables: Costs and Markets to 2030. (2017).

22. Ecker, M., Nieto, N., Kabitz, S., Schmalstieg, J., Blanke, H., Warnecke, A., Sauer, D. U. Calendar and cycle life study of Li(NiMnCo)O2-based 18650 lithium-ion batteries. J. Power Sources **248**, 839–851 (2014).

23. Grolleau, S., Delaille, A., Gualous, H., Gyan, P., Revel, R., Bernard, J., Redondo-Iglesias, E., Peter, J. Calendar aging of commercial graphite/LiFePO4 cell – Predicting capacity fade under time dependent storage conditions. J. Power Sources **255**, 450–458 (2014).

24. Gantenbein, S., Schönleber, M., Weiss, M. & Ivers-Tiffée, E. Capacity Fade in Lithium-Ion Batteries and Cyclic Aging over Various State-of-Charge Ranges. Sustainability **11**, 6697 (2019).

25. Battaglia, V. Interview on Utility-Scale Lithium-Ion Battery Energy Storage Cost Modeling. (2020).

26. Srinivasan, V. Interview on Utility-Scale Lithium-Ion Battery Energy Storage Cost Modeling. (2020).

27. Fu, R., Feldman, D. & Margolis, R. U.S. Solar Photovoltaic System Cost Benchmark: Q1 2018. (2018).

28. RS Means 2018. Building Construction Costs with RSMeans Data 2018. vol. 76 (Gordian, 2018).

29. NFPA. NFPA 2001: Standard on Clean Agent Fire Extinguishing Systems. (2017).

30. NFPA. NFPA 855: Standard for the Installation of Stationary Energy Storage Systems. (2019).

31. Blodgett, D. & Hudson, R. PV Inverter Useful Life Considerations. (2019).

32. NFPA. NFPA 70: National Electric Code. (2019).

33. Bird, L., Flores, F., Volpi, C., Ardani, K., Manning, D., McAllister, R. Review of Interconnection Practices and Costs in the Western States. (2018).

34. Fritts, J. State and Local Sales Tax Rates, Midyear 2020. https://taxfoundation.org/state-and-local-sales-tax-rates-2020/ (2020).

35. Frith, J. Lithium-Ion Batteries: State of the Industry 2021. (2021).

36. Feldman, D., Ramasamy, V., Fu, R., Ramdas, A., Desai, J., Margolis, R. U.S. solar photovoltaic system and energy storage cost benchmark: Q1 2020. (2021) doi:10.2172/1764908.

37. Kang, J., Yan, F., Zhang, P. & Du, C. Comparison of comprehensive properties of Ni-MH (nickel-metal hydride) and Li-ion (lithium-ion) batteries in terms of energy efficiency. Energy **70**, 618–625 (2014).

38. Wood Mackenzie Power & Renewables. The Global PV Inverter and PLPE Landscape, H1 2019. (2019).

39. United States Code. Subpart K - Distribution Transformers. (2013).

40. US DOE. Energy Conservation Program: Energy Conservation Standards for Single Package Vertical Air Conditioners and Single Package Vertical Heat Pumps. (2015).

41. Gallagher, G., Despande, B., Gupta, P. & Huang, A. California'sHigh Global Warming Potential Gases Emission Inventory - Emission Inventory Methodology and Technical Support Document. (2016).

42. Karkour, S., Ihara, T., Kuwayama, T., Yamaguchi, K. & Itsubo, N. Life cycle assessment of residential air conditioners considering the benefits of their use: A case study in indonesia. Energies **14**, 447 (2021).

43. California ISO. California ISO Oasis. Oasis Prod http://oasis.caiso.com/mrioasis/logon.do.

44. California ISO. Today's Outlook. California ISO https://www.caiso.com/todaysoutlook/Pages/supply.html#section-batteries-trend.

45. Kurland, S. D. Energy use for GWh-scale lithium-ion battery production. Environ. Res. Commun. **2**, 012001 (2019).

46. Dai, Q., Kelly, J. C., Gaines, L. & Wang, M. Life Cycle Analysis of Lithium-Ion Batteries for Automotive Applications. Batteries **5**, 48 (2019).

47. Ellingsen, L. A.-W., Majeau-Bettez, G., Singh, B., Srivastava, A. K., Valoen, L. O., Stromman, A. H. Life Cycle Assessment of a Lithium-Ion Battery Vehicle Pack. Journal of Industrial Ecology **18**, 113–124 (2014).

48. Wang, M. GREET2 Model. (Argonne National Laboratory, 2020).

49. Rahman, M. M., Gemechu, E., Oni, A. O. & Kumar, A. The greenhouse gas emissions' footprint and net energy ratio of utility-scale electro-chemical energy storage systems. Energy Conversion and Management **244**, 114497 (2021).

50. Burger Mansilha, M., Brondani, M., Farret, F. A., Cantorski da Rosa, L. & Hoffmann, R. Life cycle assessment of electrical distribution transformers: comparative study between aluminum and copper coils. Environ. Eng. Sci. **36**, 114–135 (2019).

51. Bessede, J.-L. & Krondorfer, W. Impact of High-voltage SF6 Circuit Breakers on Global Warming - Relative Contribution of SF6 Losses. https://www.epa.gov/sites/default/files/2016-02/documents/conf00_krondorfer.pdf (2017).

52. Farzad, T. Life Cycle Analysis for a DC- microgrid energy system in Fjärås. (2019).

53. Kopylov, S. N., Kopylov, P. S., Eltyshev, I. P., Kopylov, N. P. & Begishev, I. R. Highly Effective Fire Extinguishing Mixtures of Iodinated and Fluorinated Hydrocarbons as a Way to Reduce Greenhouse Gas Emissions into the Atmosphere. IOP Conf. Ser.: Earth Environ. Sci. **666**, 022011 (2021).

54. Senecal, J. & Prescott, R. FM-200 Suppression Systems: A Conservative Discharge Test Method and In-Room Pressure Variance Upon Discharge. (1995).

55. BNP Media. Fire Protection Design with FM 200. Plumbing and Mechanical Engineer (2000).

56. ACR News. R32 shows positive benefits in R410A drop-in test. ACR News https://www.acr-news.com/r32-shows-positive-benefits-in-r410A-drop-in-test (2013).

57. Cubero, E. Communications with Edward Cubero. (2021).

Appendix C

Supplemental Information

Private and External Impacts of Electrified Heavy-Duty Long-Haul Trucking with Li-ion Batteries

Figure C1 2024 Market Class 8 Trucks – Rated Capacity vs Range

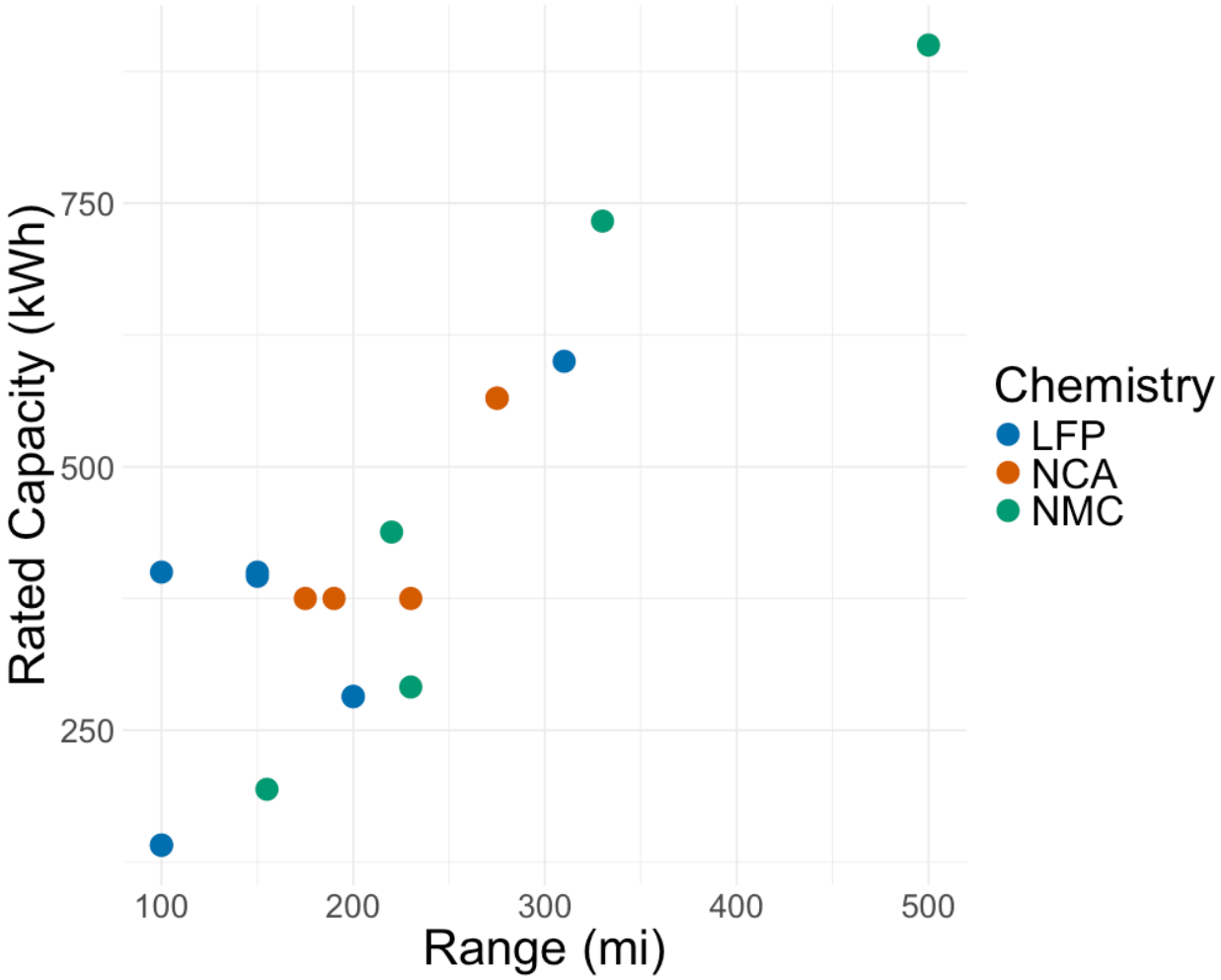

All data collected via independent review of available Class 8 trucks to date.

Table C1 Uncertainty of Truck Model Parameters

Parameter	Uncertainty
R_{Br} [%]	+/- 1%, triangle distribution
η_{BW} [%]	+/- 1%, triangle distribution
η_{Br} [%]	+/- 1%, triangle distribution
η_{GB} [%]	+/- 1%, triangle distribution
η_{E} [%]	+/- 1%, triangle distribution
η_{TW} [%]	+/- 1%, triangle distribution
C_D	+/- 5%, triangle distribution
A [m^2]	+/- 5%, triangle distribution
C_{rr}	+/- 5%, triangle distribution
m_V [kg]	+/- 5%, triangle distribution
P_{AC} [kW]	+/- 5%, triangle distribution

Table C2 Li-ion Pack Specific Energy by Cathode Chemistry[1]

Cathode Chemistry	Specific Energy [Wh/kg]	Uncertainty
LFP	165	Triangle distribution: Min = 150, Max = 180
NMC*	255	Triangle distribution: Min = 250, Max = 260
NCA	177	Triangle distribution: Min = 172, Max = 188

* Assumed NMC811

Figure C2 Discrete Probability Density of Initial Dispatch Times[2]

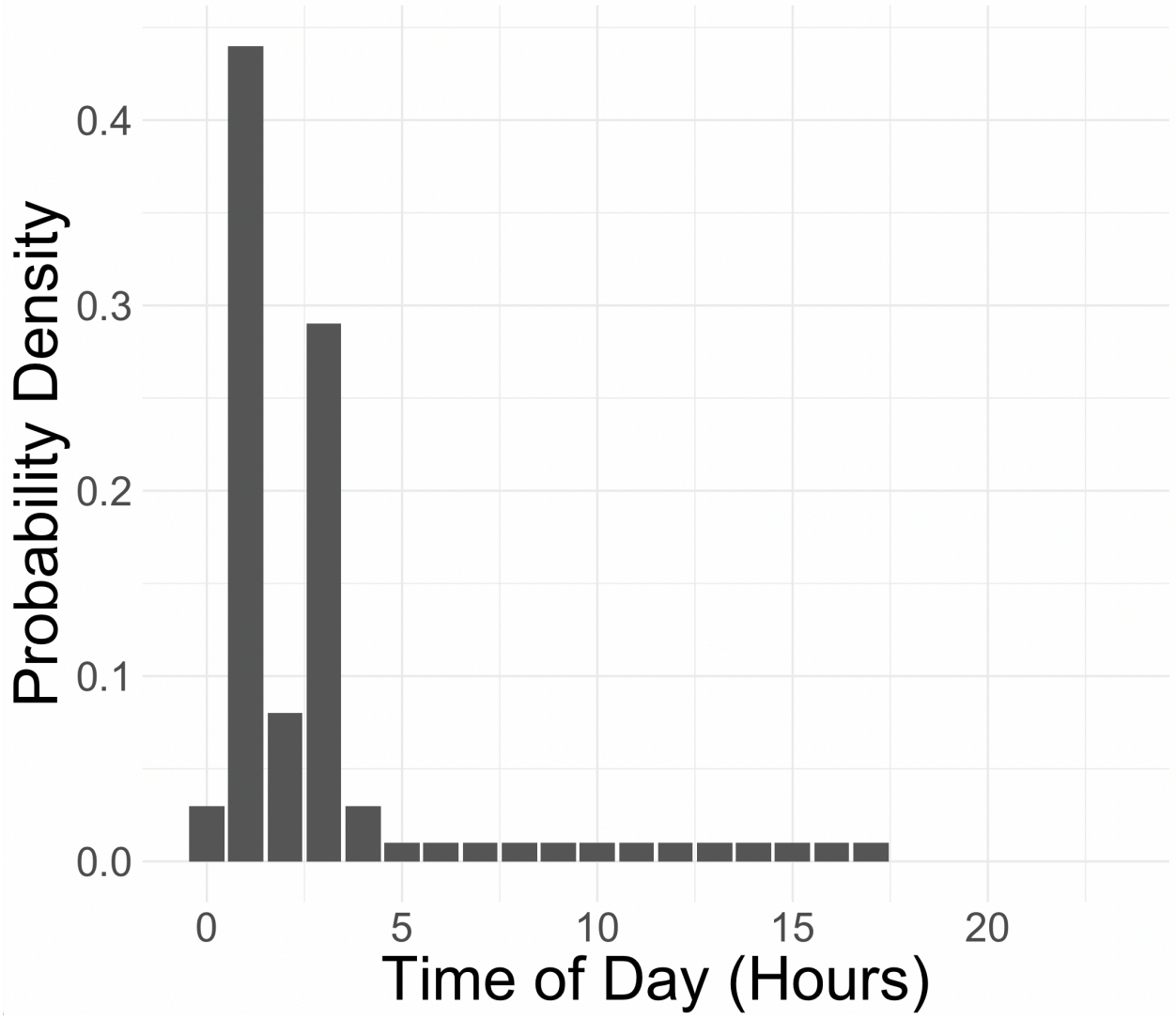

Figure C3 Class 8 Truck Drive Cycle - CARB Heavy Heavy-Duty Diesel Truck (HHDDT) Cruise Segment[3]

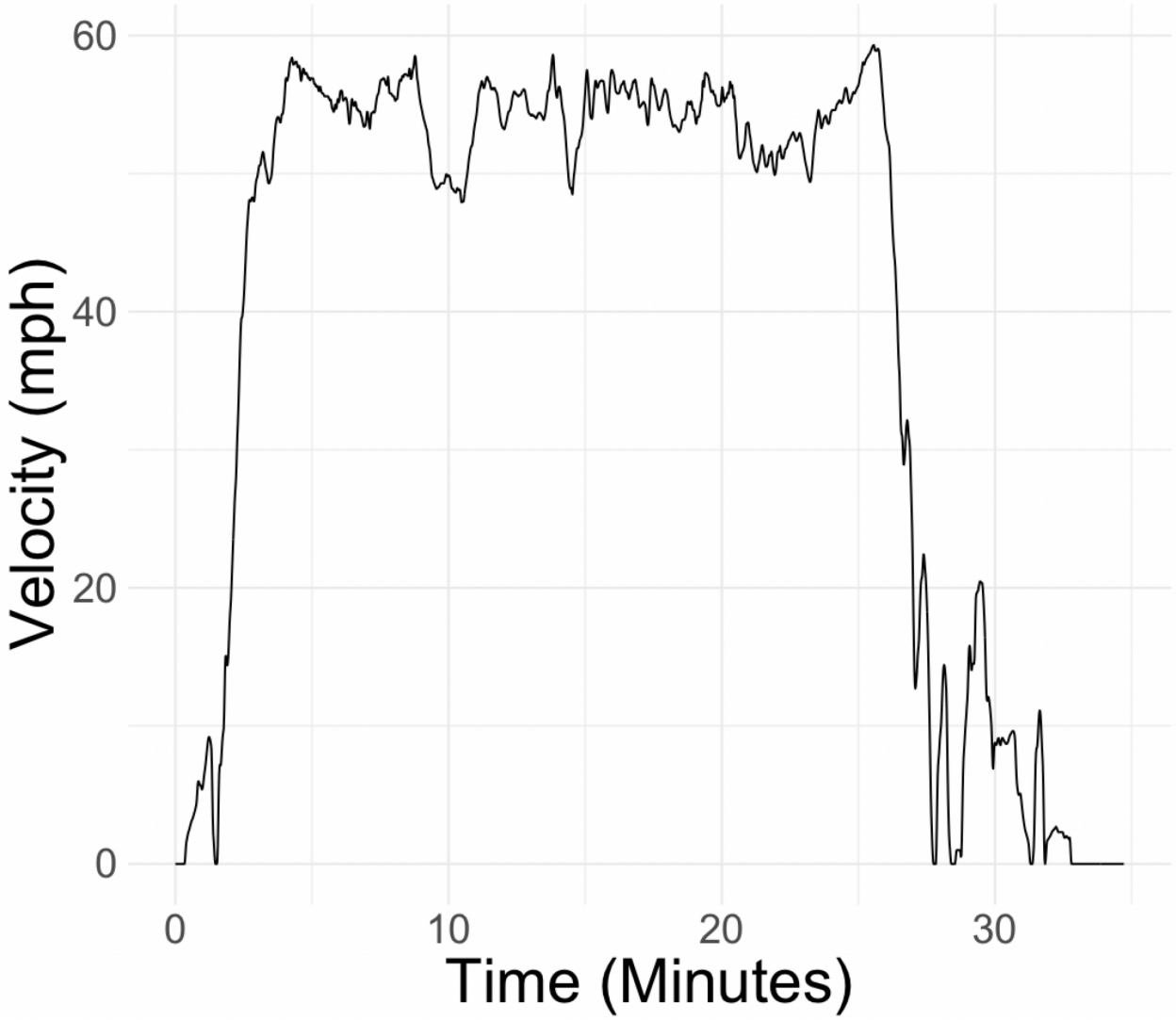

Figure C4 Modeled Charging Power vs State-of-Charge by Charging Infrastructure[4–6]

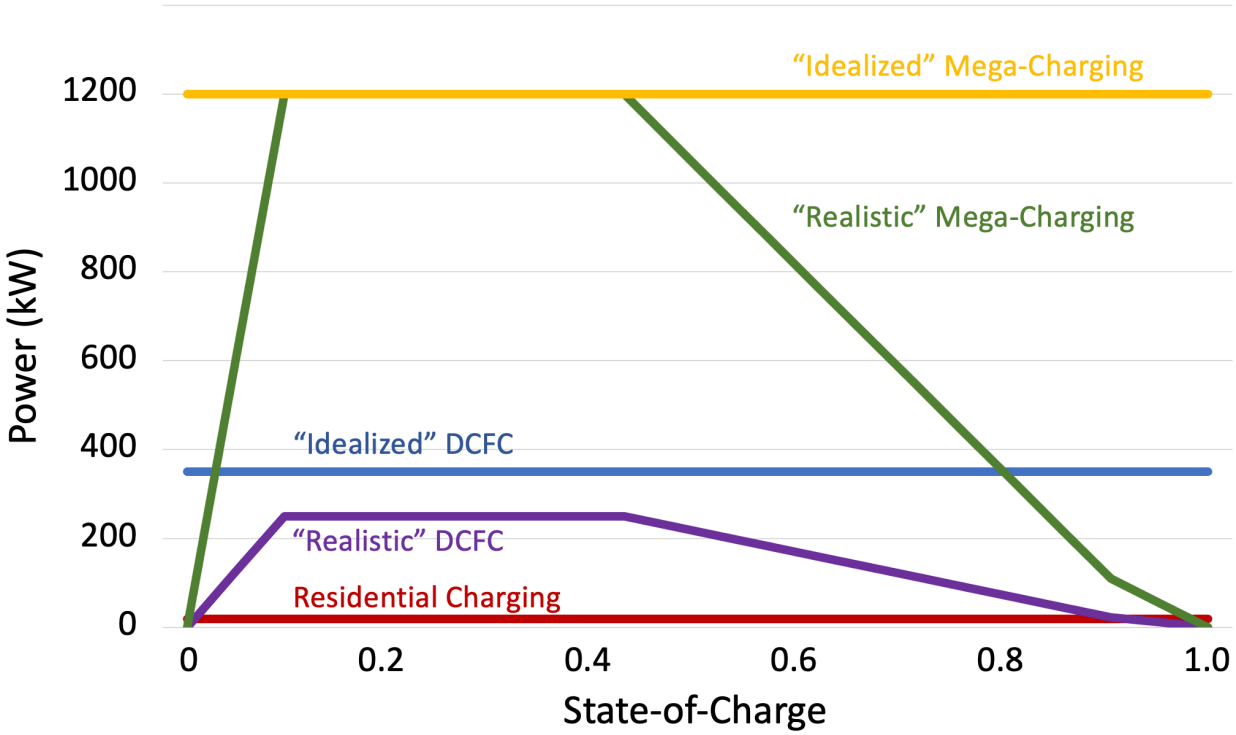

"Realistic" DCFC is the primary charging option used in this study.

Procedure C1 Determining Marginal Electricity Generators

A short run marginal grid model is employed when determining grid response to incremental changes in demand, or charging loads for this study.[7] Charging loads are assigned to a balancing area by geography which are then assigned to a transmission connected region (T-region) made up of several balancing areas.[8] The charging loads are then allocated to all the power plants in that T-region classified as the marginal generator type. We then assume that the charging load is distributed between each generator, such that the induced load is proportional to their current generation.[9] While the approach is imperfect, it provides a decent estimate for which generators are responding to a theoretical load. For greater detail, see McNeil et al.[10]

Table C3 Tailpipe emissions factors of long-haul diesel trucks by scenario[11]

Scenario:	Diesel Truck 2024	Diesel Truck 2035
Vehicle Technology:	MY 2010-2018	Advanced Design
Pollution Control Technology:	DPF*	DPF + SCR**
CO2 [g/kg-fuel]	3194	3194
CH4 [g/kg-fuel]	0.01	0.67
N2O [g/kg-fuel]	0.004	0.004
PM2.5 [g/kg-fuel]	2.2	0.3
SO2 [g/kg-fuel]	0.022	0.022
NOX [g/kg-fuel]	14.3	5.2
NH3 [g/kg-fuel]	0	0.18
Mile per Gallon	5.4	6.7

*DPF: Diesel particulate filter
**SCR: Selective catalytic reduction

Table C4 Mass Breakdown of Truck Components[11–14]

Component	Diesel Truck Percentage	Li-ion Truck Percentage
Truck Body		
Body & Glass	5.8%	6.6%
Interior	6.3%	7.1%
Exterior	1.4%	1.6%
Chassis		
Steer Axle	3.1%	3.5%
Drive Axle	3.9%	4.4%
Shafts	4.6%	5.2%
Suspensions	4.5%	5.0%
Wheels and Tires	4.1%	4.7%
Cradle	8.9%	10.1%
Powertrain		
Engine	10.6%	0.0%
Engine Fuel Storage and Exhaust	1.7%	0.0%
Electric Drive Components		
Traction Motor	0.0%	2.9%
Electronic Controller	0.0%	0.3%
Transmission		
Clutch	0.2%	0.0%
Gearbox	3.1%	1.4%
Final Drive and Coupling	0.4%	0.4%
Trailer		
Trailer Body	24.1%	27.3%
Trailer Chassis	18.8%	21.3%
Trailer Auxiliary	2.6%	2.9%

Table C5 Distribution and Assumptions for Truck Component LCAs[14]

Component/Parameter	Distribution/Characteristics
Truck Body – Body and glass	Material Breakdown by Mass: Glass fiber = 54% Aluminum = 23% Steel = 19% LDPE = 25%
Truck Body - Interior	Material Breakdown by Mass: Steel = 49% LDPE = 25% Fabric = 7% Latex = 5% Leather = 4% Rubber = 3% Aluminum = 6%
Truck Body - Exterior	Material Breakdown by Mass: LDPE = 43% Steel = 24% Glass fiber = 10% Aluminum = 10% Rubber = 8% Copper = 4%
Truck Chassis – Steer Axle	Material Breakdown by Mass: Aluminum = 100%
Truck Chassis – Drive Axle	Material Breakdown by Mass: Steel = 82% Cast iron = 17%
Truck Chassis – Shafts	Material Breakdown by Mass: Steel = 96% Cast iron = 4%
Truck Chassis – Suspension	Material Breakdown by Mass: Steel = 92% Cast iron = 2% Rubber = 6%
Truck Chassis – Wheels and tires	Material Breakdown by Mass: Aluminum = 50% Rubber = 33% Steel = 17%
Truck Chassis – Cradle	Material Breakdown by Mass: Steel = 98% Rubber = 2%
Diesel Truck Powertrain - Engine	Material Breakdown by Mass: Steel = 46%

	Cast iron = 37% Aluminum = 11% LDPE = 3% Copper = 3%
Diesel Truck Powertrain – Fuel Storage and Exhaust	Material Breakdown by Mass: Aluminum = 35% Ceramic = 23% LDPE = 19% Stainless steel = 13% Steel = 10%
Li-ion Truck Electric Drive Components – Tractive Motor	Material Breakdown by Mass: Steel = 36% Aluminum = 36% Copper = 28%
Li-ion Truck Electric Drive Components – Electronic Controller	Material Breakdown by Mass: Steel = 5% Aluminum = 47% Copper = 8% Rubber = 4% LDPE = 24%
Diesel Truck Transmission - Clutch	Material Breakdown by Mass: Steel = 86% Cast iron = 7% LDPE = 5% Rubber = 1%
Diesel Truck Transmission - Gearbox	Material Breakdown by Mass: Steel = 86% Cast iron = 7% LDPE = 5% Rubber = 1%
Diesel Truck Transmission – Final Drive and Coupling	Material Breakdown by Mass: Steel = 86% Cast Iron = 7% LDPE = 5% Rubber = 1%
Li-ion Truck Transmission – Gearbox	Material Breakdown by Mass: Steel = 86% Cast iron = 7% LDPE = 5% Rubber = 1%
Li-ion Truck Transmission – Final Drive and Coupling	Material Breakdown by Mass: Steel = 86% Cast iron = 7% LDPE = 5% Rubber = 1%
Truck Trailer - Body	Material Breakdown by Mass:

	Aluminum = 51% Wood = 38% Steel = 11%
Truck Trailer - Chassis	Material Breakdown by Mass: Steel = 58% Rubber = 18% Cast iron = 14% Aluminum = 9%
Truck Trailer - Auxiliary	Material Breakdown by Mass: Steel = 69% Glass fiber = 17% Aluminum = 6% Rubber = 5% Copper = 3%
Truck Assembly Energy Demand (MJ)	Uniform distribution; min = 6255; max = 10425
Truck Assembly Energy Demand - Thermal	Thermal energy percent of total energy: triangle distribution; min = 0%, max = 80%, mode = 40%
Truck Assembly Energy Demand - Electricity	Electrical energy percent of total energy: 100% - thermal energy percent
Truck Assembly Thermal Source – Natural Gas	Thermal energy provided by natural gas: uniform distribution; min = 0%, max = 100%
Truck Assembly Thermal Source – Diesel	Thermal energy provided by natural gas: 100% - natural gas energy percent
Diesel Engine Assembly Energy Demand (MJ)	Uniform distribution; min = 682; max = 1137
Diesel Engine Assembly Energy Demand - Thermal	Thermal energy percent of total energy: triangle distribution; min = 0%, max = 80%, mode = 40%
Diesel Engine Assembly Energy Demand - Electricity	Electrical energy percent of total energy: 100% - thermal energy percent
Diesel Engine Assembly Thermal Source – Natural Gas	Thermal energy provided by natural gas: uniform distribution; min = 0%, max = 100%
Diesel Engine Assembly Thermal Source – Diesel	Thermal energy provided by natural gas: 100% - natural gas energy percent
Electric Motor Assembly Energy Demand (MJ)	Uniform distribution; min = 363; max = 604
Electric Motor Assembly Energy Demand - Thermal	Thermal energy percent of total energy: triangle distribution; min = 0%, max = 80%, mode = 40%
Electric Motor Assembly Energy Demand - Electricity	Electrical energy percent of total energy: 100% - thermal energy percent
Electric Motor Assembly Thermal Source – Natural Gas	Thermal energy provided by natural gas: uniform distribution; min = 0%, max = 100%
Electric Motor Assembly Thermal Source – Diesel	Thermal energy provided by natural gas: 100% - natural gas energy percent

Table C6 Class 8 Truck General Ops Cost Calculation and Uncertainty

Component/Parameter	Distribution/Characteristics	Source
Vehicle Depreciation	Lifetime Cost = MSRP * (1 – exp(A * lifetime + M * annual_VMT * lifetime / 1000) * (1 – r)^lifetime MSRP: Uniform Distribution; min = 100,000; max = 140,000 A = log(0.9071) M = log(0.9990) r = discount rate	15
Insurance	Lifetime Cost = $\sum_{t=1}^{Lifetime}(ins\_per\_mile * annual\_VMT * 1/(1 - r)^t)$ ins_per_mile: Triangle distribution; min = 0.06292; max = 0.09438; mode = 0.07865 r = discount rate	13
Taxes Fixed	Lifetime Cost = (MSRP + Battery Cost) * 0.12	16
Taxes Annual	Lifetime Cost = $\sum_{t=1}^{Lifetime}(550 * 1/(1 - r)^t)$ r = discount rate	17
Fees Annual	Lifetime Cost = $\sum_{t=1}^{Lifetime}((fees\_per\_kg * vehicle\_weight + fees\_fixed) * 1/(1 - r)^t)$ fees_per_kg: Uniform distribution; min = 0.04545; max = 0.06363 fees_fixed = 5952 r = discount rate	13,15
Maintenance and Repairs	Lifetime Cost = $\sum_{t=1}^{Lifetime}((t * M + b) * Batt\_Adj * annual\_VMT * 1/(1 - r)^t)$ M = 0.03 b = 0.09 Batt_Adj: if diesel, Batt_Adj = 1 If Li-ion, Triangle distribution; min = 0.48; max = 0.72; mode = 0.6 r = discount rate	13,15
Labor Driving	Lifetime Cost = $\sum_{t=1}^{Lifetime}(lab\_per\_mile * annual\_VMT * 1/(1 - r)^t)$ lab_per_mile: Triangle distribution; min = 0.7837; max = 1.176; mode = 0.9796 r = discount rate	13,15

annual_VMT: annual vehicle miles traveled

Figure C5 Forecasted Electricity and Diesel Prices[18]

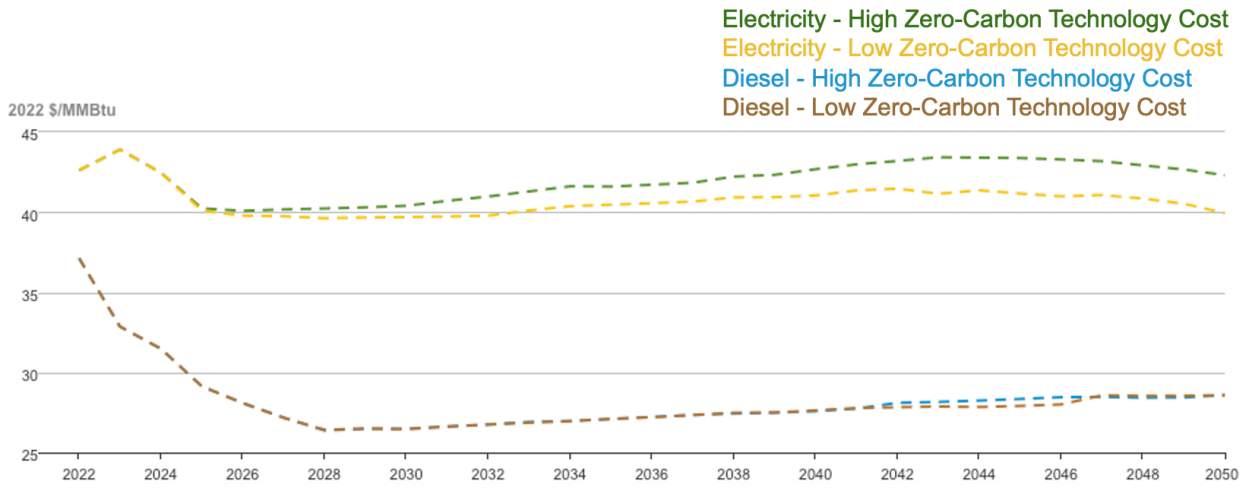

Figure C6 Forecasted Battery Prices with 17% Learning Rate[19,20]

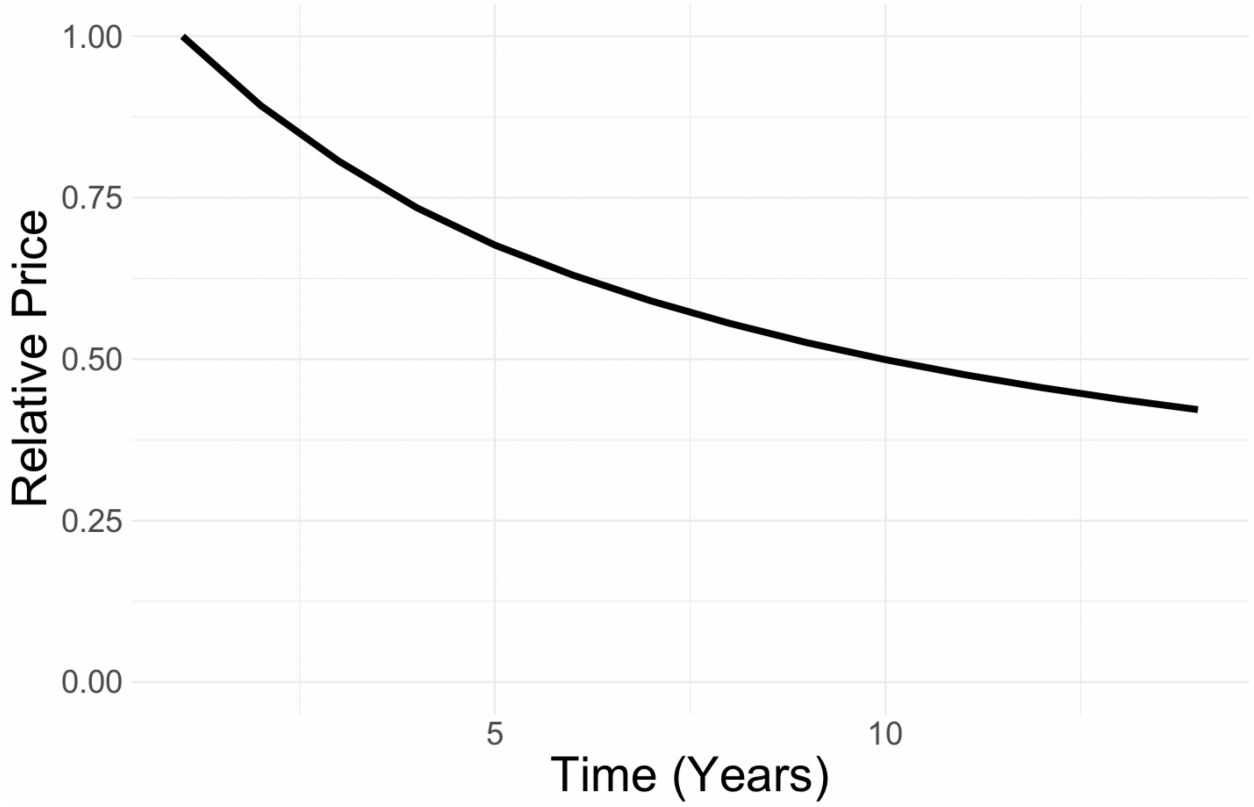

Demand growth in Table C7 used to forecast relative battery prices

Table C7 Forecasted Global Li-ion Battery Demand Scenario[19]

Year	Demand (GWh)
2022	1611
2023	2456
2024	3582
2025	5079
2026	6892
2027	8987
2028	11463
2029	14348
2030	17657
2031	21358
2032	25452
2033	29931
2034	34774
2035	39955

Table C8 2022 Li-ion Battery Pack Triangular Distribution Prices ($/kWh) by Chemistry in USD_{2024}[21]

Chemistry	Min	Max	Mode
NMC811	156	234	195
NCA	129	193	161
LFP	114	172	143

Table C9 Class 8 Truck Standing, Payload, and Tax Cost Calculation and Uncertainty

Component/Parameter	Distribution/Characteristics	Source
Standing	Lifetime Cost = $\sum_{t=1}^{Lifetime}$(lab_per_hour $*$ $annual\_charge\_time$ $*$ 1/(1 – r)^t) lab_per_hour: Triangle distribution; min = 29.76; max = 44.64; mode = 37.2 r = discount rate	13,15
Payload	Lifetime Cost = $\sum_{t=1}^{Lifetime}$(avg_penalty_weight / $GVWR * TLC$ $*$ 1/(1 – r)^t)	13,15
Tax Credit	Min(0.3*(MSRP + Battery_Cost), 40000)	22

Figure C7 TLC of Li-ion and diesel Class 8 trucks in 2024 and 2035 under high and low renewable cost scenarios with a 3% discount rate

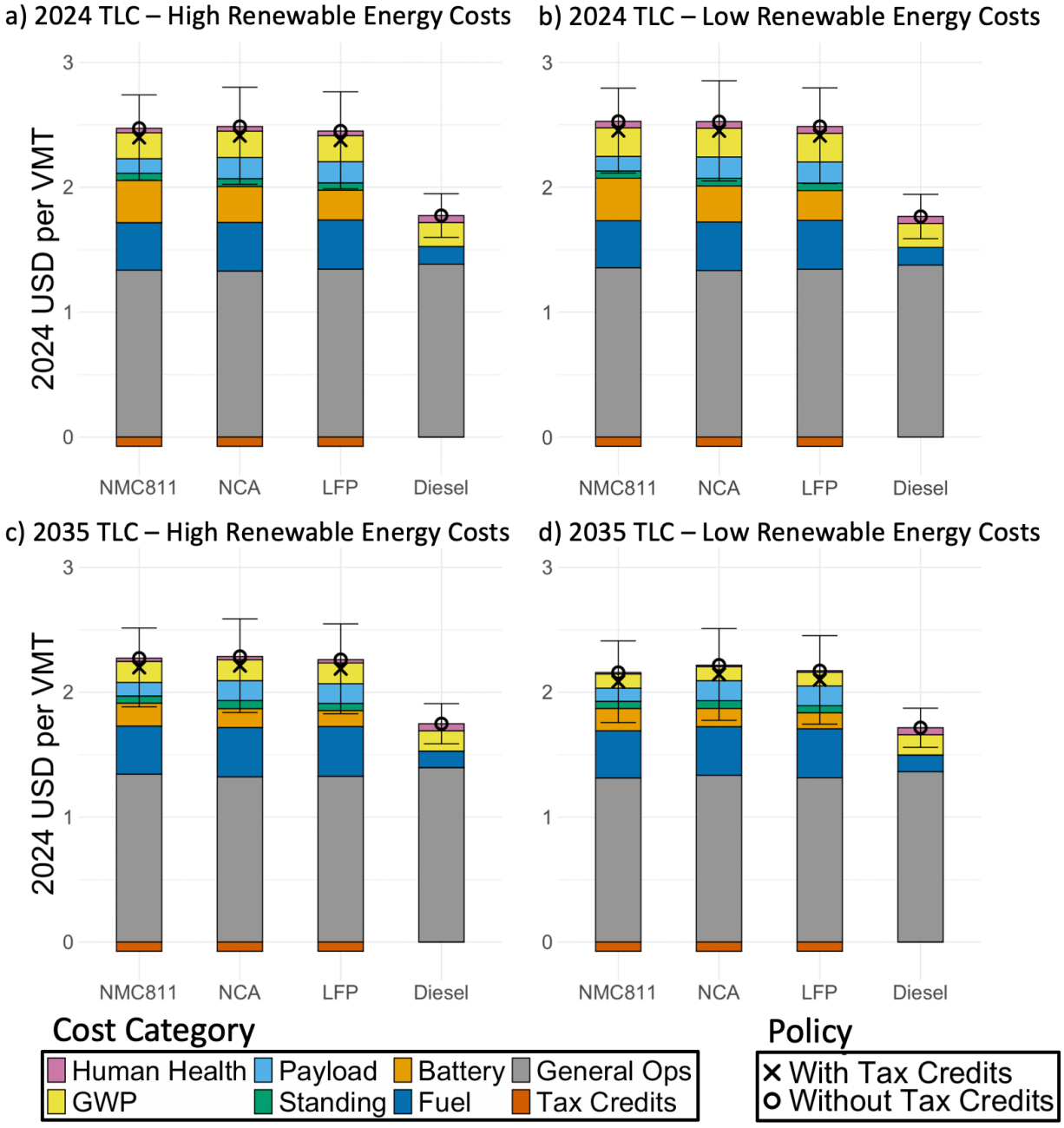

Figure C7 TLC of Li-ion and diesel Class 8 trucks in 2024 and 2035 under high and low renewable cost scenarios with a 7% discount rate

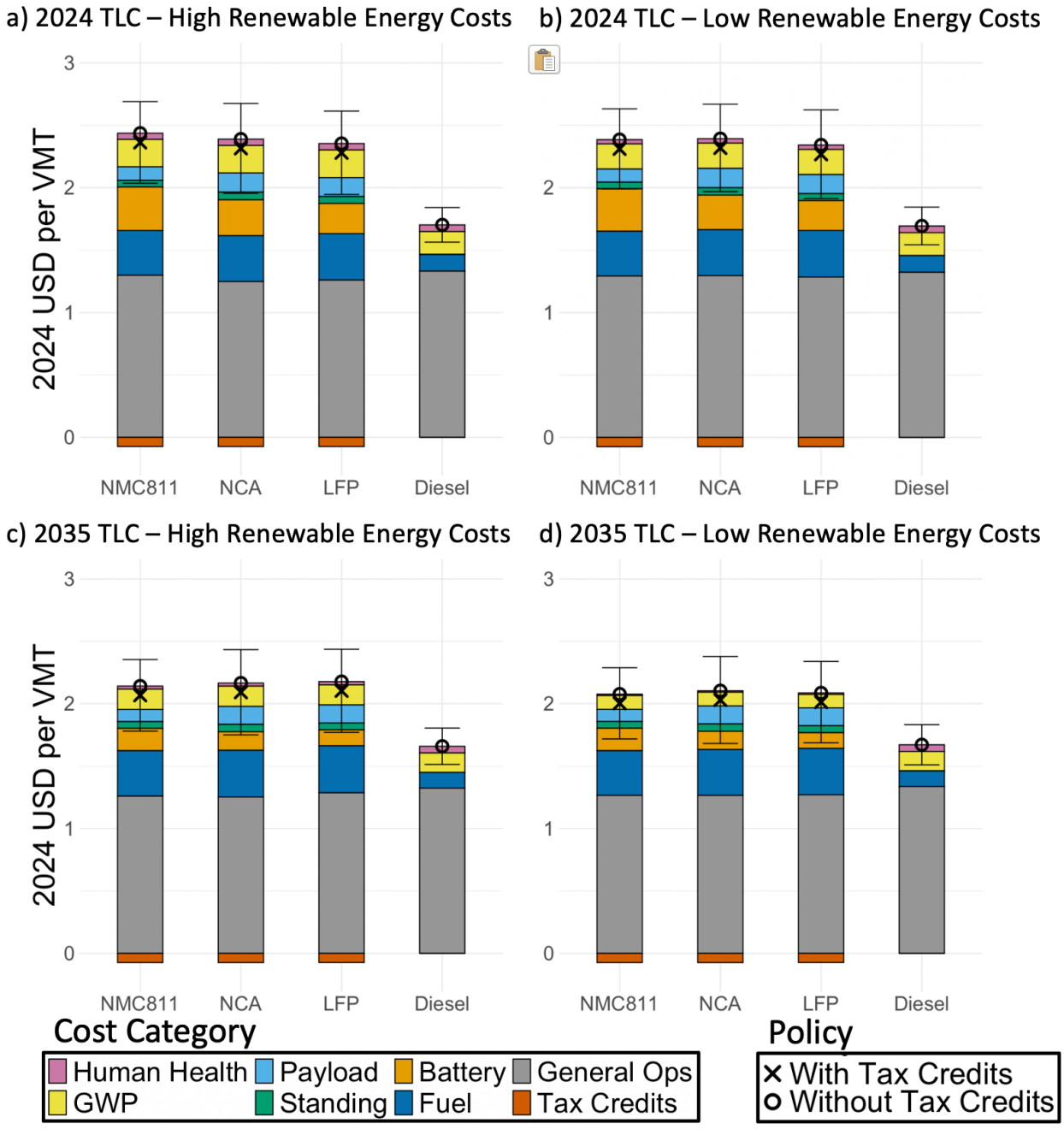

References

1. BloombergNEF. *Long-Term Electric Vehicle Outlook 2023*. (2023).

2. Boriboonsomsin, K. *et al. Collection of Activity Data from On-Road Heavy-Duty Diesel Vehicles*. (2017).

3. National Renewable Energy Laboratory. NREL DriveCAT - Chassis Dynamometer Drive Cycles. https://www.nrel.gov/transportation/drive-cycle-tool/ (2023).

4. Andrenacci, N., Karagulian, F. & Genovese, A. Modelling charge profiles of electric vehicles based on charges data. *Open Res. Europe* **1**, 156 (2021).

5. Hackmann, M. *P3 Charging Index Report 07/22 – Comparison of the Fast Charging Capability of Various Electric Vehicles*. (2022).

6. Moura, S. Interview with Prof. Scott Moura. (2023).

7. Ryan, N. A., Johnson, J. X. & Keoleian, G. A. Comparative assessment of models and methods to calculate grid electricity emissions. *Environ. Sci. Technol.* **50**, 8937–8953 (2016).

8. Gagnon, P., Frazier, W., Cole, W. & Hale, E. *Cambium Documentation: Version 2021*. (2021).

9. Jenn, A., Clark-Sutton, K., Gallaher, M. & Petrusa, J. Environmental impacts of extreme fast charging. *Environmental Research Letters* **15**, 094060 (2020).

10. McNeil, W. H., Tong, F., Harley, R. A., Auffhammer, M. & Scown, C. D. Corridor-Level Impacts of Battery-Electric Heavy-Duty Trucks and the Effects of Policy in the United States. *Environ. Sci. Technol.* **58**, 33–42 (2024).

11. Tong, F., Jenn, A., Wolfson, D., Scown, C. D. & Auffhammer, M. Health and Climate Impacts from Long-Haul Truck Electrification. *Environ. Sci. Technol.* **55**, 8514–8523 (2021).

12. Hunter, C. A. *et al.* Techno-economic analysis of long-duration energy storage and flexible power generation technologies to support high-variable renewable energy grids. *Joule* (2021) doi:10.1016/j.joule.2021.06.018.

13. Burnham, A. *et al. Comprehensive Total Cost of Ownership Quantification for Vehicles with Different Size Classes and Powertrains*. (2021).

14. Wang, M. *GREET (Greenhouse Gases, Regulated Emissions, and Energy Use in Transportation) Model*. (Argonne National Laboratory, 2023).

15. Hunter, C. *et al. Spatial and Temporal Analysis of the Total Cost of Ownership for Class 8 Tractors and Class 4 Parcel Delivery Trucks*. (2021).

16. US EPA. Learn About Federal Excise Tax Exemption. https://www.epa.gov/verified-diesel-tech/learn-about-federal-excise-tax-exemption (2023).

17. US Department of Transportation. Heavy Vehicle Use Tax. *Policy and Governmental Affairs Office of Highway Policy Information* https://www.fhwa.dot.gov/policyinformation/hvut/mod1/whatishvut.cfm (2020).

18. US Energy Information Administration. *Annual Energy Outlook 2023*. (2023).

19. BloombergNEF. *Lithium-Ion Batteries: State of the Industry 2023*. (2023).

20. Ziegler, M. & Trancik, J. *Re-examining Rates of Lithium-ion Battery Technology Improvement and Cost Declines*. (2020).

21. BloombergNEF. *2022 Lithium-Ion Battery Price Survey*. (2022).

22. Internal Revenue Service. Commercial Clean Vehicle Credit. *Commercial Clean Vehicle Credit* https://www.irs.gov/credits-deductions/commercial-clean-vehicle-credit (2024).